EPFL

Thèse n° 8013

Dynamics of brain function in preterm-born young adolescents

Présentée le 27 juillet 2020

à la Faculté des sciences et techniques de l'ingénieur
Laboratoire de traitement d'images médicales
Programme doctoral en génie électrique

pour l'obtention du grade de Docteur ès Sciences

par

Lorena
GONÇALVES DE ALCÂNTARA E FREITAS KRIKLER

Acceptée sur proposition du jury

Prof. J.-Ph. Thiran, président du jury
Prof. D. N. A. Van De Ville, Prof. P. S. Hüppi, directeurs de thèse
Prof. E. Tagliazucchi, rapporteur
Prof. F. Lazeyras, rapporteur
Prof. S. Micera, rapporteur

École polytechnique fédérale de Lausanne

2020

Para minha mãe, Iva, e meu pai, Celdes...

Acknowledgements

First and foremost, I would like to thank my PhD supervisors, without whom I would not have been able to carry out the research projects presented here. Professor Petra Hüppi gave me the opportunity to work on the fascinating world of paediatrics and prematurity. The ability to have close contact with the very subjects I was studying was paramount to having a birds-eye view of the impact of our research, and for this I am thoroughly grateful. Dimitri patiently guided me through the tortuous path of doctoral work, always available to listen and help with incredible wisdom, generosity and kindness. After every meeting, I left his office feeling encouraged and more eager to succeed (even when it took me a while to understand his brilliant ideas). I feel honoured and proud to have been their student.

Being simultaneously part of two laboratories can sometimes be challenging, but the amazing people I had the chance to work with made the journey much more enjoyable. I thank my colleagues at ChilDLab for teaching me so much about the clinical aspects of our project. In particular, thank you Chiara and Vanessa for your collaboration, friendship and endless support — no wonder we call ourselves the *dream team*. All MIP:labbers, thank you for making me feel immediately welcome upon my arrival, for all the interesting scientific discussions during meetings or around tiramisu and coffee (tea for me, please!), and for the countless hours of Mafia games. Especially, I would like to thank Dani for being a good friend and role model, Thomas for supporting me and teaching me to never give up (on my work and on French), Giuli for some of the happiest memories and proudest records of my PhD, and Laura for helping me feel good even in the occasional moments when little else would do. Finally, I would like to thank Madame Muriel Hausler and Manuela, for dealing with all the administrative issues so that we could concentrate on our work.

The analyses presented in this work would not have been possible without data – the acquisition of which was a long process involving several colleagues. Thank you Chiara and Vanessa (again!), Jiske, Fanny and Greta, for recruiting our subjects and/or sharing the arduous task of data collection with me. I extend my gratitude to Loan and Roberto, who so kindly helped us in the MRI facility and patiently forgave subject no-shows and the occasional hiccup in organisation. I am also extremely grateful to the children and their parents who participated in our study and so generously contributed their time to advance knowledge on the important topic of premature birth.

While I feel terribly lucky to have had such a well-rounded team and infra-structure to perform my work, I would not have got to this point without the love and support from my family and friends. I must absolutely thank my husband Ben for being such a super-star partner and

supporting me in any goal I set myself to achieve — including organising our two international weddings while also pursuing my PhD. Thank you for being my best friend, my boyfriend, my family, my home, my co-author and now, my proofreader (marrying an Englishman did come in handy after all!). I thank my mum Iva, who would have been absolutely thrilled to see me get here, for the strong foundation she gave me in the time we had together and for teaching me early on that education will take one very far — I just don't know if she had Switzerland in mind. My dad Celdes, for giving me his strong will and being such an inspiring fighter when it comes to the crunch. Daddy, Diego, Juliana, Heitor, aunt Ceres, Cristina and Marcinha: thank you for the unconditional support, for being such a strong foundation in my life, and for helping me believe I can do anything. Thank you for understanding that I could not visit as often as I would have loved to, especially in the final stages of the PhD. Last but not least, I would like to thank all my friends for making the world a beautiful place and my life that much happier and effortless, which allowed me to concentrate all my mental resources on this work. Especially Bee, Nanna, Sassá, Cecella, Cuka, Tristan, Sylvain and my groβe Schwester Ilki: thank you for defying physics and seemingly making the thousands of miles that separate us disappear. I feel your presence around me every single day.

Geneva, July 14, 2020 L.G.A.F.K.

Abstract

Preterm birth is a major risk factor for neurodevelopment impairments often only appearing later in life. The brain is still at a high rate of development during adolescence, making this a promising window for intervention. It is thus crucial to understand the mechanisms of altered brain function in this population. The aim of this thesis is to investigate how the brain dynamically reconfigures its own organisation over time in preterm-born young adolescents. Research to date has mainly focused on structural disturbances or in static features of brain function in this population. However, recent studies have shown that brain activity is highly dynamic, both spontaneously and during performance of a task, and that small disruptions in its complex architecture may interfere with normal behaviour and cognitive abilities.

This thesis explores the dynamic nature of brain function in preterm-born adolescents in three steps: First, we investigate changes in spontaneous brain activity over time using a resting-state paradigm. Here, we study how the variability of the blood oxygenation level dependent signal (BOLD), a measure previously linked to cognitive performance, develops in a preterm- and a term-born groups. We find that preterm participants show an altered trajectory of BOLD variability development during early adolescence. We also show that the dynamic patterns of co-activation with the dorsal anterior cingulate cortex (ACC), a key node of the salience network, also develop differently between the preterm and control groups. Secondly, we examine task-driven changes in brain activation. To this end, we select a reality filtering task known to engage the orbitofrontal cortex (OFC), a region that is particularly vulnerable in the preterm. We find that, although the preterm group is able to perform the task successfully, OFC activation is significantly higher in the control participants. Finally, inspired by the successful field of dynamic functional connectivity which has mainly flourished in resting-state paradigms, we develop a novel method to look into task-driven modulations of brain connectivity in a time-resolved way. We then apply this new approach to a third data set involving a movie watching and emotion regulation task. We find several subtle but significant seed; task; and group effects that characterise each of the dynamic co-activation patterns.

In short, we introduce a method for time-resolved evaluation of task-driven changes in brain connectivity and provide evidence of altered brain dynamics in preterm-born young adolescents. Our results thus highlight the importance of considering the dynamic aspects of brain function when studying clinical populations.

Keywords: non-invasive neuroimaging, functional MRI, dynamic analysis, preterm, BOLD signal variability, co-activation patterns, PPI-CAPs

Résumé

La naissance prématurée est un facteur de risque majeur de troubles du développement neurologique, qui souvent n'apparaissent que plus tard dans la vie. À l'adolescence, le cerveau est encore en plein développement, ce qui en fait une fenêtre d'intervention prometteuse. Il est donc crucial de comprendre les mécanismes de la fonction cérébrale altérée dans cette population. Le but de cette thèse est d'étudier comment le cerveau reconfigure dynamiquement sa propre organisation au fil du temps chez les jeunes adolescents nés avant terme. À ce jour, les recherches ont principalement porté sur les perturbations structurelles ou sur les caractéristiques statiques de la fonction cérébrale dans cette population. Cependant, des études récentes ont montré que l'activité cérébrale est très dynamique, à la fois spontanément et pendant l'exécution d'une tâche, et que de petites perturbations de cette architecture complexe peuvent interférer avec le comportement normal et les capacités cognitives.

Cette thèse explore la nature dynamique de la fonction cérébrale chez les adolescents prématurés en trois étapes : premièrement, nous analysons les changements dans l'activité cérébrale spontanée au fil du temps, à l'état de repos. Ici, nous étudions comment la variabilité du signal dépendant du niveau d'oxygénation sanguin (BOLD), une mesure auparavant liée aux performances cognitives, se développe dans un groupe prématuré et un groupe né à terme. Nous constatons que la trajectoire de développement de la variabilité BOLD est modifiée chez les participants prématurés au début de l'adolescence. Nous montrons aussi que les modèles dynamiques de co-activation avec le cortex cingulaire antérieur dorsal (ACC), un nœud clé du réseau de saillance, se développent également différemment entre le groupe prématuré et le groupe nà à terme. Deuxièmement, nous examinons les changements provoqués par les tâches dans l'activation cérébrale. À cette fin, nous sélectionnons une tâche de filtrage de la réalité connue pour engager le cortex orbitofrontal (OFC), une région particulièrement vulnérable chez le prématuré. Nous constatons que, bien que le groupe prématuré soit en mesure d'effectuer la tâche avec succès, l'activation de l'OFC est significativement plus élevée chez les participants nés à terme. Enfin, inspirés par le domaine prometteur de la connectivité fonctionnelle dynamique qui a principalement prospéré dans des expériences faites à l'état de repos, nous développons une nouvelle méthode pour étudier les modulations de connectivité cérébrale induites par une tâche d'une manière résolue dans le temps. Nous appliquons ensuite cette nouvelle approche à un troisième ensemble de données impliquant une tâche de visionnage de films et de régulation des émotions. Nous trouvons plusieurs effets subtiles mais significatifs de seed, de tâche, et de groupe qui caractérisent chacun des modèles de co-activation dynamique.

Résumé

En bref, nous introduisons une méthode d'évaluation résoluee dans le temps des changements de connectivité cérébrale liés à une tâche, et nous fournissons des preuves d'un développement altéré de la dynamique cérébrale chez les jeunes adolescents prématurés. Nos résultats mettent ainsi en évidence l'importance de considérer les aspects dynamiques de la fonction cérébrale lors de l'étude des populations cliniques.

Mots-clés : neuroimagerie non invasive, IRM fonctionnelle, analyse dynamique, prématuré, variabilité du signal BOLD, schémas de co-activation

Contents

1 Introduction

1.1 Motivation

Preterm birth (PTB) — characterised as birth before 37 full weeks of gestation — affects an estimated 7% of births in Switzerland, and 11.1% of all live births worldwide, which corresponds to nearly 15 million babies per year (Blencowe et al., 2013). This comes with a heavy societal burden as it is one of the predominant risk factors behind neurodevelopmental disorders (Pierrat et al., 2017; Twilhaar et al., 2018), besides increasing the neonatal and post-discharge costs up to 33 times (Tommiska et al., 2003) as compared to term birth. PTB has been associated with a wide range of impairments in cognitive functions spanning attention (Rommel et al., 2017), working memory (Allotey et al., 2018), affective behaviour (Hornman et al., 2016), executive functions (Costa et al., 2017; Burnett et al., 2018), among others (Moreira et al., 2014; Allotey et al., 2018). Often unveiled only when children reach school age, some of these difficulties may persist throughout life (Anderson, 2014; Kajantie et al., 2019). In Switzerland, while the majority of the patients have positive outcomes, 21% show some form of cognitive impairment, particularly in short term memory (Pittet-Metrailler et al., 2019). Understanding the neurological underpinnings of these difficulties is thus crucial to identify potential interventions and establish critical periods to restore typical development (Wolke et al., 2019).

Functional magnetic resonance imaging (fMRI) is a powerful tool to characterise brain function in a non-invasive fashion and is, therefore, ideal to investigate the neurological basis of clinical outcomes in the young population. Typically relying on the blood oxygenation level dependent signal, it indirectly measures brain activity with exceptional spatial specificity due to its signal reliability, high spatial resolution for a non-invasive method, and reproducibility. Thanks to this technique, it is now known that brain activity intrinsically oscillates in a highly organised way in rest (Damoiseaux et al., 2006), and during performance of tasks (Elliott et al., 2019). This has promoted discoveries linking brain function and the performance of cognitive demanding tasks in several domains of cognitive neuroscience (Raichle, 2001; Poldrack, 2012; D'Esposito and Kayser, 2016).

FMRI is, in many ways, well-suited to investigate paediatric populations, especially since robust measures of functional activation and connectivity can be obtained from short scanning sessions. It has been successfully employed in studies involving young cohorts tapping

into language (Centeno et al., 2014; Pigdon et al., 2020), somatomotor (Zwicker et al., 2011; Sgandurra et al., 2018), attention (Somandepalli et al., 2015; Jiang et al., 2019; Harrewijn et al., 2020), memory (Mankinen et al., 2015; de Bie et al., 2015), affective processing (Loveland et al., 2008; McRae et al., 2012), working memory (Siffredi et al., 2017; Yaple and Arsalidou, 2018), and executive functions (Wang et al., 2013; Staphorsius et al., 2015). All of these abilities are more likely to be impaired in preterm- than in term-born individuals, highlighting fMRI's fitness to study this population. Indeed, this technique has uncovered altered brain responses in regions underlying executive functions in preterm-born children in frontal (Réveillon et al., 2013; Mürner-Lavanchy et al., 2014) and temporal areas (Kwon et al., 2014; Wilke et al., 2014) which were linked to impaired language performance at age 14–15 (Wilke et al., 2014).

Recently, fMRI studies have shown that the brain activity is highly dynamic, fluctuating between large-scale brain states formed by simultaneous activation of different subsets of brain regions during rest (Chang and Glover, 2010; Preti et al., 2017; Liu et al., 2018) and task performance (Di et al., 2015; Cheng et al., 2018). Crucially, features of these moment-to-moment fluctuations of brain configuration have very recently been discovered to be linked to cognitive ability in humans, both during rest (Chén et al., 2019) and while performing attentional tasks (Fong et al., 2019). These findings indicate the high potential of brain dynamics as an avenue to further characterise the effects of prematurity in the brain, additionally shedding light on how they relate to cognitive outcomes in those who were born too soon.

1.2 Organisation and main contributions

The goal of this thesis is to advance the knowledge on the neural effects of preterm birth, in the resting state as well as during performance of cognitive tasks, through the development of state-of-the-art imaging analyses. This manuscript is thus organised as a compilation of two published articles and three preprints in preparation for submission. Chapter 2 provides an overview of the state of the art in functional MRI analysis and preterm birth research, and serves as a background for the studies presented in subsequent chapters. It starts by introducing fMRI as a powerful tool to investigate human brain function, followed by a description of currently available methodologies for human brain mapping using this technique. It then characterises the clinical aspects of preterm birth and presents the current knowledge on how its outcomes relate to brain function. Chapters 3, 4 and 5, reproduce published manuscripts and articles in preparation which contribute both through novel research, as well as complementary analyses to existing knowledge. Chapter 6 then summarises and integrates the results, and proposes avenues for future research.

Below, I summarise the main research questions and contributions of each article. In all of them I contributed to the planning, performed all data processing; methods' development; and statistical analysis where applicable, and wrote — or contributed equally to — the manuscript and revisions. Since these studies were achieved thanks to a collaboration involving large groups of people, I will often use the personal pronoun "we" when discussing the work done.

Motivation

Preterm-birth

- 11% of annual births worldwide
- Major risk of neurodevelopment problems
- Clinical consequences may last through lifetime
- Developing brain in early adolescence → potential window for intervention

Brain dynamics

- Non-invasive brain imaging using magnetic resonance imaging (MRI)
- Most studies to date rely on static analyses of brain imaging data
- Brain function is a dynamic process → dynamic analyses are crucial

Contributions

Chapter 3: Resting-state dynamics in preterm early adolescents

Freitas et al., *preprint, 2020*

- Partial least squares correlation (PLSC) multivariate pattern analysis
- BOLD variability and co-activation pattern (CAP) analysis
- Altered development of BOLD variability and of activation patterns in the preterm

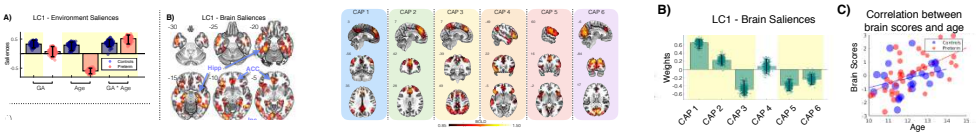

Chapter 4: Reality filtering in early adolescence

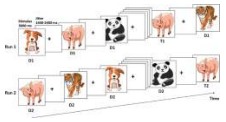

Liverani*, Freitas* et al., *Brain and Behaviour*, 2020

- Reality filtering (RF) task-based functional MRI analysis
- Orbitofrontal cortex (OFC) mediates RF in term-born early adolescents

Freitas et al., *preprint, 2020*

- Reality filtering task-based fMRI in preterm-born early adolescents
- Altered OFC activation in preterm as compared to term-born group

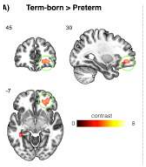

Chapter 5: Task-related dynamics and application in preterm early adolescents

Freitas et al., *NeuroImage, 2020*

- Psychophysiological interaction of co-activation patterns (PPI-CAPs)
- Time-resolved analysis of task-related effective connectivity (EC)
- Decomposed EC maps to reveal a more accurate picture of brain function

Freitas et al., *preprint, 2020*

- Early adolescents perform task alternating movie watching and emotion regulation
- PPI-CAPs uncover task-modulated patterns of activation with task, seed or group effects

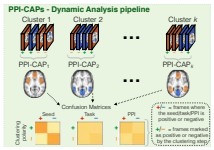

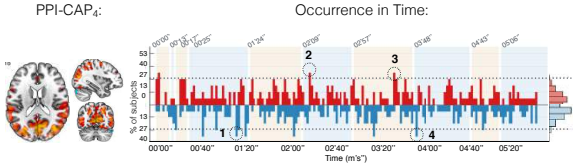

Figure 1.1 – **Thesis overview.** Main contributions on brain dynamics in preterm-birth.

Chapter 3: BOLD signal variability and dynamic spontaneous brain function in the preterm-born

Although brain analysis methods often rely on measuring and comparing the average activity in certain areas of interest, blood oxygenation level dependent (BOLD) signal variability has been shown to yield additional information on brain function that is linked to cognitive abilities. To the best of my knowledge, no one has investigated BOLD signal variability in preterm-born populations. In this chapter, I look into functional brain dynamics in two ways: first, in terms of voxelwise BOLD signal variability and its relationship with gestational age and age at assessment. Secondly, I perform a seed-based co-activation pattern analysis focusing on the dorsal anterior cingulate cortex, an area previously described to be affected by preterm-birth (White et al., 2014b; Daamen et al., 2015; Lordier et al., 2019) that was also highlighted in the analysis of BOLD variability.

Section 3.1: *(Journal Article)* Altered BOLD variability development and brain dynamics in preterm-born young adolescents

Is the development of BOLD signal variability affected by preterm birth?
Does preterm birth affect finer temporal scale brain dynamics?

BOLD signal variability, calculated as the standard deviation of BOLD signal time series, is a measure of how dynamic brain activity is throughout the duration of an fMRI experiment. It has been shown to change with age and cognitive ability (Garrett et al., 2013a) and to be altered in clinical populations (Zöller et al., 2017; Nomi et al., 2018; Easson and McIntosh, 2019). These studies support its role in reflecting the brain's dynamic range and complexity and, when present at the optimal levels, in allowing greater flexibility for brain function (McIntosh et al., 2010; Deco et al., 2011). It is thus a promising avenue to investigate brain "dynamism" in preterm populations.

In this article, I investigate the link between dynamic brain function and gestational age, as well as with age at assessment, using a multivariate partial least squares (PLS) approach in a resting-state fMRI paradigm. I have addressed this in two steps: First, I compare how those relationships evolve during early adolescence in a preterm-born and a fullterm control group of children. Then, because BOLD variability is closely linked to functional connectivity, I delve deeper into how the relationship between a region of interest identified in this analysis — namely, the anterior cingulate cortex — and other parts of the brain evolve over time in these two groups by using co-activation patterns as brain measures for the PLS. We identify interesting interactions between age at assessment and gestational age in both analyses, suggesting that preterm birth alters the development of dynamism in the brain at later stages in life.

Chapter 4: Studying cognition with task-based fMRI: Reality Filtering in young populations

While resting-state analyses provide profound insight into brain function, task-based fMRI paradigms are crucial to understand how the brain works under specific cognitive demands. In the case of preterm populations, there is particular interest in cognitive functions involving frontal brain areas, as neuroimaging studies have highlighted widespread alterations in the prefrontal cortex's structure and function in preterm individuals across lifetime. In this chapter, we thus employ a Reality Filtering (RF) task, known to recruit the orbitofrontal cortex (OFC) in adults, to study brain function in this area in young adolescents. To the best of our knowledge, no one has looked into brain function related to RF in children so far. Therefore, this chapter is divided in two steps: First, we confirm the OFC's involvement in RF in typically developing, fullterm-born children. Then, we look into whole-brain, as well as OFC-seed differences, between a preterm-born and a control group while performing an RF task.

Section 4.1: *(Journal Article)* "Get real: orbitofrontal cortex mediates the ability to sense reality in early adolescents"

What are the neural processes underlying reality filtering in early adolescents?

The typical approach to understand the neural underpinnings of cognition is to investigate how brain function changes as a direct effect from task performance. Here, we focus our study on the orbitofrontal cortex (OFC), known to be crucial for the ability to sense reality in adults but to be still under development in young adolescents, to understand how activation in this area changes in the latter population depending on stimuli presentation. Using a previously validated task paradigm adapted to children we confirmed, for the first time using fMRI and in young adolescents, that the OFC mediates reality filtering already at this age.

Section 4.2: *(Journal Article)* Altered orbitofrontal activation in preterm-born young adolescents during performance of a reality filtering task

Are preterm-born young adolescents able to perform a reality filtering task?
What are the neural processes underlying reality filtering in preterm-born young adolescents?

Because the prefrontal cortex —– of which the OFC is a constituting part — is known to be affected by preterm birth in several ways, we wanted to investigate both whether preterm-born young adolescents are capable of reality filtering and, if this is the case, whether the OFC is involved. Using the same task as in the previous section, we found that although children in the preterm group were able to perform the task with comparable accuracy to the fullterm group, the levels of OFC activation in the former group are lower and no other regions were more activated than in controls. This suggests that preterm-born individuals may have developed mechanisms to optimise OFC activity such that they are still able to perform the task without depending on the same level of activation as the control group.

Chapter 5: Time-resolved brain dynamics during task performance

While typical task-based studies compare and contrast how brain activity changes between different task contexts, they still mostly assume stationary within task blocks. This provides a limited, incomplete snapshot of how the brain works under these circumstances. Resting-state fMRI has benefited from methods that uncover dynamic features of large-scale neuronal function for over a decade (Chang and Glover, 2010), but task-based paradigms have only recently started to explore this important avenue (Gonzalez-Castillo and Bandettini, 2018).

Section 5.1: *(Journal Article)* "Time-Resolved Effective Connectivity in Task fMRI: Psychophysiological Interactions of Co-Activation Patterns"

Can we capture relevant task-related functional dynamics in a frame-wise way?

Previous studies have shown that relevant information on brain function is condensed in specific moments of high amplitude peaks in the BOLD signal (Tagliazucchi et al., 2011), meaning that large parts of the fMRI time series contain information that does not necessarily add information for certain analyses. This means the fMRI data can reduce to a point-process (Tagliazucchi et al., 2012) characterised by a sequence of time points when a seed signal traverses a given threshold. If these points are then averaged, one obtains patterns of co-activation with a seed that are recurring throughout the experiment, at a single-frame resolution (Liu and Duyn, 2013).

In this article I develop a seed-based method called Psychophysiological Interactions of Co-Activation Patterns (PPI-CAPs) to investigate such dynamic modulations of functional brain connectivity in a task-based context. In a naturalistic setting in which participants watched a short TV program, several patterns of co-activation were yielded using a posterior cingulate cortex seed — chosen due to its well documented connectivity arrangements (Liu and Duyn, 2013; Karahanoglu and Van De Ville, 2015; Lin et al., 2017) and its description as a hub region (Andrews-Hanna et al., 2010). These patterns' occurrence rates and polarity varied according the context; the seed activity; or an interaction between the two. Moreover, this method unveiled the consistency in effective connectivity patterns over time and across subjects, which allowed us to uncover links between PPI-CAPs and specific stimuli contained in the video. The main contribution of this study was revealing that explicitly tracking connectivity pattern transients is paramount to advance our understanding of how different brain areas dynamically communicate when presented with a set of cues. Given its ability to concentrate the analysis on very limited amounts of data, this represents a promising avenue for further study of dynamic features of task-modulated brain function in clinical or young populations, such as the preterm-born young adolescents most of this thesis concentrates on.

The code developed to perform the analysis described in this work has been made available on https://github.com/lorenafreitas/PPI_CAPs

Section 5.2: *(Journal Article)* "Tracking moment-to-moment functional connectivity in preterm-born young adolescents during movie watching and emotion regulation"

Do preterm-born young adolescents present altered configurations of task-related functional dynamics as compared to fullterm-born controls?

Having shown that PPI-CAPs is a compelling avenue for the study of dynamic features of context-driven brain function in clinical populations (Freitas et al., 2020) in Section 5.1, I then proceed to employ this approach to study dynamic connectivity in preterm-born young adolescents as compared to age-matched controls. To this end, our participants undergo a block-type task which alternates between moments of movie watching — where the films have an emotional valence (*i.e.*, amusing or repulsive) to them — followed by moments of emotion regulation and concentration on their own breathing. We recover six robust and reoccurring patterns of co-activation with a dorsal anterior cingulate cortex seed. Moreover, we show that several of the data-driven patterns have a seed, task, or group main effects, as well as interactions between those. This study further highlights the importance of investigating task-driven brain dynamics in the context of clinical populations to obtain a more accurate picture of healthy and altered brain function.

2 Background

Magnetic resonance imaging (MRI) is a powerful tool to characterise brain function non-invasively, and has proven a successful way to investigate the neurological substrate of clinical outcomes in young populations. In order to understand its capabilities as well as its limitations, it is important to understand the biophysical underpinnings of the technology. Thus, in this chapter, I initially introduce this technique and provide an overview of the related state-of-the-art analytical methods in Section 2.1.1, followed by an introduction on the clinical aspects of preterm birth in Section 2.2. I then summarise currently available knowledge provided by brain imaging in the preterm population in Section 2.3.

2.1 Magnetic resonance imaging (MRI) as a tool to investigate brain function

Magnetic resonance imaging (Lauterbur, 1973) of bodily tissues is a relatively young technique (Damadian et al., 1977) which depends on a basic set of physics principles concerning the interaction of protons, radio frequencies and magnetic fields. The following is a summary of how it produces images of living tissues, such as the ones used in the studies presented in the next chapters — for a detailed review see Grover et al., 2015. The main element that enables the use of MRI technology for this purpose is hydrogen, due to its high concentration in all tissues. Each atom of this substance can be seen as a sphere carrying a positive charge and is always spinning along random orientations, which causes it to "wobble" (Figure 2.1A/B). Since moving charges produce a magnetic field, we can think of these protons as tiny bar magnets.

In the presence of a strong magnetic field, such at the static magnetic field generated by the MRI machine (B_0), the protons' axes align with the field lines created by the magnet, creating a net magnetization (M_0; Figure 2.1B). M_0 can be considered as a vector containing two components: A longitudinal component M_L, parallel to B_0; and a transverse component M_T, perpendicular to it. The hydrogen nuclei's spinning motion combined with an external force causes them to precess about B_0 with an angular frequency according to the Larmor frequency

(Larmor, 1897), but at random phases. The time it takes for a proton to sweep out a 'cone' once is called its resonance frequency. Different protons precess with different frequencies, and this property has an important role in informing their physical location. This is because gradient coils (X, Y and Z) create a secondary magnetic field which distorts B_0 in a predictable pattern, causing the proton's resonance frequency to vary according to position. This is what allows the MR signal to be spatially encoded, currently to a resolution of 1–3 mm.

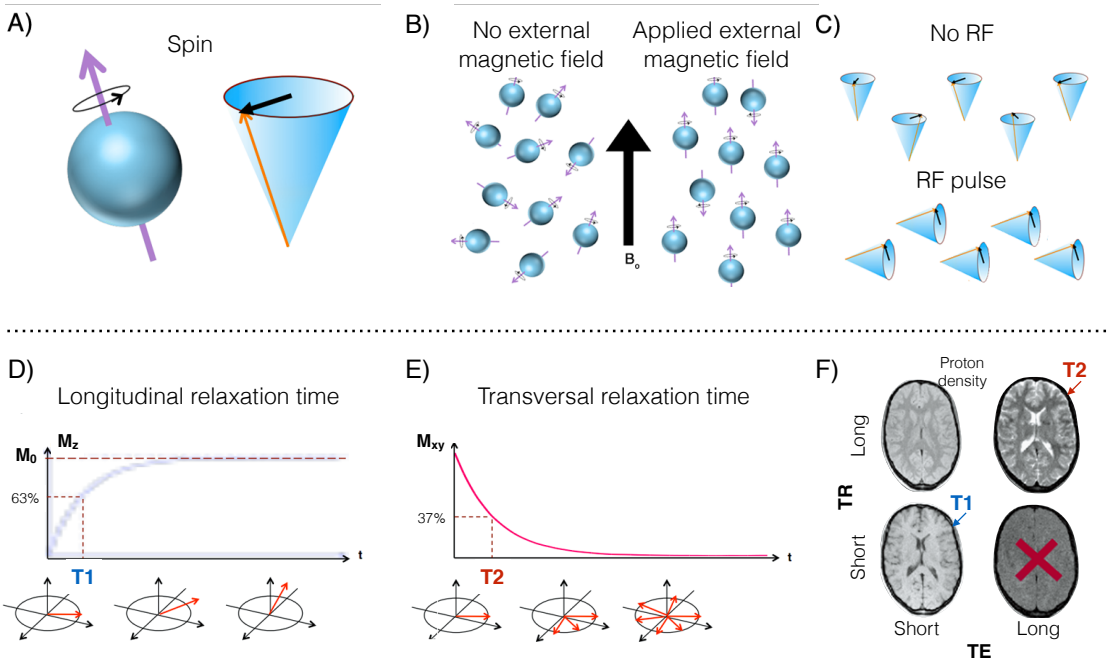

Figure 2.1 – **Magnetic resonance Imaging.** A) A proton's spin. B) Alignment of protons in the present of a magnetic field B_0, creating a net magnetisation M_0 which contains two components: a longitudinal M_L which is parallel to B_0; and a transverse component M_T which is perpendicular to it. C) When an electromagnectic radio frequency (RF) pulse transmitted by the RF coil present in the MR machine is applied, the hydrogen nuclei's phases align and they tip over, decreasing the longitudinal magnetisation and establishing a new transverse magnetisation. D) when the RF pulse is stopped, the system slowly returns to equilibrium: the transversal magnetisation begins to disappear (transversal relaxation, described by time constant T_2), while the longitudinal magnetisation returns to its original size (*i.e.*, longitudinal relaxation, described by time constant T_1). E) By altering the repetition (TR) and the echo time (TE), we can select the characteristic that we want to emphasise in the tissues.

When an electromagnectic radio frequency (RF) pulse transmitted by the RF coil present in the MR machine is applied, the hydrogen nuclei's phases align and they tip over (Figure 2.1C), decreasing the longitudinal magnetisation and establishing a new transverse magnetisation. Then, when the RF pulse is stopped, the system slowly returns to equilibrium: the transversal magnetisation begins to disappear (a phenomenon called transversal relaxation, described by time constant T_2), introduction of tissue in B0 will lead to small variations in magnetic field

as a function of local magnetic susceptibility, while the longitudinal magnetisation returns to its original size (*i.e.*, longitudinal relaxation, described by time constant T_1) — see Figure (2.1D/E). This process creates a signal that can be measured by a receiver coil contained in the MR machine. A third property, T_2^*, describes the combined effect of local inhomogeneities (for example caused by field distortions near blood vessels which contain deoxyhemoglobin) and T_2 in the magnetic field. The MRI scanner can be programmed to emphasise the effects of those inhomogeneities, and this forms the foundation of blood oxygenation level dependent (BOLD) functional MRI, as discussed in the next section.

By altering how often an RF pulse is applied and the echo time (TE; that is, the time between the onset of the RF excitation pulse and the highest signal induced in the coil), we can select the characteristic that we want to emphasise in the tissues (Figure 2.1F). The measured signal is then given by $M_0(1-e^{-TR/T_1})e^{-TE/T_2^{(*)}}$, where T_1 and T_2 are tissue properties, which allows representing boundaries between different brain tissues (namely gray and white matter, and cerebrospinal fluid, in the case of brain imaging).

In addition to tissue localisation, information on spatial field inhomogeneities can be acquired using an MR machine, which may be an important asset when combining anatomical data with the functional images that we describe in the next section. This is because areas of boundaries between tissues are particularly susceptible to causing local field inhomogeneities which can hamper the signal acquisition. As described earlier in this section, the spatial localisation of the acquired signal is encoded by magnetic field gradients positioned in three dimensions. Local field inhomogeneities which interfere with the deliberate imaging gradients may thus cause the local field of view to be miscalculated, which leads to spatial distortion and causes changes in signal intensity. Luckily, if a field-map scan is acquired, it can be used in image post-processing steps to correct the occasional signal distortion. This can be done by acquiring two regular T_2^*-weighted images acquired with different TE times, such that they produce different weightings. The phase-difference of the resulting signal from each voxel is linked to the 3 dimensional field variation in this voxel, which means post-processing algorithms are able to work out by how much each voxel needs to be "un-distorted" based on its field variation. While other methods exist for the acquisition of a field-map, this is the approach used for the all studies presented in this thesis.

2.1.1 Functional magnetic resonance imaging (fMRI)

The previous section provides an overview of the physical principles that enable the acquisition of a full image representing a brain volume, and is how the anatomical images used in this work are obtained — the main goal now is to obtain images that reflect brain function across time. To this end, the steps described in Section 2.1 are repeated every time a new image needs to be obtained, and the time between the acquisition of two volumes is called Repetition Time (TR). Typical fMRI studies use a TR of 2s but, especially more recently, this number has fallen to a bellow-second scale. By adjusting some of the parameters mentioned in the previous

section, a sequence of images can be acquired that reflect brain function.

After a number of preprocessing steps, which typically consist of motion correction; brain segmentation; co-registration; and spatial smoothing, fMRI images can be used to study intrinsic brain activity (resting-state fMRI) or brain responses to different stimuli (task-based fMRI). The results of brain activity investigations are usually shown in the form of maps that illustrate regions that activate or deactivate in a certain context. Since its beginning almost 30 years ago, fMRI has enabled a myriad of studies that greatly improved our understanding of the brain, as discussed in the next sections.

Interaction with physiology: Functional brain imaging is possible thanks to the balance between energy needs from busy brain tissues and the blood flow that supplies those regions, which was discovered in the late 80's when Ogawa et al. (1990) found that the blood's oxygenation level can be informative of cerebral activity.

Active neurons require more oxygen and glucose to fuel its ion pumps than inactive cells. Those are supplied thanks to a link between neuronal activity and the heamodynamic response, called *neurovascular coupling*. Most of the brain tissues are diamagnetic — that is, they are repelled by the magnetic field. Haemoglobin, however, has two states: it is diamagnetic when oxygenated, but strongly paramagnetic (attracted by the magnetic field) when deoxygenated, as the release of oxygen from the molecule exposes the iron atoms' unpaired electrons. The latter creates inhomogeneities in (B_0) and affects T_2^* relaxation. Thanks to this phenomenon, the measured blood oxygenation level dependent (BOLD) signals reflect the magnetic field's inhomogeneities caused by these changes in oxygen levels in the blood. fMRI signals are, therefore, an *indirect* measure of neuronal activity via its haemodynamic correlate. Several hypotheses have been proposed to explain the underlying mechanisms of neurovascular coupling (Attwell et al., 2011), but the exact nature of this complex link remains largely unknown (Logothetis and Wandell, 2004; Logothetis, 2008). However, the BOLD response has been shown to be proportional to neuronal firing rates or population-level activity both using electrode implants (Heeger et al., 2000), optogenetics (Lee et al., 2010; Kahn et al., 2011) and a combination of calcium imaging and two-photon microscopy (Ma et al., 2016; O'Herron et al., 2016), among others. Figures 2.2 A and B illustrate the relationship between the haemodynamic response and neuronal activity after direct stimulation or under spontaneous conditions, respectively.

It is important to note that the haemodynamic response (HRF) which enables BOLD signals to be measured is not instantaneous. Instead, it can be seen as a temporally blurred version of neural activity, due to the time course of neurovascular coupling, and peak response typically appears after a 5—6 s lag (Menon, 2001; Logothetis et al., 2001). The HRF is usually described by a combination of two gamma functions, peaking 6 s after stimulus delivery, followed by a negative overshoot peaking at 16 s, until it returns to baseline 20–25 s post-stimulus, with a peak–undershoot amplitude-ratio of 6 (see Figure Figures 2.2C). These numbers were

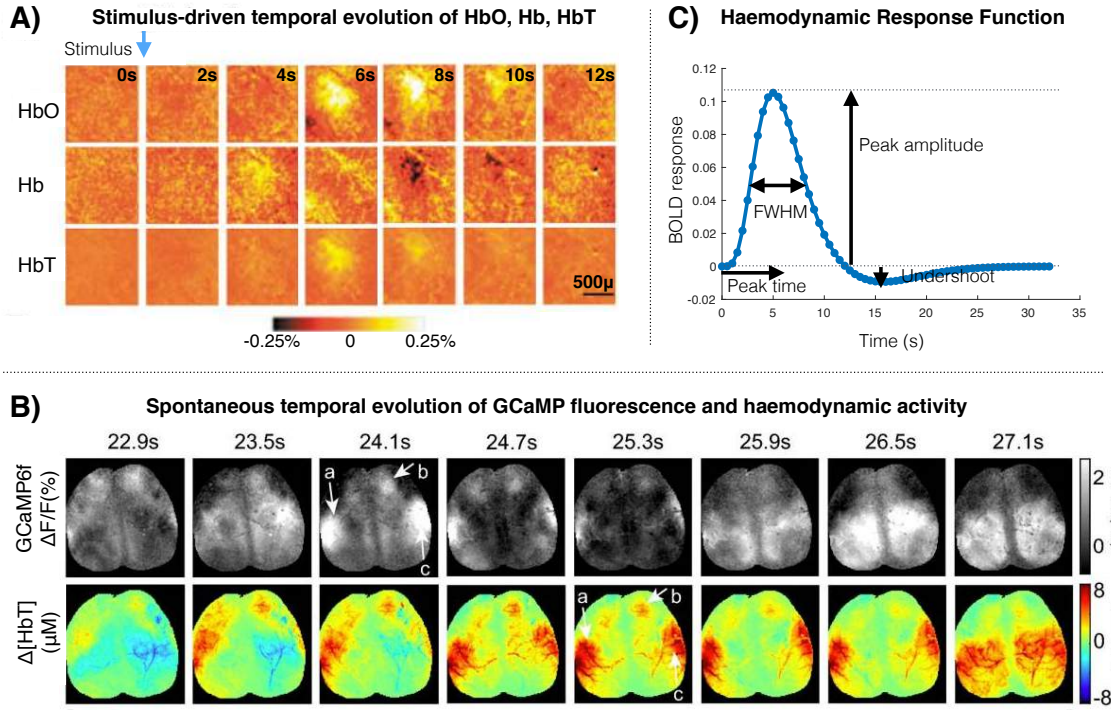

Figure 2.2 – **The haemodynamic response and its link to neuronal activity.** A) Stimulus-driven spontaneous temporal evolution of oxygenated haemoglobin (HbO), deoxyhaemoglobin (Hb) and total haemoglobin (HbT, calculated as the sum of Hb and HbO) in the rat somatosensory cortex. Each image represents the average individual frame of 990 trials. The Hb and HbO signals are expressed in percent change relative to baseline concentration (40 and 60 M, respectively). Image adapted with permission from Devor et al. (2003). In this study, electrophysiological recordings of local field potential (LFP) and multiple unit activity (MUA) were performed simultaneously to the haemoglobin measurements, revealing a strong non-linear relationship between the hemodynamic response and electrophysiological measures. B) Simultaneous imaging of *(top)* wide-field imaging of GCaMP fluorescence (600 ms window average) and *(bottom)* hemodynamic activity in the awake mouse brain without stimulation, showing comparable spatial patterns (a—c) with a time delay. Image taken with permission from Ma et al. (2016). C) The so-called *canonical* haemodynamic response function based on parameters reported by Friston et al. (1998).

obtained from a principal component analysis (PCA) of the data from Friston et al. (1998), and are still widely used today. In general, it can be seen as a delayed and smoothed version of the underpinning neuronal activity. This is key for the steps that follow data acquisition, as accurately modeling the evoked haemodynamic response to neural events plays a crucial role fMRI data analysis (Lindquist et al., 2009).

2.1.2 Task-based fMRI in the study of brain function

A popular experimental design in functional studies is task-based fMRI (tb-fMRI). In this paradigm, participants are asked to repeatedly perform a specific task for a certain time (often referred to as a "block"), followed by a contrasting block (*e.g.*, a "resting" period). By probing into BOLD signal differences between these conditions, it becomes then possible to identify parts of the brain which selectively activate or de-activate according to the task (Friston et al., 1995).

2.1.2.1 Static analysis of task-Based fMRI

Task-based paradigms (as opposed to resting-state ones, see Section 2.1.3) rely on prior knowledge about external stimuli that may be driving brain activity. The most traditionally used approach to tb-fMRI analysis is the General Linear Model (GLM). This method examines the temporal synchrony between predicted responses and a voxel's time series by modeling the latter as a linear combination of several factors that contribute to the signal (Friston et al., 1995). In that way, the GLM is more flexible than, for example, a simple correlation analysis, in that it allows the inclusion as model factors of several experimental conditions, as well as of other known (*e.g.*, motion parameters) or possible (*e.g.*, behavioural information, subjects' age, etc.) sources of variability. Typically, a comparison between task response is then done by subtracting conditions (*e.g.*, task A - task B), or a factorial analysis is performed when the experimental design includes more than one factor (*e.g.*, cognitive process). The statistical significance of the GLM's results then reflects how well an experimental observation is fit by the model (Worsley and Friston, 1995). One of the drawbacks of this approach is that, although it reveals the magnitude of an effect, it does not provide information about its duration, nor is it possible to capture inter-subject differences in timing (Robinson et al., 2009). Nonetheless, this has been one of the most widely used methods in fMRI analysis with several applications and extensions being proposed (Dale, 1999; Glover, 1999; Goldman et al., 2000; Laufs et al., 2003).

From all GLM extensions, Psychophysiological Interaction (PPI) analysis is of particular interest here, as it concerns *modulation* of functional connectivity. Originally proposed by Friston et al. in 1997, PPI determines which voxels enhance their relationship with a user-defined seed in a particular context (*i.e.*, during a specific behavioural task). This is achieved by including at least three regressors in the model: 1) the time course of the seed; 2) the task time course; and 3) the interaction regressor, calculated as an element-by-element multiplication of the seed's activity and the task time courses. Including the first two guarantees that the variance explained by the PPI is over and above that explained by the task or by physiological correlations' main effects (O'Reilly et al., 2012). In that sense, voxels whose activity is well described by the interaction regressor (also called the PPI regressor) are those that have a stronger relationship with the seed during the task of interest.

An alternative to these confirmatory analyses is to employ exploratory methods, which do

not rely on prior knowledge. Principal component analysis, for example, can be used for dimensionality reduction by mapping the data into a reduced space that maximises the variance, and is often used as a first step in the fMRI analysis pipeline (Zhong et al., 2009). Of note, partial least squares (PLS) analysis (Randal and Lobaugh, 2004) maximises the covariance between two modalities, making it possible to find links between multi-modal data (*i.e.*, fMRI and behavioural data). By analysing task-related brain metrics in conjunction with behavioural or clinical outcomes, for example, this method makes it possible to characterise the neurological substrate of cognitive functions (Roberts et al., 2017).

2.1.3 Resting-state fMRI in the study of brain function

In the mid 90's, (Biswal et al., 1995) showed in an original study that even at rest, activity in the motor cortex is remarkably structured and bilaterally coherent, despite the absence of an explicit motor task. Since then, resting-state functional magnetic resonance imaging (rs-fMRI) has become a widely used tool to investigate temporal fluctuations in neuronal activity by looking into BOLD signals across the brain (Damoiseaux et al., 2006; Fox et al., 2007). Thanks to the absence of goal-directed stimulation or activity, this paradigm is particularly well suited for studying and comparing brain function between populations who might respond to task instructions with different levels of cognitive ability or attention such as clinical; ageing; or very young cohorts, because it has minimal compliance requirements. Additionally, provided that the same image acquisition parameters are used, this allows data recorded across multiple research centers to be pooled or compared, given that there is no variability task demands. These results are comparable even when the conditions slightly differ across studies (*e.g.*, eyes closed; open; with or without fixation; etc.), so those can be appropriately chosen according to the comfort of the targeted population (Soares et al., 2016). Furthermore, this data can be acquired in a relatively short time, with sessions of 5–7 min yielding a reasonable trade-off between acquisition time and the robustness of results in adults (Van Dijk et al., 2010; Whitlow et al., 2011). In young children, 5.5 min has been shown to be an acceptable duration, to avoid head motion due to their becoming too restless (White et al., 2014a).

In the preterm population, rs-fMRI has often been used in the context of functional connectivity (FC) analyses (see Section 2.1.3.1), measuring temporal correlations between the activity of different brain regions or networks (Lordier et al., 2019). Thanks to these studies, it is now known that alterations in FC may begin even before birth (Thomason et al., 2017) and often last through adolescence (Wehrle et al., 2018) into adult life (Papini et al., 2016).

2.1.3.1 Static analysis of Resting-State fMRI

Resting-state paradigms rely on intrinsic changes in brain activity for which no prior information is available, and so the most widely adopted approach to analyse these data has been to investigate temporal relationships between the spontaneous activity in different brain regions. Typically, this is achieved by looking into correlations between these time series over the entire

duration of the scanning session. This method generally known in the literature as static functional connectivity (sFC), as it assumes those relationships are stable across time. It has been used to uncover correlations between all pairs of regions of interest (ROIs), unveiling the so-called functional connectome, or in seed-based analyses, to find correlation maps which illustrate all regions whose activity correlates with a chosen ROI (Lee et al., 2013; Smitha et al., 2017).

These initial approaches led to the discovery that some of these relationships are recurrent and robust, such that several resting-state networks (RSNs) can be observed across subjects and experiments. A popular way to look into the static connectivity between these networks is independent component analysis (Mckeown et al., 1998; Calhoun et al., 2001), a data-driven approach based on blind-source separation. It assumes that the signal from whole-brain voxels can be decomposed into groups of spatially and/or temporally independent signals, and these components can then be used to study within– or between–network correlations. Figure 2.3 illustrates some of the networks that have been widely reproduced in different studies.

In an alternative method for brain network analysis, rs-fMRI can be seen in terms of graphs, where brain regions represent nodes and high correlation values represent edges (Rubinov and Sporns, 2010; Farahani et al., 2019). The application of graph theory concepts in FC analysis reveals complex aspects of connectivity using graph parameters (*e.g.*, nodal degrees, average path length, clustering coefficient, etc.) which complement traditional analysis methods. These metrics may then be used to shed light on the brain's ability to rapidly combine information from distributed regions, its resilience to external perturbations, among others.

2.1.4 A dynamic approach to fMRI analysis

2.1.4.1 Dynamic analysis of Resting-State fMRI

Although static methods are still the most widely-adopted approach for resting-state fMRI analysis, over the past decade a growing body of research has shown that FC is actually dynamic over time (Chang and Glover, 2010). Importantly, these time-varying properties of brain activity contain invaluable information to understand brain function (Hutchison et al., 2013; Christoff et al., 2016).

An initial parameter of brain dynamics is BOLD signal variability, usually calculated as the standard deviation of the BOLD time series at each voxel (McIntosh et al., 2010). Often overlooked as noise in traditional analyses, over the past decade it has been increasingly thought of as a potentially vital feature of brain function (Garrett et al., 2010), with higher variability seeming relevant to guarantee systems' stability and dynamic range (Deco et al., 2011) as well as development and cognition in healthy (Garrett et al., 2013a) and clinical (Zöller et al., 2017; Nomi et al., 2018; Easson and McIntosh, 2019) populations.

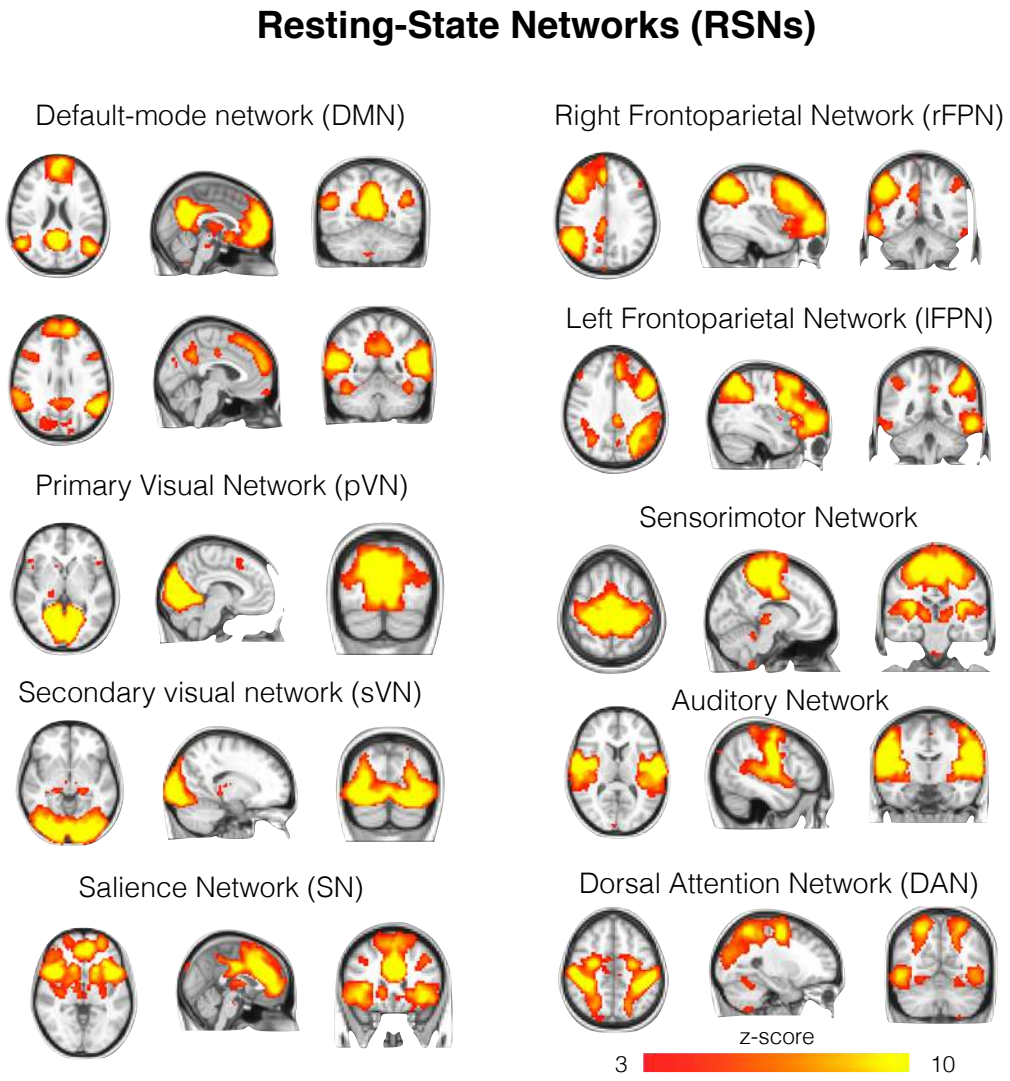

Figure 2.3 – **The resting-state networks.** Some networks have been repeatedly reproduced in resting-state experiments. The ones illustrated above were obtained from an independent component analysis using data from 35 subjects. Figure adapted from Akbar et al. (2016)

Besides the dynamics of brain activity, changes in the *relationships* between different brain regions over time have also been increasingly found to be relevant, spawning the field now known as dynamic functional connectivity (Hutchison et al., 2013; Preti et al., 2017). The most popular approach quickly became using a sliding window, where the FC is typically computed over subsequent, temporally shifted windows to capture connectivity fluctuations (Chang and Glover, 2010; Sakoğlu et al., 2010; Kucyi and Davis, 2014). This yields a series of FC matrices which contain the time courses of the fluctuation of pairwise correlations, and further analysis can then follow to detect dynamic brain states using a variety of additional methods such as

principal component analysis (Leonardi et al., 2013), hidden Markov models (Vidaurre et al., 2017), etc. Despite its prominence, this framework remains limited by its dependence on window parameters, its inherently lowered temporal resolution Leonardi and Van De Ville (2015), and its sensitivity to outliers since all time points within a window are given equal importance Lindquist et al. (2014).

An alternative approach to sliding windows focuses on performing a point process analysis (PPA) by looking into subsets of single fMRI frames instead of focusing on entire time courses. This is possible because, when averaged, frames where a selected seed region is highly active reveal a pattern containing all regions that co-activate with that ROI (Tagliazucchi et al., 2012). This can be seen as a computationally efficient proxy of a seed-based static FC described in section 2.1.3.1. As described above, however, FC patterns are known to be variable over time, and so a natural development of the PPA approach is to temporally cluster these selected frames into co-activation patterns (CAPs; Liu et al., 2018). Each CAP is then a dynamic building block of the overall connectivity map, each varying in duration, number of appearances, etc. Going a step further, innovation-driven CAPs (iCAPs) cluster frames based not on similarity between patterns of *activation*, but between patterns of activation *changes* (Karahanoglu and Van De Ville, 2015). The interest here lies in finding groups of regions whose activation change (activate or deactivate) simultaneously, allowing for temporal and spatial overlaps.

2.1.4.2 Dynamic analysis of task-Based fMRI

Similar to the resting state, activation time courses upon the execution of a task are also known to show exquisite complexity that cannot be captured by standard stationary approaches (Gonzalez-Castillo and Bandettini, 2018). Although dynamic FC has increasingly become a natural avenue for resting-state research (Preti et al., 2017), task-based experiments have not yet fully benefited from this approach: only a few studies so far have explicitly investigated task-related dFC using fMRI Braun et al. (2015); Di et al. (2015); Simony et al. (2016). Di et al. (2015), for example, used sliding windows to calculate the Time-Varying Correlation Coefficient (TVCC) between different regions' activities and found substantial fluctuations in FC patterns during stimulation periods. The method allowed them to observe a decrease in FC between visual areas shortly after stimulation onset, followed by a return to baseline. The disadvantages of this approach are twofold: firstly, the TVCC estimation is, as expected, dependent on the choice of window size; and secondly, to account for the low signal-to-noise ratio of the BOLD signal, the technique involves averaging each subject's experimental blocks, which may be at the expense of relevant variability in FC dynamics. However, this study provides additional evidence that explicitly tracking connectivity pattern transients is paramount to advance our understanding of how different brain areas dynamically communicate in a task context. As expected from their importance in resting state, time-varying properties of brain activity during task performance have been recently shown to also contain relevant information to understand cognition (Fong et al., 2019). Taken together, the above corroborate the idea that moment-to-moment FC dynamics contain relevant information about behaviour, and thus

promise to hold considerable translational value (Gonzalez-Castillo and Bandettini, 2018).

2.2 Preterm birth

A birth is defined as preterm (PT) when delivery occurs after less than 37 completed gestational weeks, in contrast to the expected duration of 40 weeks, on average, in a healthy pregnancy. This can be further characterised as a moderate to late PT (32—36 weeks), very PT (28—31 weeks), or extremely PT (≤ 27 weeks). These conditions have been associated with a wide range of behavioural, cognitive and neuropsychological difficulties that have been identified at various stages in life. In the sections below, I provide an overview of the challenges brought by preterm birth to the child, their family, and society as a whole. I then explain the problems preterm-born individuals are at higher risk of facing later in life, the body of knowledge that has been build to date around the neural mechanisms for their clinical problems, and identify a gap in the literature regarding investigations of dynamic brain function in this population, which this thesis aims to fill.

2.2.1 The global challenge of prematurity

Every year, an estimated 15 million babies are born too soon around the world, representing 5–18% of all births depending on the country. Especially in the more extreme cases, complications related to an early birth are the leading cause of death among children up to 5 years old, and these complications are responsible for the loss of approximately 1 million infants each year (Liu et al., 2016). Although PT birth may be caused by various reasons and several well known biological pathways leading to it exist (Behrman and Butler, 2007), the majority of the cases are "idiopathic", meaning that it happens spontaneously and without an obvious cause. Importantly, the number of PT births has been on the rise over the past 20 years (Costeloe et al., 2012), possibly as a consequence of an increase in maternal age and changes in obstetric practices. Additionally, with the continuous improvements in medical treatment, the rates of survival have also increased across the world, meaning that more and more children will live with the effects of prematurity each year. Besides the consequences to the children's health and behaviour, this increase is expected to escalate the economic impact of PT birth not only in the short term (*i.e.,* immediate medical care), but also in the longer term. In fact, according to the Institute of Medicine of the National Academy of Sciences, special education services related with a higher prevalence of disabling conditions in PT-born children cost U$1.1 billion yearly in the United States alone, while the lost household and labour market productivity had an impact of approximately U$5.7 billion (Behrman and Butler, 2007).

2.2.2 Behavioural consequences of preterm birth

Preterm birth puts children at a considerably higher risk of developing a broad range of cognitive deficits (Brydges et al., 2018; Twilhaar et al., 2018). By school age, up to 50% of these

children develop cognitive, language, or socio-emotional disabilities that are likely linked to neurological abnormalities starting before birth, lasting through life and into adulthood (Gozzo et al., 2009; Chaminade et al., 2013; Moiseev et al., 2015; Hornman et al., 2016; Thomason et al., 2017; Burnett et al., 2018).

A meta-analysis of cognitive outcomes in more than 7000 children and teenagers born very preterm and aged 5–20 years old found that this population showed significant deficits in intelligence Twilhaar et al. (2018). A similar study by Brydges et al. (2018), involving more than 6000 individuals, showed that they scored significantly lower on intelligence tests; measures of executive functioning; and processing speed, as compared to their term born peers across a wide range of ages (4–17). This study found no association between the children's age at assessment and cognitive impairment, indicating that very preterm born children fail to catch up with term born ones throughout childhood and adolescence. In that sense, it seems that the differences between the two groups are due to a deficit in PT children, rather than a delay (Brydges et al., 2018). This is in line with (Linsell et al., 2018)'s study, which found that cognitive function did not recover or deteriorate between infancy and adulthood in extremely preterm individuals, and explain why Doyle and Anderson (2010) find long-lasting effects of extremely preterm birth in an adult cohort. Importantly, socio-economic status at birth has been shown to affect IQ scores in adults born very preterm (Breeman et al., 2017), and to modify the relationship between early-life events and neurodevelopmental outcomes in preterm born children. Further understanding these complex relationships may shed light into potential avenues for promoting improved outcomes for infants at higher risk of neurodevelopmental issues (Benavente-Fernández et al., 2020).

Besides difficulties in executive functions, children who were born prematurely are also at a higher risk for socio-emotional disabilities (Zmyj et al., 2017), with impaired interactions being present in relationships with family, teachers and friends (Twilhaar et al., 2019). In particular, PTB children are less likely to initiate and respond to peers' efforts to participate in joint attention (Zmyj et al., 2017), which may aggravate later social cognition impairments and thus hinder social interaction skills. Whether these differences in social competences are a product of faulty or delayed maturation remains a topic for debate: some studies point towards the former hypothesis, since these effects have also been found in individuals through adolescence (Healy et al., 2013; Saigal et al., 2016); while others put it down to a maturational lag, with findings that PTB children catch up with their full term peers by the age of 5 (Witt et al., 2018). These inconsistencies emphasise the complexity of the effects of preterm birth and the importance of further characterising the link between brain and behaviour.

The most recent research indicates cognitive control impairment as a central basis for social problems in PTB adolescents (Twilhaar et al., 2019). This finding further highlights the importance of understanding the neural substrate of cognitive disabilities in this population, with a view to detecting potential targets for early intervention.

2.2.3 Consequences of preterm birth on brain structure

To identify potential interventions that would be able to recover some of the behavioural difficulties mentioned above it is important to, first, understand how the brain is affected by preterm birth. The brain undergoes significant growth and development in the last months of gestation, which naturally puts preterm-born infants at a considerably greater risk for abnormal neurodevelopment. A great body of research has thus been dedicated to understanding the consequences of prematurity on brain structure.

The most common pathology affecting babies born very preterm is the encephalopathy of prematurity, which is characterised by a subtle brain injury followed by disrupted brain growth and the development of internal (such as basal ganglia and thalamus) and external (cerebral cortex) structures (Kunz et al., 2014). In addition, prematurity has been associated with reduced white matter volume and myelination, decreased cortical grey matter as well as lower hippocampal, basal ganglia and cerebellar volume that lasts through childhood and adolescence. Moreover, these alterations have been linked to poorer neurodevelopmental (Inder et al., 2005; Ment et al., 2009; Nosarti, 2013; Padilla et al., 2015) and educational (Cheong et al., 2013) performance across childhood.

Recently, studies have investigated regional volume changes and how they relate to specific neuropsychological consequences of preterm birth. Reduced dorsal prefrontal cortex (dPFC) volume was found to be linked to children's attention and hyperactivity problems (Bora et al., 2014). In adolescents, volume changes in the fusiform and orbitofrontal cortices have been associated with socialisation problems (Healy et al., 2013), and autism (Johnson and Marlow, 2014). A reduction in hippocampal volume has also been shown to correlate with memory deficits in preterm children. Taken together, these studies emphasise the vulnerability of the brain after preterm birth.

Most neuroimaging studies involving preterm young adolescents rely on structural features, relating brain volumes or microstructure to clinical and cognitive outcomes (Hüning et al., 2018; Groeschel et al., 2019; Boardman et al., 2020). While these structural studies provide relevant insights into brain injuries that are associated with prematurity and potentially underlie neurocognitive dysfunction, they cannot provide information on brain activation driven by specific demands. Studies that investigate brain function are thus necessary to provide complementary information on the consequences of preterm birth, as discussed in the next section.

2.2.4 Consequences of preterm birth on brain function

With the wide range of behavioural alterations related to PT birth, it is no surprise that the brain may be deemed more vulnerable to dysfunction in children who are born too early. A recent meta-analysis involving more than sixty-four thousand children found that prematurity of any degree affects neurodevelopment, and that these adverse effects persist at various

follow up stages (Allotey et al., 2018).

Several studies have investigated structural differences in preterm-born children (Huppi et al., 1998; Brown et al., 2014; Kersbergen et al., 2014; Kostović Srzentić et al., 2019), but functional activation and connectivity has only been popularised in this population over the last decade, with studies primarily relying on resting-state static analysis. Fransson et al. (2007) were the first to show the presence of resting-state networks (RSNs) in the preterm, which were later found to be similar to those found in adults (Doria et al., 2010). Notably, different RSNs formed at different rates during gestation. Many studies identified an incomplete set of RSNs in preterm subjects at term-equivalent age, although not all compared them to term-born controls (Lin et al., 2008; Fransson et al., 2007, 2011; Gao et al., 2015; Lordier et al., 2019). Additionally, alterations in the functional connectivity between and within RSNs were found in infants (Gozdas et al., 2018) and adolescents (Wehrle et al., 2018) born very preterm , providing evidence for the long-lasting impact that very PT birth has on the organisation of the brain (Damaraju et al., 2010; White et al., 2014b; Johns et al., 2019).

Common to all of the studies mentioned above, was the stationary aspect of the analysis and the use of a resting-state approach. Given the high incidence of cognitive abnormalities in preterm born children at a later stage, the study of brain function under specific cognitive tasks in this cohort is highly desirable, albeit largely lacking at present.

2.2.5 Interventions for preterm newborns and children

Early interventions are usually implemented shortly after birth, often relying on improving the care-giving environment and with the goal of subsequently improving clinical outcomes. They typically involve the family, including following integrative programs such as the Newborn Individualized Developmental Care and Assessment Program (NIDCAP; Peters et al., 2009); the Infant Behavioral Assessment and Intervention Program (IBAIP; Van Hus et al., 2016); the Victorian Infant Brain Studies (VIBeS PLus; Spittle et al., 2018); or using Kangaroo Mother Care position and method (Peters et al., 2009). A meta-analysis of these family-centred interventions has shown that they have a positive effect on cognition in children born very preterm, accompanied by a positive but weaker impact on motor abilities, and inconclusive results on language (Ferreira et al., 2020). Importantly, although these interventions have been beneficial, the exact environmental factors responsible for enhancing brain development remain largely unknown.

Socio-emotional and executive function skills are still in plain development during childhood and adolescence, suggesting that this age may still be within the intervention window. There has been growing evidence that children's capacity to understand emotions affects their social adjustment. Those who are more sensitive to emotional cues tend to have better relationships with friends and adults, are less likely to present behavioural problems, are more inclined to solve conflicts, and tend to perform better at school (Denham, 2006; Domitrovich et al., 2007; Harrington et al., 2020). Socio-emotional training has been shown to reduce

aggressive behaviour and to improve both emotion recognition and executive functions in typically developing children and children from disadvantaged families, providing further evidence for the link between different cognitive abilities (Pons et al., 2002; Sprung et al., 2015; Grazzani et al., 2018; de Mooij et al., 2020). In recent years, mindfulness meditation training has emerged as a potential tool to help young populations manage a wide variety of symptoms including disruptive behaviour (Perry-Parrish et al., 2016). A study involving typically developing children at 11 years old showed that 8 weeks of mindfulness training already has the potential to improve attentional self-regulation (Felver et al., 2017). Another, found that meditation programs can enhance cognitive and social-emotional development in young populations (Schonert-Reichl et al., 2015). Taken together, these results further suggest a link between these cognitive domains and that mindfulness meditation may be an avenue for intervention in clinical populations. In fact, several studies have investigated the benefits of a meditation-based intervention for children with attention deficit hyperactivity disorder, but their varying methodological quality means that so far no clinical recommendation can be made and further, well-designed analyses, must be performed (Evans et al., 2018).

Crucially, a recent neuroimaging study involving typically developing, fullterm-born, early adolescents found that mindfulness meditation related to dynamic features of brain function and network connectivity over time, as opposed to static characteristics of neural activation(Marusak et al., 2018). This brain function trait remains largely unexplored in preterm-born early adolescents, which highlights the importance of this thesis to fill this gap.

2.3 FMRI in the study of prematurity

Thanks to recent advances in the field, fMRI has been increasingly used to characterise healthy brain function at different stages in life (Power et al., 2010). One important extension of these investigations is to understand alterations related to atypical neurodevelopment. This may lead to interventions aimed at preventing, reverting or minimising the effects of altered brain function.

FMRI is particularly well-suited to investigate paediatric populations, especially since robust measures of functional activation and connectivity can be obtained from short scanning sessions. It has been employed to uncover atypical connectivity patterns and their links to a wide range of neurodevelopmental disabilities. For instance, this technique has exposed altered brain responses in regions underlying executive functions in preterm-born children in frontal (Réveillon et al., 2013; Mürner-Lavanchy et al., 2014) and temporal areas (Kwon et al., 2014; Wilke et al., 2014) which were linked to impaired language performance at age 14–15 (Wilke et al., 2014).

Most of the studies to date, however, employ analytical methods that assume brain function to be static — that is, they investigate averaged brain activity across the entire experiment. Given that the brain is known to be highly dynamic, there is an urgent need to know how prematurity affects the dynamic features of neural function. The aim of this thesis is thus to fill this gap.

2.3.1 Challenges and considerations for paediatric MRI studies

MRI studies often require that participants lay completely still for lengthy periods of time, especially when the experimental protocol includes several imaging modalities or task paradigms. Head movement is one of the most intractable and potentially harming confounds in this type of data, causing misalignment of subsequent frames and, as a consequence, BOLD signal or structural estimates that do not correspond to true effects (Friston et al., 1996; Siegel et al., 2017). Compared to adults, children have decreased inhibitory control (Bedard et al., 2002), and may thus find it harder to remain still during experiments, particularly given the distracting environment of scanning sessions (Greene et al., 2016). Unsurprisingly, then, children and adolescents tend to present much higher total head motion than adult participants (Satterthwaite et al., 2013), making the data potentially more susceptible to results that do not reflect reality (Power et al., 2012). Motion scrubbing has become and increasingly accepted — and stringent — way of dealing with this type of artefact over recent years (Power et al., 2014; Laumann et al., 2016), but when the data is highly affected by motion it leads to significant data loss. The best approach is, therefore, to avoid movement as much as possible.

Unsurprisingly, head motion in fMRI experiments involving children tends to increase with the duration of experiments both in terms of run and session time (Engelhardt et al., 2017). While taking breaks between sessions has been suggested as a way to reduce run length-related artefacts, a trade-off must be found between implementing these and keeping the total recording time as short as possible (Meissner et al., 2019). Another design-related consideration that influences head motion in child studies is the experimental paradigm (Yuan et al., 2009). Children are less likely to move when they have something to pay attention to, such as in task-based experiments, as compared to resting-state ones (Engelhardt et al., 2017). Given the above, a potentially reasonable trade-off for protocols that include both types of experimental paradigms would be to perform the resting-state session as early as possible, and task-based sessions in sequence, all while trying to keep the total scanning time as short as possible.

An approach that has been increasingly agreed as a measure to reduce head motion or dropouts due to scanner-anxiety is to familiarise children with the scan environment as much as possible before the scan itself takes place (Greene et al., 2016), to help them feel safe and relaxed. A simple strategy is to manage the participants' expectations by showing a child-friendly information video describing the MRI procedure (Thomason, 2009). In addition, requests for the child to remain still may be done in a fun way, such as suggesting they are playing "Statue". Mock scanners can also be used as a way to reduce scanning time, giving the child the chance to live through the experiment in advance, either through commercial mock scanners or improvised versions (de Bie et al., 2010; Barnea-Goraly et al., 2014). Furthermore, implementing training sessions to teach participants what levels of movement are acceptable or not may also improve data quality. Many children simply do not understand to what degree they are moving or just forget having been asked to stay still during the scan, so receiving some form of feedback — be it verbal or otherwise — helps them understand what it really means to remain immobile (de Bie et al., 2010). Finally, decorating the scanner with child-friendly,

colourful stickers to make it look less like a medical device has been shown to be a simple yet efficient measure (Nordahl et al., 2016). Figure 2.4 shows the scanner used at Campus Biotech, in Geneva, Switzerland, where the data for the studies presented in this thesis were collected.

Figure 2.4 – **The MRI machine at Campus Biotech, decorated with stickers to make the environment more child-friendly.** Approaches to familiarise children with the scanning environment have been shown to benefit data acquisition, resulting in better quality data that is less affected by motion-related artefacts.

Despite the increasing application of fMRI studies in infants, for example, the deployment and interpretation of such investigations in neonatal populations also remain a challenge. This is partly due to our still relatively limited understanding of the effects of brain development on the BOLD signal. It has been shown that the haemodynamic response changes during development, a phenomenon probably related to differences in neurovascular coupling at each stage (Arichi et al., 2012). Furthermore, the accuracy of task-based fMRI studies highly depends on the choice of HRF models: it has been shown that even small amounts of inaccuracy in HRF modeling may cause significant loss in validity and power (Lindquist and Wager, 2007; Loh et al., 2008). While Arichi et al. (2012) have shown differences in the response elicited in the somatosensory cortex of adults, termborn, and preterm children, age-appropriate HRF parameters (as well as its inter-region variability) are still to be firmly established.

Existing brain templates and atlases are typically based on adult brains and thus not optimised for spatial normalization and parcellation of infant data and small children. Using them might thus reduce the accuracy of any quantitative analysis and generate mislocalisations in some cases. While several volumetric atlases have been proposed (Habas et al., 2010; Kazemi et al., 2007; Shi et al., 2014), no approach has been widely agreed upon since most obscure important spatial relationships among nearby locations in the cortex by blurring key structures, potentially leading to less accurate results (Li et al., 2016). Until spatial locations are well defined in the infant brain, analytical methods that do not rely on atlasing are more suitable for this population. For the young adolescents whose data were analysed in this thesis, we used a Montreal Neuroimaging Institute (MNI) template based on adult brains, as this has been consistently and successfully used in children above 7 years old (Ashburber and Friston, 1998; Burgund et al., 2002).

Finally, a recent review by Smid et al. (2016) has highlighted that, although most of the global preterm birth disease burden is on the shoulders of low and middle income countries (LMICs), only a very limited amount of research evidence for its prevention or treatment comes from studies in these settings. Instead, most of the research available on this population comes from high income countries and may thus offer an incomplete view of the global issue of preterm birth. Primary research involving LMICs thus also remains urgently needed. Nonetheless, research carried out in developed countries such as this one may still bring us closer to the development of interventions for which the need for expensive equipment will prove less essential, and LMIC populations will also benefit from them.

3 BOLD signal variability and dynamic spontaneous brain function in the preterm-born

Methods for brain imaging analyses often rely on measuring and comparing the activity in certain areas of interest after averaging across the duration of the experiment. This means that any information about variations in the signal is completely ignored. Recently, however, the blood oxygenation level dependent (BOLD) signal's variability has been shown to yield important information on brain function that is linked to cognitive abilities (Garrett et al., 2013b). It is thought to reflect the brain's flexibility and ability to rearrange itself in different ways to allow increased complexity and cognitive range (Deco et al., 2011; McIntosh et al., 2010). It is thus a simple, but potentially valuable measure to investigate brain dynamics in clinical populations.

To the best of my knowledge, at the time of this publication no one has investigated BOLD signal variability in preterm-born populations. In this chapter, I look into the dynamic aspects of brain function in two ways: first, in terms of voxelwise BOLD signal variability and its relationship with gestational age, age at assessment, and an interaction between the two. Secondly,I perform a seed-based co-activation pattern (CAP) analysis focusing on the dorsal anterior cingulate cortex, an area previously found to be affected in studies involving preterm-born individuals (White et al., 2014b; Daamen et al., 2015; Lordier et al., 2019) and which was also highlighted in the analysis of BOLD variability. Through these two analyses I thus start from a global measure of brain dynamics, namely BOLD variability, and follow up with a dynamic analysis of functional brain states. This provides a broad overview of the dynamic aspects of spontaneous brain function in preterm-born young adolescents.

3.1 Journal Article: Altered BOLD variability and whole-brain dynamics development in preterm-born young adolescents

(Preprint of article to be submitted to NeuroImage)

Lorena G. A. Freitas[a,b,c], Vanessa Siffredi[a,c], Maria Chiara Liverani[c], Thomas A. W. Bolton[a,b], Cristina Borradori-Tolsa[c], Russia Ha-Vinh Leuchter[c], Petra S. Hüppi[c], Dimitri Van De Ville[a,b]

[a] Institute of Bioengineering, École Polytechnique Fédérale de Lausanne, Switzerland
[b] Department of Radiology and Medical Informatics, University of Geneva, Switzerland
[c] Division of Development and Growth, Department of Pediatrics, University of Geneva, Switzerland

Abstract

Preterm birth is one of the leading causes for neurodevelopmental complications in surviving infants, and has been associated with a wide range of behavioural and cognitive problems later in life. Functional magnetic resonance imaging (fMRI) studies have helped to uncover the underlying neural mechanisms of these difficulties, which is paramount to identify potential avenues for interventions that will improve the preterm population's clinical outcome. A growing body of research has shown links between dynamic aspects of brain function and cognition. In particular, the variability of the blood oxygenation level dependent (BOLD) signal from fMRI has been found to relate to cognitive abilities throughout life. During adolescence the brain, as well as cognitive and socio-emotional skills, are still in full blown development, making this age a potential window for intervention. Here, we investigate BOLD variability in preterm-born young adolescents as compared to a control group of age-matched fullterm-born individuals. Furthermore, we delve into dynamic functional connectivity in this population by deriving several co-activation patterns and looking into their relationship with age, gestational age, and their interaction using a partial least squares correlation approach. We find that the development of BOLD variability and whole-brain dynamics in preterm-born individuals follows a different trajectory compared to the fullterm-born.

Keywords: fMRI, Resting-state, BOLD variability, Co-activation Patterns (CAPs), Partial least squares correlation (PLSC), Preterm, Adolescence

3.1.1 Introduction

Preterm birth — birth before 37 full weeks of gestational age (GA) — affects an estimated 11.1% of all live births yearly (Blencowe et al., 2013), and is one of the predominant risk factors for neurodevelopmental disorders (Twilhaar et al., 2018). It has been associated with a wide range of impairments in cognitive functions spanning attention (Rommel et al., 2017), working

memory (Allotey et al., 2018), affective behaviour (Hornman et al., 2016), executive functions (Costa et al., 2017; Burnett et al., 2018), among others (Moreira et al., 2014; Allotey et al., 2018). Often unveiled only when children reach school age, some of these difficulties may persist throughout life (Anderson, 2014; Kajantie et al., 2019). Understanding the neurological underpinnings of these difficulties is thus crucial to identify potential interventions and establish critical periods to restore typical development (Wolke et al., 2019).

Resting-state functional magnetic resonance imaging (rs-fMRI) is a powerful tool to investigate temporal fluctuations in neuronal activity by looking into blood oxygenation level-dependent (BOLD) signals across the brain (Fox et al., 2007). Thanks to the absence of goal-directed stimulation or activity, this paradigm is particularly well suited for studying and comparing brain function between populations who might respond to task instructions with different levels of attention or understanding, because it has minimal compliance requirements. In the preterm population, resting-state fMRI has often been used in the context of functional connectivity (FC) analyses, measuring temporal correlations between the activity of different brain regions or networks (Lordier et al., 2019). Thanks to these studies, it is now known that alterations in FC may begin even before birth (Thomason et al., 2017) and last through adolescence (Wehrle et al., 2018) into adult life (Papini et al., 2016).

The limitation of typical FC analyses is that they assume that the inter-regional relationships are stationary, that is, they do not change over time. It has been shown, however, that FC fluctuates temporally in resting-state fMRI recordings (Chang and Glover, 2010), suggesting that methods based on averaging over long runs provide an incomplete picture of brain function. As a consequence, techniques that offer insight into the *dynamic* aspects of functional connectivity (dFC) have gained increasing interest in recent years (Preti et al., 2016). Of note, co-activation patterns (CAP) analysis (Liu et al., 2018) breaks correlation maps down into building blocks that repeatedly appear over time, providing a more accurate view into resting-state dynamics than the commonly used sliding-window methods. This approach has been recently used to reveal the nuances of dFC in health and disease (Kaiser et al., 2019). In preterm birth, however, dFC remains largely unexplored.

A related aspect of brain signals that has gained popularity in recent years is its variability. Commonly ignored in conventional rs-fMRI analysis, this feature is now thought to be a key component of healthy brain functioning, taking part in the formation of functional networks (Fuchs et al., 2007) and the exploration of different functional states (Ghosh et al., 2008; McIntosh et al., 2010). Moment-to-moment variations of BOLD signals have been found to be related to age and cognitive performance (Garrett et al., 2013a), and to be altered in several neuropsychiatric disorders, such as Autism Spectrum Disorder (ASD; Di Martino et al., 2014; Easson and McIntosh,2019), and Attention-Deficit/Hyperactivity Disorder (ADHD; Zang et al., 2007; Nomi et al., 2018), some of which with symptoms that overlap with the behavioural consequences of preterm birth. The above makes BOLD signal variability a promising avenue to delve into the neurological effects of preterm birth. To the best of our knowledge, this approach has not yet been explored in this population.

Partial least squares correlation (PLSC; McIntosh et al., 2004; Krishnan et al., 2011) is an effective approach to identify relationships between different sources of data, and has become increasingly popular as a method to reveal links between brain and clinical measures. For instance, it has been used to predict clinical outcomes of depression from resting-state FC (Yoshida et al., 2017); to investigate risk factors for psychosis in 21q11DS patients from dFC features (Zöller et al., 2019); to identify the neurocorrelates of impulsivity in ADHD patients (Barker et al., 2019); among others. Easson and McIntosh (2019) recently showed, using PLSC, that BOLD signal variability in certain brain regions correlated negatively with symptom severity in children and adolescents with ASD. In a similar study, (Nomi et al., 2018) revealed that brain signal variability in medial prefrontal areas comprising the default mode network was positively correlated with inattention and symptoms of ADHD. These studies have demonstrated the relevance of PLSC to expose relationships between brain function and clinical measures. Importantly, PLSC has a critical advantage over typical voxelwise brain analyses that use mass-univariate methods in that it it does not assume independence between the voxels, making it more aligned with brain function and with the data itself, since neighbouring voxels are smoothed as a preprocessing step. Also as a consequence of being a multivariate approach, PLSC is less affected by the problem of multiple comparisons.

The teenage years are a critical period for brain development. During adolescence, functional connections across the brain become more robust (Power et al., 2010), and the coordination between networks becomes more dynamic during task performance (Hutchison and Morton, 2015) and at rest (Marusak et al., 2017; Faghiri et al., 2018). Thus, diving into the subtleties of the dynamic features of brain function at this age has great potential to improve our understanding of the effects of preterm birth in neurodevelopment. In this work, we employ PLSC analysis to characterise links between brain function and age in preterm-born young adolescents compared to full-term controls. First, we investigate the relationship between BOLD signal variability and life course measures, namely gestational age at birth; age at assessment; and an interaction between the two. Since it has been found to be linked to cognition and development, and given that preterm-born children miss the third trimester in utero when cortical folding develops more rapidly, we hypothesise that BOLD variability is widely altered in this population. Finally, we explore how dynamic functional connectivity, measured by co-activation patterns, relates to the same life course measures.

3.1.2 Methods

3.1.2.1 Participants

Forty-two very preterm-born (VPT) and twenty-seven term-born children (TB) aged between 10 and 13 years old were recruited for this study. One TB subject, who wore dental braces, was excluded after data collection due to the strong signal distortions in the BOLD signals caused by the metallic device. Additionally, one participant from the TB group, as well as six subjects from the VPT group were excluded from data analyses due to high head-motion

artefacts as detailed in Section 3.1.2.4. The results discussed in this paper thus relate to the analysis of thirty-six VPT subjects (20 female; mean age = 12.13 ±1.2 years; mean gestational age = 28.95± 1.95 weeks) and twenty-five TB children (10 female; mean age = 12.05±1.01 years, mean gestational age = 39.68±1.65 weeks). None of the children included in either of the groups had any major disabilities, neurological or psychiatric disorders.

This study was approved by the Ethics Committee of the Canton of Geneva. Both the participants and their caregivers provided informed written consent. Each subject received a gift voucher of 100 Swiss francs upon concluding their participation in the study.

3.1.2.2 MRI acquisition

MRI data were acquired at Campus Biotech in Geneva, Switzerland, using a Siemens 3T Magnetom Prisma scanner. Structural T1-weighted MP-RAGE (Magnetization Prepared Rapid Gradient Echo) sequences were acquired using the following parameters: voxel size = 0.9 x 0.9 x 0.9 mm; repetition time (TR) = 2300 ms; echo time (TE) = 2.32 ms; inversion time (TI) = 900 ms; flip angle (FA) = 8°; field of view (Fov) = 240 mm. Functional images were T2*-weighted with a multislice gradient-echo-planar imaging (EPI) sequence of 64 slices; voxel size = 2 x 2 x 2 mm; TR = 720 ms; TE = 33 ms; Fov = 208 mm. Finally, a field map was acquired with TR = 627 ms; TE_1 = 5.19 ms; TE_2 = 7.65 ms; and FA = 60°.

3.1.2.3 MRI data preprocessing

Our data were preprocessed using SPM12 (Wellcome Department of Imaging Neuroscience, UCL, UK) in Matlab R2016a (The MathWorks, Inc., Natick, Massachusetts, United States). First, a field map was calculated for each participant from the additional stock double-echo field map sequence included in our MRI protocol (Jezzard and Balaban, 1995; Hutton et al., 2002) in order to correct signal distortions caused by field inhomogeneities around the air-filled sinuses (Gorno-Tempini et al., 2002). The fMRI images from each subject were then spatially realigned and unwarped to correct, respectively, for motion artefacts and potential geometric distortions. Thanks to the distortion correction of vulnerable brain regions for each participant, this unwarping step not only improves the co-registration between structural and functional images, but it also reduces the distortion variability across subjects during spatial normalization to a common space (Hutton et al., 2002; Togo et al., 2017). This solution has been successfully used in several adult (Togo et al., 2017) and children (Wozniak et al., 2011) studies. Functional images were then co-registered to structural images in subject space and smoothed with a Gaussian filter of full width at half maximum (FWHM) = 6 mm. In addition to these initial preprocessing steps, we controlled for nuisance confounding by regressing out the average white matter and cerebrospinal fluid signals, as well as the 24-Volterra expansion of the motion parameters obtained from the realignment step. The voxelwise time series were then filtered with a bandwidth of 0.01—0.15 Hz. To be able to perform a group level comparison, BOLD variability maps (see Section 3.1.2.5), as well as the smoothed fMRI images, were warped

into MNI (Montreal Neurologic Institute) space via a study-specific Diffeomorphic Anatomical Registration Through Exponentiated Lie algebra (DARTEL) template. Normalisation methods such as these have been demonstrated to be robust to age differences in participants of 7 years and above (Ashburber and Friston, 1998; Burgund et al., 2002). Additionally, the inclusion of the DARTEL template as an intermediate step is among the top ranked currently available deformation algorithms (Klein et al., 2009).

3.1.2.4 Dealing with motion

In addition to regressing out motion parameters, we measured total head motion on our subjects by framewise displacement (FD), which calculates the total amount of movement in all directions between any two subsequent frames (Power et al., 2014). To guarantee that our analyses only includes high quality data and as recommended by Power et al., all frames with FD > 0.5 mm, as well as one frame before and two after, were excluded – an approach known as scrubbing. Finally, we excluded subjects from whom more than 30% of the frames were flagged as high motion ones. In total, one TB and six VPT subjects were excluded based on these criteria. Out of the remaining participants, for the term-born group the mean FD per frame was 0.15 mm with a standard deviation (SD) of ±0.04 mm; for the preterm-born group the mean FD was 0.16 mm ±0.04 mm. There were no significant differences in the amount of movement between the two groups.

3.1.2.5 BOLD variability

BOLD variability was calculated on a voxelwise basis as the standard deviation of the time courses in subject space, excluding scrubbed frames. Each participant's variability map was then spatially z-scored and warped to MNI space via the study-specific DARTEL template. Applying spatial normalisation on these maps as opposed to on the fMRI data used to calculate them is preferred, as voxelwise measures (*e.g.*, the amplitude of low-frequency fluctuations) are more affected by the latter (Wu et al., 2011).

3.1.2.6 Co-activation patterns (CAPs)

To reveal how patterns of co-activation in the brain were rearranged over time we performed a co-activation patterns analysis, which was calculated using the tbCAPs toolbox (Bolton et al., 2020b), openly available online on https://c4science.ch/source/CAP_Toolbox/. For this part of the study, we used fMRI images in MNI space so that frames from different participants would be comparable in the clustering step. Prior to the analysis, all subjects' voxelwise time courses were initially z-scored over time (Liu and Duyn, 2013). Then, for each subject, a seed was placed on the dorsal anterior cingulate cortex (ACC) centred at MNI coordinates [0, 32, 42] (Kolling et al., 2016) with a 10 mm radius, and the time courses of voxels within this mask were averaged. The group-wise z-scored seed activity was then thresholded such that only

15% of the frames (Liu and Duyn, 2013) were kept, which corresponded to threshold at the BOLD signal value of 0.85. These suprathreshold frames were then grouped using k-means clustering based on their euclidean similarity to obtain ACC-CAPs.

To determine the most appropriate number of clusters into which to categorize the data we employed Consensus Clustering (Monti et al., 2003). This approach applies K-means clustering on several subsamples of the data (for this study we used 100 subsamples) and calculates the consensus matrix $\mathscr{M}$. Each element $\mathscr{M}(a,b)$ indicates the fraction of subsamples in which two frames a and b were both retained and clustered together. The optimal number of clusters can then be inferred using the proportion of ambiguously clustered (PAC) measure (Senbabaoglu et al., 2014).

Finally, we calculated occurrence metrics for each CAP such as number of entries; average duration; number of transitions to and from baseline; and total number of occurrences. The latter were used as brain measures for the CAP-PLSC analysis, as it summarises the other metrics.

3.1.2.7 Partial least squares correlation (PLSC) analysis

To reveal and quantify the strength of the relationship between brain measures and life course measures, we applied partial least squares correlation analysis (McIntosh et al., 2004; Krishnan et al., 2011). We thus included either BOLD variability maps or CAP metrics as brain measures in separate analyses and, in both cases, we included Gestational Age (GA), age at assessment and an interaction between then two as life course measures. Before applying PLSC, all life course variables and voxelwise BOLD variability maps were z-scored across subjects (Krishnan et al., 2011). The toolbox used for the PLSC analyses is openly available at https://github.com/danizoeller/myPLS.

PLSC analysis starts by computing the group-wise correlation **R** between the matrix of brain measures per subject, **X**, and the matrix of life course variables per subject, **Y**. Since these data are z-scored (centred and normalised), this corresponds to the cross-product $\mathbf{R} = \mathbf{X}^T\mathbf{Y}$. The group-wise cross-correlation matrices are subsequently stacked. **R** is then factorised via singular value decomposition into three matrices $\mathbf{USV}^T$ to produce latent components (LCs) that capture relationships between brain and life course measures. Each LC is thus associated with a vector of life course saliences (or “weights") in **U**, a vector of brain saliences in **V**, and a corresponding singular value in **S**, which indicates the amount of correlation that is explained by that pair of salience vectors. The aim of PLSC is thus to yield pairs of latent vectors in **U** and **V** with maximal covariance. Each value in a salience vector indicates how strongly the corresponding measure contributes to the correlation between brain and life course measures that this LC explains. By projecting each subject's original (brain or life course) data onto the corresponding salience pattern, we obtained brain ($\mathbf{L}_X = \mathbf{XV}$) and life course ($\mathbf{L}_Y = \mathbf{YU}$) scores, respectively. In other words, each subject's brain score is a weighted sum of their brain measures (*e.g.,* BOLD variability within a voxel), where the weights are given by the brain

saliences calculated from the PLSC. Note that **YU** is computed separately for each group and stacked in $\mathbf{L}_Y$.

To test whether the correlation explained by each LC was significant, we performed 1000 permutations of the life course measures (while keeping grouping intact), and factorised the resulting cross-correlation matrix in each case, to determine the null distribution of singular values. If an LC's singular value was higher than 95% ($\alpha = 0.05$) of the null distribution, it was considered significant. For each significant LC, we then performed cross-validation on the brain and life course saliences to find the elements that contributed significantly to the relationship expressed by that LC. To do this, we created 500 random bootstrap samples obtained by random sampling with replacement on the brain and life course saliences. By dividing the mean of the bootstrap distribution by its standard deviation we obtain the bootstrap ratio (BSR), which is roughly equivalent to a z-score (McIntosh et al., 2004; Krishnan et al., 2011). For instance in the BOLD variability - life course measures PLSC, this ratio represents how robustly each voxel contributes to the LC.

In the results presented here, we threshold the brain patterns of bootstrap scores at $abs(\text{BSR}) > 3$ (when *abs* represents the absolute value), which corresponds approximately to $p < 0.001$ (Garrett et al., 2013a).

3.1.3 Results

3.1.3.1 BOLD variability

Figure 3.1 shows the mean variability map across all subjects from both groups. There was no significant difference between groups when comparing the subject-wise mean variability maps that were subtracted during the PLSC's z-scoring step, as measured by a Student's t-test.

The PLSC analysis of voxelwise BOLD variability yielded one significant LC ($p = 0.006$), which captured an effect of GA; age; and an interaction between the two. These effects were expressed differently between groups as detailed in the following sections.

BOLD variability evolves differently in preterm-born children

Figure 3.2 shows the brain and life course saliences for the significant latent component ($p = 0.006$) yielded by the PLSC analysis. For fullterm-born children, there was a positive effect of GA and age, as well as an interaction between the two, on BOLD variability. This indicates that, as young adolescents grow older, and the longer they have spent in the womb, the more variability they will present in the regions shown in Figure 3.2B. As for preterm-born children, contrary to their peers, age had a negative effect on BOLD variability, suggesting an altered trajectory for the development of this feature in this group. Moreover, although GA alone had no significant effect on BOLD variability, an interaction between GA and age did have a positive effect, suggesting that in older children, a longer gestation is linked to increased

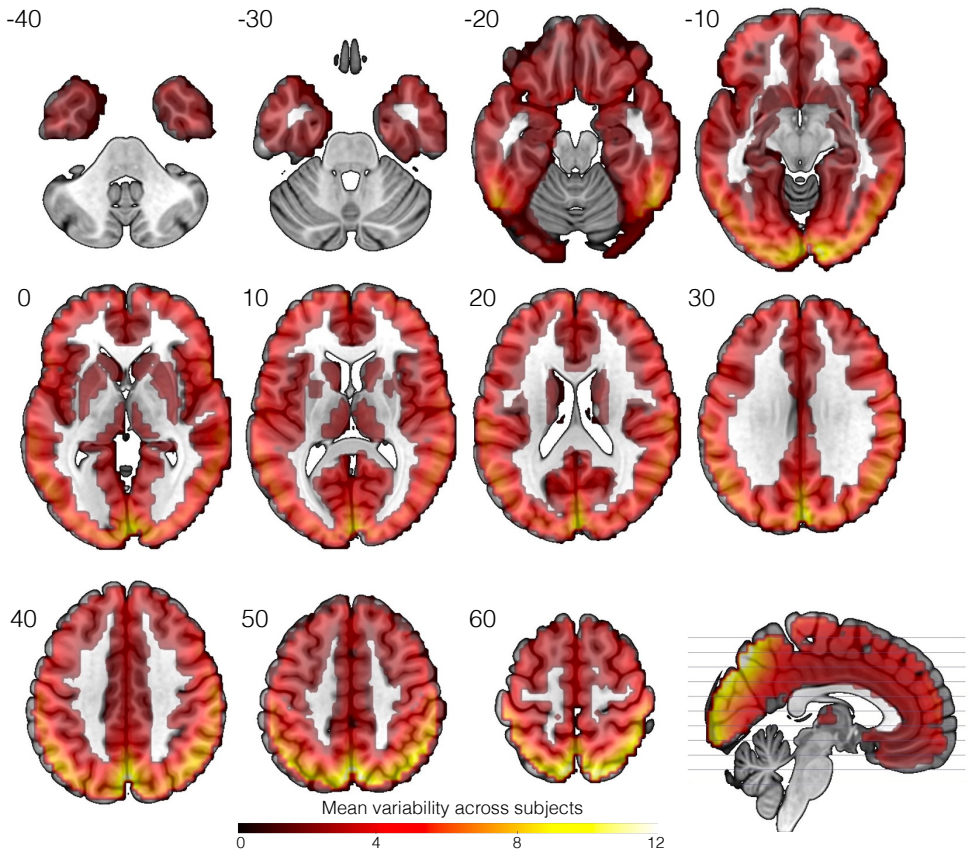

Figure 3.1 – **Mean variability map across the population.** Calculated as the average of the standard deviation of the BOLD signals from each subject from both groups. Numbers on the top left indicate MNI coordinates in the Z axis. There was no significant difference between the mean variability maps of each group separately, as measured by Student's T-tests.

BOLD variability, bringing them closer to fullterm controls. The brain regions most implicated in the relationship uncovered by the significant latent component are shown in Figure 3.2B with a bootstrap ratio threshold of BSR = 3, which is equivalent to p-values less than 0.001. In particular, the bilateral hippocampi (Hipp), insulae (Ins), ventral and dorsal anterior cingular cortex (ACC) all have a BSR < 6, which corresponds to a p-value less than 0.00001.

3.1.3.2 Co-activation patterns

Out of the brain areas highlighted in our BOLD variability analysis' results, the dorsal anterior cingulate cortex (ACC) has been previously reported to showcase alterations in both function and static connectivity in preterm-born individuals at various stages in life (White et al., 2014b; Daamen et al., 2015; Lordier et al., 2019). We thus selected this region as a seed for further investigation using CAP analysis.

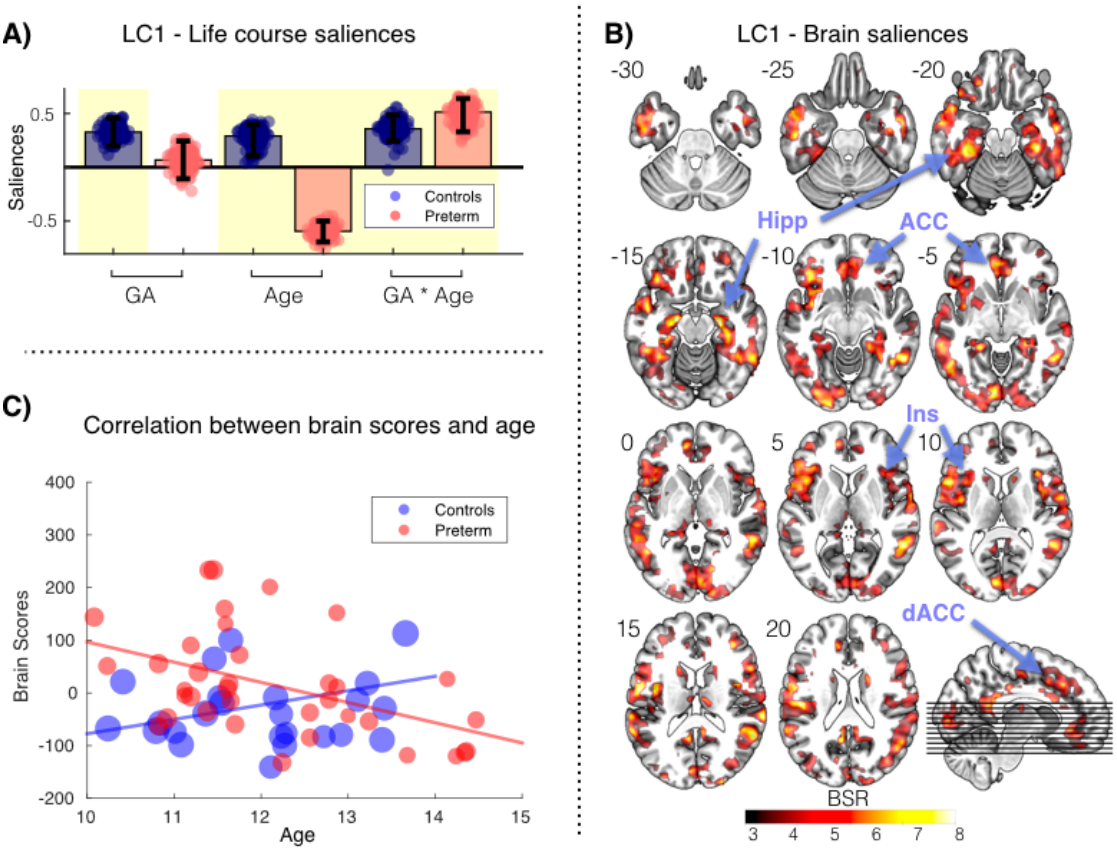

Figure 3.2 – **BOLD variability and its link to life course measures.** Partial least squares correlation (PLSC) results for BOLD variability and life course measures for preterm-born young adolescents and fullterm-born controls. A) Life course measures' weights for latent component (LC) 1. GA = Gestational Age. Error bars correspond to bootstrapping 5th–95th percentiles. B) Brain weights for LC 1. Numbers on the top left of each slice correspond to planes in Montreal Neurological Institute coordinates. C) Correlations between brain scores (subject-wise weighted average of BOLD variability maps, with the Brain Saliences as weights) and age at assessment in the two groups (r_{tb} = 0.3, p = 0.01; r_{vpt} = -0.4, p = 0.006). For this plot, brain scores (Lx) were calculated using brain data normalised across all participants (as opposed to within-group), to allow group baselines to be compared. Each bubble's size is proportional to the corresponding subject's GA.

ACC co-activates with typical resting-state networks in young adolescents

Consensus clustering was performed on K = 2–20, and the lowest proportion of ambiguously clustered frames indicated K = 6 as the ideal number of centroids for the clustering step. The co-activation patterns obtained correspond to well known resting-state networks and can be seen in Figure 3.3. CAP 1 corresponds to the default mode network (DMN), including the anterior medial prefrontal cortex, posterior cingulate cortex and angular gyri. CAP 2 includes the anterior cingulate cortex and the dorsolateral prefrontal cortex. CAP 3 corresponds to the dorsal attention network (DAN). CAP 4 includes nodes typically associated with the language

network. CAP 5 includes the insula and dorsal ACC, nodes associated with the salience network (SN). Finally, CAP 6 corresponds to the visual network.

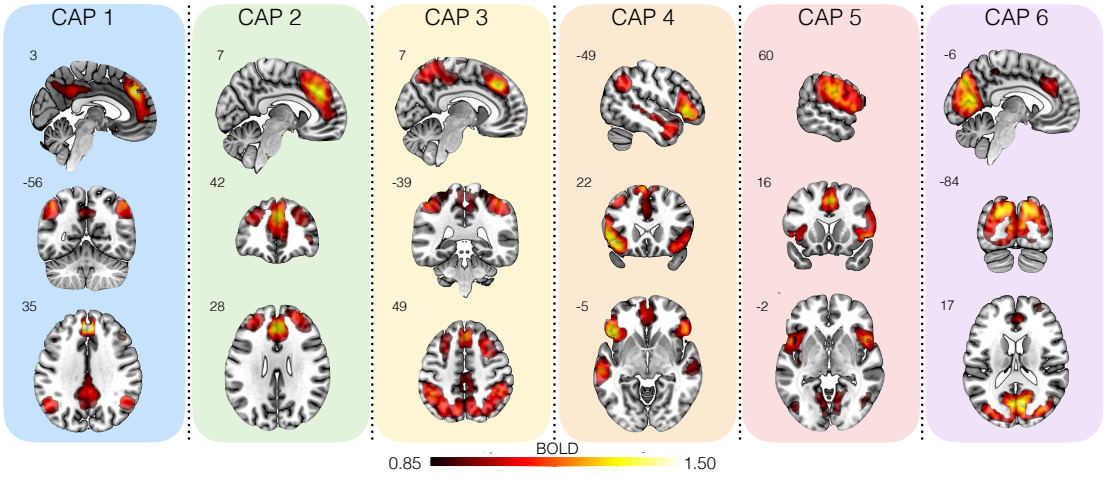

Figure 3.3 – **Spatial patterns of co-activation with the anterior cingulate cortex in young adolescents.** Co-activation Patterns (CAPs) were obtained from all subjects, including preterm-born young adolescents and fullterm controls. Numbers on the top left corner of slices correspond to Montreal Neurological Institute coordinates. Voxels were thresholded at 0.85, the same threshold used on the seed time course to keep 15% of frames for clustering in the CAP analysis. CAP 1 = default mode network ; CAP 2 = anterior cingulate cortex and dorsolateral prefrontal cortex; CAP 3 = dorsal attention network; CAP 4 = language network; CAP 5 = salience network; CAP 6 = visual network.

No group differences in individual CAP metrics between preterm- and fullterm-born participants

None of the individual CAP metrics we analysed (*i.e.*, number of entries; average duration; number of transitions to and from baseline; and total number of occurrences) were significantly different between groups, as compared using two-sample t-tests ($p > 0.05$, *n.s.*).

Altered trajectories of ACC-CAPs over time in preterm-born young adolescents

We then tested whether there were significant interplays between the six CAPs that were expressed differently between the two groups over time. To this end, we employed a PLSC analysis including the total number of occurrences per CAP and the life course measures. We found one significant latent component (LC1, $p = 0.001$) as shown in Figure 3.2. Life course weights for LC1 indicate robust weights of gestational age (GA), age at assessment and an interaction of the two for preterm young adolescents, whereas age at assessment and its interaction with GA contributed robustly to LC1 in the control group (Figure 3.4A). CAP occurrence saliences show that internally oriented networks such as the DMN have a positive weight in the relationship uncovered by LC1, while externally oriented networks (*e.g.*, language,

visual) are negatively weighted (Figure 3.4B). The correlation plot between brain scores and age shows that this relationship is altered in preterm-born young adolescents as compared to their fullterm peers (Figure 3.4C). Specifically, brain scores start lower for the VPT group at the age of 10, but increase at a higher pace than for the control group, eventually surpassing it.

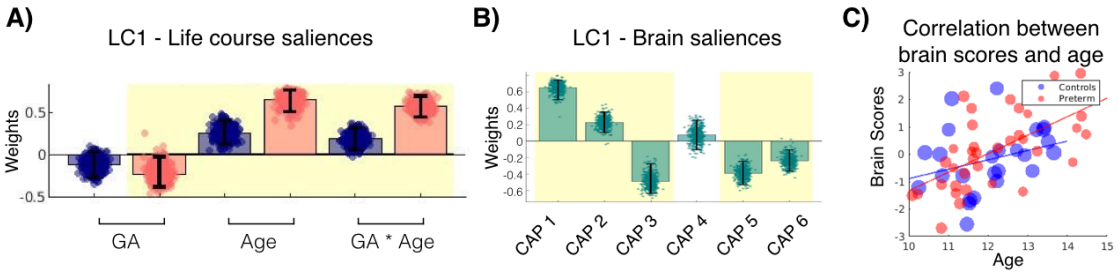

Figure 3.4 – **Altered trajectory of ACC-CAPs development over time in preterm-born young adolescents.** Partial least squares correlation between CAP occurrence and age-related measures lead to one significant latent component ($p = 0.001$). A) Life course measures' weights for LC1 indicate robust weights of gestational age (GA), age at assessment and an interaction of the two for preterm young adolescents (red bars), whereas age at assessment and its interaction with GA contributed robustly to LC1 in the control group (blue bars); blue bars represent fullterm controls. B) CAP occurrence saliences show that internally oriented networks have a positive weight in the relationship uncovered by LC1, while externally oriented networks (*e.g.*, language, visual) have a negative weight. C) The correlation plot between brain scores (subject-wise weighted average of CAP occurrences, based on brain saliences as weights) and age shows the different trajectories of CAP occurrence across age in the two groups ($r_{tb} = 0.4$, $p = 0.05$; $r_{vpt} = -0.6$, $p = 0.0001$).

3.1.4 Discussion

This study investigated dynamic features of brain activity and connectivity in preterm-born young adolescents, with the particular goal of tracking their evolution during this phase of development. To the best of our knowledge, we were the first to investigate BOLD variability in this population. We additionally employed co-activation pattern (CAP) analysis using a brain area previously shown to be vulnerable in this population — the dorsal anterior cingulate cortex — as a seed to reveal several different spatial patterns, representing well-known resting-state networks, that dynamically co-activate with this ROI over time. Finally, we revealed that the development of both BOLD variability and the balance between CAPs is altered in VPT young adolescents as compared to fullterm controls.

Altered BOLD variability evolution in the Very Preterm BOLD variability is broadly altered in the preterm group, for which we found a negative effect of age as compared to a positive effect within the control group (Figure 3.2A). Of note, the pattern of alterations includes large parts of the DMN such as the medial prefrontal cortex and the posterior prefrontal cortex.

Garrett et al. (2011) found differences in a similar set of regions when studying BOLD variability in healthy adults during the performance of a task, with the elderly, low performing group showing decreased variability. Importantly, the posterior cingulate cortex and precuneus have been singled-out as functional and structural network hubs, linked to theory-of-mind and self-referential processes (Spreng et al., 2009; van den Heuvel and Sporns, 2013), both of which are affected in the preterm-born (Papini et al., 2016; Witt et al., 2018). In pre-adolescents, a recent study in normative functional connectivity development found that FC within the DMN was anti-correlated with age and cognitive performance (Jiang et al., 2018). The increase in BOLD variability with age in the same regions in our fullterm group aligns with the idea that variability at the right level is necessary to yield a greater dynamic range and complexity, allowing flexibility in brain function and connectivity (McIntosh et al., 2010; Deco et al., 2011; Garrett et al., 2013b). Along these lines, the development of variability found in the preterm participants may be linked to other functional and behavioural alterations seen in this group. For instance, exacerbated variability in the medial prefrontal cortex in ADHD patients aged 9.91 ± 1.24 (as compared to typically developing children) is strongly correlated with the severity of ADHD symptoms and inattention (Nomi et al., 2018). The positive effect of the interaction between gestational age and age at assessment in our preterm group shows a similar relationship between BOLD variability and prematurity in our younger preterms (Figure 3.2A, B). In particular, the fact that variability is higher in the preterm group at an early age and gradually decreases past the fullterm point may indicate a compensation mechanism that overshoots, and thus does not reach ideal levels (*e.g.*, comparable to typically developing controls) within this period of life. Note that although there was a coincidental weak correlation between gestational age and age at assessment in the preterm group (Supplementary Figure A.4), we do not expect this to have had a large effect in the results due to the weakness of this relationship. It would be interesting to follow up this study with a BOLD variability analysis in preterm-born adults to check if, like with other brain measures and behavioural traits, the alterations last throughout life.

The pattern of BOLD variability alterations includes other brain regions such as the bilateral hippocampus/amygdala and the insula – areas involved in a variety of functions ranging from affective processing to higher level cognition (Uddin et al., 2018). These regions have been previously found to be affected in the young preterm population, with accounts of altered developmental trajectories (Thompson et al., 2014), volumetry (Chau et al., 2019), and function (Nosarti et al., 2006). In general, our results agree with research showing that insular BOLD variability increases linearly with age in the resting state (Nomi et al., 2018) in typically developing individuals, and show that this trajectory is altered in the preterm group. In our group comparison, there was no evidence of the previously found cortical-subcortical dichotomy in which BOLD variability increases with age in subcortical areas as opposed to cortical areas (Garrett et al., 2013b). This may be partly due to the fact that Garrett's study was performed using a task-based design. More importantly, PLSC extracts the multivariate pattern that most differentiates the two groups, suggesting a complex pattern of development alterations in the preterm group.

Altered ACC connectivity pattern in the Very Preterm To further understand the effects of BOLD variability and relate it to conventional functional connectivity, we investigate how the patterns of activation of the dorsal ACC — a region that has been previously shown to be compromised in the preterm-born (White et al., 2014b; Daamen et al., 2015; Lordier et al., 2019) — relate to other areas in the brain. In keeping with our interest in the dynamic aspects of brain function, we chose to perform a co-activation pattern (CAP) analysis to achieve this, retrieving 6 CAPs that included well known resting-state networks. There was no difference between the two groups when we compared the number of occurrences of each CAP individually. However, a multivariate analysis showed that the occurrence of certain combinations of CAPs developed differently in the two groups. Of note, the difference was mainly driven by the number of entries in each state, as opposed to the duration of each brain state. Sherman et al. (2014) found that DMN integration increased from ages 10 to 13 in typically developing children, and segregation between the DMN and dorsal attention networks increased (*i.e.*, the between-network correlations weakened). This is in line with what we found in our control group. Interestingly, the preterm group follows the same trend, but in a much more accentuated way. Similarly to our results on BOLD variability, this suggests that there is a mechanism in place that fails to identify the optimal point of balance and thus overshoots. Nosarti et al. (2006) found that, in preterm adults, a weaker connectivity in the salience network (which includes the dorsal ACC and the insula) is related to worse outcomes, which is in line with our result that, in the preterm group, co-occurrence of the ACC and the insula decreases more rapidly than in the control group. These findings, combined, further highlight early adolescence as a significant time for maturation of the brain's functional architecture, and corroborate the idea that this development fails to find the optimal compensatory balance in preterm-born individuals.

Interestingly, the combination of patterns that co-occur with the ACC found in our CAPs PLSC analysis reveals a dichotomy between the occurrences of internally- (*i.e.*, DMN, mPFC) versus externally-oriented (*i.e.*, DAN, visual) networks (Zabelina and Andrews-Hanna, 2016). Internally-oriented cognition comprises creative thinking; making social inferences; prospection; and mind-wandering (Zabelina and Andrews-Hanna, 2016; Buckner and DiNicola, 2019). Networks which support externally-oriented cognition, in turn, are typically involved in language; visual; and somatosensory tasks, attention regulation, and are usually positively correlated at rest (Lee et al., 2012), in line with our results. A study on resting-state functional connectivity including young adolescents aged 10–16 found that very preterm participants showed weaker connectivity in externally-oriented networks such as the visual and DAN (Wehrle et al., 2018). The results considered the groups in a categorical way, but includes a slightly older population than ours. This could explain the finding of a weaker task-oriented network connectivity in preterm as compared to controls, which is in line with what is seen in our older participants. This weakened connectivity has also been found in adult preterm-born individuals aged 28 and above (White et al., 2014b). Our study thus provides complementary insight into the trajectory of the differences seen between the two groups, and suggests that the disconnectivity seen in later life stages may be related to faulty compensation mechanisms

that start during the highly dynamic age range of early adolescence.

Study considerations

While we discuss the development of dynamic features during young adolescence, the measures at different ages were acquired by different individuals. Given that this is a stage in life in which the brain is in full blown development and that there is high heterogeneity in the clinical outcomes of preterm infants, it would have been ideal to perform repeated measures in the same participants in a longitudinal study. Moreover, it has been shown that extremely preterm-born individuals (<28 weeks of gestational age) tend to be less resilient and therefore more likely to present brain abnormalities. Here, we grouped extremely and very (28—31 weeks) preterm-born individuals together. Subsequent analyses should take this into consideration by looking for effects that are specific to each of these groups separately.

Conclusions

Our study shows for the first time that the trajectory of BOLD signal variability development is altered in young adolescents born prematurely, and that these alterations follow a broad spatial pattern in the brain comprising regions previously found to be affected by preterm birth. The previous implication of the brain areas observed in our study in preterm birth and cognitive performance suggests exploring the relationship between the development of BOLD signal variability and behavioural outcomes as a promising avenue for further research. In addition, we explored the development of dynamic functional connectivity in this population by examining how the interplay between different multivariate co-activation patterns changes with age. We found that the change in the balance between internally- and externally-oriented networks across age is more accentuated in the preterm group. Taken together, our observations suggest that the preterm-born brain triggers neurological compensation mechanisms that start during the highly dynamic age range of early adolescence and fail to find an optimal balance.

Acknowledgements

This work was supported by the Swiss National Science Foundation, grant no. 324730-163084 to PSH. The authors thank Loan Mattera, Roberto Martuzzi and Greta Mikneviciute for their help in data acquisition.

Conflict of Interest Statement

The authors declare that the research was conducted in the absence of any commercial or financial relationships that could be construed as a potential conflict of interest.

4 Studying cognition with task-based fMRI: reality filtering in young populations

While resting-state studies provide insightful information on spontaneous brain function, task-based functional magnetic resonance imaging (fMRI) paradigms are essential to probe into brain activation driven by specific demands. As described in more detail in this chapter, the prefrontal cortex — specifically the orbitofrontal cortex (OFC) — has been shown to be essential for the ability to process reality filtering tasks in adults (Schnider, 2018). This region is, however, known to be underdeveloped in preterm-born individuals (Thompson et al., 2007). The goal of this chapter is thus twofold: to investigate whether, as in adults, the OFC mediates reality filtering in young adolescents; and whether preterm-born young adolescents use the same brain resources as fullterm-born controls to perform a reality filtering task.

The first article included in this section has been published in the peer-reviewed Brain and Behaviour journal. Its goal was to test the hypothesis that the OFC mediates reality filtering processing in young adolescents. Maria Chiara Liverani and Lorena Freitas are considered joint first-authors for the paper, having performed the behavioural and neuroimaging analyses, respectively. In addition, Liverani and Freitas both participated in data collection for this study. The remaining authors participated in different stages of ideation for the overarching project (*Building the Path to Resilience in Preterm Infants*) and/or provided funding.

The second article is a preprint of the followup study looking into reality filtering in preterm-born children as compared to the control group from the first study.

4.1 Journal Article: Get real: orbitofrontal cortex mediates the ability to sense reality in early adolescents

(Postprint version of the article published in: Brain and Behaviour, 2020, DOI: https://doi.org/10.1002/brb3.1552)

Maria Chiara Liverani*[1], Lorena G. A. Freitas*[1,2], Vanessa Siffredi[1,2], Greta Mikneviciute[1], Roberto Martuzzi[3], Djalel-Eddine Meskaldij[1,4], Cristina Borradori Tolsa[1], Russia Ha-Vinh Leuchter[1], Armin Schnider[5], Dimitri Van De Ville[2], Petra S. Hüppi[1]

** M.C.L. and L.G.A.F. have contributed equally and are considered joint-first authors.*

[1] Department of Paediatrics, Gynecology and Obstetrics, Division of Development and Growth, Geneva University Hospitals, 6 rue Willy – Donzé, 1205 Geneva, Switzerland
[2] Institute of Bioengineering, École Polytechnique Fédérale de Lausanne, Rue Cantonale, 1015 Lausanne, Switzerland
[3] Foundation Campus Biotech Geneva, Chemin des Mines 9, 1202 Geneva, Switzerland
[4] Institute of Mathematics, École Polytechnique Fédérale de Lausanne, Rue Cantonale, 1015 Lausanne, Switzerland
[5] Department of Clinical Neurosciences, Division of Neurorehabilitation, Geneva University Hospitals, 26 Avenue de Beau-Séjour, 1211 Geneva, Switzerland

Abstract

Introduction: Orbitofrontal reality filtering (ORFi) is a memory mechanism that distinguishes if a thought is relevant to present reality or not. In adults, it is mediated by the orbitofrontal cortex (OFC). This region is still not fully developed in pre-teenagers, but ORFi is already active from age 7. Here we probe the neural correlates of ORFi in early adolescents, hypothesizing that OFC mediates the sense of reality in this population.

Methods: Functional magnetic resonance images (fMRI) were acquired in 22 early adolescents during a task composed of two runs: Run 1 measuring recognition capacity; Run 2 measuring ORFi; each containing two types of images (conditions): distractors (D: images seen for the first time in the current run) and targets (T: images seen for the second time in the current run). Group region of interest (ROI) analysis was performed in a flexible factorial design with two factors (run and condition) using SPM12.

Results: We found significant main effects for the experimental run and condition. The bilateral OFC activation was higher during ORFi than during the first run. Additionally, the OFC was more active while processing distractors than targets.

Conclusion: These results confirm, for the first time, the role of OFC in reality filtering in early

adolescents.

Keywords: *Orbitofrontal reality filtering, fMRI, orbitofrontal cortex, early adolescents, memory.*

4.1.1 Introduction

Orbitofrontal reality filtering (ORFi) is a memory control mechanism that allows to filter upcoming memories and thoughts according to their relation with ongoing reality (Schnider, 2013, 2018). The first description of ORFi was based on the observation of patients with orbitofrontal lesions, suffering from behaviourally spontaneous confabulations and disorientation. These patients typically turn to currently inappropriate memories to guide their present actions or to shape their future plans, failing to verify the connection of these memories with the "now". In addition, they are disoriented in time and space (Schnider, 2018). For example, a retired psychiatrist hospitalised after rupture of an aneurysm of the anterior communicating artery, repeatedly tried to leave the hospital in the conviction that she had to meet her own patients (Schnider et al., 2005). Schnider and colleagues (Schnider et al., 1996) developed an experimental paradigm to test ORFi and to reliably discriminate reality-confusing patients from healthy participants. It consists of two runs of a continuous recognition task in which the same images are shown twice. Participants are asked to indicate picture recurrences only within the ongoing run. The first run assesses the ability to encode and recognize items, and familiarity alone is sufficient to correctly perform the task. In the second run all images are familiar, and thus familiarity alone is not enough to perform the task. In this second run ORFi is needed, representing the ability to sense whether the memory of an item relates to the present (the currently ongoing run), or not (Schnider and Ptak, 1999).

Behaviourally, confabulating patients markedly and specifically increased their false positives in the second run (Nahum et al., 2012; Schnider and Ptak, 1999). Lesion analysis on these patients revealed that the ORFi mechanism depends on the orbitofrontal cortex (OFC) or structures directly connected with it (Schnider et al., 1996; Schnider, 2018). Functional neuroimaging studies using Positron Emission Tomography further corroborated the dependence of ORFi on the intact OFC (Schnider et al., 2000; Treyer et al., 2003, 2006). Electrophysiological studies revealed that ORFi is expressed by a frontal positivity at about 200-300 ms, before the content of a thought is recognised (Schnider, 2002).

Children are more vulnerable to memory distortions and more prone to errors than adults (Ceci and Bruck, 1993). Using a child-adapted version of the continuous recognition task, we recently found that ORFi is present in 7-year-old children, improves from 7 to 11 years in parallel with memory capacity, but does not attain adult efficacy at that age (Liverani et al., 2017).

The neural correlates of this mechanism in children and adolescents has never been investigated. While the implication of the OFC in ORFi has clearly been shown in adults (Treyer et al., 2003, 2006), no such evidence exists in a younger population.

The aim of this study was to examine, with advanced functional neuroimaging techniques, to which extent the ability of early adolescents to sense whether a memory or a thought refers to the present reality or not depends on the OFC, similar to what has been found in adults.

4.1.2 Methods

4.1.2.1 Participants

Twenty-three healthy early adolescents from 10 to 13 years of age (10 females, mean age 12 ± 1.01 years) were recruited through advertisements. One participant was excluded due to strong signal distortions on fMRI images caused by the subject's dental braces. Twenty-two participants were finally included in the analysis.

Cognitive assessment at the time of the scan was performed using the French version of the Wechsler Intelligence Scale for Children – Fifth Edition (WISC - V; Wechsler, 2014). For one participant IQ score was evaluated using the Kaufman Assessment Battery for Children, second edition (KABC-II; Kaufman and Kaufman, 2004). All participants scored within the normal range of intellectual functioning (mean = 117.04 ± 11.35). Parents were asked to fill a questionnaire assessing the presence of serious physical illness or neurological problems. None of the participant had major disabilities, psychiatric or neurological diseases.

The Ethics Committee of the Canton of Geneva approved the study, which was carried out in accordance with the Declaration of Helsinki. Caregivers and participants provided informed written consent. Participants received a gift voucher of 100 Swiss francs for their participation in the study.

4.1.2.2 fMRI Paradigm

Participants performed a child-adapted version of the continuous recognition task assessing recognition memory and orbitofrontal reality filtering (Figure 4.1; Liverani et al., 2017; Schnider et al., 1996; Schnider, 2003, 2013), associated with an event-related fMRI paradigm.

The task was composed of two runs in which the same set of images was presented and repeated twice, with a break of around 3 minutes between the two runs. In the first part, assessing recognition memory (item recognition, IR) participants were asked to indicate picture recurrence ("Have you already seen this picture in this task?") by pressing the left button of an MRI-compatible mouse if the image was seen for the first time (distractors run 1, D1), and the right button if it was seen for the second time (targets run 1, T1). This run can be solved on the basis of familiarity alone. In the second run, the same set of pictures was presented in a different order and repeated twice. Participants were instructed to indicate if each item was presented for the first or the second time in this ongoing run ("Is this the first or the second time that you see that image in this ongoing run?"), pressing the left button of the mouse for images seen for the first time (distractors run 2, D2), and the right button for

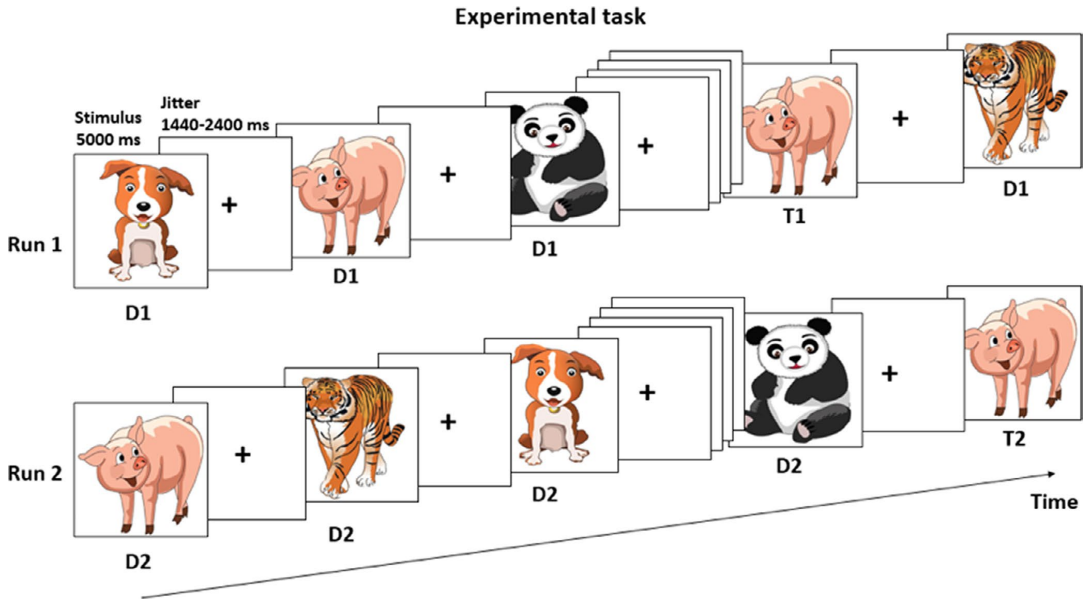

Figure 4.1 – **Task design.** The task was composed of 2 runs, separated by a break of 3 minutes. Distractors (D1, D2) are images presented for the first time within a run; targets (T1, T2), are images repeated within the same run.

images presented for the second time (targets run 2, T2). In this run all images have already been seen. Therefore, familiarity alone is not enough to correctly perform the task, and the ORFi mechanism is needed to process distractors (D2).

Pictures were a set of 30 cartoon drawings of animals and were presented for 5 seconds on the screen. In each run, 30 images were presented for the first time (distractors, D) and then repeated once (targets, T) after 6 to 9 intervening pictures, has already done in a previous study with children (Liverani et al., 2017). After each image, a fixation cross was presented during between 1440 and 2400 milliseconds. Each run lasted approximately 7.5 min. Stimuli were displayed on a white screen at the head of the scanner via a 45° angled mirror fixed to the MRI head coil. Responses were given by pressing two buttons with the right index and middle finger, on an MRI-compatible mouse. Task programming, stimuli display and responses logging were done using E-Prime 2 (Psychology Software Tools, Pittsburg, USA). All participants successfully completed a short training with a different set of images in the mock MRI scanner before the MRI.

4.1.2.3 Behavioural data analysis

Reaction times and accuracy were recorded for each condition (D1, T1, D2, T2). A 2 X 2 repeated measures analysis of variance (ANOVA) was performed on accuracy and reaction time with the within-subject factors Run (1, 2) and Stimulus (distractor D, target T).

4.1.2.4 Image acquisition

MRI data were acquired on a Siemens 3T Magnetom Prisma scanner at Campus Biotech, Geneva, Switzerland. Structural T1-weighted MP-RAGE (Magnetization Prepared Rapid Gradient Echo) sequences were acquired using the following parameters: voxel size = 0.9 x 0.9 x 0.9 mm; repetition time (TR) = 2300 ms; echo time (TE) = 2.32 ms; inversion time (TI) = 900 ms; flip angle (FA) = 8°; field of view (Fov) = 240 mm. Functional images were T2*-weighted with a multislice gradient-echo-planar imaging (EPI) sequence of 64 slices; voxel size = 2 x 2 x 2 mm; TR = 720 ms; TE = 33 ms; Fov = 208 mm. Finally, a fieldmap was acquired each time a participant entered the scanner, with TR = 627 ms; TE1 = 5.19 ms; TE2 = 7.65 ms; and FA = 60°.

4.1.2.5 MRI data preprocessing

Our data were preprocessed using SPM12 (Wellcome Department of Imaging Neuroscience, UCL, UK) in Matlab R2016a (The MathWorks, Inc., Natick, Massachusetts, United States). One particular challenge in studying frontal brain areas using fMRI is the considerable vulnerability of these regions to signal distortions caused by field inhomogeneities around the air-filled sinuses (Gorno-Tempini et al., 2002). To correct for the resulting geometrical distortions, a field map was calculated from an additional stock double-echo field map sequence included in our MRI protocol (Hutton et al., 2002). The fMRI images from each participant were then spatially realigned and unwarped, respectively, to correct for motion artefacts and potential geometric distortions. Thanks to the distortion correction of vulnerable brain regions on the single-subject level, this additional unwarping step not only improves the co-registration between structural and functional images, but it also reduces the distortion variability across subjects during spatial normalization to a common space (Hutton et al., 2002). This solution has been successfully used in several recent studies in adults including task (Daw et al., 2011) and resting-state (Togo et al., 2017) experimental paradigms, as well as in presurgical planning (Lima Cardoso et al., 2018) and in children (Wozniak et al., 2011).

In general, total head motion was very low on our participants as measured by framewise displacement (FD; Power et al., 2014): for the first fMRI run the mean FD per frame was 0.16 mm with a standard deviation (SD) of ± 0.04 mm; for the second run the mean FD was 0.15 mm ± 0.05 mm. Therefore, no participant was excluded due to high motion. Functional images were then coregistered to structural images in subject space and smoothed with a Gaussian filter of full width at half maximum (FWHM) = 6 mm. To be able to perform a group level comparison, data were warped into MNI (Montreal Neurologic Institute) space via a study-specific DARTEL (Diffeomorphic Anatomical Registration using Exponentiated Lie algebra) template. Normalisation methods such as these have been demonstrated to be robust to age differences in participants of 7 years and above (Ashburber and Friston, 1998; Burgund et al., 2002). Additionally, the inclusion of the DARTEL template as an intermediate step is among the top ranked currently available deformation algorithms (Klein et al., 2009).

4.1.2.6 Region of Interest (ROI analysis)

Statistical analyses were performed using SPM12 scripts implemented in Matlab R2016a in a two-step process, so that both intra and inter-subject variance were taken into account (Friston et al., 1995). First-level (subject level) analyses were assessed on a voxel-wise basis using a General Linear Model (GLM). Within each condition, the corresponding regressors were generated from all trials regardless of a correct or incorrect response. This was motivated by two main reasons: 1) this would ensure a similar number of trials per condition, and 2) our participants had consistently high rates of correct responses, which characterises a ceiling effect as discussed later. The condition regressors were produced by convolving SPM12's canonical hemodynamic response function (HRF) with the onsets of each trial in an event-related design and included as regressors-of-interest in the individual design matrix. To further account for potential individual movement effects, we included in our model covariates-of-no-interest calculated in the following fashion: first, we computed the 24-parameter Volterra Expansion (VE) of the 6 motion parameters stored during the realignment step of the preprocessing pipeline. Secondly, we extracted the top 6 components (or those that explained 95% of the variance in the VE) via singular value decomposition (SVD). Then, we included these components as nuisance regressors in the subject-level design matrix. This approach has been successfully used on our previous analyses of child data (see Adam-Darque et al., 2018 for an example). Finally, we employed the scan-nulling strategy (Lemieux et al., 2007) to ignore information contained in fMRI images in which FD > 0.5mm, by adding extra regressors-of-no-interest for each of these time points.

The first-level results from all participants were then used in a second-level (group level) analysis in a factorial design with two factors (run and condition) with two levels each (2 runs and 2 types of stimuli, namely distractor and target). This design provides the flexibility to analyse main effects as well as a possible interaction effects between the factors. Given the a priori hypothesis of the involvement of the OFC in the reality filtering task based on neuropsychological data, lesion studies and PET imaging studies (Schnider et al., 1996; Schnider and Ptak, 1999; Treyer et al., 2003) , we performed an ROI analysis based on this brain region. Our ROI mask was defined as follows: first, we downloaded a z-scored mask from NeuroSynth (Wager, 2011), which was calculated as a meta-analysis of 665 independent studies for the term "orbitofrontal cortex". This initial mask (nMask) was thresholded at z-value > 3, which is equivalent to a p-value < 0.001, and the largest continuous cluster was maintained. The nMask covered the entire bilateral OFC and can be seen highlighted in yellow in Figure 4.2. Last, to ensure an equal contribution of all subjects to the analysis, we created a final mask (iMask) calculated as the intersection of all voxels within nMask that were present in the grey matter of every subject in our dataset. This can be seen as the blue highlight in Figure 4.2. The contrast values for voxels within the ROI iMask from each subject were then averaged, and the resulting value entered in a 2-way analysis of variance (ANOVA). This strategy has two main advantages: it increases the signal to noise ratio, which improves the power of detecting true signals, and avoids the problem of multiple testing inherent in massive univariate approaches (Benjamini and Heller, 2007; Meskaldji et al., 2015). Although the ANOVA allows us to identify main, as

well as interaction effects, it does not describe the effect's direction – for example, it may tell us that the means between conditions are different, but not which one is greater. Thus, we performed additional t-tests within factors to clarify the direction of the effects found with the ANOVA and report the corresponding p-values, Bonferroni corrected for the number of effects that we find. Furthermore, in order to provide an estimate of each voxel's contribution to the effects detected by these tests, we calculated the voxelwise t-values within the ROI.

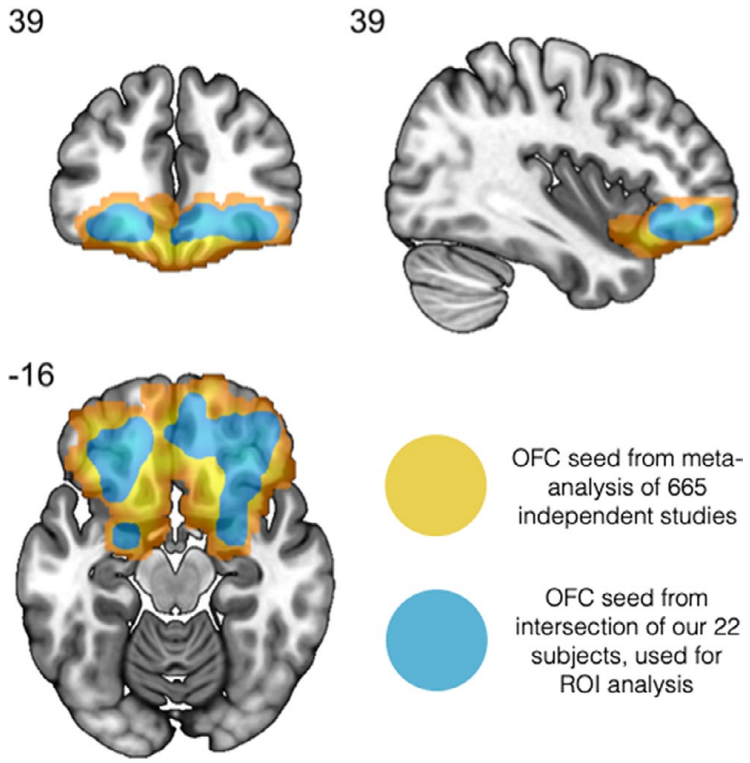

Figure 4.2 – **The shaded areas show the orbitofrontal cortex ROI.** The region highlighted in yellow indicates the initial mask calculated from 665 independent studies using NeuroSynth. The area highlighted in blue corresponds to the intersection of grey matter voxels available for all participants within the initial mask. The latter was the final ROI used for this study. Brain images follow the neurological convention (left side shown on the left; right side shown on the right).

4.1.3 Results

4.1.3.1 Behavioural results

Behavioural descriptive results on accuracy and reaction times are summarised in Table 4.1. Overall, a ceiling effect was found for the task accuracy, since participants had a very high rate of correct responses. The 2 X 2 repeated measures ANOVA on reaction times revealed a significant main effect of the factor Run ($F_{(1, 21)} = 12.14$, $p < 0.005$, $\eta_p^2 = 0.366$), with faster

Stimulus type	Correct responses, % (SD)	Reaction times, ms (SD)
Distractor, Run 1	96.06 (4.78)	1454 (406)
Target, Run 1	90.30 (16.93)	1454 (369)
Distractor, Run 2	93.63 (6.24)	1579 (339)
Target, Run 2	89.39 (13.97)	1577 (413)

Table 4.1 – Descriptive statistics of behavioural results on the reality filtering task. *Distractor, Run 1* and *Distractor, Run 2* are images seen for the first time in the first and in the second run, respectively. *Target, Run 1* and *Target, Run 2* are images seen for the second time in the first and in the second run, respectively.

responses for the first compared to the second run. No significant difference was found between Distractors and Targets reaction time ($F(1, 21) = 0.001$, $p = 0.977$, $\eta_p^2 = 0.000$). The interaction between the factor Run and the factor Condition was not significant.

Accuracy analysis revealed no difference between the two runs ($F_{(1, 21)} = 1.36$, $p = 0.257$, $\eta_p^2 = 0.061$), as well as no difference between Distractors and Targets ($F_{(1, 21)} = 3.14$, $p = 0.91$, $\eta_p^2 = 0.13$). The interaction between the factor Run and the factor Condition was not significant. Violin plots in Figures 4.3 and 4.4 show the distribution of correct responses and reaction times for each condition, respectively.

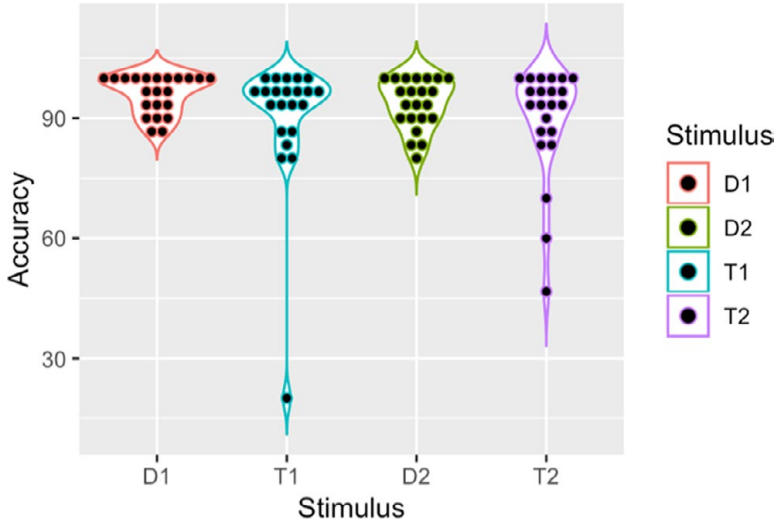

Figure 4.3 – **Accuracy distributions by stimulus type.** The violin plots show the accuracy distribution per stimulus in the population. D1 = Distractor images in Run 1; T1 = Target images in Run 1.

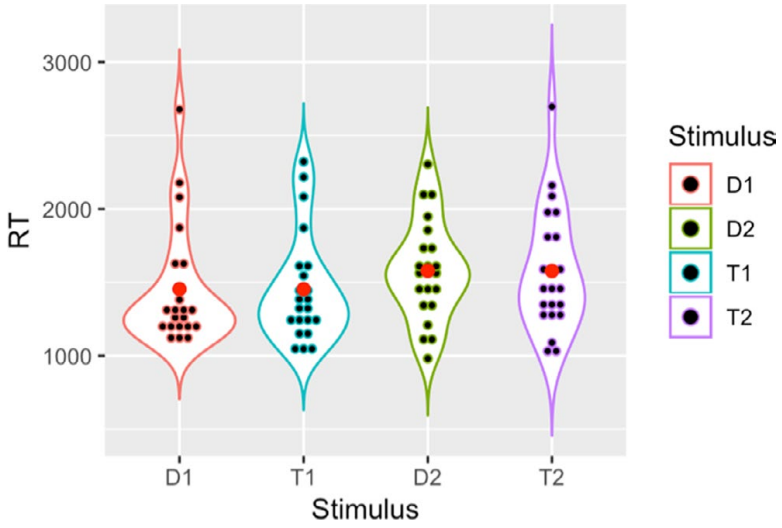

Figure 4.4 – **Reaction Times by stimulus type.** The violin plots show the distribution of participant-averaged reaction times per stimulus in the population. D1 = Distractor images in Run 1; T1 = Target images in Run 1.

Factors	Mean Squared	F-statistic	p-value
Run	1.3219	556.65	0.027
Condition	2.4095	1014.64	0.02
Run * condition	0.0024	0	0.9455

Table 4.2 – 2-way ANOVA with factors "run" and "condition" for brain activations in the orbitofrontal cortex. Run = Run 1 and Run 2; Condition = Distractors and Targets.

4.1.3.2 ROI task-related activity

To investigate whether there were main effects of run or condition, or an interaction between the two in the OFC, we first ran a 2-way ANOVA test (see Table 4.2). We found a significant main effect for the experimental “run” ($F(1, 21) = 556.65$, $p = 0.027$). Additionally, we found a significant main effect of the factor “condition” ($F(1, 21) = 1014.64$, $p = 0.02$). The interaction effect between run and condition was non-significant.

We next sought to clarify the direction of the effects found from the ANOVA test. To this end, we first carried out a t-test comparing Run 2 and Run 1 (see Table 4.3). As we hypothesised that the mean activation of the OFC during Run 2 would be higher than during Run 1, we first performed a one-tailed test. Indeed, we found that the overall bilateral OFC activation was higher during Run 2, which specifically assessed the reality filtering mechanism, than during Run 1 ($T(21) = 2.12$, $p_{(bonf)} = 0.04$). Secondly, we performed a one-tailed t-test to compare the condition levels, with the hypothesis that the OFC would present a higher activity

Comparison	t-statistic	p-value
Run 2 > Run 1	2.1172	0.04
D > T	3.7002	0.0006
D2 > T2	2.41	0.01

Table 4.3 – Post-hoc T-tests on activation in the OFC. D = Distractors; T = Targets; D2 = Distractors during Run 2; T2 = Targets during Run 2.

while processing distractors (D) than targets (T) all Run 1 and Run 2 together. This effect was also highly significant ($T(21) = 3.70$, $p_{(bonf)} = 0.0006$). The comparison between D2 and T2 (distractors and targets from the second run, respectively) showed that their means were also significantly different in the same direction ($T(21) = 2.41$, $p = 0.01$). Figure 4.5 shows the voxelwise contribution to these results.

4.1.4 Discussion

With this study we assessed for the first time in a young population and using fMRI, the neural correlates of ORFi, a memory control mechanism crucial to maintain thoughts and behaviour in phase with reality.

Behaviourally, participants performed the test without difficulties, no differences in the accuracy were found, neither between the two types of stimuli (Distractors and Targets) nor between the two runs (1, 2). Moreover, the majority of participants performed well, making very few errors. This is similar to healthy adults, who had no difficulties to correctly perform the task even when runs were separated by only 1 minute (Schnider and Ptak, 1999; Wahlen et al., 2011). Our results corroborate the idea that at this age ORFi is already an intuitive and efficacious cognitive process, corresponding to the storage capacity at that age (Liverani et al., 2017).

Regarding reaction times, responses were slower in the second run of the task compared to the first run, reflecting the main challenge of the task, which is consistent with previous studies (Bouzerda-Wahlen et al., 2015; Liverani et al., 2016, 2017). It appears that distinguishing between memories that are pertinent with the ongoing reality or not is more time consuming and takes more cognitive effort than simply recognising previously seen images. Our previous study assessing orbitofrontal reality filtering in children highlighted a significant difference between Distractors and Targets both for accuracy and reaction times (Liverani et al., 2017). In the current study participants were older, and they managed to distinguish almost perfectly between images seen in the current or previous run, performing at ceiling effect. Therefore, this could explain why no differences in accuracy and reaction time have been found between the two conditions.

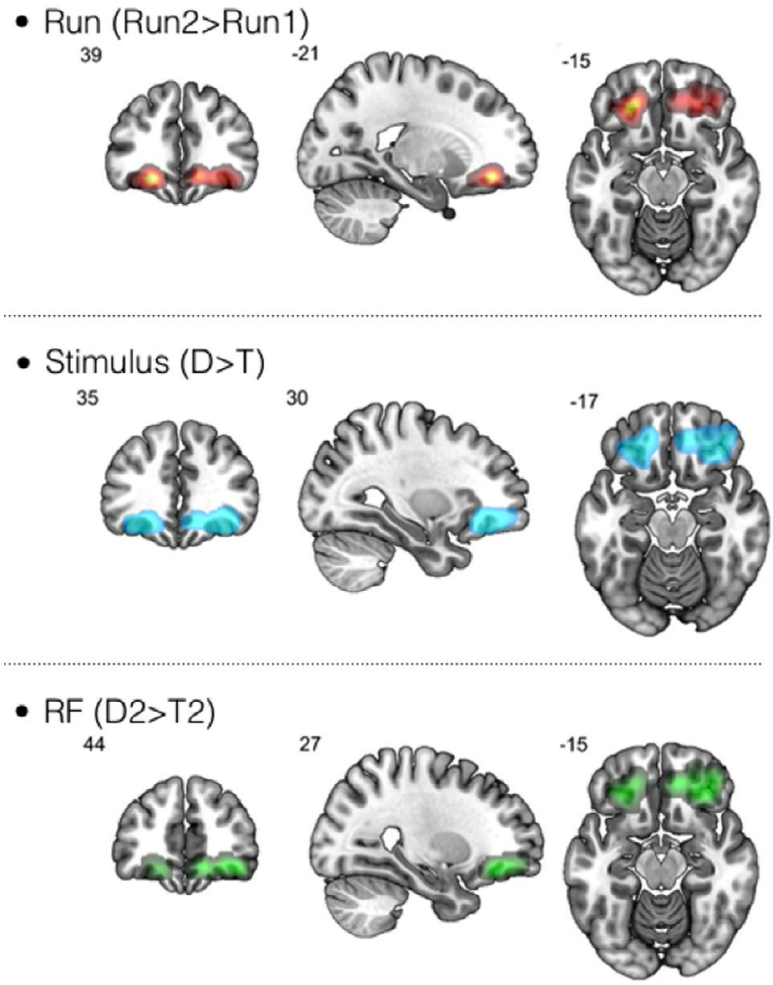

Figure 4.5 – **Voxelwise contribution to each effect.** Brighter colours indicate a stronger contribution. D = Distractors; T = Target; D2 = Distractor stimuli during the second run; T2 = Target stimuli during the second run.

OFC activation was significantly stronger during the second run, which tests ORFi. Thus, our neuroimaging data in early adolescents were in line with lesion and imaging studies in adults, indicating that in this younger population, like in adults, the ORFi mechanism is needed to accomplish the second run of the task, and it is associated with specific OFC activation. Moreover, compared to Targets, OFC activation significantly increases in response to Distractors, stimuli that specifically require ORFi. Thus, using fMRI to explore ORFi for the first time, we confirmed previous findings showing that the ability to select information pertaining to the ongoing reality and to suppress irrelevant memory traces is associated with the activation of the OFC.

Another added value of our study is that it extends these findings to a younger population: early adolescents aged between 10 and 13. Adolescence is a critical period in the development

of the prefrontal cortex. There is a general consensus that the OFC – and the whole PFC – reaches complete maturity only at 20 years of age or more (Diamond, 2002; Gogtay et al., 2004; Galvan et al., 2006). Grey matter volume in the prefrontal cortex attains its maximal volume between 11 and 12 years old and then starts to decrease (Giedd et al., 1999), with a parallel improvement in cognitive functions such as source memory (SOWELL et al., 2001). Given the late development of these prefrontal regions, one might speculate that the neural substrates of certain cognitive functions differ from early adolescence to adulthood. Nevertheless, our findings showing OFC activation while performing the reality filtering task in early adolescents of 10 to 13 years old indicate that this brain structure has matured enough to assume this function.

The filtering of current irrelevant memories – that is, ORFi – bears conceptual resemblance with inhibitory control, defined as the ability to deliberately inhibit dominant, automatic or prepotent responses that are currently irrelevant (Harnishfeger, 1995; St Clair-Thompson and Gathercole, 2006). According to Schnider (2018), ORFi does not effectively "inhibit" memories that are not pertinent with the ongoing reality, but it adapts their format, labelling and differentiating them as "fantasy" or "reality". This process allows healthy individuals to then act differently and adequately according to fantasies or daydreams (Nahum et al., 2009; Schnider, 2018). Behavioural and neuroimaging data support this dissociation between ORFi and inhibitory control. Firstly, the ability to reject memories that are irrelevant to the present moment is already effective at the age of 7 (Liverani et al., 2017) and does not correlate with behavioural inhibition measures, which is one of the last high-order functions to develop, continuing to consistently improve during adolescence Luna et al. (2010). Secondly, the present study confirms that the neural basis of ORFi already resides in the OFC by the age of 10. This finding corroborates the anatomical dissociation between the two mechanisms, since inhibition of unwanted memories has been associated with the activation of other prefrontal regions, such as dorsolateral prefrontal cortex, inferior frontal gyrus, and medio-temporal lobe (Anderson, 2004; Luna et al., 2010).

In addition to being separate from inhibition processes, ORFi also needs to be differentiated from another memory monitoring ability, called source monitoring. Source monitoring is defined as the ability to accurately verify under which circumstances a memory has been acquired, and if it was self-generated or not (Mitchell and Johnson, 2009). Previous studies demonstrated a behavioural and electrophysiological dissociation between the two mechanisms (Bouzerda-Wahlen et al., 2015). Behaviourally, the retrieval of the source of a memory is a more demanding process compared to ORFi, as indicated by slower reaction times and higher error rates. Electrophysiologically, ORFi is characterised by a frontal positivity at 200-300 ms, while source monitoring is associated with a prolonged positivity from 400 ms onwards (Bouzerda-Wahlen et al., 2015). Unlike ORFi, the developmental trajectory of source monitoring is unclear: young children may be more prone than adults to confuse memories from different sources (Lindsay et al., 1991), but the debate is still open. Anatomically, different brain areas participate in source monitoring, including the precuneus (Lundstrom et al., 2005), the medial-temporal lobe (Ross and Slotnick, 2008), and the prefrontal cortex

(Mitchell et al., 2004; Mitchell and Johnson, 2009) but not the OFC, specifically. Even if more whole-brain exploratory analyses would be needed, our results indicate a distinct activation pattern between ORFi and source monitoring. This corroborates the idea of the existence of two separate memory-monitoring mechanisms that dissociate at the behavioural, anatomical and electrophysiological level.

Given the crucial importance of ORFi for the correct adaptation of behavioural demands in everyday life, it is of major interest to better investigate what is the impact of a deficit in this mechanism in other clinical populations characterised by lesions or atypical development in the OFC region. One promising field of research concerns schizophrenia, a psychiatric condition associated with loss of grey matter in this region. Indeed, recent studies showed that an abnormal ORFi activation can be an early biomarker of schizophrenia spectrum disorder (Thézé et al., 2019). Another population characterised by specific alteration in the OFC region is preterm-born children (Gimenez et al., 2006). Up to now, no studies assessing the function of the OFC in the context of preterm birth have been done. Future research should address this point, using the paradigm assessing ORFi as a reliable task to explore OFC functions in premature children and adolescents.

Conclusion

This research investigated for the first time using fMRI technique the neural correlates of orbitofrontal reality filtering in early adolescents. Results showed that, as in adults, the orbitofrontal cortex is involved in filtering memories and thoughts according to their relevance to the present in this young population.

Acknowledgements

This work was supported by the Swiss National Science Foundation (PI P.S. Hüppi, Number 324730_163084) and the Fondation Campus Biotech Geneva (FCBG), a foundation of the Swiss Federal Institute of Technology Lausanne (EPFL), the University of Geneva (UniGe), and the Hôpitaux Universitaires de Genève (HUG). The authors thank Loan Mattera for her precious help in data acquisition and for her constructive suggestions.

Conflicts of interest

We wish to confirm that there are no known conflicts of interest associated with this publication and there has been no significant financial support for this work that could have influenced its outcome.

Data availability statement

The data that support the findings of this study are available from the corresponding author upon reasonable request.

4.2 Journal Article: Altered orbitofrontal activation in preterm-born young adolescents during performance of a reality filtering task

(Preprint or article to submit to Cerebral Cortex)

Lorena G. A. Freitas[1,2], Maria Chiara Liverani[1], Vanessa Siffredi[1,2], Cristina Borradori Tolsa[1], Russia Ha-Vinh Leuchter[1], Dimitri Van De Ville[2], Petra S. Hüppi[1]

[1] Department of Paediatrics, Gynecology and Obstetrics, Division of Development and Growth, Geneva University Hospitals, 6 rue Willy – Donzé, 1205 Geneva, Switzerland
[2] Institute of Bioengineering, École Polytechnique Fédérale de Lausanne, Rue Cantonale, 1015 Lausanne, Switzerland

Abstract

Preterm birth — that is, before 37 full weeks of gestational age — is one of the predominant risk factors for neurodevelopmental problems, and has been associated with a wide range of impairments in cognitive functions spanning attention, working memory, executive functions, among others. Understanding the neurological underpinnings of these difficulties is crucial to identify potential interventions and establish critical periods to restore typical development. Indeed, neuroimaging studies have highlighted widespread alterations in regions such as the prefrontal cortex's structure and function in preterm individuals across lifetime.

Reality filtering (RF) — the ability to distinguish if a thought is relevant to present reality or not — has been found to be mediated by the orbitofrontal cortex (OFC) in adults and typically developing early adolescents. Since this region is particularly vulnerable in individuals born prematurely, our aim was to investigate whether they rely on the OFC to complete an RF task.

Here, we compare the neural correlates of reality filtering in early adolescents born preterm with fullterm-born controls. Our findings indicate that the preterm group show lower activation of the OFC during performance of an RF task than controls, despite being able to successfully perform the task, with no significant increase in activation in other brain regions. This suggests that our preterm cohort have developed optimal mechanisms for reality filtering processing that do not require full activation of the OFC.

Keywords: Preterm, Orbitofrontal Cortex, Reality Filtering; fMRI

4.2.1 Introduction

Preterm birth, defined as when delivery happens before 37 full weeks of gestational age (GA), affects an estimated 11.1% of all live births every year (Blencowe et al., 2013). It has been associated with a wide range of impairments in cognitive functions and is one of the predomi-

nant risk factors for neurodevelopmental problems (Twilhaar et al., 2018), affecting attention (Rommel et al., 2017), working memory (Allotey et al., 2018), affective behaviour (Hornman et al., 2016), executive functions (Costa et al., 2017; Burnett et al., 2018), among others (Moreira et al., 2014; Allotey et al., 2018). Crucially, although some of these difficulties are often unveiled only when children reach school age, it has been shown that they may persist throughout life (Anderson, 2014; Kajantie et al., 2019). Therefore, understanding the neurological underpinnings of these difficulties is paramount to identify potential interventions and establish critical periods to restore typical development (Wolke et al., 2019).

One of the regions that deserve special attention in the context of the premature brain is the orbitofrontal cortex (OFC). It is crucial for a variety of complex and adaptive behaviors, such as affect recognition and emotional reappraisal (Blair, 2000; Adolphs, 2001; Wager et al., 2008; Dixon et al., 2017), assignment of value to a specific stimulus (Montague and Berns, 2002), prediction of specific outcomes (Rudebeck and Murray, 2014), reward processing (Kahnt, 2018) and hedonic experiences (Kringelbach, 2004). Additionally, it is implicated in decision making (Bechara, 2000; McClure et al., 2004), social cognition and appropriate social behavior (Rolls, 2004; Jonker et al., 2015). As part of the prefrontal cortex, the OFC has a critical period of development in the last trimester of pregnancy (Huttenlocher and Dabholkar, 1997; Ruoss et al., 2001). Consequently, OFC maturation is impacted by pretern birth, which usually takes place during this delicate period. The preterm brain can be characterized by brain volume reduction specifically in the OFC (Thompson et al., 2007). Gimenez et al. (2006) showed a reduction in the secondary sulci depth of the OFC, together with a reduced gray matter volume in the same region in very preterm children. Fischi-Gómez et al. (2015) found altered connectivity in the orbitofrontal and the medial network in extreme preterm children, and this weakness correlated with impaired social skills, simultaneous processing and hyperactivity. Cortical thickness in the frontal area, including OFC, has been correlated with internalizing and externalizing behavioral problems, common in premature children (Zubiaurre-Elorza et al., 2012). Finally, Ganella et al. (2015) found an altered distribution of the orbitofrontal sulcogyral folding pattern in adolescents born preterm, which correlated with deficits in executive functions. Taken together, all these data highlight the particular vulnerability of the OFC structure in the brain of individuals who were born prematurely.

While preterm birth has been shown by several neuroimaging studies to be linked to structural, functional and connectivity alterations in the prefrontal cortex (Gimenez et al., 2006; Bjuland et al., 2013; Nosarti et al., 2014; Sripada et al., 2018), to the best of our knowledge studies investigating OFC function are still missing in this context. The aim of our study was thus to fill this gap, using a task that specifically taps into this region while recording the functional activation of the brain in preterm-born young adolescents.

In this study, we look into reality filtering (RF) — a memory-related mechanism that distinguishes if a thought is relevant to current reality or not. In adults (Schnider, 2018) and in typically developing young adolescents aged 10-14 years old (Liverani, Freitas et al., 2020), it is mediated by the OFC. Given this region's vulnerability in the preterm, we examined both

whether this population is able to perform well in an RF task and, if this is the case, whether the OFC is also involved in this population, or a compensation mechanism has been put in place. Finally, we compare the neural correlates of reality filtering (RF) in early adolescents born preterm with fullterm-born controls.

4.2.2 Methods

4.2.2.1 Participants

For this study, twenty-seven healthy term-born (TB) early adolescents from 10 to 14 years of age (12 females, mean age 12 ± 1.01 years) and thirty-seven age-matched preterm-born (PTB) individuals (20 females, mean age 12.1 ± 1.2 years) were recruited through advertisements. One TB participant was excluded due to strong signal distortions on fMRI images caused by the subject's dental braces. One TB and two PTB participants were excluded due to high head-motion. Twenty-five TB and thirty-five PTB participants were finally included in the analysis.

Cognitive assessment at the time of the scan was performed in the same way as described in Liverani, Freitas et al. (2020)'s work (see Section 4.1.2.1). Participants scored within the normal range of intellectual functioning (TB mean = 116.22 ± 11.33; PTB mean = 106.66 ± 11.98). Parents were asked to fill a questionnaire assessing the presence of serious physical illness or neurological problems. None of the participant had major disabilities, psychiatric or neurological diseases.

The Ethics Committee of the Canton of Geneva approved the study, which was carried out in accordance with the Declaration of Helsinki. Caregivers and participants provided informed written consent. All participants received a gift voucher of 100 Swiss francs for their participation in the study upon completion of the protocol.

4.2.2.2 fMRI Paradigm

All participants performed the reality filtering task described in section 4.1.2.2 and illustrated in Figure 4.1 (Liverani, Freitas et al., 2020). In short, subjects performed two runs of an experiment in which a sequence of animal images were shown, and were asked to identify animals that had already been seen within the current run. Images shown for the first time within a run were called "Distractors (D)", while images seen for the second time within that same run were called "Target (T)". The set of images used in both runs were the same, meaning that the second run has the added difficulty of inhibiting the recognition of images seen in the previous run – the ability to perform the second run correctly is key for reality filtering.

4.2.2.3 Image acquisition

MRI data were recorded on a Siemens 3T Magnetom Prisma scanner at Campus Biotech, Geneva, Switzerland. Structural T1-weighted MP-RAGE (Magnetization Prepared Rapid Gradient Echo) sequences were acquired using the following parameters: voxel size = 0.9 x 0.9 x 0.9 mm; repetition time (TR) = 2300 ms; echo time (TE) = 2.32 ms; inversion time (TI) = 900 ms; flip angle (FA) = 8°; field of view (Fov) = 240 mm. Functional images were T2*-weighted with a multislice gradient-echo-planar imaging (EPI) sequence of 64 slices; voxel size = 2 x 2 x 2 mm; TR = 720 ms; TE = 33 ms; Fov = 208 mm. Finally, a fieldmap was acquired each time a participant entered the scanner, with TR = 627 ms; TE1 = 5.19 ms; TE2 = 7.65 ms; and FA = 60°.

4.2.2.4 MRI data preprocessing

Our data were preprocessed using SPM12 (Wellcome Department of Imaging Neuroscience, UCL, UK) in MATLAB R2016a (The MathWorks, Inc., Natick, Massachusetts, United States) as in Liverani, Freitas et al. (2020). The fMRI images from each participant were spatially realigned and unwarped, respectively, to correct for motion artefacts and potential geometric distortions. The unwarping step brings two main advantages: it improves the co-registration between structural and functional images, and reduces the distortion variability across subjects during spatial normalization to a common space (Hutton et al., 2002). Functional images were then coregistered to structural images in subject space and smoothed with a Gaussian filter of full width at half maximum (FWHM) = 6 mm. To be able to perform a group level comparison, data were warped into MNI (Montreal Neurologic Institute) space via a study-specific DARTEL (Diffeomorphic Anatomical Registration using Exponentiated Lie algebra) template. Such normalisation methods have been shown to be robust to age differences in participants from the age of 7 (Ashburber and Friston, 1998; Burgund et al., 2002). In addition, including the DARTEL template as an intermediate step is among the top ranked currently available deformation algorithms (Klein et al., 2009).

4.2.2.5 Head motion

Head motion was assessed in terms of Framewise Displacement (FD; Power et al., 2014). One TB and two PTB subjects for whom more than 20% of frames would be affected by motion (that is, frames with FD > 0.5 mm, one frame before, and two after those) were excluded. For the remaining subjects, total head motion was quite low in both groups: In the control group, for the first fMRI run the mean FD per frame was 0.159 mm with a standard deviation (SD) of ± 0.05 mm; for the second run the mean FD was 0.154 mm ± 0.05 mm; In the Preterm group, for the first fMRI run the mean FD per frame was 0.163 mm with a standard deviation (SD) of ± 0.05 mm; for the second run the mean FD was 0.165 mm ± 0.06 mm. The two groups did not significantly differ in mean FD neither for Run 1 (unpaired t-test, p = 0.74) nor for Run 2 (p = 0.54).

4.2.2.6 fMRI analysis

Whole brain analysis: The fMRI data were analysed using SPM12 (Wellcome Department of Imaging Neuroscience, UCL, UK) in MATLAB R2016a (The MathWorks, Inc., Natick, Massachusetts, United States). For each subject, we built a first-level General Linear Model (GLM) including the condition (Distractor or Target images) regressors, as well as regressors of no interest that might affect the signal. Specifically, to account for effects potentially caused by head motion, we included in our model covariates-of-no-interest calculated in the following fashion: first, we computed the 24-parameter Volterra Expansion (VE) of the 6 motion parameters stored during the realignment step of the preprocessing pipeline. Secondly, we extracted the top 6 components (or those that explained 95% of the variance in the VE) via singular value decomposition (SVD). Then, we included these components as nuisance regressors in the subject-level design matrix. This approach has been successfully used on our previous analyses of child data (Adam-Darque et al., 2018; Liverani, Freitas et al., 2020). Finally, we employed the scan-nulling strategy (Lemieux et al., 2007) to ignore information contained in fMRI images in which FD > 0.5mm, by adding extra regressors-of-no-interest for each of these time points. Finally, the results from this first-level analysis were included in a second-level factorial model including run and condition as factors. Statistical analysis was performed on a voxelwise basis searching for run, group, or interaction effects.

Region of interest (ROI) analysis: Given the known involvement of the orbitofrontal cortex in the Reality filtering task studied here (Schnider, 2018; Liverani, Freitas et al., 2020), we have delved deeper into the analysis of this area as a region of interest (ROI). To avoid confounding the results, the ROI we selected was based on a mask obtained from Neurosynth.org using a combination of 666 independent studies that included the OFC (for details of how the seed was created, see section 4.1.2.6). Group, run and condition effects were analysed using Student's t-tests. Interactions involving any combination of the three were analysed using a factorial analysis of variance (ANOVA).

4.2.3 Results

4.2.3.1 Comparison of whole-brain activation during the two task runs

In order to investigate general differences in activation between the two runs, we performed a second-level analysis where all the participants from both groups were pooled together. These results are depicted in Figure 4.6. During performance of Run 2, three clusters were significantly more active than during Run 1. These are: right superior parietal lobule [MNI coordinates x = -54 y = -18 z = 49; $p_{FWE\text{-}corr} = 0.001$], right amygdala [x = 21 y = -9 z = -18; $p_{FWE\text{-}corr} = 0.01$], and left amygdala [x = -21 y = -9 z = -18; $p_{FWE\text{-}corr} = 0.02$] – see Figure 4.6A. During performance of Run 1, the posterior parietal cortex was more activated [x = 0 y = -51 z = 20; $p_{unc} = 0.001$]. This contrast can be seen in Figure 4.6B.

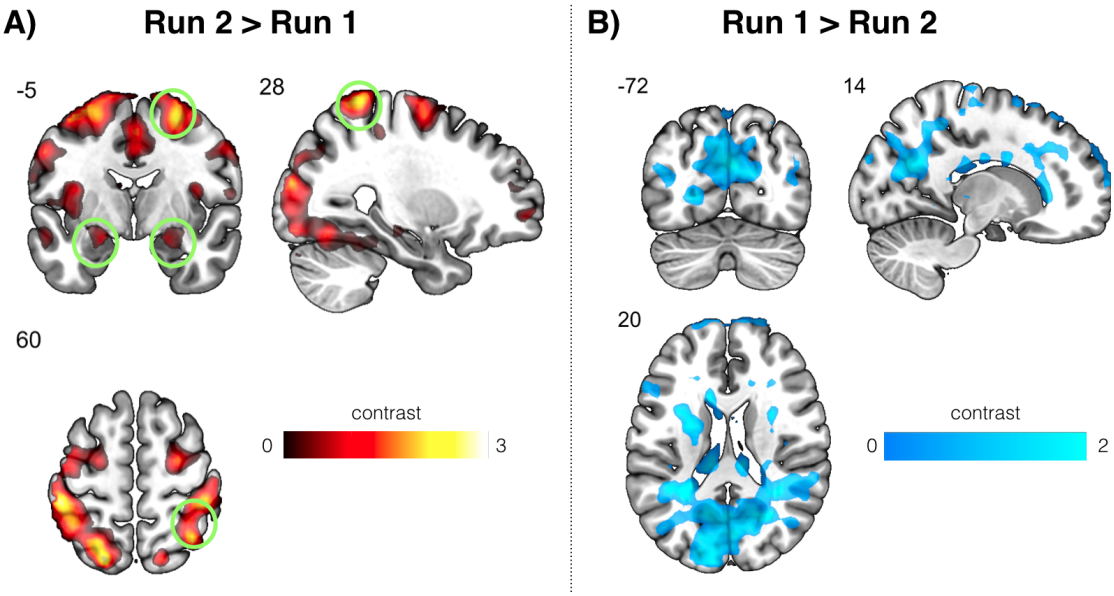

Figure 4.6 – **Comparison between the whole brain activation of the two runs.** The brain maps show regions that were most activated (at $p < 0.001$), with subjects from both groups pooled together A) During Run 2 (relevant for reality filtering), regions typically involved in external attention (*e.g.*, superior parietal lobule) were more more activated than during Run 1. Green circles highlight regions that survived FWE correction at $\alpha = 0.05$. *Post hoc* analysis of activation during the two individual runs indicates that this difference is due to increased activation of these regions during Run 2, as opposed to decreased activity during Run 2. B) During Run 1, regions that typically form networks involved in internally-oriented processes (*e.g.*, default mode network) are more highly activated. *Post hoc* analysis of activation during the two individual runs indicates that this difference is due to increased activation of these regions during Run 1. Note that no regions were significantly more active during Run 1 than during Run 2 after FWE correction.

4.2.3.2 Group comparison of whole-brain activation during the two task runs

We next sought to identify whether there was a group difference in activation during performance of the task runs. These results are illustrated in Figure 4.7. Term-born controls had higher activation of the medial temporal gyrus (MNI coordinates x = -39 y = -39 z = 9; $p = 0.001$, *unc*) and the right orbitofrontal cortex (x = 21 y = 42 z = -9; $p_{\text{FWE-corr}} = 0.02$). *Post hoc* analysis of activation during the two individual runs indicates that this difference is due to increased activation of these regions in the term-born group, as opposed to decreased activity in the preterm group (not shown). Preterm participants showed higher activation in visual attention areas (x = 40 y = -74 z = 20; $p_{\text{FWE-corr}} = 0.04$) and motor areas related to finger movement (x = -42 y = -39 z = 66; $p_{\text{FWE-corr}} = 0.04$) as compared to controls. *Post hoc* analysis of activation during the two individual runs indicates that this difference is due to increased activation of motor regions in the preterm group, and decreased activation in attention areas in the

term-born group.

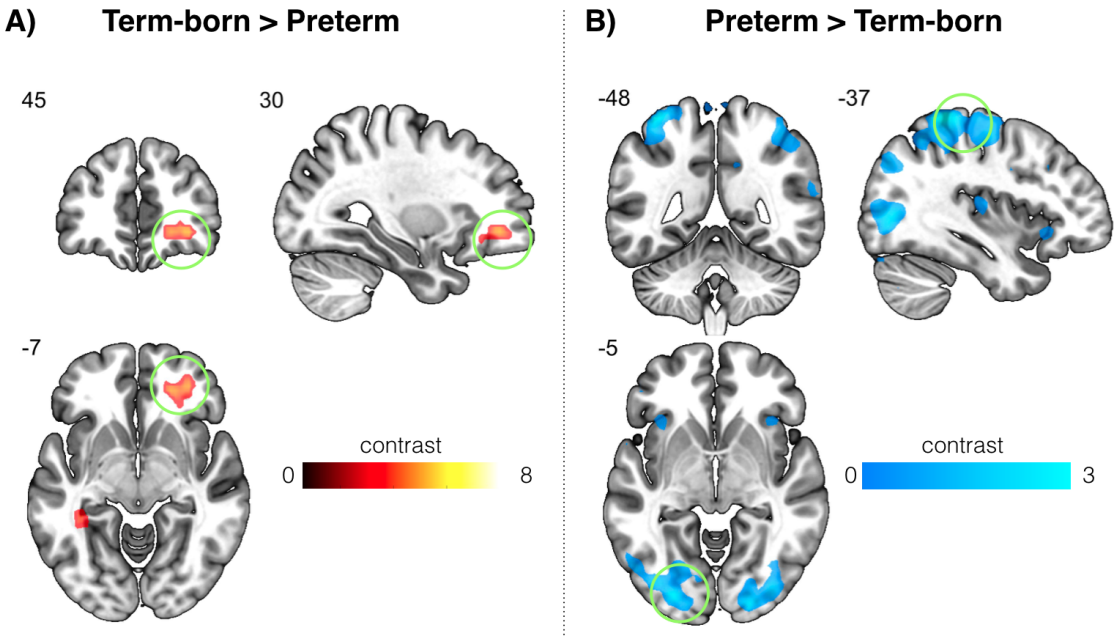

Figure 4.7 – **Group differences in activation across the two runs.** The brain maps show regions that were most activated at height threshold $p = 0.001$, with maps from both runs pooled together. Green circles highlight regions that survived FWE correction at $\alpha = 0.05$. A) Term-born controls had higher activation of the medial temporal gyrus (MNI coordinates x = -39 y = -39 z = 9; $p = 0.001$, *unc*) and the right orbitofrontal cortex (x = 21 y = 42 z = -9; $p_{\text{FWE-corr}} = 0.02$). B) Preterm participants showed higher activation in visual attention areas (x = 40 y = -74 z = 20; $p_{\text{FWE-corr}} = 0.04$) and motor areas related to finger movement (x = -42 y = -39 z = 66; $p_{\text{FWE-corr}} = 0.04$).

4.2.3.3 Interactions between group and run effects

A group versus run interaction contrast identified several clusters as depicted in Figure 4.8. They include the orbitofrontal cortex (x = 15 y = 39 z = -6; $p = 0.001$), nodes of the frontoparietal network such as dorsolateral prefrontal cortex and posterior parietal cortex (x = -24 y = 30 z = 48; $p = 0.001$), insula (x = -43 y = -3 z = -15; $p = 0.001$) and visual attention areas (x = -27 y = -63 z = 21; $p = 0.001$). A *post hoc* comparison between the two runs in the two groups separately revealed that these differences are mainly due to increased activation of these regions during the second run in the control group (Figure 4.8, right).

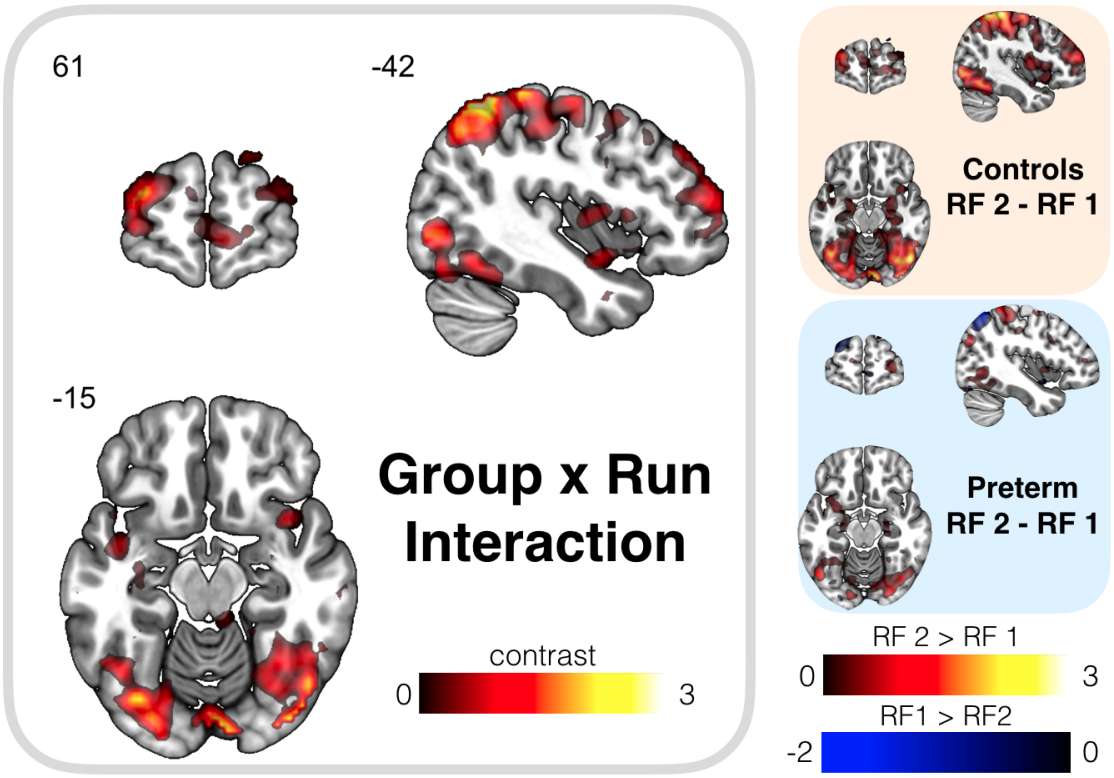

Figure 4.8 – **Group versus Run interaction effects.** (Left) The brain maps show regions whose activation showed an interaction of Group and Run effects at height threshold $p = 0.001$. (Right, orange inset) Contrast between the two runs in the Control group. Red areas indicate higher activation during Run 2 (RF 2), while blue regions indicate higher activation during Run 1 (RF 1). (Right, blue inset) Contrast between the two runs in the preterm group. Red areas indicate higher activation during Run 2, while blue regions indicate higher activation during Run 1.

4.2.3.4 Orbitofrontal cortex as an ROI

An ROI analysis focused on the orbitofrontal cortex (OFC) revealed a Run effect (t = 2.47, $p = 0.007$), where the activation during Run 2 was higher than during Run 1 and a tendency for a Group effect (t = 1.4, $p = 0.05$). Finally, OFC activation during presentation of Distractor images in the reality filtering run (RF2) was higher in controls than in preterm-born individuals (t = 2.38, $p = 0.01$). The ANOVA analysis revealed the interactions shown in Figure 4.9. OFC activation was higher in both groups during performance of the second run (RF 2), and higher in the fullterm-born (Control) group than in the preterm-born group during both runs, but the difference in activation between the two runs was larger in the Control group, as indicated by the steeper slope of the yellow line in the Run vs. Group interaction plot from Figure 4.9. Blood oxygenation level dependent (BOLD) signal was stronger during the presentation of both types of stimuli (Distractor, D; and Target, T) during the second run, and the difference

in activation between runs was larger for stimuli of the Target type, as shown by the red dotted line in the Stimulus vs. Run interaction plot from Figure 4.9. Finally, the control group has a much steeper increase in activation during presentation of Distractor stimuli from moments when Target stimuli where presented, as compared to their preterm peers (orange dotted line in the Group vs. Stimulus interaction plot from Figure 4.9). The difference in activation between groups was higher for Distractor images than for Target images (green full line in the Stimulus vs. Group plot from Figure 4.9). None of the interactions were statistically significant, but the trends identified here are discussed in the next session.

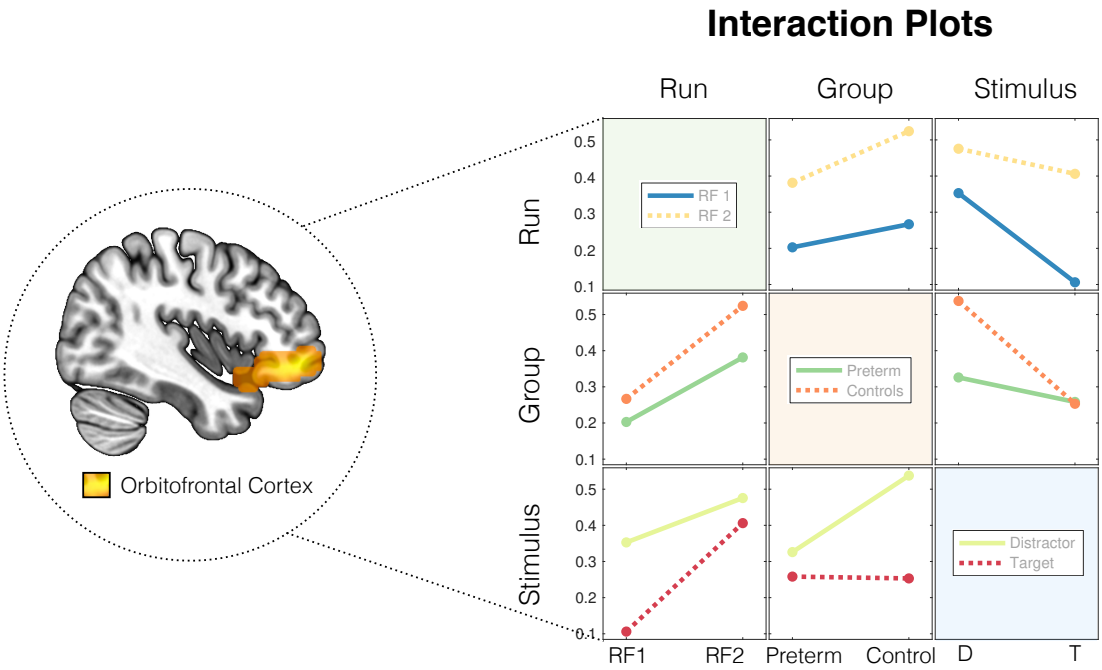

Figure 4.9 – **Group, Run and Stimulus interaction effects in activation of the orbitofrontal cortex as a region of interest.** (Left) The orbitofrontal cortex (sagittal plane with MNI coordinate x = 40). (Right) Interaction plots involving runs, groups and stimulus types. The y-axis of all plots represent the average BOLD signal for the corresponding factor (*e.g.*, run, group or stimulus).

4.2.4 Discussion

4.2.4.1 Comparison of whole-brain activation during the two task runs

During performance of the first run of the experiment, the activation of regions typically involved in internally-oriented attention (*i.e.*, nodes of the default mode network such as the posterior parietal cortex) tended to be higher in comparison to during the second run of the experiment. Given that the same set of images is used for both runs, Run 2 (RF 2) is significantly harder than Run 1. This is because, in Run 2, subjects must not only recognise images that were already seen during the current run, but also suppress memories from the

previous one. The fact that the activation of these areas is higher during the first run is thus in line with previous studies which found that default mode network activation is inversely proportional to task demand (Čeko et al., 2015). This finding may be interpreted as a greater occurrence of moments of introspection or mind-wandering during Run 1 given the ease of the task.

Run 2, in turn, requires more effort since participants must not only recognise images that have already been seen during the current run, but also filter the memory of those images that have only been already seen during the first run. It is thus not surprising that brain regions related to attentional control and information manipulation during working memory-related tasks (Koenigs et al., 2009; Wu et al., 2016) are more highly activated during this run.

Finally, the areas more highly activated during either of the runs are not specific to the task we are studying: in fact, they have been widely found to be part of well-known networks which are involved in other cognitive tasks and / or present during the resting state (van den Heuvel and Hulshoff Pol, 2010). This is probably due to the participants from both groups being pooled together for this part of the analysis —– if they evoke different brain regions to perform the task, these results could be expected to be averaged out when all subjects are grouped together. Our results so far may thus suggest that either participants from the two groups use different underlying mechanisms to perform the reality filtering task, or at least that the level of activation in these two groups differs, decreasing the power to find these task-specific regions.

4.2.4.2 Group comparison of whole-brain activation during the two task runs

We found significant differences in activation during the performance of the reality filtering task when comparing the two groups. We identified increased activation of the orbitofrontal cortex in Term-Born young adolescents as compared to their Preterm-Born peers. By itself, this result could have been achieved under three scenarios: 1) high activation of the OFC in the control group during task performance; 2) de-activation of the OFC in the preterm group; 3) or a combination of the two. The *post hoc* analysis of the individual groups indicated that the first hypothesis is true: this difference is due to high activation of the OFC in the Term-Born participants. The high activation of OFC in the control group is inline with previous work that identify the OFC as a mediator of Reality Filtering in healthy populations (Schnider et al., 2000; Treyer et al., 2003; Bouzerda-Wahlen et al., 2015; Schnider, 2018; Thézé et al., 2019), including our own previous work on healthy young adolescents (Liverani, Freitas et al., 2020). Failure to process reality filtering functions has been a consistent marker of reality confusion in clinical patients with damage in the OFC or in structures directly connected to it (Schnider and Ptak, 1999; Nahum et al., 2012). The fact that the preterm individuals did not activate the OFC as highly may be linked to previous findings of delayed development of frontal areas in this population (Nosarti et al., 2014; Sripada et al., 2018). However, that they are still able to perform the task despite lower activation in the OFC can mean one of two things: either they have developed a more efficient way of performing the same task that requires less use of this

region, or the lack of development of this area has been compensated by other processes. This is further discussed in the next subsection.

Preterm young adolescents had significantly higher activation in motor areas related to finger movement than their Term-Born counterparts. This difference was due to an increase in activation in these areas in the preterm, rather than de-activation in the control group. While this may seem unexpected, given that all participants performed both runs of the task by clicking mouse buttons with the right hand fingers, it is in line with previous research (Heep et al., 2009a; Arichi et al., 2010; Allievi et al., 2016). Heep et al. (2009a) and Arichi et al. (2010) found in separate studies that unilateral motor stimulation led to bilateral activation of the sensorimotor cortex in preterm infants. In our results, regions related to visual attention were also more active in the Preterm than in the control group. This was surprising, since nodes of the attention network have been consistently found to be less active in the preterm population (Olsen et al., 2018). Our inspection of the contrast values for individual groups revealed that this was due to decreased activation of attention-related areas in the control group. This is probably due to the fact that the task was too easy, which is in line with the ceiling effect we observed in the participants' answers.

4.2.4.3 Interactions between whole-brain group and run effects

Although the two runs of our experiment have the same instruction (*i.e.*, to identify images that were repeated during the current run), it is during the second run that reality filtering processing is required. This is because during Run 2, while recognising images as already seen, participants must also decide whether those have been already seen during the current run or only the previous one. Thus, investigating interactions between group and run effects was important for us to further understand what aspects of reality filtering were really different between groups. Although the results from this analysis did not survive multiple comparison correction, they point towards a few interesting trends. For instance, the dorsolateral prefrontal cortex and posterior parietal cortices were more highly activated in the control group during Run 2. These regions are key nodes of the frontoparietal network, which is crucial for the ability to coordinate behaviour in a flexible, accurate and timely manner (Marek and Dosenbach, 2018). In addition, the control group showed higher increase in orbitofrontal cortex activation during the second run than the preterm-born individuals. This is in line with previous research showing that preterm birth is linked to altered development of frontal structure, function and connectivity (Sripada et al., 2018). Interestingly, however, young adolescents born preterm were able to perform the task successfully with a low rate of errors. This may be due to different hypotheses. Firstly, there may be a compensatory mechanism involving other parts of the brain that allow the preterm group to perform the task through different routes. However, no brain areas were significantly more active in this population than in the control group during the second run. An alternative possibility is that the preterm group does indeed rely on the orbitofrontal cortex to perform the task and that, given the alterations in frontal cortices, have developed a more efficient way to perform the task that optimises OFC activation. Finally,

since there was a ceiling effect in the accuracy of the responses from both groups, this could be due to the task having been too easy for this age. Our results indicate the second or third options as potential explanations. However, as discussed in Section 4.2.4.4 (Challenges and Limitations), further studies involving a more difficult version of the task would help clarify this issue.

4.2.4.4 Group, Run and Stimulus interaction effects on OFC activation

Given the known role of the OFC in mediating reality filtering processing, we performed additional analyses using this area as a region of interest. Although the results were not statistically significant (and we discuss the possible reasons in Section 4.2.4.4), the trends we found were extremely interesting, and we chose to report them to serve as a base for future studies. For instance, while the fact that OFC activation was higher in both groups during performance of Run 2, and higher in the fullterm-born (Control) group than in the preterm-born group during both runs agrees with our whole-brain results, this analysis illustrates that the difference in activation between the two runs was larger in the Control group.

BOLD signal in the OFC was stronger in general during the second run independently of the type of stimulus, and the increase in activation was higher for stimuli of the Distractor type rather than of the Target type. This is in line with previous research indicating that the role of the OFC in reality filtering relates to suppressing memories that are not currently relevant (thus while processing images of the Distractor type during Run 2) (Schnider, 2018). Further, the control group shows a larger increase in activation during presentation of Distractor stimuli from moments when Target stimuli where presented, as compared to their preterm peers. Since the young adolescents that were born preterm were able to perform the task with high accuracy, this suggests that this group have found an optimal way to process this function that does not require activation of the OFC to the same levels as typically developing children.

Challenges and future directions

As described before, there is a ceiling effect in the participants from both groups' responses, such that nearly no mistakes were ever made, preventing us from being able to investigate potential correlations between brain activation and accuracy levels. This effect may have been due to the fact that we used the same task that had been described as used for children from 7 years of age. It is thus possible that we have missed higher activation of regions involved in the processing of this task. Future studies involving young adolescents should thus increase the difficulty of the task by methods such as increasing the number of trials, shortening the time for individual trials, and / or adding different types of distractor elements (*e.g.*, images never repeated during Run 1 that reappear during Run 2, and images that appear for the first time in Run 2). By increasing the difficulty of the task in these ways, regions that activate specifically for the reality filtering task may become more evident due to an increased effect. In addition, this will allow us to investigate differences in functional processing of accurately

(versus incorrectly) recognised trials.

Crucially, although there is room for improvement, this study already sheds important light into differences between reality filtering processing in individuals born preterm or at term, and presents compelling avenues for future research.

Conclusion

In this study, we investigated the neurological underpinnings of a reality filtering task performance in young adolescents born prematurely as compared to their term-born peers. We identified differences in activation in the two groups while performing the two steps of the task and framed them within previous knowledge on preterm birth and reality filtering processing. Our results corroborate the idea that compensatory mechanisms are in place to make up for preterm birth-related difficulties, allowing individuals to perform functional tasks. Such results may be used as biomarkers for future studies on potential interventions to help this population.

Acknowledgements

This work was supported by the Swiss National Science Foundation, grant no. 324730-163084 to PSH. The authors thank Loan Mattera, Roberto Martuzzi and Greta Mikneviciute for their help in data acquisition.

Conflict of Interest Statement

The authors declare that the research was conducted in the absence of any commercial or financial relationships that could be construed as a potential conflict of interest.

5 Time-resolved brain dynamics during task performance

Dynamic approaches to analyse resting-state data have blossomed in recent years (Chang and Glover, 2010; Preti et al., 2017), but task-related paradigms to study cognition are yet to fully benefit from these methods. Most analyses available to date are based on sliding-window procedures (Kucyi and Davis, 2014; Di et al., 2015; Gonzalez-Castillo and Bandettini, 2018), thus relying on averaging over relatively long intervals of data. As a consequence, these methods do not fully explore the dynamic range that fMRI is able to unveil, which is down to sub-second scale. Point process analysis (Tagliazucchi et al., 2012; Liu and Duyn, 2013) select subsets of single fMRI frames when a seed is highly active and, when those are clustered, reoccurring patterns are unveiled containing all regions that co-activate with that region of interest. This allows brain function to be linked to specific moments of the experiment at frame resolution.

With the above in mind, in this chapter I introduce a method to examine moment-to-moment changes in brain connectivity during performance of a task, which has been published in the peer-reviewed journal NeuroImage (Freitas et al., 2020). I illustrate that this analysis captures information on brain function which is impossible to obtain using conventional static approaches. Given its ability to concentrate the analysis on limited amounts of data, this represents a promising avenue for the study of the dynamic features of task-modulated brain function in clinical or young populations. Therefore, on a second study, I apply this method to a data set in which preterm-born young adolescents and age-matched controls perform a task which involves movie watching and emotion regulation. We thus argue that explicitly examining changes in connectivity patterns is paramount to advance our understanding of how different brain areas dynamically communicate when presented with a set of cues, and of what abnormalities may arise in this interplay as a consequence of clinical conditions such as preterm birth.

5.1 Journal Article: Time-resolved effective connectivity in task fMRI: psychophysiological interactions of co-activation patterns (PPI-CAPs)

(This article has been published in NeuroImage on Volume 212, 15 May 2020)

Lorena G. A. Freitas[a,b,e], Thomas A. W. Bolton[a,b], Benjamin E. Krikler[c], Delphine Jochaut[d], Anne-Lise Giraud[d], Petra S. Hüppi[e], Dimitri Van De Ville[a,b]

[a] Institute of Bioengineering, École Polytechnique Fédérale de Lausanne, Switzerland
[b] Department of Radiology and Medical Informatics, University of Geneva, Switzerland
[c] Department of Physics, University of Bristol, United Kingdom
[d] Department of Basic Neurosciences, University of Geneva, Switzerland
[e] Division of Development and Growth, Department of Pediatrics, University of Geneva, Switzerland

Abstract

Investigating context-dependent modulations of functional connectivity (FC) with functional magnetic resonance imaging is crucial to reveal the neurological underpinnings of cognitive processing. Most current analysis methods hypothesise sustained FC within the duration of a task, but this assumption has been shown too limiting by recent imaging studies. While several methods have been proposed to study functional dynamics during rest, task-based studies are yet to fully disentangle network modulations.

Here, we propose a seed-based method to probe task-dependent modulations of brain activity by revealing psychophysiological interactions of co-activation patterns (PPI-CAPs). This point process-based approach temporally decomposes task-modulated connectivity into dynamic building blocks which cannot be captured by current methods, such as PPI or Dynamic Causal Modelling. Additionally, it identifies the occurrence of co-activation patterns at single frame resolution as opposed to window-based methods.

In a naturalistic setting where participants watched a TV program, we retrieved several patterns of co-activation with a posterior cingulate cortex seed whose occurrence rates and polarity varied depending on the context; on the seed activity; or on an interaction between the two. Moreover, our method exposed the consistency in effective connectivity patterns across subjects and time, allowing us to uncover links between PPI-CAPs and specific stimuli contained in the video.

Our study reveals that explicitly tracking connectivity pattern transients is paramount to advance our understanding of how different brain areas dynamically communicate when presented with a set of cues.

Keywords: PPI-CAPs; Dynamic functional connectivity (dFC); Task fMRI; Psychophysiological interaction (PPI); Co-activation patterns (CAPs); Framewise analysis

5.1.1 Introduction

Since its introduction in the early 1990s (Ogawa et al., 1990), functional magnetic resonance imaging (fMRI) has played a growing role in advancing our knowledge of brain activity. Its technical developments have allowed the study of brain function at increasingly high spatial and, moreover, temporal resolution (Van Essen et al., 2013). Simultaneously, the progress in analysis techniques has exposed the joint importance of, on the one hand, how brain regions activate and, on the other hand, how their activity interacts to support complex cognitive processes. This view of the brain as a network of functionally linked regions has spawned the field of Functional Connectivity (FC) which, traditionally, uses Pearson's correlation to study temporal dependencies between separate brain regions over the duration of an entire resting-state fMRI run—typically in the order of several minutes (van den Heuvel and Hulshoff Pol, 2010).

The discovery that FC significantly fluctuates over time in resting-state fMRI recordings (Chang and Glover, 2010) first suggested that methods driven by averaging over long runs offer an incomplete picture of brain function, which led to a widespread effort to investigate *dynamic* Functional Connectivity (dFC; Hutchison et al., 2013; Calhoun et al., 2014; Preti et al., 2016; Karahanoğlu and Van De Ville, 2017). Since then, several methodological developments have been proposed to capture this feature. The most common technique involves computing a metric characterising FC over gradually shifted temporal windows of data (*sliding window approach*; Leonardi et al., 2013; Allen et al., 2014). While this increases the temporal refinement of the analysis from minutes to several seconds, it cannot fully benefit from the current sub-second resolution of fMRI recordings because a minimal window size of at least 30 seconds is required to obtain reliable correlation estimates (Kucyi and Davis, 2014; Shen et al., 2016; Preti et al., 2016). Furthermore, shorter windows demand more stringent high-pass filtering of the original time courses to avoid spurious correlations due to aliasing, thus limiting the available information (Leonardi and Van De Ville, 2015; Zalesky and Breakspear, 2015).

Essentially, the sliding window approach keeps the idea of computing second-order statistics, but within each window. Dynamic Conditional Correlation (DCC; Lindquist et al., 2014), a method based on multivariate generalized autoregressive conditional heteroskedasticity models, overcomes some of the methodological issues inherent to traditional sliding window correlation by gradually refining the FC estimate with each new sample, thus requiring no *ad hoc* parameter settings. However, the associated gain of performance in capturing meaningful neuronal fluctuations has been inconsistent across studies (Choe et al., 2017; Damaraju et al., 2018). Other extensions include a more systematic use of the wavelet coherence transform (Rack-Gomer and Liu, 2012; Yaesoubi et al., 2015) as originally proposed in the exploratory results of Chang and Glover (2010).

Another category of analyses follows a framewise approach. Good examples of these are point process analysis (PPA)-based methods (Tagliazucchi et al., 2012), which select a subset of frames where a chosen seed is highly active and proceed from there. Liu et al. (2013) benefited from this to identify co-activation patterns (CAPs) by clustering the retained frames into groups of similar activation arrangements. Another way of performing an implicit selection of relevant information is through sparsity-driven detection of neuronal activation time points (through Sparse Paradigm Free Mapping; Caballero Gaudes et al., 2011; Petridou et al., 2013) or moments of transient activity (innovation-driven CAPs; Karahanoglu and Van De Ville, 2015). All of these approaches have been mainly used to study resting-state data.

Unsurprisingly, the dynamic nature of connectivity in the brain is also expressed in the presence of external stimulation or during task performance (Gonzalez-Castillo and Bandettini, 2018). The natural assumption is thus that certain brain areas interact differently during the course of a task experiment. Beta Series Correlations (BSC, Rissman et al.,2004) analysis, for example, reveals the absolute FC between brain regions under different stages of task performance. Another reasonable expectation is that different regions may *change* the way they interact with each other when performing different tasks. These can be studied using methods such as Effective Connectivity (EC) analyses to look into the influence one neural system has on another and how this relationship changes between task settings (which we will refer to as *contexts* or *conditions* in what follows). This can be done using methods as varied as regression models such as Psychophysiological Interaction (PPI) analysis (Friston et al., 1997) and its generalizations (McLaren et al., 2012); differential equation models such as dynamic causal modelling (Friston et al., 2003) and causal dynamic network modelling (Cao et al., 2019); structural equation modelling (Zhuang et al., 2008); and Granger causality (Wen et al., 2013). These approaches, however, do not explicitly reveal moment-to-moment interactions between experimental conditions and brain activity, but rather average over the duration of the task/rest epochs, which is probably too limiting as has been shown from high temporal resolution neuroimaging techniques (Ploner et al., 2009; Zhang et al., 2012). As a natural development from these, window-based approaches to compute time-varying networks have been used to capture changes in task-related functional connectivity (Di et al., 2015; Baczkowski et al., 2017; Ge et al., 2019), although this also comes with known disadvantages as discussed above. Recent studies (*e.g.*, Fransson et al., 2018) have steered away from windowed correlations, but there is still a great need for novel techniques to study how tasks modulate moment-to-moment connectivity at high temporal resolution.

Here, we introduce psychophysiological interaction of co-activation patterns (PPI-CAPs) as a novel seed-based approach to investigate time-resolved effective connectivity. Our aim was to create a method that reveals the modulation of moment-to-moment connectivity between brain regions under a specific context or during performance of a task. To illustrate our framework, we applied PPI-CAPs to an fMRI dataset where subjects were exposed to a naturalistic paradigm by watching a short episode of a TV program containing two types of scenes (conditions). Our method dissected the connectivity patterns elicited by subjects across time, and found several PPI-CAPs with at least one of three possible effects: 1) a seed

effect, indicating that the pattern was highly correlated with the seed activity in general; 2) a condition effect, meaning that the pattern in question was significantly more elicited during one of the types of scenes than during the other one; and 3) an interaction effect, representing an interaction between condition and the relationship of that co-activation pattern with the seed. Additionally, we shed light on the consistency in effective connectivity patterns across subjects and time, allowing to uncover links between PPI-CAPs and specific movie cues. Overall, our approach contributes to the state-of-the-art by unraveling time-resolved, relevant information on brain dynamics during task performance that cannot be captured by other methods.

5.1.2 Methods

We first provide a global overview of the PPI-CAPs analysis pipeline (see Figure 5.1). We start from fMRI data where an experimental modulation has been applied and the timing is known (Figure 5.1A). Similar to the framework of conventional PPA and CAPs, we start by selecting frames at time points when a predefined seed is most highly (de-)activated (Figure 5.1B/C). A static analysis illustrates the relevance of the frames that have been selected (Figure 5.1D). Then, we proceed to the dynamic (PPI-CAPs) analysis (Figure 5.1E/F).

For the static analysis, we first multiply the selected frames by the sign of the seed and the centred modulating term (*i.e.*, the contrast variable, as it encodes knowledge of the task paradigm) at the corresponding time points. Note that this sequence is equivalent to multiplying the original selected frames by the PPI variable, which corresponds to the multiplication of the sign of the seed and the task time courses. The average of these selected frames leads to a proxy of the conventional PPI results (Figure 5.1D, bottom), which we refer to as the *static interaction map* (siMap). For a mathematical motivation as well as a toy example that intuitively illustrates this relationship between conventional PPI and static PPI-CAP analyses, we refer to Appendix B and Supplementary Figure B.1, respectively.

For the dynamic analysis, all the originally retained frames are subjected to K-means++ clustering (Arthur and Vassilvitskii, 2007) as described in Section 5.1.2.3 (Figure 5.1E). This step yields PPI-CAPs, their occurrence in time and the polarity of their constituting frames, which allows us to eventually identify meaningful statistics (*i.e.*, effects of task, seed, or their interaction). The next sections further detail the different steps of the pipeline.

5.1.2.1 Seed-based frame selection

The first step of the PPI-CAPs framework is to select a seed region according to prior knowledge about the task being studied or on an exploratory basis—a good discussion on how to choose a seed can be found in O'Reilly et al. (2012). The fMRI frames in which the seed reaches high magnitude values are then selected for further analysis. We refer to frames in which absolute seed activity is above the stipulated threshold as *suprathreshold frames*.

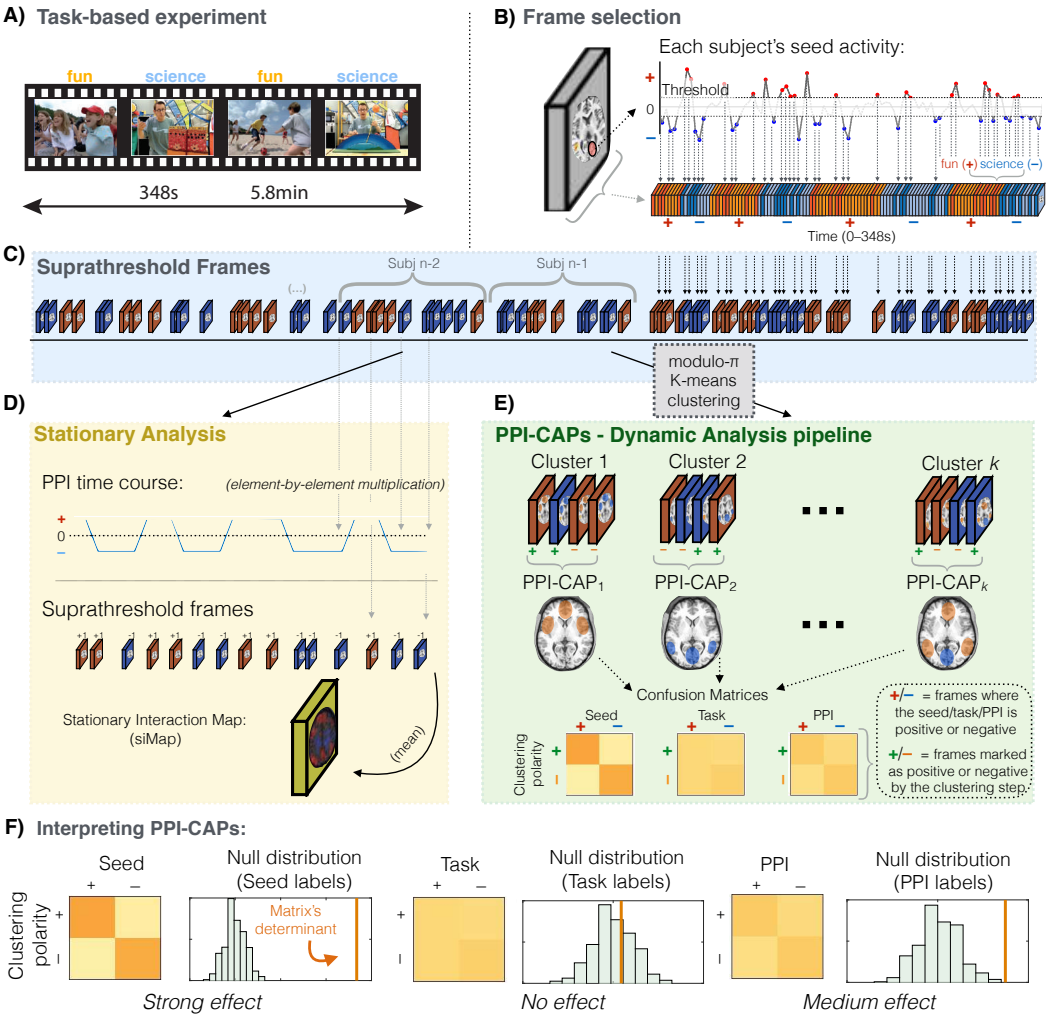

Figure 5.1 – **The PPI-CAPs analysis pipeline.** A) We begin with an experimental design containing different task blocks or contexts. Here, we used data acquired in a naturalistic paradigm in which subjects watched a film containing two main types of scenes: *fun* and *science*. B) For each subject, the z-scored signal from a selected seed is thresholded so that frames in which it is highly active or deactive (darkened in the subject time course) can be considered for further analysis. Orange and blue frames occur during *fun* and *science* scenes, respectively. C) Suprathreshold frames from all subjects are concatenated. From here on, we can proceed to a static or a dynamic analysis. D) Static analysis: suprathreshold frames from each condition are multiplied by the sign of the seed and task time courses (which corresponds to the PPI time course) and then averaged, yielding a proxy of the PPI analysis results: the static interaction map, or siMap, at either subject or group level. E) Dynamic analysis: suprathreshold frames from all subjects are clustered into a set of PPI-CAPs. Frame labels allow us to count how often a PPI-CAP occurs in each condition in its positive or negative polarity and compare these to the signs of each effect of interest. F) The frames' polarity after clustering tends to correlate with the sign of the effects it represents. By examining the confusion matrix for each effect (seed, task or PPI), we can determine if a PPI-CAP is strongly related to it (*i.e.*, when the confusion matrix is highly diagonal) or when there is no such effect (*i.e.*, when the confusion matrix has no obvious pattern).

5.1.2.2 Static analysis

In the context of point process analyses (Tagliazucchi et al., 2012; Liu and Duyn, 2013), simple averaging of selected frames provides a good proxy for seed-based functional connectivity (see Appendix B), showing that the chosen subset of data contains relevant information. For large datasets, this observation holds for a wide range of thresholds retaining 15–90% of frames (Liu and Duyn, 2013, Figure 1B), while for smaller datasets the threshold must aim at a trade-off between dramatically decreasing the amount of data used for analysis while keeping enough frames to reduce the effects of noise. Note that, besides improving the signal-to-noise ratio, including more frames in the analysis of smaller datasets improves the chance that enough frames will be available for the dynamic analysis.

In a similar validation step, we perform an initial static analysis procedure that can be compared against conventional PPI. Specifically, suprathreshold frames were multiplied by a centred contrast variable—the sign of the PPI regressor, as explained in Section 5.1.2—and subsequently averaged (Figure 5.1D, yellow inset). Here, we used the strategy described in Liu and Duyn (2013) to improve the signal-to-noise ratio of an fMRI frame, where a mask was created to cover voxels with the highest 10% and lowest 5% values, and all other voxels were set to zero. The spatial correlation between the resulting static interaction map (siMap) and the PPI results is measured using spatial Pearson's correlation coefficient. This correlation was repeatedly calculated for siMaps including 5–100% of all frames both at subject and group levels, to test the robustness of the method to the choice of threshold. Since correlation values are range-constrained, when calculating their averages as described in Section 5.1.3.1 and shown in Figure 5.2C we first applied Fisher's z transform (the inverse hyperbolic tangent) to all Pearson's r values (Cox, 2008). After calculating the means, we then converted the results back to Pearson's r values by calculating the former's hyperbolic tangent. For the group maps, z-scored seed activations were calculated for all subjects, whose data were concatenated and frames selected as per individual subjects. The PPI analysis was performed using the standard procedure from SPM8 where three regressors are included in a general linear model design, relating to the time courses of the PPI, the seed, and the task, respectively. Note that the PPI regressor in SPM is derived by deconvolving the haemodynamic response function (HRF) from the seed time course, multiplying the latter by the task time course, and then reconvolving the final series with the HRF. The exact same task time course and seed region were used for both analyses.

5.1.2.3 Dynamic analysis

For a dynamic analysis of brain function during task, we identify the PPI-CAPs that may present a seed, task, or interaction effect (Figure 5.1E). To this end, we applied K-means++ clustering on the suprathreshold frames of all subjects, using a *modulo-π* cosine distance as a similarity measure, which we have named as such because it consists in the following: frames among which only the signs of the voxels were reversed were considered to be representations of the same pattern, with opposite polarity (*e.g.*, if frame *a* showed an active prefrontal cortex

and deactive occipital cortex, while frame *b* displayed a deactive prefrontal cortex and active occipital cortex, then, assuming $\mathbf{F}_a$ and $\mathbf{F}_b$ are the frames' voxel patterns, $\mathbf{F}_a \approx -\mathbf{F}_b$).

Traditionally, the iterative algorithm to implement K-means consists of two steps: 1) assigning each data point to its closest centroid given the defined similarity metric *d*; 2) updating the centroids according to their assigned data points (*e.g.*, by updating each centroid with the average of the normalized data points most recently assigned to it). At each iteration, the cluster label assigned to the i^{th} frame, $\mathbf{L}_i$, is given by:

$$\mathbf{L}_i = \underset{\kappa}{\operatorname{argmin}} \big(\mathrm{d}(\mathbf{C}_\kappa, \mathbf{F}_i)\big), \tag{5.1}$$

where κ runs over the number of clusters, $\mathbf{C}_\kappa$ is the value of the κ^{th} cluster's centroid, $\mathbf{F}_i$ is the voxelwise activation pattern for the i^{th} frame, and *d* is the selected distance metric.

To add information regarding the frame polarity in PPI-CAPs, in our approach we set *d* to be the *modulo-π* cosine distance (mpcos):

$$d(\mathbf{x}, \mathbf{y}) = \mathrm{mpcos}(\mathbf{x}, \mathbf{y}) = 1 - \left| \frac{\mathbf{x} \cdot \mathbf{y}}{\|\mathbf{x}\| \ \|\mathbf{y}\|} \right|, \tag{5.2}$$

where $\mathbf{x} \cdot \mathbf{y} = \sum_k x_k y_k$ is the standard inner product and the norm is $\|\mathbf{x}\| = \sqrt{\mathbf{x} \cdot \mathbf{x}}$. The polarity P_i of frame F_i is thus equivalent to $\mathrm{sign}(\mathbf{C}_\kappa \cdot \mathbf{F}_i)$. From here on, we will describe frames for which $P_i = 1$ as having a "positive polarity", and those for which $P_i = -1$ as having a "negative polarity". Note how the metric in equation (5.2) compares to the standard cosine distance, given by:

$$\cos(\mathbf{x}, \mathbf{y}) = 1 - \frac{\mathbf{x} \cdot \mathbf{y}}{\|\mathbf{x}\| \ \|\mathbf{y}\|}, \tag{5.3}$$

meaning that *modulo-π* cosine implies no additional complexity as compared to the standard cosine distance metric. The value of each centroid $\mathbf{C}_\kappa$ is then updated as such:

$$\mathbf{C}_\kappa = \frac{1}{N_\kappa} \sum_{i=1}^{N_\kappa} P_i \frac{\mathbf{F}_i}{\|\mathbf{F}_i\|}, \tag{5.4}$$

where N_κ is the number of frames in the κ^{th} cluster and $\|\mathbf{F}_i\|$ is the magnitude of frame $\mathbf{F_i}$.

The final cluster centroids then form the PPI-CAPs. Each frame is thus annotated according to: 1) the time point it corresponds to; 2) the task or condition label which corresponds to that time; 3) the subject to whom it belongs; and 4) the polarity in which it occurred (positive or negative). This information can then be used to investigate differences in PPI-CAP occurrence across settings.

5.1.2.4 Significance assessment

If a PPI-CAP has a strong main or interaction effect, the polarity of the frames that constitute it will tend to correlate with the sign of that effect for the same time points. To visualise if this is the case, we can thus generate confusion matrices for each effect and PPI-CAP. When there is a strong correlation, the higher values of a confusion matrix will tend to load on one of its diagonals, and the relevance of this relationship can be measured by taking the matrix's determinant, which we will call the *det-index*. To test whether this value is significant, we can thus generate a null distribution by performing random permutations of the effect of interest's labels and re-calculate the det-index each time. Finally, we see where the real det-index stands in the distribution (Figure 5.1F). For the results shown here, we performed 3000 random permutations for each test. We disclose the uncorrected p-values and indicate the significance level that should be used to correct for multiple corrections, controlling for the number of PPI-CAPs.

5.1.2.5 Choosing the number of PPI-CAPs

Effective Connectivity methods such as PPI provide a summary spatial map of task-specific seed relationship modulation. To disentangle which and when instantaneous patterns of activity support the summarized PPI findings, we must first determine the number of clusters into which to categorize the data. To this end, we employed Consensus Clustering (Monti et al., 2003). This approach applies K-means clustering on several subsamples of the data and calculates the *consensus matrix* $\mathscr{M}$. Each element $\mathscr{M}(a,b)$ indicates the fraction of subsamples in which two frames a and b were both retained and clustered together. The optimal number of clusters can then be inferred by visual inspection of the ordered matrix $\mathscr{M}$, as well as of the cumulative distribution function (CDF) of $\mathscr{M}$ for different values of k.

Additionally, for every $k = 3,4,...,8$ we calculated the number of frames from each subject that contributed to each of the k PPI-CAPs. This helped us choose a k value for which the distribution of PPI-CAPs across subjects was roughly uniform. We applied consensus clustering for $k = 3,4,...,8$ using 10 random subsamples for every k. Each subsample included 80 % of the suprathreshold frames of all subjects, and K-means was computed for 50 random initialisations for each subsample. To obtain the final clustering result, we applied K-means clustering with the optimum k on 100 % of the suprathreshold frames and kept the best result from 50 random initialisations, *i.e.*, the one that minimised the total sum of modulo-π cosine distances between frames and centroids.

5.1.2.6 Experimental data

To validate the method, we used fMRI data from 16 healthy subjects (mean age 22.92 ± 8.14 years) watching a short TV program about the effects of sun exposure. The video alternated between two contexts: 1) images of several children playing by the beach (from here on

described as *fun*); 2) scenes where scientific concepts were explained in a laboratory (we will call this context *science*). The movie can be watched online[1], and a detailed description of the dataset can be found in Jochaut et al. (2015). One subject was excluded due to high motion for having >25% of frames with framewise displacement (Power et al., 2010) higher than 0.5 mm. Thus, 15 subjects were analysed (mean percentage of scrubbed frames = 2.2%, SD = 5.8%). 179 volumes (Tim-Trio; Siemens, 40 transverse slices, voxel size = 3 mm × 3 mm × 3 mm; repetition time = 2000 ms; echo time = 50 ms; field of view = 192) were available per subject, as well as an anatomical T1-weighted rapid acquisition gradient echo sequence (176 slices, voxel size = 1 mm × 1 mm × 1 mm, field of view = 256), acquired at the end of the scanning. All participants have given their written informed consent, which was approved by the local ethics committee (Biomedical Inserm protocol C08–39).

5.1.2.7 fMRI preprocessing

Functional images were preprocessed using SPM8 (Wellcome Department of Imaging Neuroscience, UK) where they were realigned to correct for head motion; coregistered with structural images; normalized in the Montreal Neurological Institute (MNI) stereotactic space; and spatially smoothed using a 6 mm full width at half maximum isotropic Gaussian kernel. In order to remove haemodynamic temporal blurring and better approximate neural activity, blood oxygenation level-dependent (BOLD) signals were deconvolved with the canonical haemodynamic response function from SPM8. This was done using an implementation of the Wiener filter from spm_peb_ppi.m, an SPM8 function that computes BOLD deconvolution in the context of PPI analyses. Voxels were then z-scored in time (Liu and Duyn, 2013).

5.1.2.8 Considerations for the application of PPI-CAPs

We applied PPI-CAPs on a movie-watching dataset to illustrate its potential to uncover task-related time-resolved effective connectivity in a realistic setting. To this end, the posterior cingulate cortex (PCC) was selected as a seed region for this study due to its well documented connectivity arrangements (Lin et al., 2017) and description as a hub region (Andrews-Hanna et al., 2010). A previous study by our group on transient brain activity also revealed the PCC as the node with the most spatial overlap between networks (Karahanoglu and Van De Ville, 2015). We used SPM8's Check Orthogonality tool to understand how collinear the PCC activity was with our task paradigm, MATLAB's Skewness function to check that the activity was not skewed, and we verified that the magnitude of the seed time course did not correlate with the sign of the task (Supplementary Material B.2). To keep in line with previous work that inspired our method (Liu and Duyn, 2013), we report the thresholding step based on the percentage of data points kept for the dynamic analysis. As discussed later, PPI-CAPs is robust to a very wide range of seed activity thresholds for selecting frames to retain for analysis. For the results presented here, we use 60% of the available frames as a trade-off between optimising data

[1] https://miplab.epfl.ch/index.php/miplife/research/supplement-asd-study

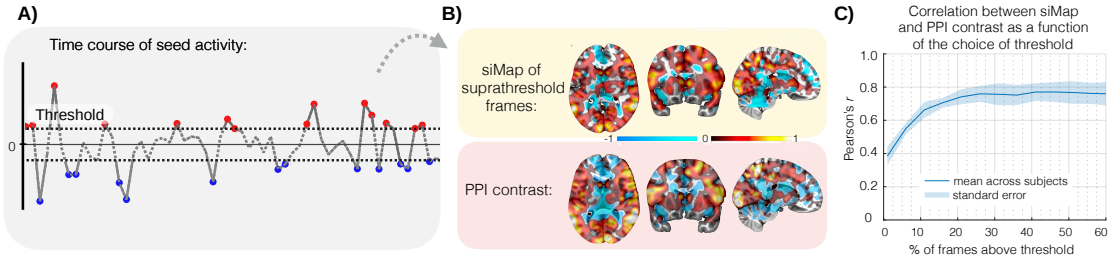

Figure 5.2 – **The static interaction Map (siMap) using a subset of fMRI frames accords with the PPI contrast obtained from all the available data.** A) Frames from time points when the considered seed is highly active are selected. A fraction of seed time course is shown for one subject. B) Retained frames are then multiplied by the PPI variable and averaged, yielding the static interaction map (siMap), as shown for the same subject with a yellow background. For comparison, the contrast map resulting from a PPI analysis using all frames is also shown with a red background. C) The siMap and PPI contrast map are reasonably correlated ($r > 0.7$) even when the former is computed using only 15% of the frames, and this similarity remains high as more frames are used, showing that the selection of relevant frames is robust to the choice of threshold. The dark blue curve represents the average correlation between the siMap and 1st level PPI contrast map across subjects, and the light blue shading denotes the standard error. The correlation means were calculated by averaging Fisher's z transforms of the Pearson's r values, and transforming the result back to Pearson's r.

usage from our dataset and obtaining clear brain patterns in the dynamic analysis, avoiding noise that is not averaged out due to a lack of frames in some PPI-CAPs.

5.1.3 Results

5.1.3.1 Static analysis

Single subject level: At a single subject level, the spatial pattern from the corresponding siMap, generated as the average of the 60% suprathreshold fMRI frames (when the PCC seed was highly active), was reasonably correlated with the resulting map from a 1st level PPI Analysis (average spatial correlation: r=0.76 $\pm$ 0.28). This was the threshold we chose in order to keep enough frames for the dynamic analysis, but the similarity was robust to the choice of threshold for frame selection across subjects (Figure 5.2C): correlation was already high even when only 15% of suprathreshold frames were kept (r=0.71 $\pm$ 0.1). To further illustrate that the correlation strength remains stable for varying cutoff values, we first calculated the mean subject-level Fisher's z-transformed correlations (see Section 5.1.2.2) for each threshold that kept from 15 to 60% of original frames. Then, we computed the average of these means and transformed it back to Pearson's r, for which we obtained 0.76 with SD±0.04. The correlation gradually drops when fewer than 15% of the frames are used, which is expected as not enough frames are selected to average out the noise.

Group level: At the group level, the spatial pattern from the siMap obtained using 60% of frames also correlated (r = 0.85) with the pattern obtained from a 2nd level PPI analysis (Supplementary Figure B.3), which showed a significant increase in effective connectivity between the PCC and the right V5 during *fun* scenes (height threshold T = 3.8, p < 0.001; right V5 MNI coordinates x = 39, y = -67, z = -2; cluster size = 185 voxels; $p_{fwe\text{-}corr} < 0.001$).

Together, these results demonstrate that even a subset of fMRI frames, selected when the seed activity is highly active or strongly deactivated, contains relevant information about how its co-activation with other regions changes based on task context.

5.1.3.2 Dynamic analysis

Choice of number of clusters An analysis of PPI-CAP occurrences for $k = 3, 4, ..., 8$ showed that for $k \geq 6$, some patterns never occurred in some subjects, while $k = 4$ and $k = 5$ were the cases with the most homogeneous distribution of pattern occurrence per subject (see Supplementary Fig. B.4). Visual inspection of the consensus matrices showed that the most stable values for k (*i.e.*, the values for which any two frames would most consistently be clustered together or separately) were $k = 3$ and $k = 4$. Taking these observations together, we proceeded with the analysis generating 4 clusters, as this k value combined the beneficial features of: 1) yielding PPI-CAPs that are homogeneously distributed across subjects; 2) being highly stable (*i.e.*, running the clustering several times would always produce similar results); and 3) representing a reasonable balance between variety and redundancy (Liu and Duyn, 2013).

Temporal decomposition of psychophysiological interactions into co-activation patterns Our dynamic analysis revealed four recurring patterns of co-activation (Fig. 5.3A), all of which were significantly modulated by the seed, the context or an interaction between the two (PPI effect) after correcting for multiple comparisons (significance level $\alpha_{0.05/4} = 0.0125$). PPI-CAP$_1$ includes nodes of the visuospatial (VSN) and attention (AN) networks correlated with the PCC and nodes of the fronto-parietal network (FPN) and salience networks (SN) anti-correlated with the PCC (p = 0.008). Additionally, the VSN and AN had a tendency to be more active, while the FPN and SN were more deactive, during *science* scenes as compared to *fun* ones (p = 0.019). PPI-CAP$_2$ combines the FPN correlated, plus the posterior insula and visual nodes anti-correlated, with the seed (p = 0.0009). PPI-CAP$_3$ corresponds to the default mode network (DMN) and was significantly correlated with the seed (p = 0.0009). It also appeared more often during *fun* scenes rather than *science* ones (p = 0.008). PPI-CAP$_4$, in turn, which contains the V5 and nodes of the VSN, showed not only a significant seed effect (p = 0.0009), but also a PPI effect (p = 0.0009). Supplementary Figure B.6 shows the exact times where each PPI-CAP appeared more consistently in their positive—or negative (meaning that the signs of the voxels should be flipped)—configuration across subjects, and Supplementary Figure B.5 shows their corresponding permutation histograms.

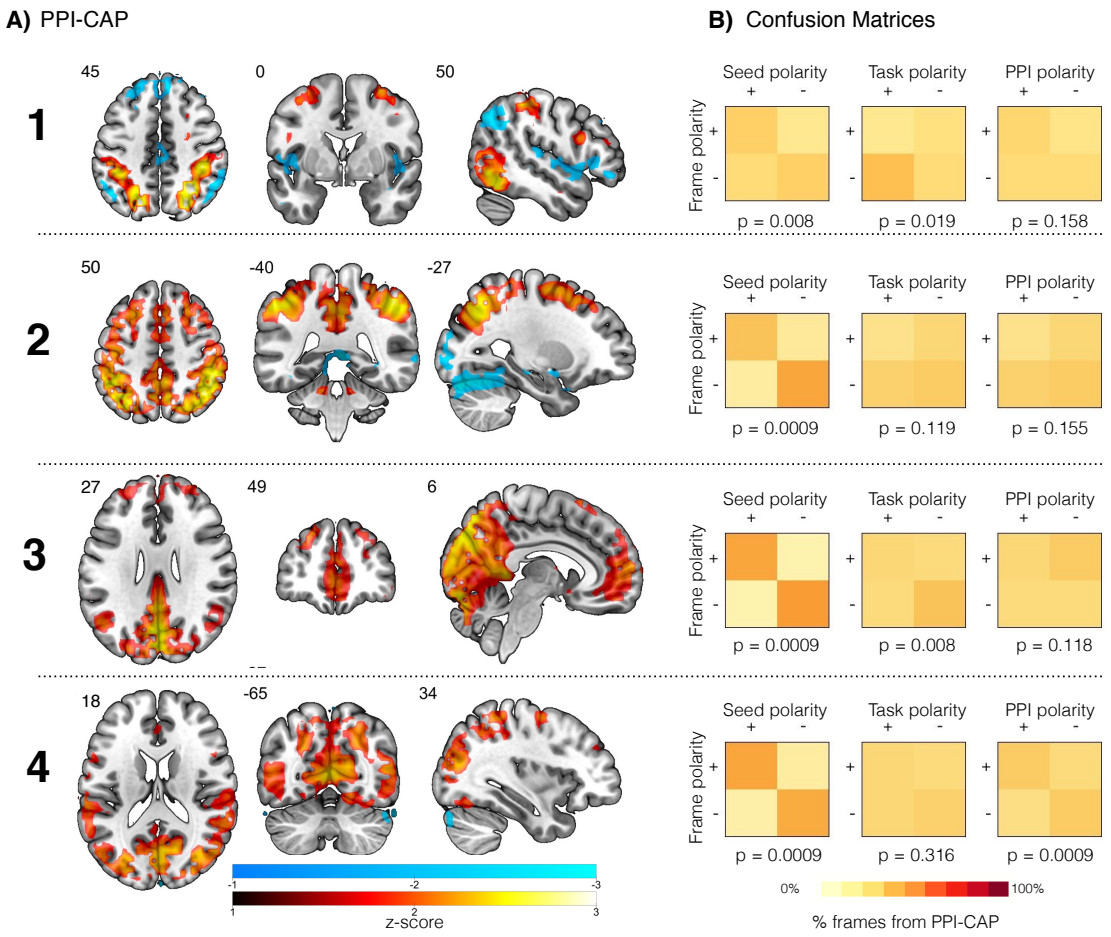

Figure 5.3 – **PPI-CAPs reveal patterns of co-activation that have a seed; task; or an interaction effect.** A) We retrieved four PPI-CAPs from the Movie Watching dataset by clustering suprathreshold frames: PPI-CAP$_1$ includes activated visuospatial and attention networks and deactive nodes of the fronto-parietal network (FPN) and salience networks; PPI-CAP$_2$ includes an activated FPN plus deactive posterior insula and visual nodes; PPI-CAP$_3$ corresponds to nodes of the default mode network; and PPI-CAP$_4$ contains the V5 and visuospatial network. B) Confusion matrices depict how closely the polarity of the frames that make up each PPI-CAP relate to the sign of each effect. A clear diagonal (or anti-diagonal) pattern indicates a strong effect. All PPI-CAPs show a significant seed effect, PPI-CAP$_3$ shows a significant task effect, and PPI-CAP$_4$ shows a significant PPI effect, after Bonferroni correction for the number of PPI-CAPs. Raw p-values reported below the corresponding confusion matrices.

Consistency of PPI-CAPs across subjects and brain activity decoding Our time-resolved method allowed us to investigate how consistent each PPI-CAP was across subjects and throughout the experiment. Figure 5.4 illustrates this analysis for PPI-CAP$_4$. By inspecting moments when the PPI-CAP appeared consistently for several subjects, we were able to identify specific video frames that elicited the co-activation pattern. For PPI-CAP$_4$, moments of positive activation, that is, moments when the V5 and visuospatial network were more active,

corresponded to scenes in which there was high motion (*e.g.*, a group of children playing football), whereas a negative polarity of this pattern was related to moments of stillness (Figure 5.4). Supplementary Figure B.6 shows these results for all four PPI-CAPS: for PPI-CAP_1, moments of positive polarity corresponded to scenes in which the main object (or character) was zoomed into and movements were slow, whereas a negative polarity (meaning a negative VSN and AN, with activated FPN and SN) was related to moments when some goal-oriented action was being performed. For example, at 1'38", while a group of children are sat at the beach, one of the girls is clearly reaching out for sand to build her castle. PPI-CAP_2 seemed to be more strongly active during moments when there are lots of people on the scene, and more consistently negative (*i.e.*, deactivated FPN and activated posterior insula) when the scene changes to only one person on screen, explaining concepts about the danger of sun exposure. PPI-CAP_3 appeared more with a positive polarity during zoomed-out scenes where many people were present and interacting, or when science concepts had been explained for a while in the laboratory scenario. These results illustrate PPI-CAPs' ability to link a pattern's occurrence to specific moments of the experimental paradigm.

5.1.4 Discussion

PPI-CAPs: a tool to more accurately reveal task-based brain dynamics For decades, parametric statistical methods have been used for the analysis of task fMRI data (Friston et al., 1994; Eklund et al., 2016). Notably, the information revealed by the family of PPI approaches, where statistical analysis is performed on fMRI signal time courses to extract brain locations with context-dependent seed correlation, has greatly expanded our knowledge of brain function in health and disease in that time. For instance, Decety et al. (2008) investigated how healthy children experience empathy and moral reasoning when they view someone in pain. The connectivity observed in areas consistently engaged in moral behaviour and social interaction depended highly on intention and on whether the pain was self-inflicted or not, providing an empirical framework for studies of social cognition disorders in children. Steuwe et al. (2015) showed that subcortical limbic and frontal loci become more connected to the locus coeruleus in female post-traumatic stress disorder patients when facing direct eye contact rather than averted gaze, potentially indicating an innate alarm system. More recently, a PPI analysis revealed that music intervention for preterm-born babies in neonatal intensive care units induces functional connectivity changes which suggest that music induces a more arousing and pleasant state (Lordier et al., 2018).

Meanwhile, point process analyses (Tagliazucchi et al., 2012) have proven to be a powerful tool for the study of resting-state brain data, by showing that large-scale brain activity could be condensed by solely analysing the time points when seed activity exceeds a given threshold, while nonetheless closely approximating seed-based correlation findings (Liu et al., 2013).

In this work, we brought the advantages of these two methodologies together to expand the analysis of task-based recordings. Indeed, we showed that after modulation by the centred

Figure 5.4 – **PPI-CAPs enables the time-resolved analysis of effective connectivity consistency across subjects.** For PPI-CAP$_4$: (Top) The plot shows the percentage out of all 15 participants (y-axis) of subjects for whom this PPI-CAP was present at each fMRI frame (x-axis). Red and blue bars indicate the percentage for appearances in positive and negative configurations, respectively. Orange and blue background patches correspond to *fun* and *science* scenes, respectively. The histogram on the rightmost side of the top panel depicts the distribution of random consistency across subjects for each polarity, calculated by randomly permuting the time points on which the PPI-CAP appeared for each subject, then re-calculating the subject consistency across time. The dashed line represents the value of the 99% percentile from the random distribution, indicating that a subject consistency above this threshold is significant. Four sample time points of high consistency were highlighted. Numbers above the brain slices correspond to MNI coordinates. (Bottom) Video frames spanning a duration of 2 seconds, centred at each frame which corresponds to the timing of high consistency indicated in the top plot. For other PPI-CAPs see Supplementary Figure B.6.

contrast variable, averaging as few as 15% fMRI frames with the strongest absolute seed activity yielded a spatial interaction pattern resembling the conventional PPI map calculated from the whole example dataset (Fig. 5.2C).

Beyond this initial equivalence as a first sanity check of the approach, we showed that functional brain connectivity across task conditions could be disentangled into a set of distinct building blocks, the PPI-CAPs, in analogy to the resting-state CAP methodology (Liu and Duyn, 2013; Liu et al., 2018). Whereas a traditional PPI map reflects, *on average*, the functional seed interplays that differ across task conditions, PPI-CAPs break this information down into separate seed co-activation patterns with their own spatiotemporal features. In addition, our approach also extends the information provided by traditional CAPs by capturing interaction effects between the task and the relationship of a co-activation pattern with the seed.

Of note is the fact that the retrieved PPI-CAPs that do not show a context or PPI effect highlight shared functions between task settings, thus displaying common temporal expression features (*i.e.*, similar occurrence levels across conditions). Statistically probing for a context effect enables, then, to distinguish these from co-activation patterns that are indeed task-modulated. This information cannot be obtained from previous PPI approaches. Further, extracting PPI-CAPs also enables the analyst to overcome the caveats arising from multiple comparisons that plague PPI analysis. This is because rather than mass univariate testing, K-means++ clustering (a multivariate, unsupervised technique) is performed to establish characteristic activation patterns, and only then followed by statistical testing on a much lower dimensional space.

Our methodological pipeline also yields polarity labels for each frame that contributes to a PPI-CAP, revealing moments among which a certain pattern has opposite signs—that is, regions that are highly activated in a frame labelled as “positive" will be deactivated in a “negative" frame of that PPI-CAP, and vice-versa. Since a given pattern may contain activated and deactivated voxels simultaneously, this also provides subregion-specific information on their relationship with the seed, task, or both, at any point in time. For instance, for a PPI-CAP whose frames’ polarities correlate with the polarity of the seed (*i.e.*, the confusion matrix with the seed is clearly diagonal), both jointly show their strongest signal values at the same time in all positively labelled frames. Accordingly, areas that appear in blue on that same PPI-CAP represent areas of seed-to-voxel anti-correlation when frames are labelled as positive, and vice-versa. Conversely, when a PPI-CAP has, for instance, a seed effect with the corresponding confusion matrix’s pattern being anti-diagonal, we know that voxels depicted as red are, in fact, discordant with the seed at time points when a negative frame appears. This is why the interpretation of a PPI-CAP requires both the visualization of the co-activation map and the confusion matrix that shows how the polarity labels of its contributing frames relate to each effect’s time course.

In the current version of our method the appearance of a PPI-CAP is defined only by averaging constituting frames, whose labels were assigned automatically during the clustering step. Since the first centroid initialization is made at random by K-means++ clustering, the polarity

labels and, consequently, the pattern of the PPI-CAP they constitute, may be inverted in different runs. If preferred, this could be changed as a post-processing step so that, if desired, the default pattern would be the one with the largest polarity. For example, if a PPI-CAP is made up mainly of negative frames, its flipped version could become the default (meaning that the voxels that currently appear in the pattern as deactive would be shown as active). In this case, the frame polarity labels would therefore be updated for their distribution to be correctly represented in the plots. Alternatively, polarity labels (as well as the pattern formed by the corresponding frames) could be arranged to default to the arrangement that favours a diagonal confusion matrix with the seed, to facilitate the interpretation of voxels in red or blue in relation to that region when there is a seed effect. Yet another option would be for the appearance of a PPI-CAP to default to the one that contains the most activated voxels (with frame labels being updated when necessary). Note, however, that none of these choices affects the interpretation of the results, as switching the labels will also invert the appearance of the PPI-CAP when it is updated as per Equation 5.4, so in the end the conclusions are unchanged; these suggestions are merely for visualization purposes.

Neuroscientific relevance The above touches upon the striking complexity of functional brain activation during a task (Simony et al., 2016; Bolton et al., 2018b; Gonzalez-Castillo and Bandettini, 2018): in this, although standard PPI analysis already provides valuable insight into brain function at the cross-condition level (Kucyi et al., 2016), appropriately capturing truly occurring activity requires the deployment of better temporal resolution approaches as introduced here. Along this line of reasoning, none of the PPI-CAPs extracted in the present study strongly correlated with the results of a second-level PPI analysis ($r_{\text{PPI-CAP}_1}$ = 0.33; $r_{\text{PPI-CAP}_2}$ = -0.07; $r_{\text{PPI-CAP}_3}$ = 0.06; $r_{\text{PPI-CAP}_4}$ = 0.31). The diversity of the patterns revealed by PPI-CAPs in this work confirms the heterogeneity of PCC connectivity to large scale networks seen in previous studies (Liu and Duyn, 2013; Karahanoglu and Van De Ville, 2015), and their occurrence counts reveal how some of these relationships are modulated according to task. This suggests that the results from a conventional PPI analysis may yield a distorted picture of modulated activity as it likely never occurs as presented in the resulting map, and highlights PPI-CAPs' ability to reveal this effect more accurately.

The ability to characterise functional brain changes at the single frame level also offers the advantage to tie PPI-CAPs to specific subparts of the analysed task paradigm (see Spiers and Maguire, 2007 for a more general review on this analytical direction): in the results illustrated here, PPI-CAP_4 (a visuospatial network) occurred upon strong movement during the displayed movie (Figure 5.4), and all four patterns showed consistent, time-locked expression across subjects at specific time points (Supplementary Figure B.6). The vivid and homogeneous recruitment of posterior motion processing areas actually squares well with previous findings considering the same dataset from another methodological angle (Bolton et al., 2018a).

Recently, the fMRI research community has striven to improve robustness and reproducibility by creating *large-scale data* acquisition and sharing initiatives (Van Essen et al., 2013; Poldrack

et al., 2013; Van Horn and Toga, 2014), which brought along novel issues regarding data analysis (Smith and Nichols, 2018; Choudhury et al., 2014). This is because alongside the increase in data size, methods to analyse brain data have become increasingly complex. This combination may make some analyses simply computationally infeasible. It is thus an advantage for new analytical methods to obtain robust results even if running only on a portion of data, thereby circumventing computational cost issues that could make them impractical. From a researcher's point of view, even a linear decrease in computation time is significant, as a reduction of analysis time from weeks to several days can be decisive when trying to meet deadlines. This further highlights the importance of PPI-CAPs' *efficient* use of brain data, which is achieved by selecting a subset that already contains the relevant information needed to uncover our method's novel results.

Potential extensions of the PPI-CAPs approach In the current methodology, PPI-CAPs are derived through a K-means clustering step, and are thus mutually exclusive in time. Previous work has already shown the merit of considering separate brain states to accurately describe task-based data (Leonardi et al., 2014; Gonzalez-Castillo et al., 2015). However, a possible avenue to be explored would be to disentangle patterns that may overlap in time. An interesting option to achieve this would be to translate a recent total variation framework tailored to fMRI data (Karahanoglu and Van De Ville, 2015) to the task-based setting. As part of this new approach, the deconvolution method we currently apply would be replaced by Total Activation (TA) (Karahanoglu et al., 2013), which deconvolves BOLD signals and the haemodynamic response function using spatio-temporal regularisation to recover *activity-inducing signals*. These signals more closely reflect true neuronal activation than the indirect and noisy BOLD signals. Still based on Karahanoglu et al.'s work, by differentiating those, *innovation signals* are obtained—which reflect *changes* in activation intensity rather than pure amplitude. The development of our method would thus be to apply the frame selection and clustering steps on these signals to yield innovation-driven PPI-CAPs, which would represent spatial patterns of voxels whose signals *transition* simultaneously. Backprojecting these would then recover their time courses, thus revealing moments when different combinations of those patterns may overlap.

Another attractive avenue would be to consider the introduction of temporal relationships between successive time points, a feat that can be achieved both when considering sequential (Eavani et al., 2013; Chen et al., 2016; Vidaurre et al., 2017) or overlapping (Sourty et al., 2016; Bolton et al., 2018b) brain states. For instance, given that the present results revealed default mode network (PPI-CAP$_3$), fronto-parietal network (PPI-CAP$_1$ and PPI-CAP$_2$) and salience network (PPI-CAP$_2$) contributions during movie-watching, causal interplays across these networks could be assessed in accordance with the so called triple network model (Menon, 2011).

Aside from addressing temporal dynamics, an equally important issue is to optimally tackle the spatial dimension of the data. One extension could be the injection of a spatial prior in

deriving PPI-CAPs (Zhuang et al., 2018). Another interesting aspect could be to study more closely the spatial variability of task-related functional activity patterns (Kiviniemi et al., 2011). A possible direction for this purpose could be to separately consider, for each PPI-CAP, the pools of frames linked to given task contexts, and carry out statistical comparisons at this level (Amico et al., 2014). Subtle spatial differences across task setting could then be revealed. However, this aspect also depends on the number of clusters used in the analysis: at larger values of K, different spatial patterns across contexts may rather be seen as context-specific PPI-CAPs. Here, given the relatively low amount of available data and the clearly optimal choice of $K = 4$ (Supplementary Figure B.4), we did not pursue this side of the analyses.

Yet other extensions could be, on the one hand, to consider more sophisticated measures than PPI-CAP occurrences as features of interest (Chen and Glover, 2015) and, on the other hand, to broaden the analysis of PPI-CAPs to a meta-state perspective (Miller et al., 2016; Vidaurre et al., 2017), where a meta-state would symbolise a particular combination of expression and polarity of the investigated patterns.

Ultimately, the goal is of course the application of the developed tools to better understand both brain functions in healthy individuals, but also dysfunction in the case of neurological pathologies. Our approach enables us to easily address this last point, by adding a group factor to the employed nonparametric statistical assessment, enabling at the same time to gain insight into which features (seed, task, interaction) relate to the studied disease.

Study considerations A natural limitation of this method is a consequence of the type of data: the spatiotemporal resolution can only be as good as that of the fMRI data used. The threshold for seed activation is the main free parameter in PPI-CAPs, but we showed that, as has been confirmed in other independent studies that followed a PPA approach (Liu et al., 2013; Tagliazucchi et al., 2012), the choice of this value does not affect the results within a very wide range of options. If the magnitude of the seed activity is not correlated with the sign of the task, then the resulting siMap will be proportional to the results of a PPI analysis, and its interpretation can follow the same guidelines as for PPI (see Friston et al., 1997 Figure 5).

Recent work by Cole et al.(2019) has highlighted some challenges related to analysis of task-based functional connectivity. The authors find that simply describing the task paradigm as a dedicated regressor convolved with a canonical HRF, such as in PPI analysis, leaves a relatively large amount of false positives in the data. This is partly explained by the facts that the actual HRF shape varies across regions, and that task-related increases in activation will not necessarily always have the same amplitude, leaving residual activity in the data despite the use of a task regressor. In our work, we consider data that is deconvolved, a step for which we assume a canonical HRF shape. Given the impact of HRF variability on task-based analyses, and the advantage offered by approaches in which the HRF can be modeled individually across regions, future work should enable the use of similar strategies in a deconvolution setting. A second point made by the authors relates to the possible impact of differences in task-evoked

activation amplitude across epochs. In our case, while we consider a naturalistic paradigm, we delineate *fun* and *science* task sub-blocks. There is thus the risk that during one type of block, task-based activation takes varying amplitudes, which would not be accounted for in the modeling of the task. Note that we do not explicitly rely on amplitude information in deriving and interpreting PPI-CAPs: rather, we examine how much the expression of a PPI-CAP (the polarity that it takes) across frames is in line with that of the task paradigm, the seed paradigm, or the PPI. A whole-brain pattern seen in a PPI-CAP thus may jointly represent those three effects. In any case, future work should keep the points above in mind.

Conclusion

We presented a novel analysis that temporally decomposes task-modulated functional connectivity into dynamic building blocks which cannot be captured by static methods such as PPI analysis. We demonstrated that the PPI-CAPs approach successfully identifies dynamic task-dependent patterns using only a subset of the available data, which will lead to a linear decrease in computation time for large datasets proportional to the reduction in data size. Moreover, we illustrated how our method can be used to analyse brain activity at a resolution as low as the scanner's repetition time. Finally, we indicated how our method can expand other existing techniques and proposed new avenues for future research. Taken together, these show that our approach provides a more accurate picture of brain activity during task performance.

Funding

This research was supported by the Swiss National Science Foundation (SNF) [grant number 320030B_182832]. It was also supported in part by the Bertarelli Foundation (to TB and DVDV); the Center for Biomedical Imaging (CIBM); and the National Agency for Research (tempofront grant number 04701 to ALG).

5.2 Journal Article: Tracking moment-to-moment functional connectivity in preterm-born young adolescents during movie watching and emotion regulation

(Preprint with preliminary results)

Lorena G. A. Freitas[a,b,c], Maria Chiara Liverani[c], Vanessa Siffredi[a,c], Cristina Borradori-Tolsa[c], Russia Ha-Vinh Leuchter[c], Dimitri Van De Ville[a,b], Petra S. Hüppi[c]

[a] Institute of Bioengineering, École Polytechnique Fédérale de Lausanne, Switzerland
[b] Department of Radiology and Medical Informatics, University of Geneva, Switzerland
[c] Division of Development and Growth, Department of Pediatrics, University of Geneva, Switzerland

Abstract

Preterm birth is one of the leading causes of impaired neurodevelopment. Some of its consequences only become apparent later in life, impacting children's and their family's lives. The brain is, however, still in development during young adolescence, indicating that this age may be within the intervention window. Understanding the mechanisms of altered brain function in this population is thus paramount to identifying potential interventions. Functional magnetic resonance studies have shown that brain function is highly dynamic at rest and during task performance. Alterations in its complex organisation have been found to lead to impairments in a variety of abilities ranging from cognition to the processing of emotions. Here, we employ psychophysiological interaction of co-activation patterns (PPI-CAPs) analysis to investigate moment-to-moment changes in task-driven modulation of brain activity during a task involving movie watching and emotion regulation. We identify several patterns of co-activation, including one involving the limbic network, which show a main seed; task; or group effects, or an interaction between these. This study highlights the relevance of dynamic approaches to study brain function.

5.2.1 Introduction

Infants born prematurely (*i.e.*, before 37 completed weeks of gestation) are at significantly higher risk for executive and cognitive functions impairment, including difficulties in emotion reactivity and regulation later in life (Evrard et al., 2011; Langerock et al., 2013; Yaari et al., 2018). These abilities are, however, still in plain development during childhood and adolescence, suggesting that this age may still be within the intervention window. In order to identify and develop interventions that promote positive outcomes in this population, it is paramount to understand the neurological underpinnings of these difficulties.

Most neuroimaging studies involving preterm adolescents rely on structural features, relating brain volumes or microstructure to clinical and cognitive outcomes (Hüning et al., 2018; Groeschel et al., 2019; Boardman et al., 2020). These structural studies provide relevant insights into brain injuries that are associated with prematurity and potentially underlie neurocognitive dysfunction, however they cannot provide information on brain activation driven by specific demands. Functional MRI (fMRI) has thus become an increasingly popular approach for this objective. For instance, Johns et al. (2019) have recently found that altered functional connectivity in preterm-born adolescents was linked to socio-emotional impairments.

Of note, studies that investigate dynamic features of brain function and their links to cognition have gained popularity in recent years. For instance, Garrett et al. (2013b) showed that the variability of the blood oxygenation level dependent (BOLD) signal from fMRI is related to cognitive ability at different stages in life. Moving from activation to a connectivity perspective, studies relying on sliding-window approaches have established a link between dynamic functional connectivity (dFC) and executive functions by showing that the former's modulation correlates with ongoing cognitive impairment (Nguyen et al., 2017) and meditative states in children and adolescents (Marusak et al., 2018). Interestingly, using a similar approach, Tobia et al. (2017) found that dFC may be the mechanism responsible for individual variation in emotional responses to stress. Studies that probe into the link between dFC and emotional processing in preterm-born individuals are still largely missing.

A recent development to sliding-window approaches is time-resolved analysis, allowing specific modulations of brain connectivity to be analysed at fMRI frame resolution. Freitas et al. (2020) developed such a method called Psychophysiological Interaction of Co-Activation Patterns (PPI-CAPs) to capture moment-to-moment changes in connectivity during performance of a task. Importantly, the authors showed the method's ability to link dynamic brain states to specific stimulus cues within a Movie Watching (MW) paradigm. Studies including MW tasks have the added benefit of approximating a real-life setting where subjects watch naturalistic videos as opposed to the traditionally constrained experiments used in research (Vanderwal et al., 2019). Naturalistic paradigms are thus intrinsically well-suited for dynamic analyses in clinical populations, as has been recently been shown by Bolton et al. (2020a).

In this study, we employ PPI-CAPs to investigate functional connectivity changes over time in preterm-born young adolescents and an age-matched control group of fullterm-born individuals. Our participants watched a series of emotionally-loaded videos followed by moments of self-regulation while focusing on their own breathing. Our goal was to explore whether moment-to-moment rearrangements between brain regions differ across the two groups in internally- versus externally-oriented tasks.

5.2.2 Methods

5.2.2.1 Participants

Twenty-seven healthy term-born (TB) early adolescents from 10 to 14 years of age (12 females, mean age 12 ± 1.01 years) and thirty-seven age-matched preterm-born (PTB) individuals (20 females, mean age 12.1 ± 1.2 years) were recruited through advertisements. One TB participant was excluded due to strong signal distortions on fMRI images caused by the subject's dental braces. Two TB and twelve PTB participants were excluded due to high head-motion. Twenty-four TB and twenty-five PTB participants were finally included in the analysis.

Cognitive assessment at the time of the scan was performed using the French version of the Wechsler Intelligence Scale for Children – Fifth Edition (WISC - V; Wechsler, 2014). For one participant IQ score was evaluated using the Kaufman Assessment Battery for Children, second edition (KABC-II; Kaufman and Kaufman, 2004). All participants scored within the normal range of intellectual functioning (mean = 117.04 ± 11.35). Parents were asked to fill a questionnaire assessing the presence of serious physical illness or neurological problems. None of the participant had major disabilities, psychiatric or neurological diseases.

The Ethics Committee of the Canton of Geneva approved the study, which was carried out in accordance with the Declaration of Helsinki. Caregivers and participants provided informed written consent. Participants received a gift voucher of 100 Swiss francs for their participation in the study.

5.2.2.2 fMRI Paradigm

Participants received instructions in text form on the screen, which was also read out loud by the experimenter. They were requested to watch a series of 20 s-long videos and instructed to, at the end of each one, relax and focus on their breathing for 20 s. At the end of this interval, the children we asked to rate the video they have watched from *negative* to *positive* on a scale from 1 to 5 by clicking on the corresponding number on the screen, using a mouse. A rating of "1" would mean that the video brings very negative emotions such as fear, sadness or that it is scary, while "5" means it brings very positive emotions such as happiness, laughter, or it was cute. A rating of "3" would thus mean that the video's emotional valence was neutral. At the end of the rating, the trial was finished. This was repeated 12 times for a total time of 12 minutes and 1000 fMRI frames. Participants were asked to move as little as possible in general and especially when rating the videos (*e.g.*, by moving only their wrist rather than the whole arm while making their choice using a mouse). Figure 5.5 illustrates the task paradigm. The 12 videos were selected from a published database (Samson et al., 2016) which includes 300 videos with emotional valence ratings from 75 adult participants. For our selection, we used the following criteria: we chose the 6 most positive videos (excluding those that would be likely to cause bursts of laughter, to avoid motion artefacts in the fMRI scans) and the 6 most repulsive videos (excluding those that would have been too scary, since our study involved

children).

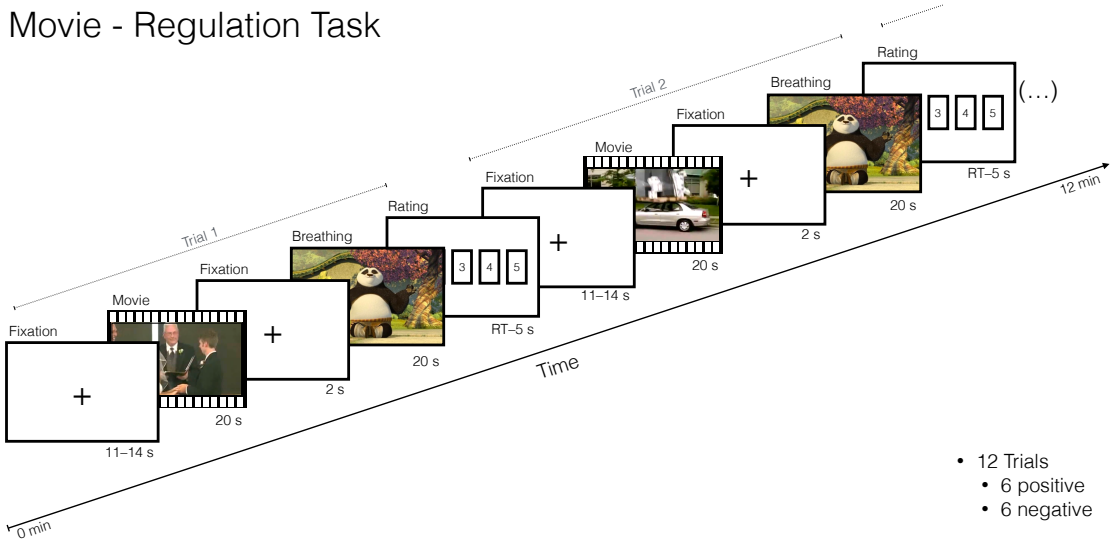

Figure 5.5 – **The movie-regulation task paradigm.** After instructions are shown on the screen and read out loud, the first trial starts with a fixation cross of variable duration, followed by a 20 s-long video. This is followed by a 2 s cross and then a 20 s interval where participants are asked to concentrate on their breathing. At the end of the trial, participants must rate the video on a scale from 1 to 5, where 1 represents "negative" and 5 indicates "positive". Each trial lasts roughly one minute, and the total protocol includes 12 such trials.

5.2.2.3 MRI acquisition

MRI data were acquired on a Siemens 3T Magnetom Prisma scanner at Campus Biotech, Geneva, Switzerland. Structural T1-weighted MP-RAGE (Magnetization Prepared Rapid Gradient Echo) sequences were acquired using the following parameters: voxel size = 0.9 x 0.9 x 0.9 mm; repetition time (TR) = 2300 ms; echo time (TE) = 2.32 ms; inversion time (TI) = 900 ms; flip angle (FA) = 8°; field of view (Fov) = 240 mm. Functional images were T2*-weighted with a multislice gradient-echo-planar imaging (EPI) sequence of 64 slices; voxel size = 2 x 2 x 2 mm; TR = 720 ms; TE = 33 ms; Fov = 208 mm. In addition, a fieldmap was acquired every time a participant entered the scanner, with TR = 627 ms; TE1 = 5.19 ms; TE2 = 7.65 ms; and FA = 60°.

5.2.2.4 MRI data preprocessing

All data were preprocessed using SPM12 (Wellcome Department of Imaging Neuroscience, UCL, UK) in MATLAB R2019a (The MathWorks, Inc., Natick, Massachusetts, United States). The fMRI images from each participant were spatially realigned and unwarped, respectively,

to correct for motion artefacts and potential geometric distortions. The unwarping step brings two main advantages: it improves the co-registration between structural and functional images, and reduces the distortion variability across subjects during spatial normalization to a common space (Hutton et al., 2002). Functional images were then coregistered to structural images in subject space and smoothed with a Gaussian filter of full width at half maximum (FWHM) = 6 mm.

In order to approximate BOLD signals as much as possible to actual brain data, one of the initial steps in PPI-CAPs analysis is to deconvolve the time series with the haemodynamic response function (Freitas et al., 2020). To this end, here we apply total activation (TA) deconvolution (Karahanoglu et al., 2013), a method based on sparse spatio-temporal priors to uncover the underlying activity-inducing signal of fMRI without relying on timing information.

After Total Activation deconvolution, data were warped into MNI (Montreal Neurologic Institute) space via a study-specific DARTEL (Diffeomorphic Anatomical Registration Through Exponentiated Lie algebra) template to be allow group level comparisons. This normalisation method has been shown to be robust to age differences in participants from the age of 7 (Ashburber and Friston, 1998; Burgund et al., 2002) and is among the top ranked currently available deformation algorithms (Klein et al., 2009).

5.2.2.5 Head motion

Head motion was assessed in terms of framewise displacement (FD; Power et al., 2014). Two TB and fourteen PTB subjects for whom more than 20% of frames would be affected by motion (that is, frames with FD > 0.5 mm, one frame before, and two after those) were excluded from further analyses. For the remaining subjects, total head motion was quite low in both groups: In the control group, for the first fMRI run the mean FD per frame was 0.159 mm with a standard deviation (SD) of ± 0.05 mm; for the second run the mean FD was 0.154 mm ± 0.05 mm; In the Preterm group, for the first fMRI run the mean FD per frame was 0.163 mm with a standard deviation (SD) of ± 0.05 mm; for the second run the mean FD was 0.165 mm ± 0.06 mm. The two groups did not significantly differ in mean FD (unpaired t-test, p = 0.65).

5.2.2.6 fMRI analysis

To explore moment-to-moment changes in functional connectivity during movie watching or breathing intervals and to see how this changes across groups, we employed a psychophysiological interaction of co-activation patterns (PPI-CAPs) analysis (Freitas et al., 2020). This approach selects moments in which a seed is highly active and clusters frames based on their activation patterns, allowing positive and negative polarities of the same pattern (that is, moments in which activation patterns have completely opposite signs) to be grouped together. It is then possible to test, for each obtained PPI-CAP, whether it varies according to the seed activity, the task progression, or an interaction between the two.

For this study we selected the dorsal anterior cingulate cortex (ACC) as a seed, as it is a key node of the Salience Network and has been previously shown to be affected by preterm birth in studies involving both static (White et al., 2014b; Daamen et al., 2015; Lordier et al., 2019) and dynamic (Chapter 3) analyses. As all of these studies involved resting-state paradigms so, to the best of our knowledge, this is the first investigation of task-related dynamic ACC connectivity in this population. In addition, to show that interesting task-related dynamics may be found independently of the seed choice, we also conducted the analysis using the PCC as a seed given its description as a hub region (Andrews-Hanna et al., 2010), and its wide variety of connection arrangements (Lin et al., 2017), including during internally- (Raichle, 2001) and externally-oriented cognition (Freitas et al., 2020). These additional results can be found in Supplementary Material Section B.3. In both cases, 30% of the frames in which the seed was most highly (de)active were selected as a trade-off between using less data while keeping enough frames to obtain stable results (Freitas et al., 2020). The clustering step was performed across both groups together, to avoid the problem of matching similar PPI-CAPs between groups if these were calculated separately.

To identify the optimal number of PPI-CAPs that must be retrieve, we performed a Consensus Clustering analysis(Monti et al., 2003). This approach applies K-means clustering on several subsamples of the data and calculates the *consensus matrix* $\mathscr{M}$. Each element $\mathscr{M}(a,b)$ indicates the fraction of subsamples in which two frames a and b were both retained in the subsample and clustered together. The optimal number of clusters can then be inferred by visual inspection of the ordered matrix $\mathscr{M}$, as well as of the cumulative distribution function (CDF) of $\mathscr{M}$ for different values of k. Once the final k was identified, the final clustering step was performed using 100 replicates.

5.2.2.7 Network assignment

After PPI-CAPs were obtained in the clustering step, we identified the regions and networks highlighted in each pattern by comparing them to those from previous studies using two approaches. First, we compared them to the 7 functional networks identified by Thomas Yeo et al. (2011). This was achieved by calculating what proportion of each functional network was activated or deactivated in each PPI-CAP, and then applying the Hungarian Algorithm Munkres (1957) to the resulting matrix, to assign networks to each pattern. In addition, we uploaded the PPI-CAPs' files to NeuroSynth.org (Wager, 2011) and investigated the regions most associated with each PPI-CAP according with the automated meta-analysis tool.

5.2.2.8 Significance assessment

For each PPI-CAP, we tested 3 main (Seed; Task; Group) and 3 interaction (Seed vs. Task, or PPI; Group vs. Task; and Group vs. Seed). If a PPI-CAP has a strong main or interaction effect, the polarity of the frames that constitute it will tend to correlate with the sign of that effect for the same time points. To visualise if this is the case, we can thus generate confusion matrices for

each effect and PPI-CAP. When there is a strong correlation, the higher values of a confusion matrix will tend to load on one of its diagonals, and the relevance of this relationship can be measured by taking the matrix's determinant, or *det-index*. To test whether this value is significant, we generate null distributions by performing random permutations of the effect of interest's labels and re-calculate the det-index each time. Finally, we see where the real det-index stands in the distribution (Figure 5.1F). For this study, we performed 3000 random permutations for each test. We disclose the null distributions and uncorrected p-values in the Supplementary Figures for this chapter and, in the Results Section, indicate effects with significance level $\alpha_{0.05/6} = 0.008$), to correct for the number of PPI-CAPs.

5.2.2.9 Investigation of seed heterogeneity

Finally, we investigated the source of the seed activity to test how heterogeneous the seed was. To this end, we clustered the seed's voxelwise time courses — signed after z-scoring — into three subgroups. We then projected these groups back onto the brain to identify possible subdivisions of the seed and to better understand where the averaged signal likely came from.

5.2.3 Results

5.2.3.1 Consensus clustering

We performed consensus clustering using a K range from 3 to 20 to identify the most stable number of clusters for our data. Visual inspection of the confusion matrices for each value of K, as well as the plot of the proportion of ambiguously clustered frames for each case, identified K = 6 as a clear optimal value. These results can be found in Supplementary Figure B.7

5.2.3.2 Six patterns from ACC-based PPI-CAPs

Clustering ACC-selected frames yielded the patterns shown in Figure 5.6. According to the Hungarian Algorithm-based assignment of networks each PPI-CAP was identified as the following: PPI-CAP_1 corresponds to an activated somatomotor network (SMN) and deactivated default mode network; PPI-CAP_2 is assigned to an activated ventral attention Network, also known as salience network (SN), and deactivated limbic; PPI-CAP_3 contains an activated Visual and deactivated fronto-parietal network (FPN); PPI-CAP_4 includes an activated dorsal attention (DAN) and deactivated visual network; PPI-CAP_5 has an activated FPN and deactivated SMN; and PPI-CAP_6 includes an activated limbic and deactivated DAN. As visual inspection of Figure 5.6 suggests, some CAPs had similarities with more than one network. The full similarity matrix can be found in Figure B.8 in the Supplementary Material for this chapter. For simplicity, we will interpret the results based on the assigned networks.

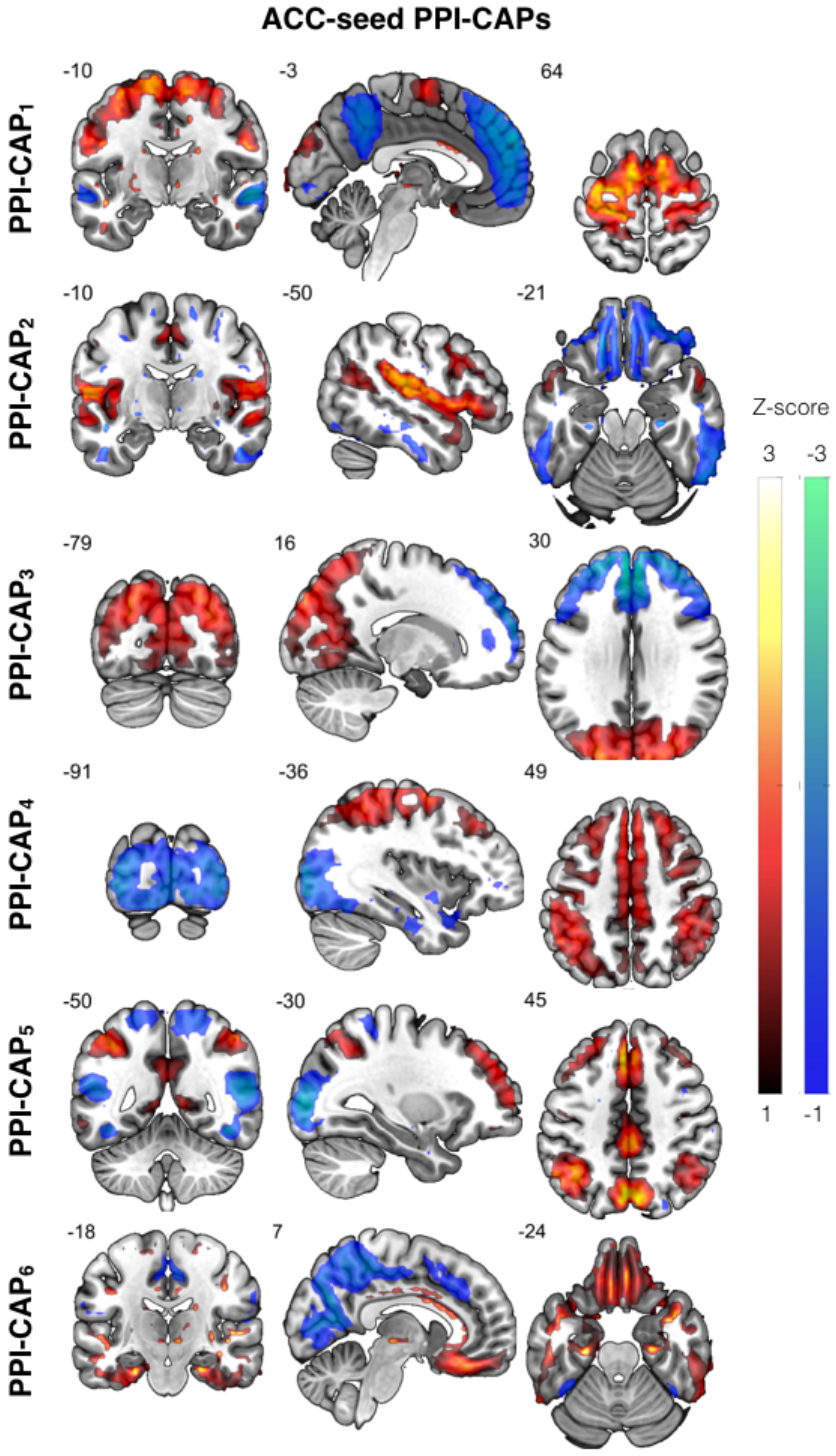

Figure 5.6 – **PPI-CAPs focused on the ACC yield six dynamic patterns.** Using K = 6 for the clustering step as defined in Figure B.7 yielded the six PPI-CAPs above. Each row corresponds to one PPI-CAP, numbers indicate slice coordinates in MNI space.

5.2.3.3 Main and interaction effects

For each PPI-CAP, we tested for main and interaction effects by checking if the flipping of each pattern correlates with the sign of each effect. The resulting confusion matrices can be seen in Figure 5.7. Each row corresponds to a PPI-CAP. Permutation testing then identified which of these effects were significant, which can be seen in Figure B.9 in the Supplementary Material.

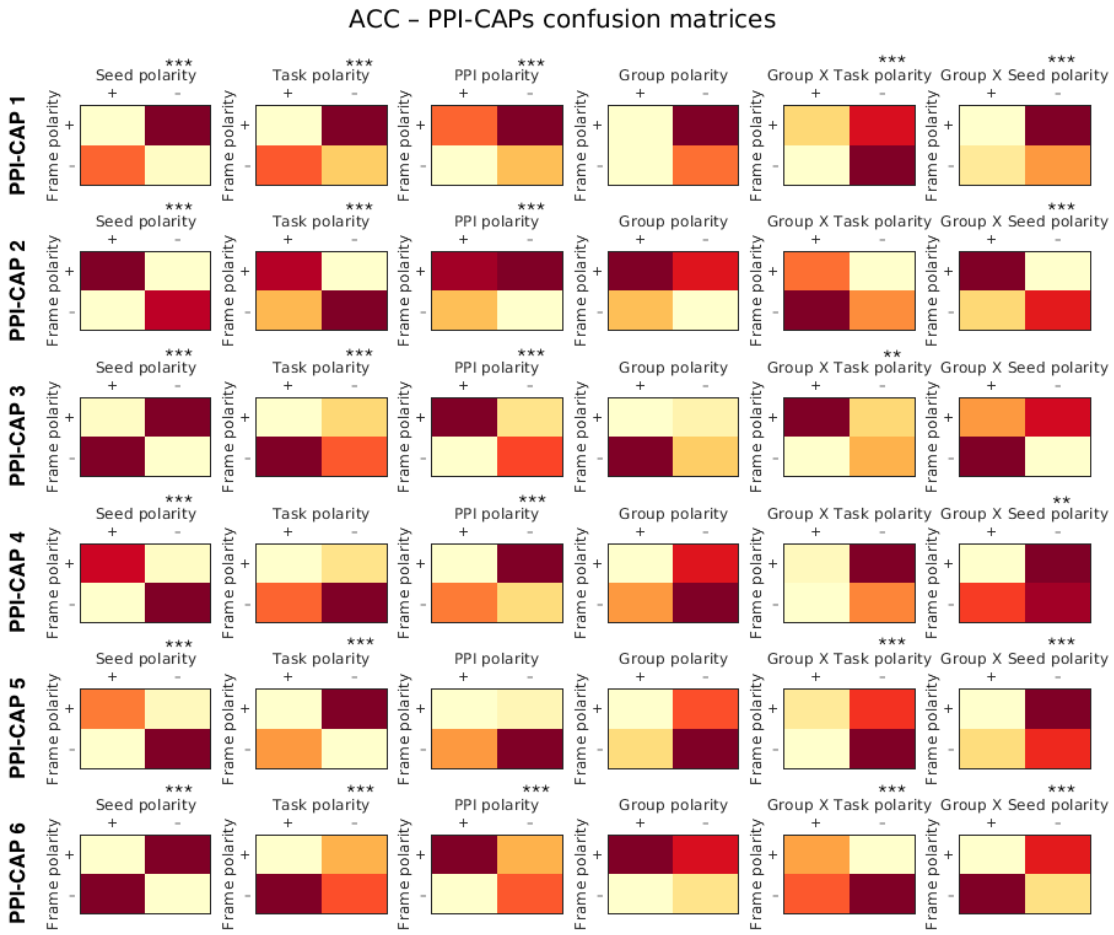

Figure 5.7 – **ACC-seed PPI-CAPs show a variety of main and interaction effects.** To identify main and interaction effects for each PPI-CAP, confusion matrices show how often the sign of a PPI-CAP switches in the same way as each of the effects. We tested three main effects (Seed; Task; and Group) and three interaction effects (Seed vs. Task (PPI); Group vs. Seed; and Group vs. Task). The signs for each effect are as follows: Seed — positive and negative signs correspond to frames when the seed was activated of deactivated, respectively; Task — positive signs correspond to "Movie Watching" while negative signs correspond to moments of "Emotion Regulation"; Group — positive signs correspond to fullterm controls, while negative signs correspond to preterm-born individuals. Interaction signs are calculated as element-by-element multiplication of the main effect signs. Light yellow indicates the lowest number of frames, while dark red indicates the highest number of frames. *** = p<0.001; ** = P<0.008. Significance level $\alpha_{0.05/6} = 0.008$).

Main effects: All the PPI-CAPs showed a significant seed effect at $p < 0.001$ (Figure B.9, first column). As the direction of the diagonals in the first column of Figure 5.7 suggests, PPI-CAPs 2, 4 and 5 we positively correlated with the seed, while PPI-CAPs 1, 3 and 6 were negatively correlated with it. PPI-CAP 2 was positively correlated with the task ($p < 0.001$), meaning that the salience network was more active during the Movie Watching Task. In contrast, PPI-CAPs 1, 3, 5 and 6 were anti-correlated with the task, meaning that the areas shown in red for these patterns in Figure 5.6 tended to be more active during the Emotion Regulation task (all, $p < 0.001$). Only PPI-CAP 1 showed a group effect, occurring more often in the preterm group ($p < 0.03$, uncorrected), with a tendency to appear more often in its positive configuration.

Interaction effects: PPI-CAPs 1, 3, and 6 show a positive interaction between seed and task (PPI effect), meaning that these patterns correlate with the seed more during Movie Watching and are anti-correlated with the ACC during Emotion Regulation (all, $p < 0.001$). In contrast, PPI-CAPs 2 and 4 show a negative PPI effect, such that they correlate more with the seed during Emotion Regulation (all, $p < 0.001$). PPI-CAPs 1 ($p < 0.001$), 3 ($p = 0.002$), 5 ($p < 0.001$) and 6 ($p < 0.001$) have a positive group versus task interaction, such that during Movie Watching, the regions shown in red for these patterns are more often activated in controls than in preterms, while during Emotion Regulation these regions are also more often de-activated for this group. Finally, PPI-CAP 2 has a positive group versus seed interaction effect ($p < 0.001$), while PPI-CAPs 1 ($p < 0.001$), 4 ($p = 0.003$), 5 ($p < 0.001$), and 6 ($p < 0.001$) have a negative group versus seed interaction effect.

5.2.3.4 Seed heterogeneity

Clustering the seed's voxels' based on their signed time courses revealed three clear spatial subdivisions. The averaged seed activation seems to come mainly from subdivisions one and two, with subdivision three having a temporal pattern that resembled the former less. Figure 5.8 illustrates this result.

5.2.4 Discussion

In this study we investigated dynamic functional connectivity in the context of a task involving movie watching and emotional regulation in a preterm-born population of young adolescents. We employed a state-of-the-art method to uncover several patterns of co-activation with an anterior cingulate cortex (ACC) seed and analyse their relationship with three main effects (namely seed; task; and group), as well as three interaction effects (namely seed versus task; group versus task; and group versus seed). We identified several patterns with a significant effect, many of which involved differences across the two groups, revealing dynamic aspects of brain function in the preterm population that had not been uncovered before.

Our exploration of ACC-based connectivity patterns revealed several reproducible PPI-CAPs,

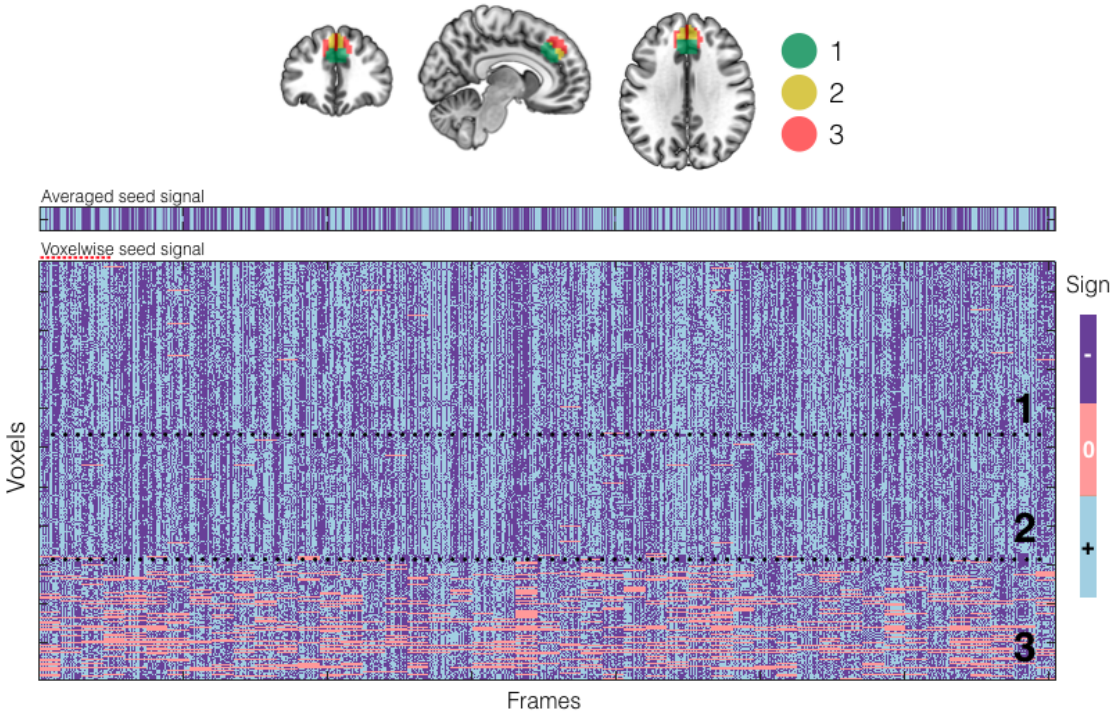

Figure 5.8 – **ACC-seed subdivisions based on temporal activity.** Temporally clustering the voxelwise seed activity's sign (large rectangle) across all subjects yielded three spatial subdivisions of the dorsal anterior cingulate cortex, indicated in green, yellow and red in the brain plot. The activity of voxels within regions one and two (as indicated by the top two layers of the large rectangle) resembled more closely and thus seem to be driving the seed's averaged signal (top rectangle).

with six being the optimal number of repeatable patterns. Previous studies had shown a wide variety of possible brain states in connection with other brain regions such as the posterior cingulate cortex (Liu et al., 2013; Lin et al., 2017; Freitas et al., 2020). The ACC, in turn, has often come up in BOLD variability studies, including some involving clinical populations (Zöller et al., 2017; Zhang et al., 2020), suggesting this brain region's high flexibility and that dynamic aspects of its function and connectivity may be implicated in the neurological mechanisms of clinical disorders. While Chapter 3 investigated resting-state co-activation pattern with an ACC seed, to the best of our knowledge this is the first study to have explored the task-related dynamic connectivity range of the ACC.

Only one PPI-CAP had a pure group effect close to significance. This was PPI-CAP 1, with somatomotor (SMN) areas being more highly active, while the default mode network (DMN) was deactive, in preterm-born children throughout the experiment. In addition, the group versus polarity effect indicates that it appears more often when this group is performing the movie watching task (note the darker colours on the right side of the corresponding confusion matrix in Figure 5.7). In typically developing individuals, motor stimulation is related to con-

tralateral activation of the motor cortex. Furthermore, not only physical stimulation, but even just the act of watching someone else move, or of imagining oneself moving, already generates similar activation (Butler and Page, 2006). Studies involving somatomotor stimulation in preterm-born infants, however, have often found bilateral (as opposed to only contralateral) activation of the motor cortex in response to unilateral stimulation (Heep et al., 2009b; Arichi et al., 2010; Allievi et al., 2016). Many of the the videos shown during Movie Watching blocks involve high movement such as sports scenes of families playing football. Taken together, the above facts may justify not only the occasional appearance of motor-related areas during this experiment, but also why it appears more for the preterm group. Further analyses based on transients (Karahanoglu and Van De Ville, 2015; Freitas et al., 2020) would help to disentangle the spatiotemporal overlapping of the different regions included in the PPI-CAP in this case.

Interestingly, PPI-CAP 6, which includes the limbic network (LN) and the dorsal attention network (DAN) with opposite signs, shows both a group versus task and a group versus seed interaction effects. In controls, the LN is more often active when movie watching than during emotional regulation, while the opposite is true for the preterm group. It is also more deactivated (and the DAN activated) when the preterm are movie watching. These results are in line with previous results which found altered structural connectivity of the cortico-basal-thalamo-cortical loop and the limbic system, which are essential for socio-emotional processing (Olson et al., 2007; Braun, 2011), in preterm-born school aged children as compared to term-born controls (Fischi-Gómez et al., 2015; Fischi-Gomez et al., 2016).

The investigation of seed homogeneity by clustering voxels based on their temporal features revealed three spatial subdivisions. This was done in a data-driven way, showing that there is a high level of consistency between neighbouring voxels. It also highlights that the seed itself is not entirely homogeneous and that the effects we found mainly related to the ventral part of the dorsal anterior cingulate cortex.

Taken together, the results presented here underline the potential of dynamic analyses to uncover brain function relationships that cannot be examined using traditional static methodologies. The potential to study these dynamic features in combination with behavioural and clinical outcomes proves a compelling direction for future research.

Considerations and future avenues

Although we identified a variety of patterns that co-activate with the ACC, it is not possible to know whether all the brain regions contained in each pattern activated (or deactivated) simultaneously — and it probably is not the case. Future studies would benefit from combining the PPI-CAPs approach with a method that extracts *transients*, or moments of change, from the data, and only then performs the clustering step (Karahanoglu and Van De Ville, 2015; Freitas et al., 2020). This would help clarify the co-occurrence of certain networks with opposite signs in some of the PPI-CAPs we uncovered.

This study includes a task block where participants are asked to focus on their breathing. The very act of concentration one one's breathing has been shown to alter breathing patterns (Conrad et al., 2007), which may cause changes not only in motion, but also CO_2 levels (Western and Patrick, 1988). A recent study by Chen et al. (2020) has shown that increased CO_2 levels induce vasodilation and an increase in blood flow, which may drive so-called "physiological networks". Thus, including physiological measures in a subsequent analysis would help control for these potential confounds when exploring task effects.

Another compelling next step would be to explore potential relationships between the occurrence of patterns identified here with behavioural and clinical measures from the participants. For example, does the occurrence of PPI-CAP 6, which has a strong emotional component, correlate with scores of emotional aptitude in these young adolescents? Future studies will help clarify this point.

Finally, recent studies have looked into another aspect of brain dynamics called quasi-periodic patterns (QPP; Majeed et al., 2011). This approach assumes that brain activity and BOLD fluctuations are dominated by a slow propagation of activity involving the DMN and task positive networks (Abbas et al., 2019). The QPPs can then be tested on their spatiotemporal pattern, frequency and strength, which is useful to identify whether not only the existence of different patterns of activity *per se*, but also *e.g.* the specific order in which they appear, brings novel information about clinical populations (Briend et al., 2020).

6 Summary and future perspectives

This work explored the dynamic features of brain function in young adolescents and how they are affected in individuals who were born preterm. To this end, both task-based and resting-state fMRI paradigms were analysed, and one methodological advancement was developed to bring the advantages of dynamic approaches also to task-based studies. Here, I summarise our main findings and identify potential avenues for future work that builds upon the analyses and clinical contributions presented so far.

6.1 Summary of findings

Resting-state brain dynamics in preterm-born young adolescents: We investigated, for the first time, the development of blood oxygenation level dependent (BOLD) signal variability and co-activation patterns (CAPs) in young adolescents born prematurely as compared to fullterm-born controls. To address the issue of high dimensionality in voxelwise BOLD variability maps, we employed a partial least squares correlation (PLSC) approach to identify multivariate patterns of alterations across groups and how they relate to life course measures, namely age at assessment; gestational age; and an interaction between the two. We used a similar PLSC approach to identify differences in CAP expression between the groups and their relationship with the aforementioned life course variables. Through this approach, we discovered that the development of BOLD signal variability is indeed altered in the preterm group in a broad pattern distributed across several areas of the brain, but especially in the bilateral hipoccampi and salience network including bilateral insulae and anterior cingulate cortex (ACC). Since the ACC has been recently identified in other studies as having altered connectivity in preterm-born individuals, we investigated this region further by performing an ACC-based CAPs analysis to uncover dynamic functional connectivity patterns that arise across age. Similarly to the BOLD variability analysis, we found different trajectories of CAP development in both groups. Indeed, the change in the balance between internally- and externally-oriented networks across age is more accentuated in the preterm group. Taken together, our observations suggest that the preterm-born brain triggers neurological compensation mechanisms that start during the highly dynamic age range of early adolescence and

fail to find an optimal balance.

Reality Filtering task processing in preterm-born young adolescents: To test whether preterm-born young adolescents would be able to complete a task that relies on a particularly vulnerable region in this population (the orbitofrontal cortex, OFC), we performed a reality filtering experiment. By looking into how brain activation changed depending on the type of stimulus being shown and comparing the preterm and control groups, we found that despite being able to perform the task with comparable accuracy to the fullterm group, the levels of OFC activation in the preterm group are lower. Moreover, no other regions were significantly more activated in the preterm than in controls. This suggests that preterm-born individuals may have developed mechanisms to optimise OFC activity such that they are still able to perform the task without depending on the same level of activation as the control group.

Time-resolved task-driven modulations of brain connectivity: We thus proceeded to investigate how brain organisation changes over time as a result of task performance in the preterm population. Given their higher risk of attentional and socio-emotional deficits, we elaborated a task that includes a movie watching aspect and an emotion regulation one. To explore this rich data set we first developed a time-resolved method to recover task-driven co-activation patterns (PPI-CAPs) and analyse their relationships with the seed, task, or an interaction between the two. We initially validate this framework in an adult data set. Once the methodology was stable, we applied it to the preterm data and extended the method to allow group comparisons. Here, we identified a series of dorsal anterior cingulate cortex (ACC)-based co-activation patterns that vary differently in preterms and controls according to the task. Interestingly, a new pattern including the limbic network emerged from this data which had not been found in the CAP analysis from Chapter 3, which was based on resting-state data. This is in line with existing evidence that the limbic network is involved in emotion processing. Together, these results highlight the relevance of studying brain dynamics in clinical populations. The code developed to perform the analysis described in this work has been made available on https://github.com/lorenafreitas/PPI_CAPs

6.2 Perspective for future research

Linking dynamic brain function and clinical outcomes

The studies presented in this thesis characterise dynamic features of brain function in preterm-born young adolescents and how they compare to fullterm-born individuals at his age. Several of these involve areas known to be part of high-order functional networks (see, for example, chapter 3). An interesting follow-up will thus be to see how the markers unveiled here relate to clinical outcomes such as attention levels, working memory, executive functions, etc. In fact, this data is available from the *Building the Path to Resilience in Preterm-Born Infants* project, of which this work is a constituting part. This would thus be a natural and feasible development for the near future.

Mindfulness meditation as a potential intervention in preterm young adolescents

Although interventions for premature babies have been routinely implemented with a positive effect on cognition and motor abilities (Ferreira et al., 2020), so far there is no consensus regarding procedures applied at later stages in life. Socio-emotional and executive function skills are, however, still in plain development during childhood and adolescence, suggesting that this age may still be within the intervention window.

Mindfulness meditation is a form of mind training to develop a reflective (as opposed to reflexive) way of responding to both internal or external events (Bishop, 2004) that involves attention, attitude and intention. As (Kabat-Zinn, 1994) describes it, it involves "paying attention (Attention), in a particular way (Attitude), on purpose (Intention), in the present moment, and non-judgmentally". Studies on its benefits for physical and mental health as well as its neurocognitive mechanisms have gained increased popularity in investigations involving adults, children and adolescents. In fact, even short sessions of meditation given to inexperienced participants have been deemed enough to improve attention levels Norris et al. (2018); Jankowski and Holas (2020). Moreover, regular practice has been shown to have long-term effects on attention (Zanesco et al., 2018) and brain funtion. Benefits such as the ones described above have put meditation in the spotlight as a potential intervention in clinical practice (Simkin and Black, 2014; Zhang et al., 2018).

In young populations, mindfulness meditation training has emerged as a potential tool to help manage a wide variety of symptoms including disruptive behaviour (Perry-Parrish et al., 2016) and lack of attention (Zhang et al., 2018). A study involving typically developing children at 11 years old showed that 8 weeks of mindfulness training already has the potential to improve attentional self-regulation (Felver et al., 2017). Another, found that meditation programs can enhance cognitive and social-emotional development in young populations (Schonert-Reichl et al., 2015). Taken together, these results further suggest a link between these cognitive domains and that mindfulness meditation may be an avenue for intervention in clinical populations.

The *Building the Path to Resilience in Preterm-Born Infants* project, of which this thesis is part, has acquired functional and structural MRI data from the preterm-born young adolescents studied here after 8 weeks of mindfulness training. Crucially, mindfulness has recently been found to relate to dynamic — as opposed to static — features of neural function and neural network interactions over time (Marusak et al., 2018). This highlights PPI-CAPs as a compelling avenue to explore the effects of mindfulness meditation as a potential intervention for young adolescents born prematurely, as its focus is precisely to uncover dynamic aspects of brain function during performance of a task.

PPI-CAPs as markers for neurofeedback

FMRI Neurofeedback (NF) is a technique in which real-time information about someone's own brain activity is fed back to them, which gives them the chance to attempt to control it. It has been found to be a promising means to reshape neural activity, and has been used as an intervention tool in several neurological and psychiatric disorders (Güntensperger et al., 2017; Misaki et al., 2019) including in adolescent clinical populations (Alegria et al., 2017). Most relevant for this work is its potential for self-driven modulation of emotion processing domains, both in adult (Koush et al., 2017; Lorenzetti et al., 2018) as well as children and adolescent populations (Cohen Kadosh et al., 2016). In most of these studies, a seed region is selected for which information on activation levels is provided to the user, who then tries to modulate that brain area's activity.

Recently, Koush et al. (2017) showed that it is also possible to gain control over entire networks related to emotion regulation using a connectivity-neurofeedback approach. This opens a promising avenue for future research built on the basis of this thesis. In Chapter 5, we introduced Psychophysiological Interaction of Co-Activation Patterns (PPI-CAPs) as a seed-based method to investigate time-resolved changes in effective connectivity also in a task-based environment. With this method, we have investigated differences in dynamic brain function during the performance of a task in the preterm group as compared to fullterm-born controls. The very PPI-CAPs which are less elicited by the clinical population could potentially be used as an NF target in future studies. In this paradigm, an initial run could be performed to identify target PPI-CAPs — that is, those which were most differently expressed between groups. Then, subsequent runs would be carried out where the subject's goal is to attempt to reproduce that pattern. It is important to note, however, that although fMRI NF has been show to successfully modulate activation and connectivity in the brain, and to lead to behavioural changes, how this translates into clinically significant improvements remains debatable (Thibault et al., 2018).

Extensions for PPI-CAPs

As described in more detail in section 5.1.4 of Chapter 5 (Potential extensions of the PPI-CAPs approach), there are several ways in which this methodology could be extended to capture additional information on the dynamic features brain function. Of note, rather than approaching brain function as a series of separately elicited brain sates (Leonardi et al., 2014; Gonzalez-Castillo et al., 2015; Freitas et al., 2020), one could think of it as several patterns that may overlap with each other in dynamic ways (Karahanoglu et al., 2013; Karahanoglu and Van De Ville, 2015). The so-called *innovation signals* from Karahanoglu et al. (2013)'s work reflect moments in which there are significant *changes* in activation intensity of certain brain areas, rather than pure amplitude. One could thus apply the frame selection and clustering steps on these signals to yield *innovation-driven* PPI-CAPs (or PPI-*i*CAPs), which would represent spatial patterns of voxels whose signals *transition* simultaneously. Backprojecting these would

then recover their time courses, thus revealing moments when different combinations of those patterns may overlap.

Another attractive route for extension would be to consider the introduction of temporal relationships between successive time points. This has been shown to be a promising avenue both when considering sequential (Eavani et al., 2013; Chen et al., 2016; Vidaurre et al., 2017) or overlapping (Sourty et al., 2016; Bolton et al., 2018b) brain states. For instance in the case of the present work, given that the results from Chapter 5.1 which revealed default mode network (PPI-CAP$_3$), fronto-parietal network (PPI-CAP$_1$ and PPI-CAP$_2$) and salience network (PPI-CAP$_2$) contributions during movie-watching, causal interplays between these networks could be assessed in the context of the so-called triple network model (Menon, 2011).

So far, PPI-CAPs address temporal dynamics alone, without taking into consideration how to optimally tackle the spatial dimension of the data. One extension could thus be to inject a spatial prior in deriving PPI-CAPs (Zhuang et al., 2018), or to study the spatial variability of task-related functional activity patterns in more detail (Kiviniemi et al., 2011). This could be achieved by separately considering, for each PPI-CAP, the pools of frames linked to given task contexts, and carrying out statistical comparisons at this level (Amico et al., 2014).

Finally, one could investigate measures that are more sophisticated than pure occurrences as features of interest (Chen and Glover, 2015; Bolton et al., 2020b), or broaden the analysis of PPI-CAPs to a meta-state perspective (Miller et al., 2016; Vidaurre et al., 2017), where a meta-state would symbolise a particular combination of expression and polarity of the investigated patterns.

The ultimate goal is to apply novel tools to better understand brain function both in health individuals and in clinical cohorts. I believe that the future avenues presented here would help provide a more accurate picture of brain function dynamics and have great potential to address these populations.

Probing into structure-function relationships

While the main goal of this thesis was to focus on the relevance of functional brain dynamics for the study of preterm birth, it is important to consider that the brain's underlying structural architecture clearly affects not only static measures of brain function (Honey et al., 2009) but also dynamic ones (Hansen et al., 2015). However, for reasons that remain to be explored — and may include non-linear neural processing in specific brain areas as well as confounding physiological artefacts — the BOLD signal contains information that does not simply reproduce that of brain structure. Therefore, analysing both together may bring relevant, additional information which previous studies had missed. For instance, Amico and Goñi (2018) demonstrated how an approach combining multimodal canonical correlation as well as joint independent component analysis can be used to investigate structural-functional alterations by recovering task-sensitive "hybrid" patterns of connectivity that represent subjects'

connectivity fingerprint.

Graph signal processing (GSP) has recently emerged in the neuroimaging field as a novel framework for brain data analysis that integrates brain structure and function (see Huang et al. (2018) for a broad overview). In this scheme, brain structure defines a graph representation where brain regions are the nodes and white matter tracts are the edges, while each frame of fMRI activity is a temporal sample of a signal living on this graph. More recently, this concept has seen an interesting extension in which high quality activity time courses within the white matter are derived through the combination of a voxel-wise structural graph, and of grey matter activity (Tarun et al., 2020).

To the best of our knowledge, graph analyses on preterm-born populations to date have solely considered either structure or function individually. Therefore, this remains a promising avenue to obtain a better-informed picture of brain function in prematurity.

A note on addressing the global challenge of prematurity

An important issue in the study of the neurodevelopmental effects of preterm birth is that, although most of the global burden of preterm birth is shouldered by low- and middle-income countries (LMICs), only a tiny portion of the currently available research evidence for their prevention and treatment come from these settings (Smid et al., 2016). However, since high-income countries tend to offer more funding for research and in many cases have better facilities at researchers' disposal, investigations in these regions of potential biomarkers for targeted intervention that improves clinical outcomes in this population are also of utmost importance. Once non-invasive interventions such as the ones the *Building the Path to Resilience in Preterm-Born Infants* project — of which this thesis is a constituting part — aims to investigate are found, the need for expensive equipment such as MRI machines will prove less essential, and LMIC populations will also benefit from them.

A Supplementary material for Chapter 3

A.1 Supplementary Figures

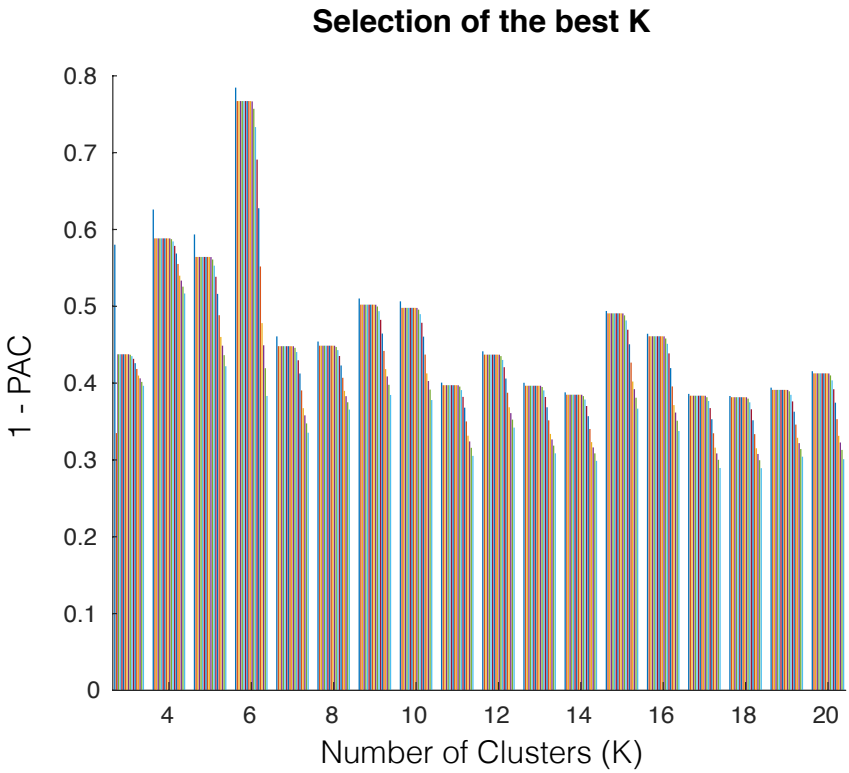

Figure A.1 – **Selecting the ideal number of Co-Activation Patterns.** The plot shows the proportion of ambiguous clustering (PAC) for cluster numbers ranging from 3 to 20. There is a clear peak of (1 - PAC) for K = 6 indicating that, when this value is chosen, different runs of k-means clustering yield the most consistent results.

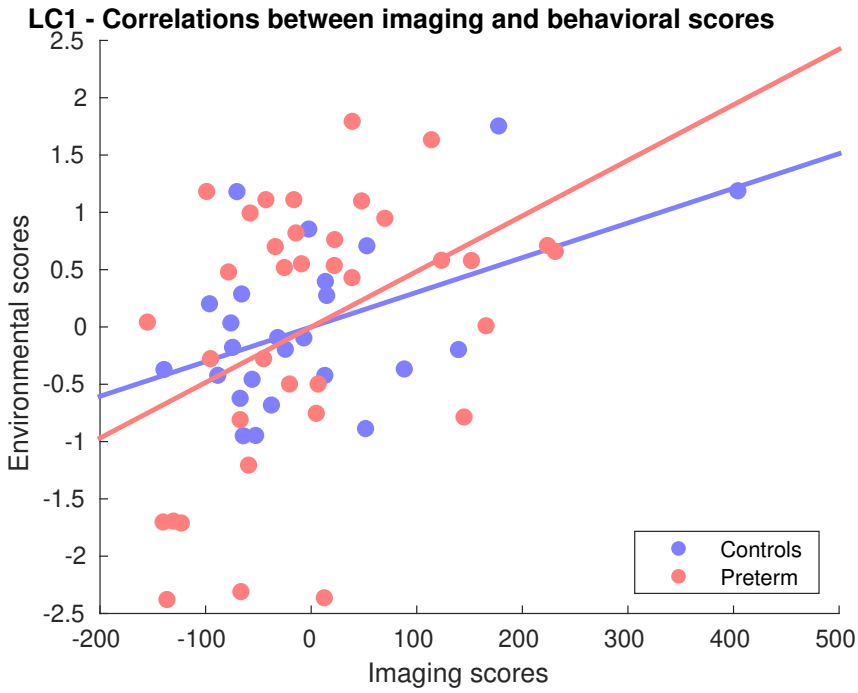

Figure A.2 – **Correlation between brain and environmental scores for BOLD variability PLS.**

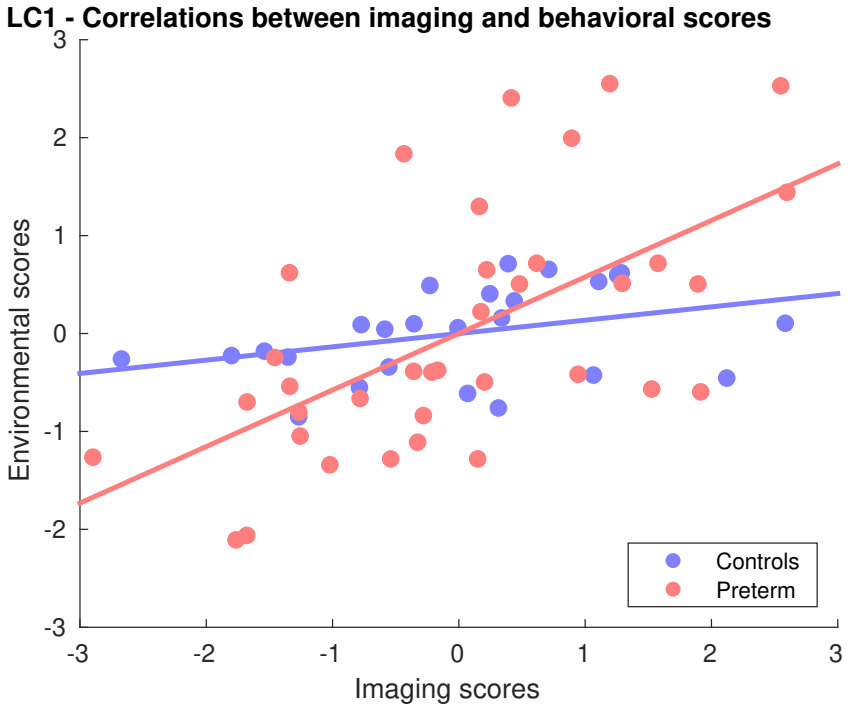

Figure A.3 – **Correlation between brain and environmental scores for CAP PLS.**

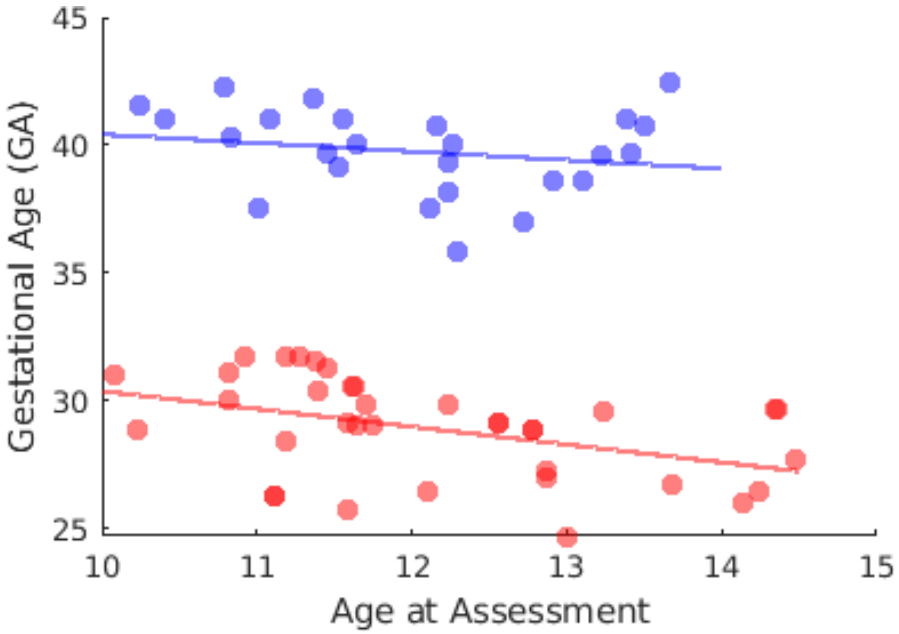

Figure A.4 – **Correlation between gestational age and age at assessment.** There was no significant correlation between the two measures in the control group ($r = -0.22$, *n.s.*). There as a weak correlation between the two measures in the preterm group ($r = -0.4$, $p = 0.02$).

B Supplementary material for Chapter 5

B.1 Link between conventional PPI and the stationary PPI-CAP

Within the PPA/CAPs framework, it is well known that averaging the frames where the seed exceeds a "well chosen" threshold ϕ, yields a proxy for the conventional seed connectivity map (Tagliazucchi et al., 2012; Liu and Duyn, 2013). This observation can be explained in the following way: let us assume that the activity time course $S(t)$ of a seed voxel is a realization over time, $t = 1,\ldots,N$, of a random variable S for which $E[S] = 0$ and $E[S^2] = 1$. To construct conventional seed connectivity, a general linear model (GLM) is put forward to explain the time course $V(t)$ of a target voxel as:

$$V(t) \quad = \quad \beta S(t) + \varepsilon(t), \qquad \text{(Eq. B.1)}$$

where β is the parameter weight (i.e., functional connectivity) and $\varepsilon(t)$ is the residual and assumed to be a realization of the noise with $E[\varepsilon] = 0$ and $E[\varepsilon^2] = \sigma^2$. In addition, we assume the noise to be independent from the seed voxel activity; i.e., $E[S \cdot \varepsilon] = 0$. Multiplying both sides of Eq. B.1 with $S(t)$ and taking the expectation leads to:

$$E[V \cdot S] \quad = \quad \beta E[S^2] + E[S \cdot \varepsilon], \qquad \text{(Eq. B.2)}$$

which simplifies into $\beta = E[V \cdot S]$.

To obtain the stationary map in the CAPs approach, we want the expectation value of the target voxel for frames where the seed exceeds a threshold ϕ:

$$\begin{aligned} I_{\text{CAP}+} &= E[V : S > \phi] && \text{(Eq. B.3)} \\ &= E[\beta S + \varepsilon : S > \phi] && \text{(Eq. B.4)} \\ &= \beta E[S : S > \phi] + E[\varepsilon : S > \phi], && \text{(Eq. B.5)} \end{aligned}$$

where in the first step we have substituted the previous GLM of Eq. B.1 and ":" implies conditioning. Due to the independence of noise and seed voxel, and $E[\varepsilon] = 0$, the second term

of Eq. B.5 will vanish, and we obtain

$$I_{\text{CAP+}} = \beta E[S : S > \phi], \tag{Eq. B.6}$$

which means that the expectation of suprathreshold frames in the PPA method will be proportional to the result of a conventional correlation map, with the constant of proportionality given by $E[S|S > \phi]$, which only depends on the seed, and not the target voxel. A similar relationship can be derived when the seed activity is below the negative threshold:

$$\begin{aligned} I_{\text{CAP-}} &= E[V : S < -\phi] && \text{(Eq. B.7)} \\ &= E[\beta S + \varepsilon : S < -\phi] && \text{(Eq. B.8)} \\ &= \beta E[S : S < -\phi] + E[\varepsilon : S < -\phi] && \text{(Eq. B.9)} \\ &= \beta E[S : S < -\phi] && \text{(Eq. B.10)} \end{aligned}$$

In the case of a two-sided threshold, using the identity $\text{sign}(A)\,A = |A|$, we can conclude that:

$$\begin{aligned} I_{CAP} &= E\big[\,\text{sign}(S)V : |S| > \phi\big] && \text{(Eq. B.11)} \\ &= E[\beta S\,\text{sign}(S) + \varepsilon\,\text{sign}(S) : |S| > \phi\big] && \text{(Eq. B.12)} \\ &= \beta E[S\,\text{sign}(S) : |S| > \phi\big] + E[\varepsilon\,\text{sign}(S) : |S| > \phi\big] && \text{(Eq. B.13)} \\ &= \beta E\big[|S| : |S| > \phi\big]. && \text{(Eq. B.14)} \end{aligned}$$

Based on this observation, we can generalize to PPI for which the GLM becomes:

$$V(t) = \beta_S S(t) + \beta_T T(t) + \beta_{PPI} P(t) + \varepsilon(t), \tag{Eq. B.15}$$

where $T(t)$ is the time course of the task and $P(t)$ is the "interaction term" given by $P(t) = S(t)T(t)$. The stationary map of the PPI-CAPs analysis then averages values of the target voxel multiplied with the sign of the interaction term, where the selection is based on the criterion of the seed exceeding the threshold:

$$\begin{aligned} I_{\text{PPI-CAP}} &= E[\text{sign}(ST)V : |S| > \phi] \\ &= E[\text{sign}(ST)(\beta_S S + \beta_T T + \beta_{PPI} P + \varepsilon) : |S| > \phi] \\ &= \beta_S E[\text{sign}(ST)S : |S| > \phi] + \beta_T E[\text{sign}(ST)T : |S| > \phi] + \beta_{PPI} E[\text{sign}(ST)P : |S| > \phi]. \end{aligned}$$

Using the identities $\text{sign}(A)\,A = |A|$ and $\text{sign}(AB)\,A = \text{sign}(B)|A|$, this becomes

$$\begin{aligned} I_{\text{PPI-CAP}} &= \beta_S E\big[\,\text{sign}(T)|S| : |S| > \phi\big] + \beta_T E\big[\,\text{sign}(S)|T| : |S| > \phi\big] + \beta_{PPI} E\big[|ST| : |S| > \phi\big] \\ &\approx \beta_{PPI} E\big[|ST| : |S| > \phi\big]. \end{aligned}$$

The last approximation can be made when the contributions of the first two terms are negligible. For the first term, we assume the absolute value of S to be independent of the task (that weights the expectation operator) and T has equal number of positive and negative values,

in which case the first term will be 0. For the second term, if the task is just a change of sign, then its absolute value will be fixed and uncorrelated to the sign of the seed. Thus the second term is proportional to $E\big[\,\mathrm{sign}(S) : |S| > \phi\big]$, which is necessarily bound between ± 1 and will be exactly 0 if S is symmetric.

Therefore, what remains is the final term and we find that the result of a PPI analysis will be proportional to the SiMap. This brief derivation also shows that the stationary PPI-CAP can be contaminated by "leakage" from the seed and/or task contributions if these assumptions are not fulfilled.

B.2 Supplementary Figures for Section 5.1

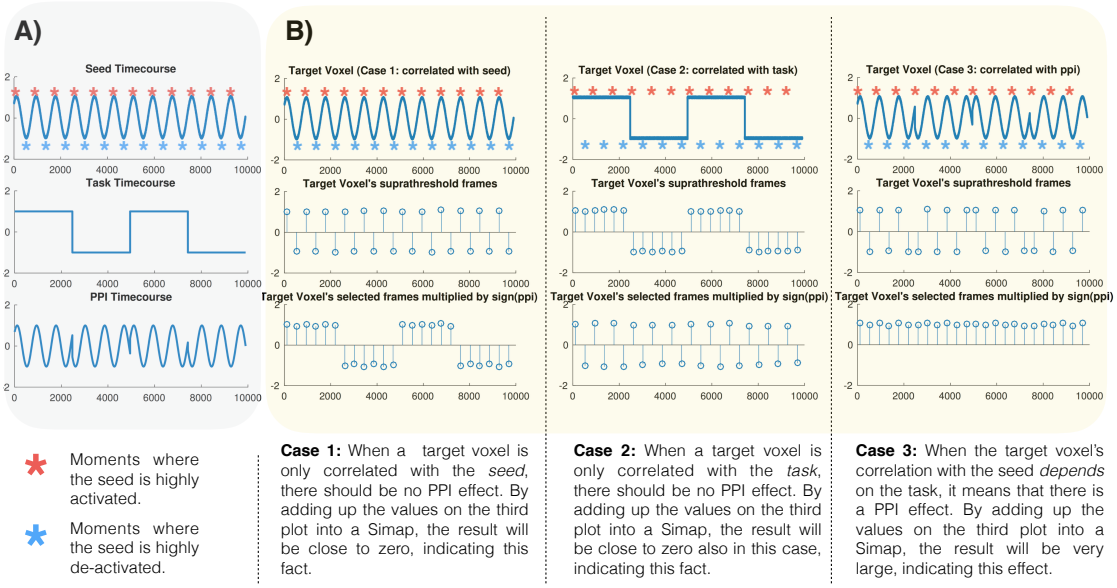

Figure B.1 – **An intuitive toy example to illustrate the relationship between the static interaction map (simap) and PPI analysis results.** A) Moments where the seed activity is significantly high (red stars) or low (blue stars) are selected. B) Three possible cases are depicted: 1) When the target voxel is correlated only with the seed (meaning that there is no interaction effect), its resulting value in the siMap will be close to zero, as would be expected for its corresponding beta value in a PPI analysis. 2) Similarly, when the target voxel is correlated only with the task, its resulting value in the siMap will be close to zero. 3) when the target voxel is correlated with the PPI regressor, meaning that its relationship with the seed changes according to the context, the averaged value from its suprathreshold frames will yield a high value, indicating a PPI effect.

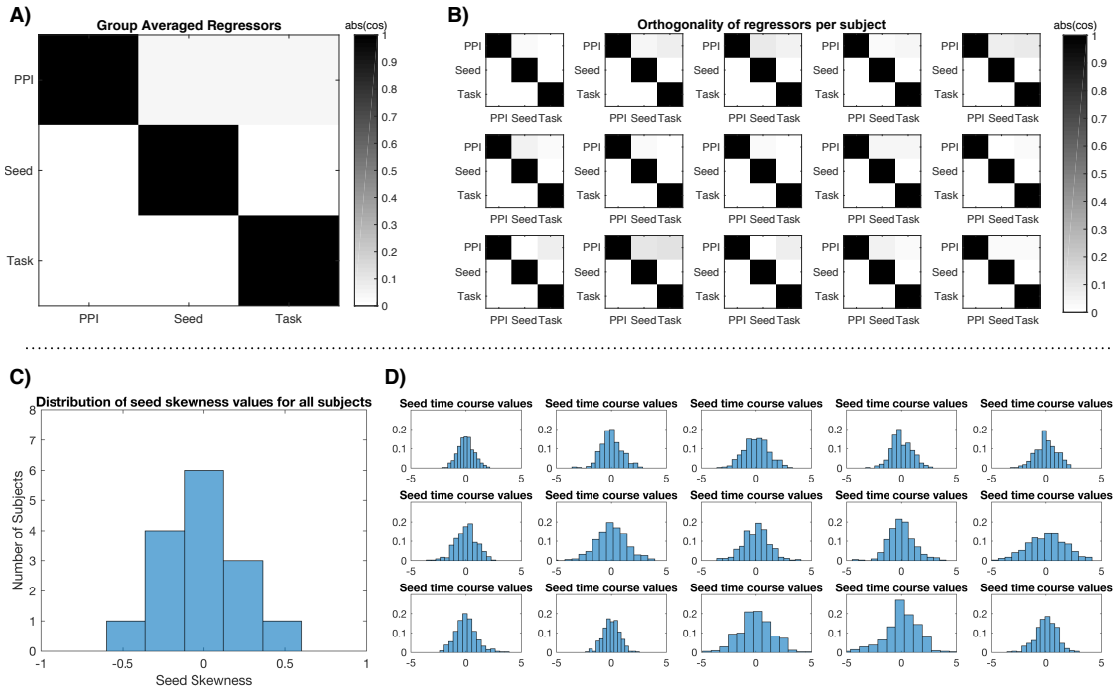

Figure B.2 – **Sanity check on the chosen seed signal.** Before proceeding with the PPI-CAPs analysis, we checked the orthogonality of the seed, task and ppi regressors using SPM's Check Orthogonality tool, as well as the skewness of the seed. A) The group-averaged matrix confirms that the regressors are not collinear at the group level. The highest off-diagonal value is 0.04. B) Shows the same matrix at the single-subject level. C) The seed signal was not skewed for any of the subjects: the skewness value stayed within the [-0.5 0.5] range for all of them. D) Shows the distribution of z-scored seed signal values for each subject. Additionally, the magnitude of the seed timecourse was not correlated with the sign of the task: the Pearson's r coefficient for the subject with the strongest correlation between the magnitude of the seed and the sign of the task was 0.11.

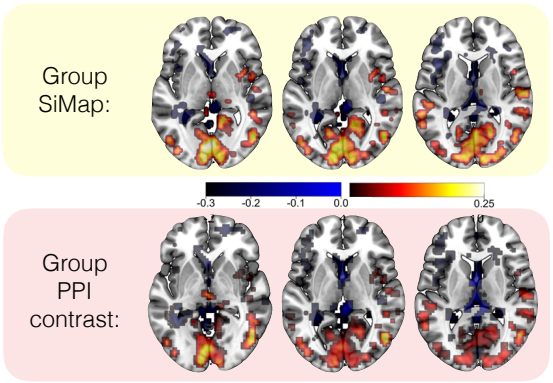

Figure B.3 – **Group-level static interaction map resembles PPI analysis results.** The spatial correlation betweeen the two analyses' results was 0.85 for the siMap calculated from 60% frames.

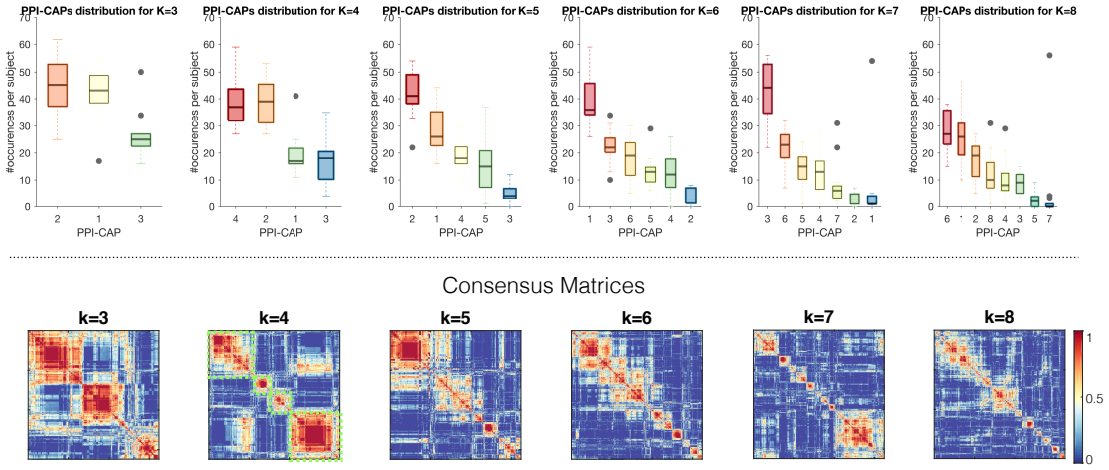

Figure B.4 – **An analysis of the number of occurrences of each PPI-CAP per subject combined with consensus clustering indicates the optimal number of groups in which to cluster the suprathreshold frames.** (Top) The PPI-CAPs distributions for $k \in [3,8]$ showed that k values of 6 and above yielded PPI-CAPs that never occurred for some subjects, while values between 4 and 5 had the most homogeneous distribution of pattern occurrence per subject. (Bottom) Visual inspection of the consensus matrices showed that the most stable values for k (that is, those for which any two frames would most consistently be clustered together or separately) were $k = 3$ and $k = 4$. Since 4 represents a better trade-off in terms of variety and robustness, we chose this value for further analysis (see its clear pattern highlighted in green). The colormap represents the proportion of time when two frames were consistently clustered either together or separately.

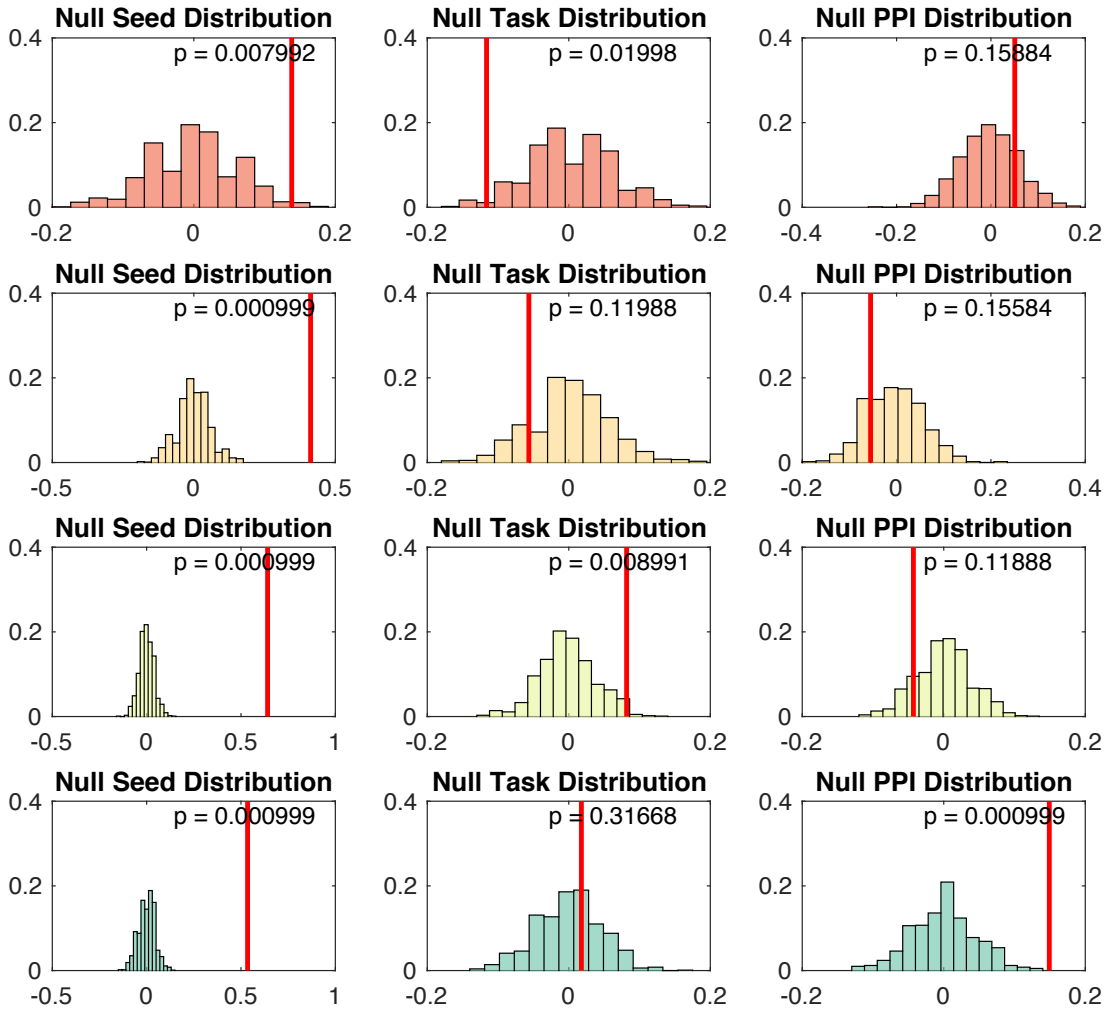

Figure B.5 – **Significance assessment of PPI-CAPs.** Each histogram illustrates the distribution of determinant values of the confusion matrices obtained from 3000 random permutations of the frame labels composing each PPI-CAP, with respect to seed, task or PPI. The red line indicates where the determinant of the confusion matrix for real data lies.

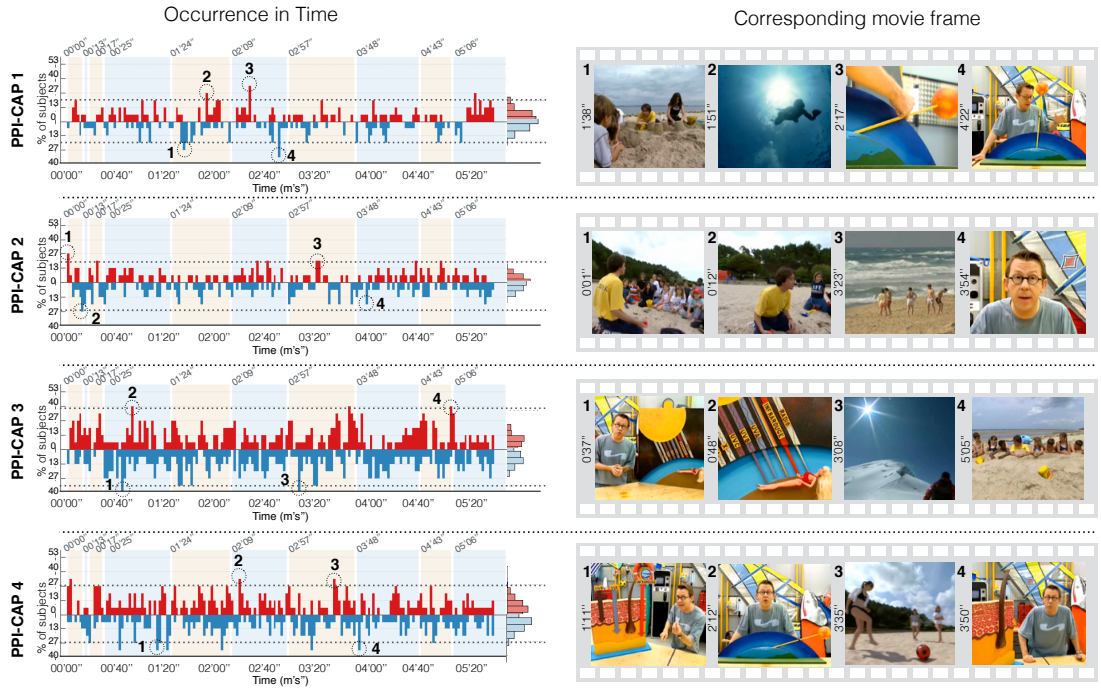

Figure B.6 – **The high temporal resolution of the PPI-CAPs approach allows us to link brain activity to stimuli presented at specific time points.** Here, we show moments when each PPI-CAP was highly consistent across participants (left). The y-axis shows the percentage of subjects, out of the total 15 participants, who expressed the PPI-CAP at each given time point. The histogram on the right hand side of the panel depicts the distribution of random consistency across subjects. This was calculated by randomly permuting the time points on which the PPI-CAP appeared for each subject, then re-calculating the subject consistency across time (the same plot as the ones on the left). Finally, we plotted the distribution of possible consistency values. The dashed line represents the value of the 99th percentile from the random distribution, indicating that a subject consistency above this threshold is significant. Selected time points of high consistency across subjects for each PPI-CAP are indicated by numbers on the left plots, and the corresponding video frames are presented for those times on the rightmost side of the figure.

B.3 Supplementary Figures for Section 5.2

ACC-seed PPI-CAPs in preterm-born adolescents

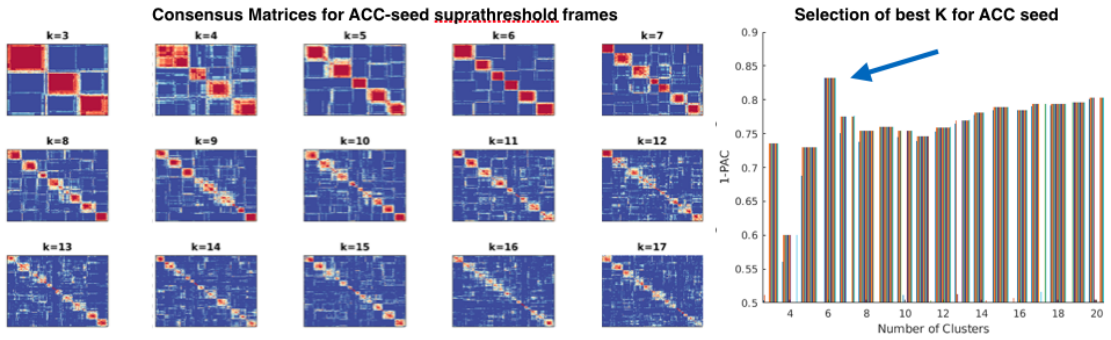

Figure B.7 – **Choosing the best number of clusters for an ACC-seed PPI-CAPs analysis.** 30% of the frames when the dorsal anterior cingulate cortex (ACC) was most (de)activated were selected for analysis. Consensus clustering was run for K ranging from 3 to 20, in 10 folds for each of which a random subsample including 80% of the subjects was used. On the left, the consensus matrices provide a visual appreciation of how often each pair of frames was consistently clustered (*i.e.,* both always in the same cluster, or both never in the same cluster). Blue indicates never, red indicates always. On the right, we plot the proportion of ambiguously clustered frames for each K. Since we want this value to be very low, a peak in the (1-PAC) plot indicates the most stable choice of K. Since K = 6 has a clear peak and means we will have a large number of frames per PPI-CAP (essential for averaging out noise), we select this as opposed to higher K numbers who also had good results.

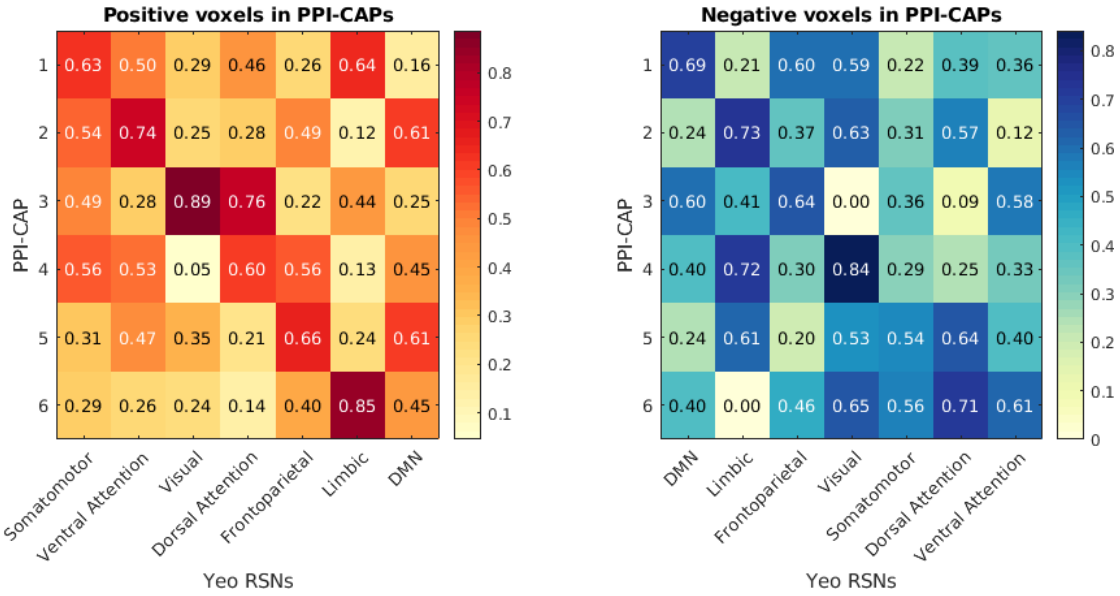

Figure B.8 – **Identifying networks present in each PPI-CAP.** The two matrices compare the activated (red) and deactivated (blue) voxels in each PPI-CAP from Figure 5.6 to the 7 functional networks from Thomas Yeo et al. (2011). Colour intensity and numbers indicate the proportion of voxels from each network that are present in the PPI-CAP. Networks were then ordered according to the Hungarian Assignment Algorithm (Munkres, 1957). According to this result, PPI-CAP$_1$ corresponds to an activated Somatomotor Network (SMN) and deactivated Default Mode Network; PPI-CAP$_2$ is assigned to an activated Ventral Attention Network, also known as Salience Network (SN), and deactivated Limbic; PPI-CAP$_3$ contains an activated Visual and deactivated Frontoparietal Network (FPN); PPI-CAP$_4$ includes an activated Dorsal Attention (DAN) and deactivated Visual Network; PPI-CAP$_5$ has an activated FPN and deactivated SMN; and PPI-CAP$_6$ includes an activated Limbic and deactivated DAN.

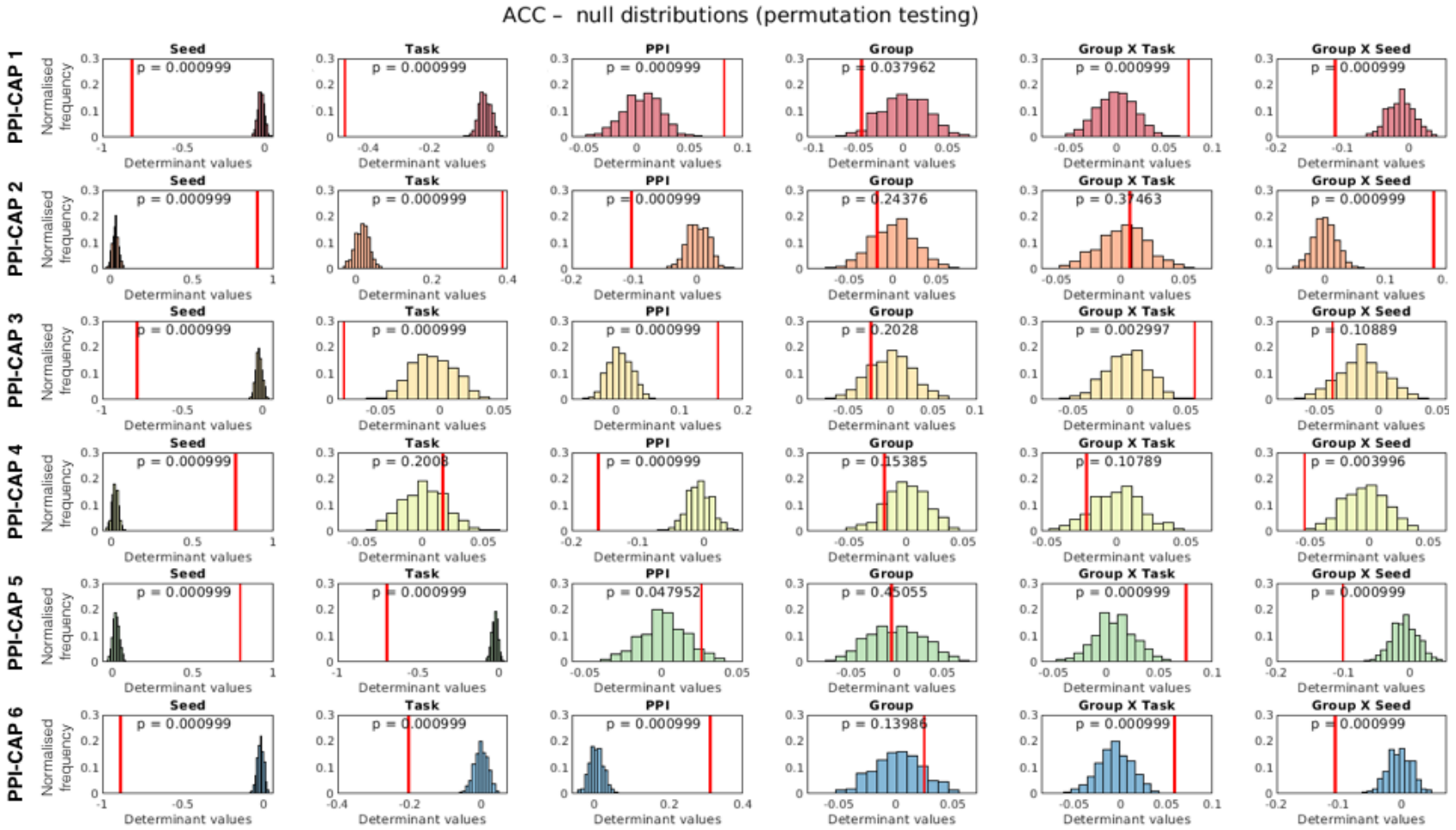

Figure B.9 – **Statistical assessment of each PPI-CAP's effects.** To check whether the effects identified in Figure 5.7 are significant, we performed permutation testing by shuffling the corresponding effect's labels 3000 times and calculating the det-index in each case, to generate a null distribution. We then check where the real data's det-index lies within this distribution and calculate the p-value.

PCC-seed PPI-CAPs in preterm-born adolescents

In Chapter 5, Section 5.2, we perform a PPI-CAPs analysis to explore task-related dynamic connectivity using the dorsal anterior cingulate cortex as a seed. Here we provide a similar analysis using the posterior cingulate cortex (PCC). While interpreting these additional results goes beyond the goal of this Section, this additional work illustrates that task-driven dynamics are a powerful and compelling strategy to uncover features of brain function in clinical populations independently of the choice of seed.

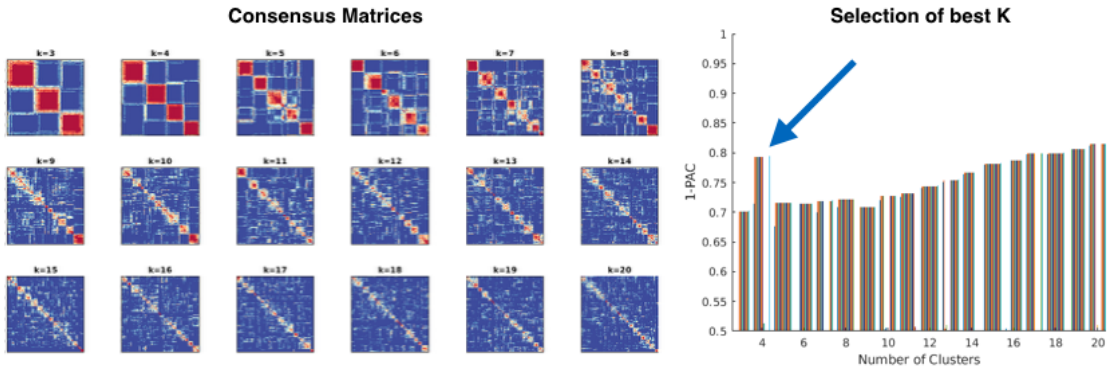

Figure B.10 – **Choosing the best number of clusters for a PCC-seed PPI-CAPs analysis.** 30% of the frames when the posterior cingulate cortex (PCC) was most (de)activated were selected for analysis. Consensus clustering was run for K ranging from 3 to 20, in 10 folds for each of which a random subsample including 80% of the subjects was used. On the left, the consensus matrices provide a visual appreciation of how often each pair of frames was consistently clustered (*i.e.,* both always in the same cluster, or both never in the same cluster). Blue indicates never, red indicates always. On the right, we plot the proportion of ambiguously clustered frames for each K. Since we want this value to be very low, a peak in the (1-PAC) plot indicates the most stable choice of K. Since K = 4 has a clear peak and means we will have a large number of frames per PPI-CAP (essential for averaging out noise), we select this as opposed to higher K numbers who also had good results.

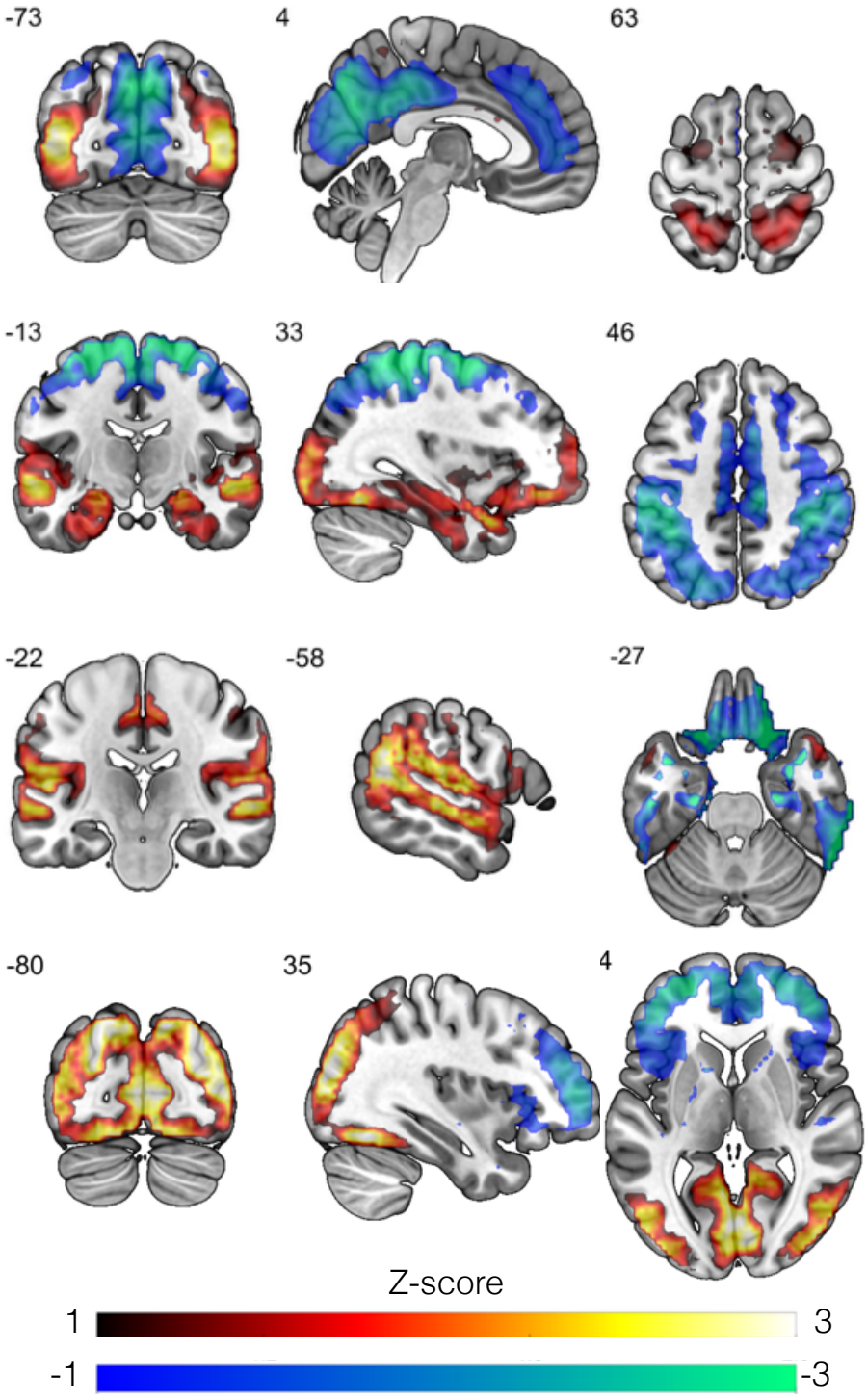

Figure B.11 – **PCC-seed PPI-CAPs.** Using K = 4 for the clustering step as defined in Figure B.10 yielded the four PPI-CAPs above. Each row corresponds to one PPI-CAP, numbers indicate slice coordinates in MNI space.

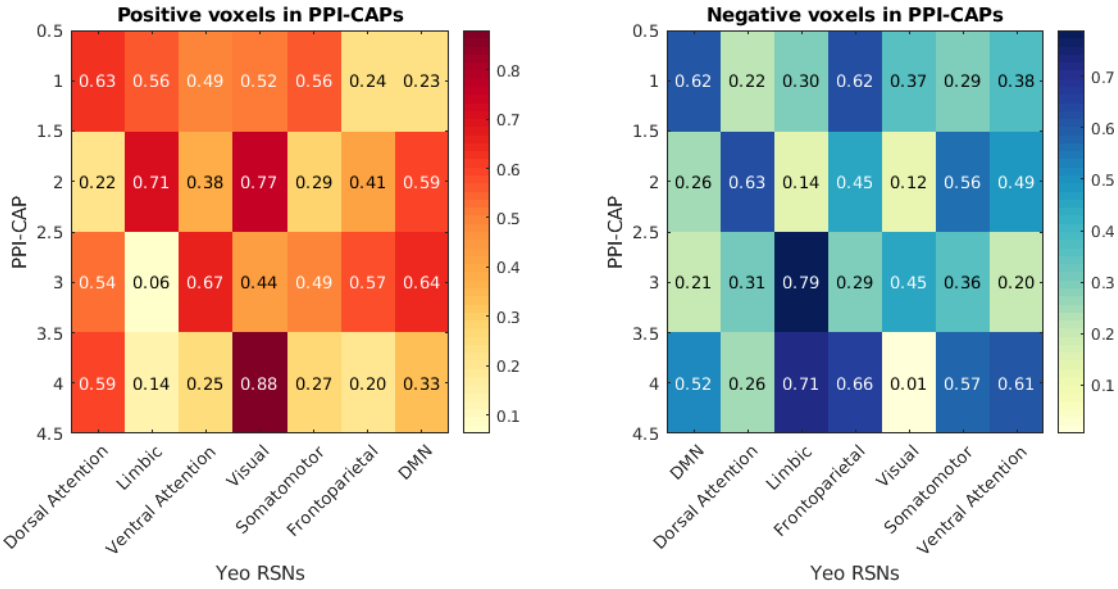

Figure B.12 – **Identifying networks present in each PPI-CAP.** The two matrices compare the activated (red) and deactivated (blue) voxels in each PPI-CAP from Figure B.11 to the 7 functional networks from Thomas Yeo et al. (2011). Colour intensity and numbers indicate the proportion of voxels from each network that are present in the PPI-CAP. Networks were then ordered according to the Hungarian Assignment Algorithm (Munkres, 1957). According to this result, PPI-CAP$_1$ corresponds to an activated Dorsal Attention Network (DAN) and deactivated Default Mode Network; PPI-CAP$_2$ is assigned to an activated Limbic Network (LN) and deactivated DAN; PPI-CAP$_3$ contains an activated Salience Network and deactivated LN; and PPI-CAP$_4$ includes an activated Visual Network and deactivated Fronto-Parietal Network.

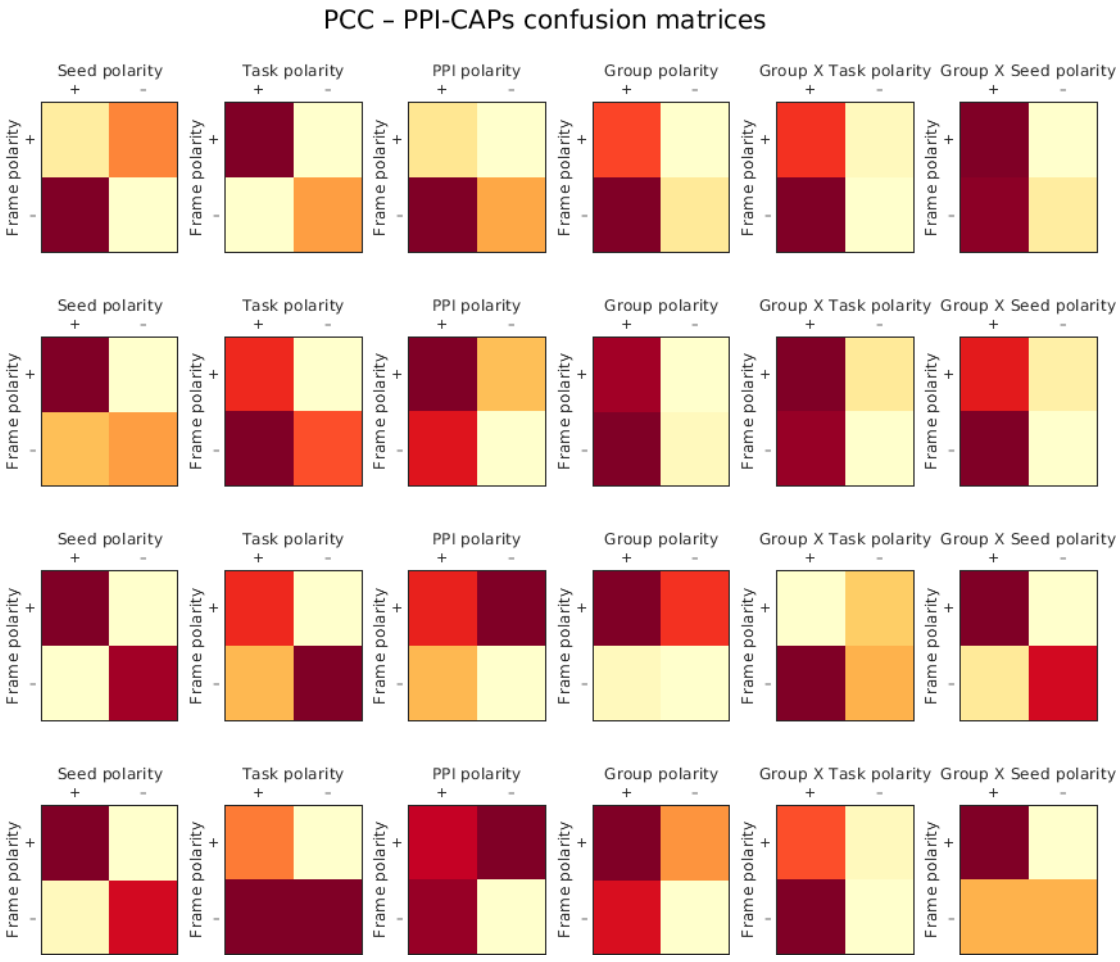

Figure B.13 – **Confusion matrices for PCC-seed PPI-CAPs.** To identify main and interaction effects for each PPI-CAP, we generate confusion matrices to see how often the sign of a PPI-CAP switches in the same way as each of the effects. We tested three main effects (Seed; Task; and Group) and three interaction effects (Seed vs. Task (PPI); Group vs. Seed; and Group vs. Task). The signs for each effect are as follows: Seed — positive and negative signs correspond to frames when the seed was activated of deactivated, respectively; Task — positive signs correspond to "Movie Watching" while negative signs correspond to moments of "Emotion Regulation"; Group — positive signs correspond to fullterm controls, while negative signs correspond to preterm-born individuals. Interaction signs are calculated as element-by-element multiplication of the main effect signs. Light yellow indicates a low number of frames, while dark red indicates the highest number of frames.

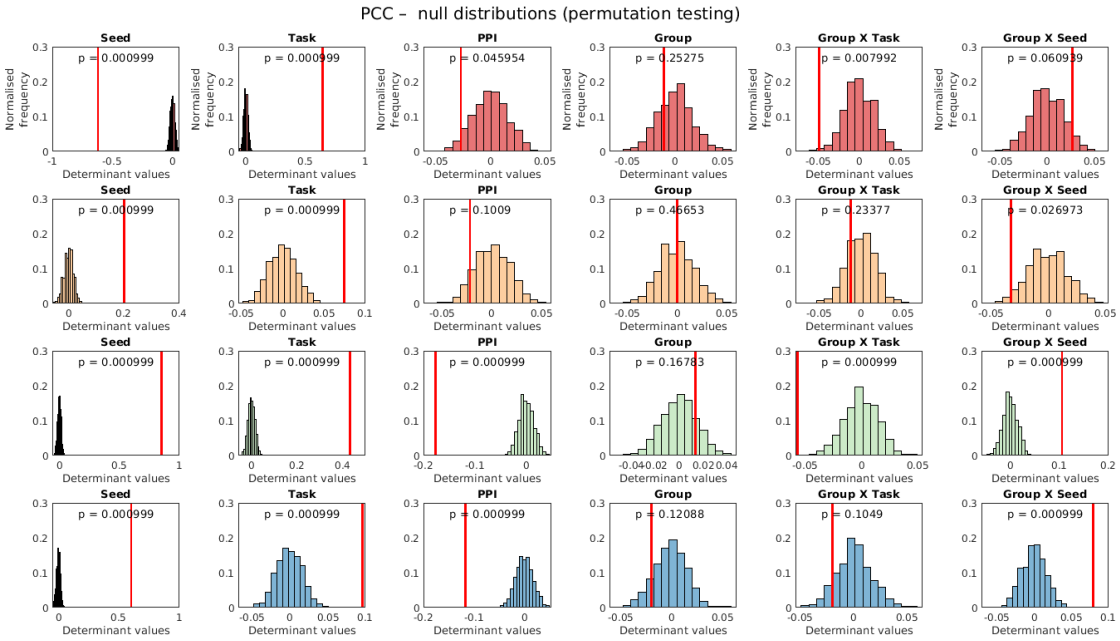

Figure B.14 – **Statistical assessment of each PPI-CAP's effects.** To check whether the effects identified in Figure B.13 are significant, we performed permutation testing by shuffling the corresponding effect's labels 3000 times and calculating the det-index in each case, to generate a null distribution. We then check where the real data's det-index lies within this distribution and calculate the p-value.

Bibliography

Abbas, A., Belloy, M., Kashyap, A., Billings, J., Nezafati, M., Schumacher, E. H., and Keilholz, S. (2019). Quasi-periodic patterns contribute to functional connectivity in the brain. *NeuroImage*, 191:193–204.

Adam-Darque, A., Grouiller, F., Vasung, L., Ha-Vinh Leuchter, R., Pollien, P., Lazeyras, F., and Hüppi, P. S. (2018). fMRI-based Neuronal Response to New Odorants in the Newborn Brain. *Cerebral Cortex*, 28(8):2901–2907.

Adolphs, R. (2001). The neurobiology of social cognition. *Current Opinion in Neurobiology*, 11(2):231–239.

Akbar, N., Giorgio, A., Till, C., Sled, J. G., Doesburg, S. M., De Stefano, N., and Banwell, B. (2016). Alterations in Functional and Structural Connectivity in Pediatric-Onset Multiple Sclerosis. *PLOS ONE*, 11(1):e0145906.

Alegria, A. A., Wulff, M., Brinson, H., Barker, G. J., Norman, L. J., Brandeis, D., Stahl, D., David, A. S., Taylor, E., Giampietro, V., and Rubia, K. (2017). Real-time fMRI neurofeedback in adolescents with attention deficit hyperactivity disorder. *Human Brain Mapping*, 38(6):3190–3209.

Allen, E. A., Damaraju, E., Plis, S. M., Erhardt, E. B., Eichele, T., and Calhoun, V. D. (2014). Tracking whole-brain connectivity dynamics in the resting state. *Cerebral Cortex*, 24(3):663–676.

Allievi, A. G., Arichi, T., Tusor, N., Kimpton, J., Arulkumaran, S., Counsell, S. J., Edwards, A. D., and Burdet, E. (2016). Maturation of Sensori-Motor Functional Responses in the Preterm Brain. *Cerebral Cortex*, 26(1):402–413.

Allotey, J., Zamora, J., Cheong-See, F., Kalidindi, M., Arroyo-Manzano, D., Asztalos, E., van der Post, J. A., Mol, B. W., Moore, D., Birtles, D., Khan, K. S., and Thangaratinam, S. (2018). Cognitive, motor, behavioural and academic performances of children born preterm: a meta-analysis and systematic review involving 64.061 children. *BJOG: An International Journal of Obstetrics and Gynaecology*, 125(1):16–25.

Amico, E., Gomez, F., Di Perri, C., Vanhaudenhuyse, A., Lesenfants, D., Boveroux, P., Bonhomme, V., Brichant, J. F., Marinazzo, D., and Laureys, S. (2014). Posterior cingulate

cortex-related co-activation patterns: A resting state fMRI study in propofol-induced loss of consciousness. *PLoS ONE*, 9(6):1–9.

Amico, E. and Goñi, J. (2018). Mapping hybrid functional-structural connectivity traits in the human connectome. *Network Neuroscience*, 2(3):306–322.

Anderson, M. C. (2004). Neural Systems Underlying the Suppression of Unwanted Memories. *Science*, 303(5655):232–235.

Anderson, P. J. (2014). Neuropsychological outcomes of children born very preterm. *Seminars in Fetal and Neonatal Medicine*, 19(2):90–96.

Andrews-Hanna, J. R., Reidler, J. S., Sepulcre, J., Poulin, R., and Buckner, R. L. (2010). Functional-Anatomic Fractionation of the Brain's Default Network. *Neuron*, 65(4):550–562.

Arichi, T., Fagiolo, G., Varela, M., Melendez-Calderon, A., Allievi, A., Merchant, N., Tusor, N., Counsell, S. J., Burdet, E., Beckmann, C. F., and Edwards, A. D. (2012). Development of BOLD signal hemodynamic responses in the human brain. *NeuroImage*, 63(2):663–673.

Arichi, T., Moraux, A., Melendez, A., Doria, V., Groppo, M., Merchant, N., and Combs, S. (2010). Somatosensory cortical activation identi fi ed by functional MRI in preterm and term infants. *NeuroImage*, 49(3):2063–2071.

Arthur, D. and Vassilvitskii, S. (2007). k-means ++ : The Advantages of Careful Seeding. *Proceedings of the eighteenth annual ACM-SIAM symposium on Discrete algorithms*, pages 1027–1035.

Ashburber, J. and Friston, K. J. (1998). Spatial normalization. *Brain Warping, W. Toga, ed*, pages 27–44.

Attwell, D., Buchan, A., Charpak, S., Lauritzen, M., MacVicar, B., and Newman, E. (2011). Glial and neuronal control of brain blood flow. *Nature*, 468(7321):232–243.

Baczkowski, B. M., Johnstone, T., Walter, H., Erk, S., and Veer, I. M. (2017). Sliding-window analysis tracks fl uctuations in amygdala functional connectivity associated with physiological arousal and vigilance during fear conditioning. *NeuroImage*, 153(March):168–178.

Barker, E. D., Ing, A., Biondo, F., Jia, T., Pingault, J. B., Du Rietz, E., Zhang, Y., Ruggeri, B., Banaschewski, T., Hohmann, S., Bokde, A. L., Bromberg, U., Büchel, C., Quinlan, E. B., Sounga-Barke, E., Bowling, A. B., Desrivières, S., Flor, H., Frouin, V., Garavan, H., Asherson, P., Gowland, P., Heinz, A., Ittermann, B., Martinot, J. L., Martinot, M. L. P., Nees, F., Papadopoulos-Orfanos, D., Poustka, L., Smolka, M. N., Vetter, N. C., Walter, H., Whelan, R., and Schumann, G. (2019). Do ADHD-impulsivity and BMI have shared polygenic and neural correlates? *Molecular Psychiatry*.

Barnea-Goraly, N., Weinzimer, S. A., Ruedy, K. J., Mauras, N., Beck, R. W., Marzelli, M. J., Mazaika, P. K., Aye, T., White, N. H., Tsalikian, E., Fox, L., Kollman, C., Cheng, P., and Reiss, A. L. (2014). High success rates of sedation-free brain MRI scanning in young children using simple subject preparation protocols with and without a commercial mock scanner–the Diabetes Research in Children Network (DirecNet) experience. *Pediatric Radiology*, 44(2):181–186.

Bechara, A. (2000). Emotion, Decision Making and the Orbitofrontal Cortex. *Cerebral Cortex*, 10(3):295–307.

Bedard, A.-C., Nichols, S., Barbosa, J. A., Schachar, R., Logan, G. D., and Tannock, R. (2002). The Development of Selective Inhibitory Control Across the Life Span. *Developmental Neuropsychology*, 21(1):93–111.

Behrman, R. E. and Butler, A. S. (2007). *Preterm birth: Causes, Consequences, and prevention*.

Benavente-Fernández, I., Siddiqi, A., and Miller, S. P. (2020). Socioeconomic status and brain injury in children born preterm: modifying neurodevelopmental outcome. *Pediatric Research*, 87(2):391–398.

Benjamini, Y. and Heller, R. (2007). False Discovery Rates for Spatial Signals. *Journal of the American Statistical Association*, 102(480):1272–1281.

Bishop, S. R. (2004). Mindfulness: A Proposed Operational Definition. *Clinical Psychology: Science and Practice*, 11(3):230–241.

Biswal, B., Zerrin Yetkin, F., Haughton, V. M., and Hyde, J. S. (1995). Functional connectivity in the motor cortex of resting human brain using echo-planar mri. *Magnetic Resonance in Medicine*, 34(4):537–541.

Bjuland, K. J., Løhaugen, G. C. C., Martinussen, M., and Skranes, J. (2013). Cortical thickness and cognition in very-low-birth-weight late teenagers. *Early Human Development*, 89(6):371–380.

Blair, R. J. R. (2000). Impaired social response reversal: A case of 'acquired sociopathy'. *Brain*, 123(6):1122–1141.

Blencowe, H., Cousens, S., Chou, D., Oestergaard, M., Say, L., Moller, A.-b., and Kinney, M. (2013). Born Too Soon: The global epidemiology of 15 million preterm births. *Born Too soon the global epidemiology of 15 million preterm births*, 10(Suppl 1):1–14.

Boardman, J. P., Hall, J., Thrippleton, M. J., Reynolds, R. M., Bogaert, D., Davidson, D. J., Schwarze, J., Drake, A. J., Chandran, S., Bastin, M. E., and Fletcher-Watson, S. (2020). Impact of preterm birth on brain development and long-term outcome: protocol for a cohort study in Scotland. *BMJ Open*, 10(3):e035854.

Bolton, T. A. W., Freitas, L. G. A., Jochaut, D., Giraud, A.-L., and Van De Ville, D. (2020a). Neural responses in autism during movie watching: Inter-individual response variability co-varies with symptomatology. *NeuroImage*, page 116571.

Bolton, T. A. W., Jochaut, D., Giraud, A. L., and Van De Ville, D. (2018a). Brain dynamics in ASD during movie-watching show idiosyncratic functional integration and segregation. *Human Brain Mapping*, 39(6):2391–2404.

Bolton, T. A. W., Tarun, A., Sterpenich, V., Schwartz, S., and Van De Ville, D. (2018b). Interactions Between Large-Scale Functional Brain Networks are Captured by Sparse Coupled HMMs. *IEEE Transactions on Medical Imaging*, 37(1):230–240.

Bolton, T. A. W., Tuleasca, C., Wotruba, D., Rey, G., Dhanis, H., Gauthier, B., Delavari, F., Morgenroth, E., Gaviria, J., Blondiaux, E., Smigielski, L., and Van De Ville, D. (2020b). TbCAPs: A toolbox for co-activation pattern analysis. *NeuroImage*, 211:116621.

Bora, S., Pritchard, V. E., Chen, Z., Inder, T. E., and Woodward, L. J. (2014). Neonatal cerebral morphometry and later risk of persistent inattention/hyperactivity in children born very preterm. *Journal of Child Psychology and Psychiatry*, 55(7):828–838.

Bouzerda-Wahlen, A., Nahum, L., Liverani, M. C., Guggisberg, A. G., and Schnider, A. (2015). An Electrophysiological Dissociation between Orbitofrontal Reality Filtering and Context Source Monitoring. *Journal of Cognitive Neuroscience*, 27(1):164–174.

Braun, K. (2011). The Prefrontal-Limbic System: Development, Neuroanatomy, Function, and Implications for Socioemotional Development. *Clinics in Perinatology*, 38(4):685–702.

Braun, U., Schäfer, A., Walter, H., Erk, S., Romanczuk-Seiferth, N., Haddad, L., Schweiger, J. I., Grimm, O., Heinz, A., Tost, H., Meyer-Lindenberg, A., and Bassett, D. S. (2015). Dynamic reconfiguration of frontal brain networks during executive cognition in humans. *Proceedings of the National Academy of Sciences*, 112(37):11678–11683.

Breeman, L. D., Jaekel, J., Baumann, N., Bartmann, P., and Wolke, D. (2017). Neonatal predictors of cognitive ability in adults born very preterm: a prospective cohort study. *Developmental Medicine & Child Neurology*, 59(5):477–483.

Briend, F., Armstrong, W. P., Kraguljac, N. V., Keilhloz, S. D., and Lahti, A. C. (2020). Aberrant static and dynamic functional patterns of frontoparietal control network in antipsychotic-naïve first-episode psychosis subjects. *Human Brain Mapping*, page hbm.24992.

Brown, C. J., Miller, S. P., Booth, B. G., Andrews, S., Chau, V., Poskitt, K. J., and Hamarneh, G. (2014). Structural network analysis of brain development in young preterm neonates. *NeuroImage*, 101:667–680.

Brydges, C. R., Landes, J. K., Reid, C. L., Campbell, C., French, N., and Anderson, M. (2018). Cognitive outcomes in children and adolescents born very preterm: a meta-analysis. *Developmental Medicine and Child Neurology*, 60(5):452–468.

Buckner, R. L. and DiNicola, L. M. (2019). The brain's default network: updated anatomy, physiology and evolving insights. *Nature Reviews Neuroscience*, 20(10):593–608.

Burgund, E. D., Kang, H. C., Kelly, J. E., Buckner, R. L., Snyder, A. Z., Petersen, S. E., and Schlaggar, B. L. (2002). The feasibility of a common stereotactic space for children and adults in fMRI studies of development. *NeuroImage*, 17(1):184–200.

Burnett, A. C., Anderson, P. J., Lee, K. J., Roberts, G., Doyle, L. W., Cheong, J. L., Callanan, C., Carse, E., Charlton, M. P., Davis, N., Duff, J., Hutchinson, E., Hayes, M., Kelly, E., McDonald, M., Opie, G., Watkins, A., Williamson, A., and Woods, H. (2018). Trends in executive functioning in extremely preterm children across 3 birth eras. *Pediatrics*, 141(1):1–10.

Butler, A. J. and Page, S. J. (2006). Mental Practice With Motor Imagery: Evidence for Motor Recovery and Cortical Reorganization After Stroke. *Archives of Physical Medicine and Rehabilitation*, 87(12):2–11.

Caballero Gaudes, C., Petridou, N., Francis, S. T., Dryden, I. L., and Gowland, P. A. (2011). Paradigm free mapping with sparse regression automatically detects single-trial functional magnetic resonance imaging blood oxygenation level dependent responses. *Human Brain Mapping*, pages n/a–n/a.

Calhoun, V. D., Adali, T., Pearlson, G. D., and Pekar, J. J. (2001). A Method for Making Group Inferences from Functional MRI Data Using Independent Component Analysis. *Human Brain Mapping*, 151:140–151.

Calhoun, V. D., Miller, R., Pearlson, G., and Adal, T. (2014). The Chronnectome : Time-Varying Connectivity Networks as the Next Frontier in fMRI Data Discovery. *Neuron*, 84(2):262–274.

Cao, X., Sandstede, B., and Luo, X. (2019). A Functional Data Method for Causal Dynamic Network Modeling of Task-Related fMRI. *Front. Neurosci.*, 13(February):1–19.

Ceci, S. J. and Bruck, M. (1993). Suggestibility of the child witness: A historical review and synthesis. *Psychological Bulletin*, 113(3):403–439.

Čeko, M., Gracely, J. L., Fitzcharles, M.-A., Seminowicz, D. A., Schweinhardt, P., and Bushnell, M. C. (2015). Is a Responsive Default Mode Network Required for Successful Working Memory Task Performance? *The Journal of Neuroscience*, 35(33):11595–11605.

Centeno, M., Koepp, M. J., Vollmar, C., Stretton, J., Sidhu, M., Michallef, C., Symms, M. R., Thompson, P. J., and Duncan, J. S. (2014). Language dominance assessment in a bilingual population: Validity of fMRI in the second language. *Epilepsia*, 55(10):1504–1511.

Chaminade, T., Millet, V., and Deruelle, C. (2013). Brain and Cognition fMRI evidence for dorsal stream processing abnormality in adults born preterm. *Brain and Cognition*, 81(1):67–72.

Chang, C. and Glover, G. H. (2010). Time–frequency dynamics of resting-state brain connectivity measured with fMRI. *NeuroImage*, 50(1):81–98.

Chau, C. M. Y., Ranger, M., Bichin, M., Park, M. T. M., Amaral, R. S. C., Chakravarty, M., Poskitt, K., Synnes, A. R., Miller, S. P., and Grunau, R. E. (2019). Hippocampus, Amygdala, and Thalamus Volumes in Very Preterm Children at 8 Years: Neonatal Pain and Genetic Variation. *Frontiers in Behavioral Neuroscience*, 13.

Chen, J. E. and Glover, G. H. (2015). Functional Magnetic Resonance Imaging Methods. *Neuropsychol Rev.*, 2:289–313.

Chen, J. E., Lewis, L. D., Chang, C., Tian, Q., Fultz, N. E., Ohringer, N. A., Rosen, B. R., and Polimeni, J. R. (2020). Resting-state "physiological networks". *NeuroImage*, 213:116707.

Chén, O. Y., Cao, H., Reinen, J. M., Qian, T., Gou, J., Phan, H., De Vos, M., and Cannon, T. D. (2019). Resting-state brain information flow predicts cognitive flexibility in humans. *Scientific Reports*, 9(1):3879.

Chen, T., Cai, W., Ryali, S., Supekar, K., and Menon, V. (2016). Distinct Global Brain Dynamics and Spatiotemporal Organization of the Salience Network. *PLoS Biology*, 14(6):1–21.

Cheng, L., Zhu, Y., Sun, J., Deng, L., He, N., Yang, Y., Ling, H., Ayaz, H., Fu, Y., and Tong, S. (2018). Principal States of Dynamic Functional Connectivity Reveal the Link Between Resting-State and Task-State Brain: An fMRI Study. *International Journal of Neural Systems*, 28(07):1850002.

Cheong, J. L. Y., Anderson, P. J., Roberts, G., Burnett, A. C., Lee, K. J., Thompson, D. K., Molloy, C., Wilson-Ching, M., Connelly, A., Seal, M. L., Wood, S. J., and Doyle, L. W. (2013). Contribution of Brain Size to IQ and Educational Underperformance in Extremely Preterm Adolescents. *PLoS ONE*, 8(10):e77475.

Choe, A. S., Nebel, M. B., Barber, A. D., Cohen, J. R., Xu, Y., Pekar, J. J., Caffo, B., and Lindquist, M. A. (2017). Comparing test-retest reliability of dynamic functional connectivity methods. *NeuroImage*, 158:155–175.

Choudhury, S., Fishman, J. R., McGowan, M. L., and Juengst, E. T. (2014). Big data, open science and the brain: lessons learned from genomics. *Frontiers in Human Neuroscience*, 8(May):1–10.

Christoff, K., Irving, Z. C., Fox, K. C. R., Spreng, R. N., and Andrews-Hanna, J. R. (2016). Mind-wandering as spontaneous thought: a dynamic framework. *Nature Reviews Neuroscience*, 17(11):718–731.

Cohen Kadosh, K., Luo, Q., de Burca, C., Sokunbi, M. O., Feng, J., Linden, D. E., and Lau, J. Y. (2016). Using real-time fMRI to influence effective connectivity in the developing emotion regulation network. *NeuroImage*, 125:616–626.

Cole, M. W., Ito, T., Schultz, D., Mill, R., Chen, R., and Cocuzza, C. (2019). Task activations produce spurious but systematic in fl ation of task functional connectivity estimates. *NeuroImage*, 189(December 2018):1–18.

Conrad, A., Müller, A., Doberenz, S., Kim, S., Meuret, A. E., Wollburg, E., and Roth, W. T. (2007). Psychophysiological Effects of Breathing Instructions for Stress Management. *Applied Psychophysiology and Biofeedback*, 32(2):89–98.

Costa, D., Miranda, D., Burnett, A. C., Doyle, L. W., Cheong, J. L., and Anderson, P. J. (2017). Executive Function and Academic Outcomes in Children Who Were Extremely Preterm Danielle. *Pediatrics*, 140(3).

Costeloe, K. L., Hennessy, E. M., Haider, S., Stacey, F., Marlow, N., and Draper, E. S. (2012). Short term outcomes after extreme preterm birth in England: Comparison of two birth cohorts in 1995 and 2006 (the EPICure studies). *BMJ (Online)*, 345(7886):1–14.

Cox, N. J. (2008). Speaking Stata: Correlation with confidence, or Fisher's z revisited. *Stata Journal*, 8(3):413–439.

Daamen, M., Bäuml, J. G., Scheef, L., Meng, C., Jurcoane, A., Jaekel, J., Sorg, C., Busch, B., Baumann, N., Bartmann, P., Wolke, D., Wohlschläger, A., and Boecker, H. (2015). Neural correlates of executive attention in adults born very preterm. *NeuroImage: Clinical*, 9:581–591.

Dale, A. M. (1999). Optimal Experimental Design for Event-Related fMRI. *Human Brain Mapping*, 114:109–114.

Damadian, R., Goldsmith, M., and Minkoff, L. (1977). NMR in cancer: XVI. FONAR image of the live human body. *Phsiol Chem Phys.*, 9(1):97–100.

Damaraju, E., Phillips, J. R., Lowe, J. R., Ohls, R., Calhou, V. D., and Caprihan, A. (2010). Resting-state functional connectivity differences in premature children. *Frontiers in Systems Neuroscience*, 4(June):1–13.

Damaraju, E., Tagliazucchi, E., Laufs, H., and Calhoun, V. D. (2018). Connectivity dynamics from wakefulness to sleep. *bioRxiv preprint*.

Damoiseaux, J. S., Rombouts, S. A. R. B., Barkhof, F., Scheltens, P., Stam, C. J., Smith, S. M., and Beckmann, C. F. (2006). Consistent resting-state networks across healthy subjects. *Proceedings of the National Academy of Sciences*, 103(37):13848–13853.

Daw, N. D., Gershman, S. J., Seymour, B., Dayan, P., and Dolan, R. J. (2011). Model-Based Influences on Humans' Choices and Striatal Prediction Errors. *Neuron*, 69(6):1204–1215.

de Bie, H. M. A., Boersma, M., Wattjes, M. P., Adriaanse, S., Vermeulen, R. J., Oostrom, K. J., Huisman, J., Veltman, D. J., and Delemarre-Van de Waal, H. A. (2010). Preparing children with a mock scanner training protocol results in high quality structural and functional MRI scans. *European Journal of Pediatrics*, 169(9):1079–1085.

de Bie, H. M. A., de Ruiter, M. B., Ouwendijk, M., Oostrom, K. J., Wilke, M., Boersma, M., Veltman, D. J., and Delemarre-van de Waal, H. A. (2015). Using fMRI to Investigate Memory in Young Children Born Small for Gestational Age. *PLOS ONE*, 10(7):e0129721.

de Mooij, B., Fekkes, M., Scholte, R. H. J., and Overbeek, G. (2020). Effective Components of Social Skills Training Programs for Children and Adolescents in Nonclinical Samples: A Multilevel Meta-analysis. *Clinical Child and Family Psychology Review*.

Decety, J., Michalska, K. J., and Akitsuki, Y. (2008). Who caused the pain? An fMRI investigation of empathy and intentionality in children. *Neuropsychologia*, 46(11):2607–2614.

Deco, G., Jirsa, V. K., and McIntosh, A. R. (2011). Emerging concepts for the dynamical organization of resting-state activity in the brain. *Nature Reviews Neuroscience*, 12(1):43–56.

Denham, S. A. (2006). Social-Emotional Competence as Support for School Readiness: What Is It and How Do We Assess It? *Early Education & Development*, 17(1):57–89.

D'Esposito, M. and Kayser, Andrewand Chen, A. (2016). *Functional MRI: Applications in Cognitive Neuroscience*, pages 317–353. Springer New York, New York, NY.

Devor, A., Dunn, A. K., Andermann, M. L., Ulbert, I., Boas, D. A., and Dale, A. M. (2003). Coupling of Total Hemoglobin Concentration, Oxygenation, and Neural Activity in Rat Somatosensory Cortex. *Neuron*, 39(2):353–359.

Di, X., Fu, Z., Chan, S. C., Hung, Y. S., and Biswal, B. B. (2015). Task-related functional connectivity dynamics in a block-designed visual experiment. *Front. Hum. Neurosci.*, 9(September):1–11.

Di Martino, A., Yan, C. G., Li, Q., Denio, E., Castellanos, F. X., Alaerts, K., Anderson, J. S., Assaf, M., Bookheimer, S. Y., Dapretto, M., Deen, B., Delmonte, S., Dinstein, I., Ertl-Wagner, B., Fair, D. A., Gallagher, L., Kennedy, D. P., Keown, C. L., Keysers, C., Lainhart, J. E., Lord, C., Luna, B., Menon, V., Minshew, N. J., Monk, C. S., Mueller, S., Müller, R. A., Nebel, M. B., Nigg, J. T., O'Hearn, K., Pelphrey, K. A., Peltier, S. J., Rudie, J. D., Sunaert, S., Thioux, M., Tyszka, J. M., Uddin, L. Q., Verhoeven, J. S., Wenderoth, N., Wiggins, J. L., Mostofsky, S. H., and Milham, M. P. (2014). The autism brain imaging data exchange: Towards a large-scale evaluation of the intrinsic brain architecture in autism. *Molecular Psychiatry*, 19(6):659–667.

Diamond, A. (2002). Normal Development of Prefrontal Cortex from Birth to Young Adulthood: Cognitive Functions, Anatomy, and Biochemistry. In *Principles of Frontal Lobe Function*, pages 466–503. Oxford University Press.

Dixon, M. L., Thiruchselvam, R., Todd, R., and Christoff, K. (2017). Emotion and the prefrontal cortex: An integrative review. *Psychological Bulletin*, 143(10):1033–1081.

Domitrovich, C. E., Cortes, R. C., and Greenberg, M. T. (2007). Improving Young Children's Social and Emotional Competence: A Randomized Trial of the Preschool "PATHS" Curriculum. *The Journal of Primary Prevention*, 28(2):67–91.

Doria, V., Beckmann, C. F., Arichi, T., Merchant, N., Groppo, M., and Turkheimer, F. E. (2010). Emergence of resting state networks in the preterm human brain. *Proceedings of the National Academy of Sciences of the United States of America*, 107:20015–20020.

Doyle, L. W. and Anderson, P. J. (2010). Adult Outcome of Extremely Preterm Infants. *PEDIATRICS*, 126(2):342–351.

Easson, A. K. and McIntosh, A. R. (2019). BOLD signal variability and complexity in children and adolescents with and without autism spectrum disorder. *Developmental Cognitive Neuroscience*, 36(March):100630.

Eavani, H., Satterthwaite, T. D., Gur, R. E., Gur, R. C., and Davatzikos, C. (2013). Unsupervised learning of functional network dynamics in resting state fMRI. *Lecture Notes in Computer Science (including subseries Lecture Notes in Artificial Intelligence and Lecture Notes in Bioinformatics)*, 7917 LNCS:426–437.

Eklund, A., Nichols, T. E., and Knutsson, H. (2016). Cluster failure: why fMRI inferences for spatial extent have inflated false-positive rates. *Proceedings of the National Academy of Sciences*, page 201602413.

Elliott, M. L., Knodt, A. R., Cooke, M., Kim, M. J., Melzer, T. R., Keenan, R., Ireland, D., Ramrakha, S., Poulton, R., Caspi, A., Moffitt, T. E., and Hariri, A. R. (2019). General functional connectivity: Shared features of resting-state and task fMRI drive reliable and heritable individual differences in functional brain networks. *NeuroImage*, 189(November 2018):516–532.

Engelhardt, L. E., Roe, M. A., Juranek, J., DeMaster, D., Harden, K. P., Tucker-Drob, E. M., and Church, J. A. (2017). Children's head motion during fMRI tasks is heritable and stable over time. *Developmental Cognitive Neuroscience*, 25:58–68.

Evans, S., Ling, M., Hill, B., Rinehart, N., Austin, D., and Sciberras, E. (2018). Systematic review of meditation-based interventions for children with ADHD. *European Child & Adolescent Psychiatry*, 27(1):9–27.

Evrard, D., Charollais, A., Marret, S., Radi, S., Rezrazi, A., and Mellier, D. (2011). Cognitive and emotional regulation developmental issues in preterm infants 12 and 24 months after birth. *European Journal of Developmental Psychology*, 8(2):171–184.

Faghiri, A., Stephen, J. M., Wang, Y. P., Wilson, T. W., and Calhoun, V. D. (2018). Changing brain connectivity dynamics: From early childhood to adulthood. *Human Brain Mapping*, 39(3):1108–1117.

Farahani, F. V., Karwowski, W., and Lighthall, N. R. (2019). Application of graph theory for identifying connectivity patterns in human brain networks: A systematic review. *Frontiers in Neuroscience*, 13(JUN):1–27.

Felver, J. C., Tipsord, J. M., Morris, M. J., Racer, K. H., and Dishion, T. J. (2017). The Effects of Mindfulness-Based Intervention on Children's Attention Regulation. *Journal of Attention Disorders*, 21(10):872–881.

Ferreira, R. d. C., Alves, C. R. L., Guimarães, M. A. P., de Menezes, K. K. P., and Magalhães, L. d. C. (2020). Effects of early interventions focused on the family in the development of children born preterm and/or at social risk: a meta-analysis. *Jornal de Pediatria*, 96(1):20–38.

Fischi-Gomez, E., Muñoz-Moreno, E., Vasung, L., Griffa, A., Borradori-Tolsa, C., Monnier, M., Lazeyras, F., Thiran, J.-P., and Hüppi, P. S. (2016). Brain network characterization of high-risk preterm-born school-age children. *NeuroImage: Clinical*, 11:195–209.

Fischi-Gómez, E., Vasung, L., Meskaldji, D.-E., Lazeyras, F., Borradori-Tolsa, C., Hagmann, P., Barisnikov, K., Thiran, J.-P., and Hüppi, P. S. (2015). Structural Brain Connectivity in School-Age Preterm Infants Provides Evidence for Impaired Networks Relevant for Higher Order Cognitive Skills and Social Cognition. *Cerebral Cortex*, 25(9):2793–2805.

Fong, A. H. C., Yoo, K., Rosenberg, M. D., Zhang, S., Li, C.-S. R., Scheinost, D., Constable, R. T., and Chun, M. M. (2019). Dynamic functional connectivity during task performance and rest predicts individual differences in attention across studies. *NeuroImage*, 188:14–25.

Fox, M. D., Snyder, A. Z., Vincent, J. L., and Raichle, M. E. (2007). Intrinsic Fluctuations within Cortical Systems Account for Intertrial Variability in Human Behavior. *Neuron*, 56:171–184.

Fransson, P., Åden, U., Blennow, M., and Lagercrantz, H. (2011). The functional architecture of the infant brain as revealed by resting-state fMRI. *Cerebral Cortex*, 21(1):145–154.

Fransson, P., Schiffler, B. C., and Thompson, W. H. (2018). Brain network segregation and integration during an epoch-related working memory fMRI experiment. *NeuroImage*, 178(May):147–161.

Fransson, P., Skiöld, B., Horsch, S., Nordell, A., Blennow, M., Lagercrantz, H., and Aden, U. (2007). Resting-state networks in the infant brain. *Proceedings of the National Academy of Sciences of the United States of America*, 104(39):15531–6.

Freitas, L. G. A., Bolton, T. A. W., Krikler, B. E., Jochaut, D., Giraud, A.-L., Hüppi, P. S., and Van De Ville, D. (2020). Time-resolved effective connectivity in task fMRI: Psychophysiological interactions of Co-Activation patterns. *NeuroImage*, 212:116635.

Friston, K., Buechel, C., Fink, G., Morris, J., Rolls, E., and Dolan, R. (1997). Psychophysiological and Modulatory Interactions in Neuroimaging. *NeuroImage*, 6(3):218–229.

Friston, K., Frith, C., Frackowiak, R., and Turner, R. (1995). Characterizing Dynamic Brain Responses with fMRI: A Multivariate Approach. *NeuroImage*, 2(2):166–172.

Friston, K., Josephs, O., Rees, G., and Turner, R. (1998). Non-linear event-related responses in fMRI. *Magnetic Resonance in Medicine*, 39:41–52.

Friston, K. J., Harrison, L., and Penny, W. (2003). Dynamic causal modelling. *NeuroImage*, 19(4):1273–1302.

Friston, K. J., Holmes, A. P., Worsley, K. J., Poline, J.-P., Frith, C. D., and Frackowiak, R. S. (1994). Statistical parametric maps in functional imaging: a general linear approach. *Human brain mapping*, 2(4):189–210.

Friston, K. J., Williams, S., Howard, R., Frackowiak, R. S. J., and Turner, R. (1996). Movement-Related effects in fMRI time-series. *Magnetic Resonance in Medicine*, 35(3):346–355.

Fuchs, E., Ayali, A., Robinson, A., Hulata, E., and Ben-Jacob, E. (2007). Coemergence of Regularity and Complexity During Neural Network Development. *InterScience*, 67(13):18021814.

Galvan, A., Hare, T. A., Parra, C. E., Penn, J., Voss, H., Glover, G., and Casey, B. J. (2006). Earlier Development of the Accumbens Relative to Orbitofrontal Cortex Might Underlie Risk-Taking Behavior in Adolescents. *Journal of Neuroscience*, 26(25):6885–6892.

Ganella, E. P., Burnett, A., Cheong, J., Thompson, D., Roberts, G., Wood, S., Lee, K., Duff, J., Anderson, P. J., Pantelis, C., Doyle, L. W., and Bartholomeusz, C. (2015). Abnormalities in orbitofrontal cortex gyrification and mental health outcomes in adolescents born extremely preterm and/or at an extremely low birth weight. *Human Brain Mapping*, 36(3):1138–1150.

Gao, W., Alcauter, S., Smith, J. K., Gilmore, J. H., and Lin, W. (2015). Development of human brain cortical network architecture during infancy. *Brain structure & function*, 220(2):1173–1186.

Garrett, D. D., Kovacevic, N., McIntosh, A. R., and Grady, C. L. (2010). Blood Oxygen Level-Dependent Signal Variability Is More than Just Noise. *Journal of Neuroscience*, 30(14):4914–4921.

Garrett, D. D., Kovacevic, N., McIntosh, A. R., and Grady, C. L. (2011). The Importance of Being Variable. *Journal of Neuroscience*, 31(12):4496–4503.

Garrett, D. D., Kovacevic, N., McIntosh, A. R., and Grady, C. L. (2013a). The modulation of BOLD variability between cognitive states varies by age and processing speed. *Cerebral Cortex*, 23(3):684–693.

Garrett, D. D., Samanez-Larkin, G. R., MacDonald, S. W., Lindenberger, U., McIntosh, A. R., and Grady, C. L. (2013b). Moment-to-moment brain signal variability: A next frontier in human brain mapping? *Neuroscience & Biobehavioral Reviews*, 37(4):610–624.

Ge, B., Wang, H., Wang, P., Tian, Y., Zhang, X., and Liu, T. (2019). Discovering and characterizing dynamic functional brain networks in task FMRI. *Brain Imaging and Behavior*.

Ghosh, A., Rho, Y., McIntosh, A. R., Kötter, R., and Jirsa, V. K. (2008). Noise during rest enables the exploration of the brain's dynamic repertoire. *PLoS Computational Biology*, 4(10).

Giedd, J. N., Blumenthal, J., Jeffries, N. O., Castellanos, F. X., Liu, H., Zijdenbos, A., Paus, T., Evans, A. C., and Rapoport, J. L. (1999). Brain development during childhood and adolescence: a longitudinal MRI study. *Nature Neuroscience*, 2(10):861–863.

Gimenez, M., Junque, C., Vendrell, P., Narberhaus, A., Bargallo, N., Botet, F., and Mercader, J. M. (2006). Abnormal orbitofrontal development due to prematurity. *Neurology*, 67(10):1818–1822.

Glover, G. H. (1999). Deconvolution of Impulse Response in Event-Related BOLD fMRI. *NeuroImage*, 9(4):416–429.

Gogtay, N., Giedd, J. N., Lusk, L., Hayashi, K. M., Greenstein, D., Vaituzis, A. C., Nugent, T. F., Herman, D. H., Clasen, L. S., Toga, A. W., Rapoport, J. L., and Thompson, P. M. (2004). Dynamic mapping of human cortical development during childhood through early adulthood. *Proceedings of the National Academy of Sciences*, 101(21):8174–8179.

Goldman, R. I., Stern, J. M., Engel, J., and Cohen, M. S. (2000). Acquiring simultaneous EEG and functional MRI. *Clinical Neurophysiology*, 111(11):1974–1980.

Gonzalez-Castillo, J. and Bandettini, P. A. (2018). Task-based dynamic functional connectivity: Recent findings and open questions. *NeuroImage*, (August):1–8.

Gonzalez-Castillo, J., Hoy, C. W., Handwerker, D. A., Robinson, M. E., Buchanan, L. C., Saad, Z. S., and Bandettini, P. A. (2015). Tracking ongoing cognition in individuals using brief, whole-brain functional connectivity patterns. *Proceedings of the National Academy of Sciences*, 112(28):8762–8767.

Gorno-Tempini, M. L., Hutton, C., Josephs, O., Deichmann, R., Price, C., and Turner, R. (2002). Echo Time Dependence of BOLD Contrast and Susceptibility Artifacts. *NeuroImage*, 15(1):136–142.

Gozdas, E., Parikh, N. A., Merhar, S. L., Tkach, J. A., He, L., and Holland, S. K. (2018). Altered functional network connectivity in preterm infants: antecedents of cognitive and motor impairments? *Brain Structure and Function*, 223(8):3665–3680.

Gozzo, Y., Vohr, B., Lacadie, C., Hampson, M., Katz, K. H., Maller-kesselman, J., Schneider, K. C., Peterson, B. S., Rajeevan, N., Makuch, R. W., Constable, R. T., and Ment, L. R. (2009). Alterations in neural connectivity in preterm children at school age. *NeuroImage*, 48(2):458–463.

Grazzani, I., Ornaghi, V., Conte, E., Pepe, A., and Caprin, C. (2018). The Relation Between Emotion Understanding and Theory of Mind in Children Aged 3 to 8: The Key Role of Language. *Frontiers in Psychology*, 9.

Greene, D. J., Black, K. J., and Schlaggar, B. L. (2016). Considerations for MRI study design and implementation in pediatric and clinical populations. *Developmental Cognitive Neuroscience*, 18:101–112.

Groeschel, S., Holmström, L., Northam, G., Tournier, J.-D., Baldeweg, T., Latal, B., Caflisch, J., and Vollmer, B. (2019). Motor Abilities in Adolescents Born Preterm Are Associated With Microstructure of the Corpus Callosum. *Frontiers in Neurology*, 10.

Grover, V. P., Tognarelli, J. M., Crossey, M. M., Cox, I. J., Taylor-Robinson, S. D., and McPhail, M. J. (2015). Magnetic Resonance Imaging: Principles and Techniques: Lessons for Clinicians. *Journal of Clinical and Experimental Hepatology*, 5(3):246–255.

Güntensperger, D., Thüring, C., Meyer, M., Neff, P., and Kleinjung, T. (2017). Neurofeedback for Tinnitus Treatment – Review and Current Concepts. *Frontiers in Aging Neuroscience*, 9.

Habas, P. A., Kim, K., Rousseau, F., Glenn, O. A., Barkovich, A. J., and Studholme, C. (2010). Atlas-based segmentation of developing tissues in the human brain with quantitative validation in young fetuses. *Human Brain Mapping*, 31(9):1348–1358.

Hansen, E. C., Battaglia, D., Spiegler, A., Deco, G., and Jirsa, V. K. (2015). Functional connectivity dynamics: Modeling the switching behavior of the resting state. *NeuroImage*, 105:525–535.

Harnishfeger, K. K. (1995). The development of cognitive inhibition. In *Interference and Inhibition in Cognition*, pages 175–204. Elsevier.

Harrewijn, A., Abend, R., Linke, J., Brotman, M. A., Fox, N. A., Leibenluft, E., Winkler, A. M., and Pine, D. S. (2020). Combining fMRI during resting state and an attention bias task in children. *NeuroImage*, 205:116301.

Harrington, E. M., Trevino, S. D., Lopez, S., and Giuliani, N. R. (2020). Emotion regulation in early childhood: Implications for socioemotional and academic components of school readiness. *Emotion*, 20(1):48–53.

Healy, E., Reichenberg, A., Nam, K. W., Allin, M. P., Walshe, M., Rifkin, L., Murray, S. R. M., and Nosarti, C. (2013). Preterm Birth and Adolescent Social Functioning–Alterations in Emotion-Processing Brain Areas. *The Journal of Pediatrics*, 163(6):1596–1604.

Heeger, D. J., Huk, A. C., Geisler, W. S., and Albrecht, D. G. (2000). Spikes versus BOLD : what does neuroimaging tell us about neuronal activity ? *Nature neuroscience*, 3(7):631–2.

Heep, A., Scheef, L., Jankowski, J., Born, M., Zimmermann, N., Sival, D., Bos, A., Gieseke, J., Bartmann, P., Schild, H., and Boecker, H. (2009a). Functional Magnetic Resonance Imaging of the Sensorimotor System in Preterm Infants. *PEDIATRICS*, 123(1):294–300.

Heep, A., Scheef, L., Jankowski, J., Born, M., Zimmermann, N., Sival, D., Bos, A., Gieseke, J., Bartmann, P., Schild, H., and Boecker, H. (2009b). Functional Magnetic Resonance Imaging of the Sensorimotor System in Preterm Infants. *PEDIATRICS*, 123(1):294–300.

Honey, C. J., Sporns, O., Cammoun, L., Gigandet, X., Thiran, J. P., Meuli, R., and Hagmann, P. (2009). Predicting human resting-state functional connectivity from structural connectivity. *Proceedings of the National Academy of Sciences*, 106(6):2035–2040.

Hornman, J., De Winter, A. F., Kerstjens, J. M., Bos, A. F., and Reijneveld, S. A. (2016). Emotional and behavioral problems of preterm and full-term children at school entry. *Pediatrics*, 137(5).

Huang, W., Bolton, T. A. W., Medaglia, J. D., Bassett, D. S., Ribeiro, A., and Van De Ville, D. (2018). A Graph Signal Processing Perspective on Functional Brain Imaging. *Proceedings of the IEEE*, 106(5):868–885.

Hüning, B., Storbeck, T., Bruns, N., Dransfeld, F., Hobrecht, J., Karpienski, J., Sirin, S., Schweiger, B., Weiss, C., Felderhoff-Müser, U., and Müller, H. (2018). Relationship between brain function (aEEG) and brain structure (MRI) and their predictive value for neurodevelopmental outcome of preterm infants. *European Journal of Pediatrics*, 177(8):1181–1189.

Huppi, P. S., Maier, S. E., Peled, S., Zientara, G. P., Barnes, P. D., Jolesz, F. A., and Volpe, J. J. (1998). Microstructural Development of Human Newborn Cerebral White Matter Assessed in Vivo by Diffusion Tensor Magnetic Resonance Imaging. *Pediatr Res*, 44(4):584–590.

Hutchison, R. M. and Morton, J. B. (2015). Tracking the brain's functional coupling dynamics over development. *Journal of Neuroscience*, 35(17):6849–6859.

Hutchison, R. M., Womelsdorf, T., Allen, E. A., Bandettini, P. A., Calhoun, V. D., Corbetta, M., Della Penna, S., Duyn, J. H., Glover, G. H., Gonzalez-Castillo, J., Handwerker, D. A., Keilholz, S., Kiviniemi, V., Leopold, D. A., de Pasquale, F., Sporns, O., Walter, M., and Chang, C. (2013). Dynamic functional connectivity: Promise, issues, and interpretations. *NeuroImage*, 80:360–378.

Huttenlocher, P. R. and Dabholkar, A. S. (1997). Regional differences in synaptogenesis in human cerebral cortex. *The Journal of Comparative Neurology*, 387(2):167–178.

Hutton, C., Bork, A., Josephs, O., Deichmann, R., Ashburner, J., and Turner, R. (2002). Image Distortion Correction in fMRI: A Quantitative Evaluation. *NeuroImage*, 16(1):217–240.

Inder, T. E., Warfield, S. K., Wang, H., and Hüppi, P. S. (2005). Abnormal Cerebral Structure Is Present at Term in Premature Infants. *PEDIATRICS*, 115(2):286–294.

Jankowski, T. and Holas, P. (2020). Effects of Brief Mindfulness Meditation on Attention Switching. *Mindfulness*, 11(5):1150–1158.

Jezzard, P. and Balaban, R. (1995). Correction for Geometric Distortion in Echo Planar Images from B, Field Variations. *Magnetic Resonance in Medicine*, 34:65–73.

Jiang, K., Yi, Y., Li, L., Li, H., Shen, H., Zhao, F., Xu, Y., and Zheng, A. (2019). Functional network connectivity changes in children with attention-deficit hyperactivity disorder: A resting-state fMRI study. *International Journal of Developmental Neuroscience*, 78:1–6.

Jiang, P., Vuontela, V., Tokariev, M., Lin, H., Aronen, E. T., Ma, Y., and Carlson, S. (2018). Functional connectivity of intrinsic cognitive networks during resting state and task performance in preadolescent children. *PLOS ONE*, 13(10):e0205690.

Jochaut, D., Lehongre, K., Saitovitch, A., Devauchelle, A.-D., Olasagasti, I., Chabane, N., Zilbovicius, M., and Giraud, A.-L. (2015). Atypical coordination of cortical oscillations in response to speech in autism. *Frontiers in Human Neuroscience*, 9(March):1–12.

Johns, C. B., Lacadie, C., Vohr, B., Ment, L. R., and Scheinost, D. (2019). Amygdala functional connectivity is associated with social impairments in preterm born young adults. *NeuroImage: Clinical*, 21(June 2018):101626.

Johnson, S. and Marlow, N. (2014). Growing up after extremely preterm birth: Lifespan mental health outcomes. *Seminars in Fetal and Neonatal Medicine*, 19(2):97–104.

Jonker, F. A., Jonker, C., Scheltens, P., and Scherder, E. J. (2015). The role of the orbitofrontal cortex in cognition and behavior. *Reviews in the Neurosciences*, 26(1):1–11.

Kabat-Zinn, J. (1994). *Wherever you go, there you are: Mindfulness meditation in everyday life*. Hyperion, New York, NY.

Kahn, I., Desai, M., Knoblich, U., Bernstein, J., Henninger, M., Graybiel, A. M., Boyden, E. S., Buckner, R. L., and Moore, C. I. (2011). Characterization of the Functional MRI Response Temporal Linearity via Optical Control of Neocortical Pyramidal Neurons. *J Neurosci*, 31(42):15086–15091.

Kahnt, T. (2018). A decade of decoding reward-related fMRI signals and where we go from here. *NeuroImage*, 180:324–333.

Kaiser, R. H., Kang, M. S., Lew, Y., Van Der Feen, J., Aguirre, B., Clegg, R., Goer, F., Esposito, E., Auerbach, R. P., Hutchison, R. M., and Pizzagalli, D. A. (2019). Abnormal frontoinsular-default network dynamics in adolescent depression and rumination: a preliminary resting-state co-activation pattern analysis. *Neuropsychopharmacology*, 44(9):1604–1612.

Kajantie, E., Strang-Karlsson, S., Evensen, K. A. I., and Haaramo, P. (2019). Adult outcomes of being born late preterm or early term – What do we know? *Seminars in Fetal and Neonatal Medicine*, 24(1):66–83.

Karahanoglu, F. I., Caballero-Gaudes, C., Lazeyras, F., and Van De Ville, D. (2013). Total activation: FMRI deconvolution through spatio-temporal regularization. *NeuroImage*, 73:121–134.

Karahanoglu, F. I. and Van De Ville, D. (2015). Transient brain activity disentangles fMRI resting-state dynamics in terms of spatially and temporally overlapping networks. *Nature Communications*, 6:7751.

Karahanoğlu, F. I. and Van De Ville, D. (2017). Dynamics of Large-Scale fMRI Networks: Deconstruct Brain Activity to Build Better Models of Brain Function. *Current Opinion in Biomedical Engineering*, pages 28–36.

Kaufman, A. S. and Kaufman, N. L. (2004). *Kaufman Assessment Battery for Children: Technical manual*. Circle Pines: American Guidance Service, 2nd edition.

Kazemi, K., Moghaddam, H. A., Grebe, R., Gondry-Jouet, C., and Wallois, F. (2007). A neonatal atlas template for spatial normalization of whole-brain magnetic resonance images of newborns: Preliminary results. *NeuroImage*, 37(2):463–473.

Kersbergen, K. J., Leemans, A., Groenendaal, F., Aa, N. E. V. D., Viergever, M. A., Vries, L. S. D., and Benders, M. J. N. L. (2014). Microstructural brain development between 30 and 40

weeks corrected age in a longitudinal cohort of extremely preterm infants. *NeuroImage*, 103:214–224.

Kiviniemi, V., Vire, T., Remes, J., Elseoud, A. A., Starck, T., Tervonen, O., and Nikkinen, J. (2011). A Sliding Time-Window ICA Reveals Spatial Variability of the Default Mode Network in Time. *Brain Connectivity*, 1(4):339–347.

Klein, A., Andersson, J., Ardekani, B. A., Ashburner, J., Avants, B., Chiang, M. C., Christensen, G. E., Collins, D. L., Gee, J., Hellier, P., Song, J. H., Jenkinson, M., Lepage, C., Rueckert, D., Thompson, P., Vercauteren, T., Woods, R. P., Mann, J. J., and Parsey, R. V. (2009). Evaluation of 14 nonlinear deformation algorithms applied to human brain MRI registration. *NeuroImage*, 46(3):786–802.

Koenigs, M., Barbey, A. K., Postle, B. R., and Grafman, J. (2009). Superior Parietal Cortex Is Critical for the Manipulation of Information in Working Memory. *Journal of Neuroscience*, 29(47):14980–14986.

Kolling, N., Behrens, T., Wittmann, M., and Rushworth, M. (2016). Multiple signals in anterior cingulate cortex. *Current Opinion in Neurobiology*, 37:36–43.

Kostović Srzentić, M., Raguž, M., and Ozretić, D. (2019). Specific cognitive deficits in preschool age correlated with qualitative and quantitative MRI parameters in prematurely born children. *Pediatrics and Neonatology*, (xxxx).

Koush, Y., Meskaldji, D.-E., Pichon, S., Rey, G., Rieger, S. W., Linden, D. E., Van De Ville, D., Vuilleumier, P., and Scharnowski, F. (2017). Learning Control Over Emotion Networks Through Connectivity-Based Neurofeedback. *Cerebral Cortex*, page bhv311.

Kringelbach, M. (2004). The functional neuroanatomy of the human orbitofrontal cortex: evidence from neuroimaging and neuropsychology. *Progress in Neurobiology*, 72(5):341–372.

Krishnan, A., Williams, L. J., McIntosh, A. R., and Abdi, H. (2011). Partial Least Squares (PLS) methods for neuroimaging: A tutorial and review. *NeuroImage*, 56(2):455–475.

Kucyi, A. and Davis, K. D. (2014). Dynamic functional connectivity of the default mode network tracks daydreaming. *NeuroImage*, 100:471–480.

Kucyi, A., Hove, M. J., Esterman, M., Hutchison, R. M., and Valera, E. M. (2016). Dynamic Brain Network Correlates of Spontaneous Fluctuations in Attention. *Cerebral Cortex*, page bhw029.

Kunz, N., Zhang, H., Vasung, L., O'Brien, K. R., Assaf, Y., Lazeyras, F., Alexander, D. C., and Hüppi, P. S. (2014). Assessing white matter microstructure of the newborn with multi-shell diffusion MRI and biophysical compartment models. *NeuroImage*, 96:288–299.

Kwon, S. H., Vasung, L., Ment, L. R., and Huppi, P. S. (2014). The Role of Neuroimaging in Predicting Neurodevelopmental Outcomes of Preterm Neonates. *Clinics in Perinatology*, 41(1):257–283.

Langerock, N., van Hanswijck de Jonge, L., Bickle Graz, M., Hüppi, P., Borradori Tolsa, C., and Barisnikov, K. (2013). Emotional reactivity at 12 months in very preterm infants born at <29 weeks of gestation. *Infant Behavior and Development*, 36(3):289–297.

Larmor, J. (1897). LXIII. On the theory of the magnetic influence on spectra; and on the radiation from moving ions. *The London, Edinburgh, and Dublin Philosophical Magazine and Journal of Science*, 44:503—-512.

Laufs, H., Kleinschmidt, A., Beyerle, A., Eger, E., Salek-Haddadi, A., Preibisch, C., and Krakow, K. (2003). EEG-correlated fMRI of human alpha activity. *NeuroImage*, 19(4):1463–1476.

Laumann, T. O., Snyder, A. Z., Mitra, A., Gordon, E. M., Gratton, C., Adeyemo, B., Gilmore, A. W., Nelson, S. M., Berg, J. J., Greene, D. J., McCarthy, J. E., Tagliazucchi, E., Laufs, H., Schlaggar, B. L., Dosenbach, N. U. F., and Petersen, S. E. (2016). On the Stability of BOLD fMRI Correlations. *Cerebral Cortex*.

Lauterbur, P. C. (1973). Image Formation by Induced Local Interactions: Examples Employing Nuclear Magnetic Resonance. *Nature*, 242:190–191.

Lee, J. H., Durand, R., Gradinaru, V., Zhang, F., Goshen, I., Kim, D.-s., Fenno, L. E., Ramakrishnan, C., and Deisseroth, K. (2010). Global and local fMRI signals driven by neurons defined optogenetically by type and wiring. *Nature*, 465(7299):788–792.

Lee, M., Smyser, C., and Shimony, J. (2013). Resting-State fMRI: A Review of Methods and Clinical Applications. *American Journal of Neuroradiology*, 34(10):1866–1872.

Lee, M. H., Hacker, C. D., Snyder, A. Z., Corbetta, M., Zhang, D., Leuthardt, E. C., and Shimony, J. S. (2012). Clustering of Resting State Networks. *PLoS ONE*, 7(7):e40370.

Lemieux, L., Salek-Haddadi, A., Lund, T. E., Laufs, H., and Carmichael, D. (2007). Modelling large motion events in fMRI studies of patients with epilepsy. *Magnetic Resonance Imaging*, 25(6):894–901.

Leonardi, N., Richiardi, J., Gschwind, M., Simioni, S., Annoni, J.-m., Schluep, M., Vuilleumier, P., and Ville, D. V. D. (2013). Principal components of functional connectivity : A new approach to study dynamic brain connectivity during rest. *NeuroImage*, 83:937–950.

Leonardi, N., Shirer, W. R., Greicius, M. D., and Van De Ville, D. (2014). Disentangling dynamic networks: Separated and joint expressions of functional connectivity patterns in time. *Human Brain Mapping*, 35(12):5984–5995.

Leonardi, N. and Van De Ville, D. (2015). On spurious and real fluctuations of dynamic functional connectivity during rest. *NeuroImage*, 104:430–436.

Li, G., Wang, L., Shi, F., Gilmore, J. H., Lin, W., Shen, D., and Engineering, C. (2016). Construction of 4D High-definition Cortical Surface Atlases of Infants: Methods and Applications. *Med Image Anal*, 25(1):22–36.

Lima Cardoso, P., Dymerska, B., Bachratá, B., Fischmeister, F. P., Mahr, N., Matt, E., Trattnig, S., Beisteiner, R., and Robinson, S. D. (2018). The clinical relevance of distortion correction in presurgical fMRI at 7 T. *NeuroImage*, 168:490–498.

Lin, P., Yang, Y., Gao, J., Pisapia, N. D., Ge, S., Wang, X., Zuo, C. S., Levitt, J. J., and Niu, C. (2017). Dynamic Default Mode Network across Different Brain States. *Nature Publishing Group*, (October 2016):1–13.

Lin, W., Zhu, Q., Gao, W., Chen, Y., Toh, C.-H., Styner, M., Gerig, G., Smith, J., Biswal, B., and Gilmore, J. (2008). Functional Connectivity MR Imaging Reveals Cortical Functional Connectivity in the Developing Brain. *American Journal of Neuroradiology*, 29(10):1883–1889.

Lindquist, M. A., Meng, J., Atlas, L. Y., and Wager, T. D. (2009). NeuroImage Modeling the hemodynamic response function in fMRI : Ef fi ciency , bias and mis-modeling. *NeuroImage*, 45(1):S187–S198.

Lindquist, M. A. and Wager, T. D. (2007). Validity and power in hemodynamic response modeling: A comparison study and a new approach. *Human Brain Mapping*, 28(8):764–784.

Lindquist, M. A., Xu, Y., Nebel, M. B., and Caffo, B. S. (2014). Evaluating dynamic bivariate correlations in resting-state fMRI: A comparison study and a new approach. *NeuroImage*, 101:531–546.

Lindsay, D., Johnson, M. K., and Kwon, P. (1991). Developmental changes in memory source monitoring. *Journal of Experimental Child Psychology*, 52(3):297–318.

Linsell, L., Johnson, S., Wolke, D., O'Reilly, H., Morris, J. K., Kurinczuk, J. J., and Marlow, N. (2018). Cognitive trajectories from infancy to early adulthood following birth before 26 weeks of gestation: a prospective, population-based cohort study. *Archives of Disease in Childhood*, 103(4):363–370.

Liu, L., Oza, S., Hogan, D., Chu, Y., Perin, J., Zhu, J., Lawn, J. E., Cousens, S., Mathers, C., and Black, R. E. (2016). Global, regional, and national causes of under-5 mortality in 2000–15: an updated systematic analysis with implications for the Sustainable Development Goals. *The Lancet*, 388(10063):3027–3035.

Liu, X., Chang, C., and Duyn, J. H. (2013). Decomposition of spontaneous brain activity into distinct fMRI co-activation patterns. *Frontiers in Systems Neuroscience*, 7(December):1–11.

Liu, X. and Duyn, J. H. (2013). Time-varying functional network information extracted from brief instances of spontaneous brain activity. *Proceedings of the National Academy of Sciences*, 110(11):4392–4397.

Liu, X., Zhang, N., Chang, C., and Duyn, J. H. (2018). Co-activation patterns in resting-state fMRI signals. *NeuroImage*, 180(September 2017):485–494.

Liverani, M. C., Manuel, A. L., Guggisberg, A. G., Nahum, L., and Schnider, A. (2016). No Influence of Positive Emotion on Orbitofrontal Reality Filtering: Relevance for Confabulation. *Frontiers in Behavioral Neuroscience*, 10.

Liverani, M. C., Manuel, A. L., Nahum, L., Guardabassi, V., Tomasetto, C., and Schnider, A. (2017). Children's sense of reality: The development of orbitofrontal reality filtering. *Child Neuropsychology*, 23(4):408–421.

Liverani, Freitas, Siffredi, V., Mikneviciute, G., Martuzzi, R., Meskaldij, D., Borradori Tolsa, C., Ha-Vinh Leuchter, R., Schnider, A., Van De Ville, D., and Hüppi, P. S. (2020). Get real: Orbitofrontal cortex mediates the ability to sense reality in early adolescents. *Brain and Behavior*.

Logothetis, N. K. (2008). What we can do and what we cannot do with fMRI. *Nature*, 453(7197):869–878.

Logothetis, N. K., Pauls, J., Augath, M., Trinath, T., and Oeltermann, A. (2001). Neurophysiological investigation of the basis of the fMRI signal. *Nature*, 412(6843):150–157.

Logothetis, N. K. and Wandell, B. A. (2004). Interpreting the BOLD Signal. *Annual Review of Physiology*, 66(1):735–769.

Loh, J. M., Lindquist, M. A., and Wager, T. D. (2008). Residual analysis for detecting mismodelling in fMRI. *Statistica Sinica*, 18(4):1421–1448.

Lordier, L., Loukas, S., Grouiller, F., Vollenweider, A., Vasung, L., Meskaldij, D., Lejeune, F., Pittet, M. P., Borradori-Tolsa, C., Lazeyras, F., et al. (2018). Music processing in preterm and full-term newborns: A psychophysiological interaction (PPI) approach in neonatal fMRI. *NeuroImage*.

Lordier, L., Meskaldji, D. E., Grouiller, F., Pittet, M. P., Vollenweider, A., Vasung, L., Borradori-Tolsa, C., Lazeyras, F., Grandjean, D., De Ville, D. V., and Hüppi, P. S. (2019). Music in premature infants enhances high-level cognitive brain networks. *Proceedings of the National Academy of Sciences of the United States of America*, 116(24):12103–12108.

Lorenzetti, V., Melo, B., Basílio, R., Suo, C., Yücel, M., Tierra-Criollo, C. J., and Moll, J. (2018). Emotion Regulation Using Virtual Environments and Real-Time fMRI Neurofeedback. *Frontiers in Neurology*, 9.

Loveland, K. A., Steinberg, J. L., Pearson, D. A., Mansour, R., and Reddoch, S. (2008). Judgments of Auditory—Visual Affective Congruence in Adolescents with and without Autism: A Pilot Study of a New Task Using fMRI. *Perceptual and Motor Skills*, 107(2):557–575.

Luna, B., Padmanabhan, A., and O'Hearn, K. (2010). What has fMRI told us about the Development of Cognitive Control through Adolescence? *Brain and Cognition*, 72(1):101–113.

Lundstrom, B. N., Ingvar, M., and Petersson, K. M. (2005). The role of precuneus and left inferior frontal cortex during source memory episodic retrieval. *NeuroImage*, 27(4):824–834.

Ma, Y., Shaik, M. A., Kozberg, M. G., Kim, S. H., Portes, J. P., Timerman, D., and Hillman, E. M. C. (2016). Resting-state hemodynamics are spatiotemporally coupled to synchronized and symmetric neural activity in excitatory neurons. *Proceedings of the National Academy of Sciences*, 113(52):E8463–E8471.

Majeed, W., Magnuson, M., Hasenkamp, W., Schwarb, H., Schumacher, E. H., Barsalou, L., and Keilholz, S. D. (2011). Spatiotemporal dynamics of low frequency BOLD fluctuations in rats and humans. *NeuroImage*, 54(2):1140–1150.

Mankinen, K., Ipatti, P., Harila, M., Nikkinen, J., Paakki, J.-J., Rytky, S., Starck, T., Remes, J., Tokariev, M., Carlson, S., Tervonen, O., Rantala, H., and Kiviniemi, V. (2015). Reading, listening and memory-related brain activity in children with early-stage temporal lobe epilepsy of unknown cause-an fMRI study. *European Journal of Paediatric Neurology*, 19(5):561–571.

Marek, S. and Dosenbach, N. U. F. (2018). The frontoparietal network: function, electrophysiology, and importance of individual precision mapping. *Dialogues in clinical neuroscience*, 20(2):133–140.

Marusak, H. A., Calhoun, V. D., Brown, S., Crespo, L. M., Sala-Hamrick, K., Gotlib, I. H., and Thomason, M. E. (2017). Dynamic functional connectivity of neurocognitive networks in children. *Human Brain Mapping*, 38(1):97–108.

Marusak, H. A., Elrahal, F., Peters, C. A., Kundu, P., Lombardo, M. V., Calhoun, V. D., Goldberg, E. K., Cohen, C., Taub, J. W., and Rabinak, C. A. (2018). Mindfulness and dynamic functional neural connectivity in children and adolescents. *Behavioural Brain Research*, 336:211–218.

McClure, S. M., York, M. K., and Montague, P. R. (2004). The Neural Substrates of Reward Processing in Humans: The Modern Role of fMRI. *The Neuroscientist*, 10(3):260–268.

McIntosh, A. R., Chau, W. K., and Protzner, A. B. (2004). Spatiotemporal analysis of event-related fMRI data using partial least squares. *NeuroImage*, 23(2):764–775.

McIntosh, A. R., Kovacevic, N., Lippe, S., Garrett, D., Grady, C., and Jirsa, V. (2010). The development of a noisy brain. *Archives Italiennes de Biologie*, 148(3):323–337.

Mckeown, M. J., Makeig, S., Brown, G. G., Jung, T.-p., Kindermann, S. S., Bell, A. J., and Sejnowski, T. J. (1998). Analysis of fMRI Data by Blind Separation Into Independent Spatial Components. *Human Brain Mapping*, 188(June 1997):160–188.

McLaren, D. G., Ries, M. L., Xu, G., and Johnson, S. C. (2012). A generalized form of context-dependent psychophysiological interactions (gPPI): A comparison to standard approaches. *NeuroImage*, 61(4):1277–1286.

McRae, K., Gross, J. J., Weber, J., Robertson, E. R., Sokol-Hessner, P., Ray, R. D., Gabrieli, J. D., and Ochsner, K. N. (2012). The development of emotion regulation: an fMRI study of cognitive reappraisal in children, adolescents and young adults. *Social Cognitive and Affective Neuroscience*, 7(1):11–22.

Meissner, T. W., Walbrin, J., Nordt, M., Koldewyn, K., and Weigelt, S. (2019). Let's take a break: Head motion during fmri tasks is reduced in children and adults if data acquisition is distributed across sessions or days. *bioRxiv*.

Menon, R. S. (2001). Imaging function in the working brain with fMRI. *Current Opinion in Neurobiology*, 11(5):630–636.

Menon, V. (2011). Large-scale brain networks and psychopathology: A unifying triple network model. *Trends in Cognitive Sciences*, 15(10):483–506.

Ment, L. R., Hirtz, D., and Hüppi, P. S. (2009). Imaging biomarkers of outcome in the developing preterm brain. *The Lancet Neurology*, 8(11):1042–1055.

Meskaldji, D.-E., Vasung, L., Romascano, D., Thiran, J.-P., Hagmann, P., Morgenthaler, S., and Van De Ville, D. (2015). Improved statistical evaluation of group differences in connectomes by screening–filtering strategy with application to study maturation of brain connections between childhood and adolescence. *NeuroImage*, 108:251–264.

Miller, R. L., Yaesoubi, M., Turner, J. A., Mathalon, D., Preda, A., Pearlson, G., Adali, T., and Calhoun, V. D. (2016). Higher Dimensional Meta-State Analysis Reveals Reduced Resting fMRI Connectivity Dynamism in Schizophrenia Patients. *PloS one*, 11(3):e0149849.

Misaki, M., Phillips, R., Zotev, V., Wong, C.-K., Wurfel, B. E., Krueger, F., Feldner, M., and Bodurka, J. (2019). Brain activity mediators of PTSD symptom reduction during real-time fMRI amygdala neurofeedback emotional training. *NeuroImage: Clinical*, 24:102047.

Mitchell, K. J. and Johnson, M. K. (2009). Source monitoring 15 years later: What have we learned from fMRI about the neural mechanisms of source memory? *Psychological Bulletin*, 135(4):638–677.

Mitchell, K. J., Johnson, M. K., Raye, C. L., and Greene, E. J. (2004). Prefrontal Cortex Activity Associated with Source Monitoring in a Working Memory Task. *Journal of Cognitive Neuroscience*, 16(6):921–934.

Moiseev, A., Doesburg, S. M., and Grunau, R. E. (2015). Altered Network Oscillations and Functional Connectivity Dynamics in Children Born Very Preterm. *Brain Topography*, 28(5):726–745.

Montague, P. and Berns, G. S. (2002). Neural Economics and the Biological Substrates of Valuation. *Neuron*, 36(2):265–284.

Monti, S., Tamayo, P., Mesirov, J., and Golub, T. (2003). Consensus Clustering : A Resampling-Based Method for Class Discovery and Visualization of Gene Expression Microarray Data. *Machine Learning*, 52:91–118.

Moreira, R. S., Magalhães, L. C., and Alves, C. R. (2014). Effect of preterm birth on motor development, behavior, and school performance of schoola-age children: A systematic review. *Jornal de Pediatria*, 90(2):119–134.

Munkres, J. (1957). Algorithms for Assignment and Transportation Problems. *Journal of the Society for Industrial and Applied Mathematics*, 5(1).

Mürner-Lavanchy, I., Ritter, B. C., Spencer-Smith, M. M., Perrig, W. J., Schroth, G., Steinlin, M., and Everts, R. (2014). Visuospatial working memory in very preterm and term born children - Impact of age and performance. *Developmental Cognitive Neuroscience*, 9:106–116.

Nahum, L., Bouzerda-Wahlen, A., Guggisberg, A., Ptak, R., and Schnider, A. (2012). Forms of confabulation: Dissociations and associations. *Neuropsychologia*, 50(10):2524–2534.

Nahum, L., Ptak, R., Leemann, B., and Schnider, A. (2009). Disorientation, Confabulation, and Extinction Capacity: Clues on How the Brain Creates Reality. *Biological Psychiatry*, 65(11):966–972.

Nguyen, T. T., Kovacevic, S., Dev, S. I., Lu, K., Liu, T. T., and Eyler, L. T. (2017). Dynamic functional connectivity in bipolar disorder is associated with executive function and processing speed: A preliminary study. *Neuropsychology*, 31(1):73–83.

Nomi, J. S., Schettini, E., Voorhies, W., Bolt, T. S., Heller, A. S., and Uddin, L. Q. (2018). Resting-state brain signal variability in prefrontal cortex is associated with ADHD symptom severity in children. *Frontiers in Human Neuroscience*, 12(March):1–8.

Nordahl, C. W., Mello, M., Shen, A. M., Shen, M. D., Vismara, L. A., Li, D., Harrington, K., Tanase, C., Goodlin-Jones, B., Rogers, S., Abbeduto, L., and Amaral, D. G. (2016). Methods for acquiring MRI data in children with autism spectrum disorder and intellectual impairment without the use of sedation. *Journal of Neurodevelopmental Disorders*, 8(1):20.

Norris, C. J., Creem, D., Hendler, R., and Kober, H. (2018). Brief Mindfulness Meditation Improves Attention in Novices: Evidence From ERPs and Moderation by Neuroticism. *Frontiers in Human Neuroscience*, 12.

Nosarti, C. (2013). Structural and functional brain correlates of behavioral outcomes during adolescence. *Early Human Development*, 89(4):221–227.

Nosarti, C., Nam, K. W., Walshe, M., Murray, R. M., Cuddy, M., Rifkin, L., and Allin, M. P. (2014). Preterm birth and structural brain alterations in early adulthood. *NeuroImage: Clinical*, 6:180–191.

Nosarti, C., Rubia, K., Smith, A. B., Frearson, S., Williams, S. C., Rifkin, L., and Murray, R. M. (2006). Altered functional neuroanatomy of response inhibition in adolescent males who were born very preterm. *Developmental Medicine & Child Neurology*, 48(04):265.

Ogawa, S., Lee, T. M., and Kay, A. R. (1990). Brain magnetic resonance imaging with contrast dependent on blood oxygenation. *Proceedings of the National Academy of Sciences*, 87(December):9868–9872.

O'Herron, P., Chhatbar, P. Y., Levy, M., Shen, Z., Schramm, A. E., Lu, Z., and Kara, P. (2016). Neural correlates of single-vessel haemodynamic responses in vivo. *Nature*, 534(7607):378–382.

Olsen, A., Dennis, E. L., Evensen, K. A. I., Husby Hollund, I. M., Løhaugen, G. C., Thompson, P. M., Brubakk, A.-M., Eikenes, L., and Håberg, A. K. (2018). Preterm birth leads to hyperreactive cognitive control processing and poor white matter organization in adulthood. *NeuroImage*, 167:419–428.

Olson, I. R., Plotzker, A., and Ezzyat, Y. (2007). The Enigmatic temporal pole: a review of findings on social and emotional processing. *Brain*, 130(7):1718–1731.

O'Reilly, J. X., Woolrich, M. W., Behrens, T. E. J., Smith, S. M., and Johansen-Berg, H. (2012). Tools of the trade: Psychophysiological interactions and functional connectivity. *Social Cognitive and Affective Neuroscience*, 7(5):604–609.

Padilla, N., Alexandrou, G., Blennow, M., Lagercrantz, H., and Ådén, U. (2015). Brain Growth Gains and Losses in Extremely Preterm Infants at Term. *Cerebral Cortex*, 25(7):1897–1905.

Papini, C., White, T. P., Montagna, A., Brittain, P. J., Froudist-Walsh, S., Kroll, J., Karolis, V., Simonelli, A., Williams, S. C., Murray, R. M., and Nosarti, C. (2016). Altered resting-state functional connectivity in emotion-processing brain regions in adults who were born very preterm. *Psychological Medicine*, 46(14):3025–3039.

Perry-Parrish, C., Copeland-Linder, N., Webb, L., and Sibinga, E. M. (2016). Mindfulness-Based Approaches for Children and Youth. *Current Problems in Pediatric and Adolescent Health Care*, 46(6):172–178.

Peters, K. L., Rosychuk, R. J., Hendson, L., Cote, J. J., McPherson, C., and Tyebkhan, J. M. (2009). Improvement of Short- and Long-Term Outcomes for Very Low Birth Weight Infants: Edmonton NIDCAP Trial. *PEDIATRICS*, 124(4):1009–1020.

Petridou, N., Gaudes, C. C., Dryden, I. L., Francis, S. T., and Gowland, P. A. (2013). Periods of rest in fMRI contain individual spontaneous events which are related to slowly fluctuating spontaneous activity. *Human Brain Mapping*, 34(6):1319–1329.

Pierrat, V., Marchand-Martin, L., Arnaud, C., Kaminski, M., Resche-Rigon, M., Lebeaux, C., Bodeau-Livinec, F., Morgan, A. S., Goffinet, F., Marret, S., and Ancel, P.-Y. (2017). Neurodevelopmental outcome at 2 years for preterm children born at 22 to 34 weeks' gestation in France in 2011: EPIPAGE-2 cohort study. *BMJ*, page j3448.

Pigdon, L., Willmott, C., Reilly, S., Conti-ramsden, G., Liegeois, F., Connelly, A., and Morgan, A. T. (2020). The neural basis of nonword repetition in children with developmental speech or language disorder : An fMRI study. *Neuropsychologia*, 138(December 2019):107312.

Pittet-Metrailler, M. P., Mrner-Lavanchy, I., Adams, M., Graz, M. B., Pfister, R. E., Natalucci, G., Grunt, S., Tolsa, C. B., and Swiss National Network and Follow-up Group (2019). Neurodevelopmental outcome at early school age in a Swiss national cohort of very preterm children. *Swiss Medical Weekly*.

Ploner, M., Schoffelen, J. M., Schnitzler, A., and Gross, J. (2009). Functional integration within the human pain system as revealed by Granger causality. *Human Brain Mapping*, 30(12):4025–4032.

Poldrack, R. A. (2012). The future of fMRI in cognitive neuroscience. *NeuroImage*, 62(2):1216–1220.

Poldrack, R. A., Barch, D. M., Mitchell, J. P., Wager, T. D., Wagner, A. D., Devlin, J. T., Cumba, C., Koyejo, O., and Milham, M. P. (2013). Toward open sharing of task-based fMRI data: the OpenfMRI project. *Frontiers in Neuroinformatics*, 7(July):1–12.

Pons, F., Harris, P. L., and Doudin, P.-A. (2002). Teaching emotion understanding. *European Journal of Psychology of Education*, 17(3):293–304.

Power, J. D., Barnes, K. A., Snyder, A. Z., Schlaggar, B. L., and Petersen, S. E. (2012). Spurious but systematic correlations in functional connectivity MRI networks arise from subject motion. *NeuroImage*, 59(3):2142–2154.

Power, J. D., Fair, D. A., Schlaggar, B. L., and Petersen, S. E. (2010). The Development of Human Functional Brain Networks. *Neuron*, 67(5):735–748.

Power, J. D., Mitra, A., Laumann, T. O., Snyder, A. Z., Schlaggar, B. L., and Petersen, S. E. (2014). Methods to detect, characterize, and remove motion artifact in resting state fMRI. *NeuroImage*, 84(2):320–341.

Preti, M. G., Bolton, T., and Van De Ville, D. (2016). The dynamic functional connectome : State-of-the-art and perspectives. *NeuroImage*, (December).

Preti, M. G., Bolton, T., and Van De Ville, D. (2017). The dynamic functional connectome : State-of-the-art and perspectives. *NeuroImage*, (December).

Rack-Gomer, A. L. and Liu, T. T. (2012). Caffeine increases the temporal variability of resting-state BOLD connectivity in the motor cortex. *Neuroimage*, 59(3):2994–3002.

Raichle, M. E. (2001). Cognitive Neuroscience. Bold insights. *Nature*, 412(12):128–130.

Randal, A. and Lobaugh, N. J. (2004). Partial least squares analysis of neuroimaging data : applications and advances. *NeuroImage*, 23:250–263.

Réveillon, M., Urben, S., Barisnikov, K., Borradori Tolsa, C., Hüppi, P. S., and Lazeyras, F. (2013). Functional neuroimaging study of performances on a Go/No-go task in 6- to 7-year-old preterm children: Impact of intrauterine growth restriction. *NeuroImage: Clinical*, 3:429–437.

Rissman, J., Gazzaley, A., and Esposito, M. D. (2004). Measuring functional connectivity during distinct stages of a cognitive task. *NeuroImage*, 23:752–763.

Roberts, R., Wiebels, K., Sumner, R., van Mulukom, V., Grady, C., Schacter, D., and Addis, D. (2017). An fMRI investigation of the relationship between future imagination and cognitive flexibility. *Neuropsychologia*, 95:156–172.

Robinson, L. F., Wager, T. D., and Lindquist, M. A. (2009). Change point estimation in multi-subject fMRI studies. *NeuroImage*.

Rolls, E. T. (2004). The functions of the orbitofrontal cortex. *Brain and Cognition*, 55(1):11–29.

Rommel, A. S., James, S. N., McLoughlin, G., Brandeis, D., Banaschewski, T., Asherson, P., and Kuntsi, J. (2017). Association of Preterm Birth With Attention-Deficit/Hyperactivity Disorder–Like and Wider-Ranging Neurophysiological Impairments of Attention and Inhibition. *Journal of the American Academy of Child and Adolescent Psychiatry*, 56(1):40–50.

Ross, R. S. and Slotnick, S. D. (2008). The Hippocampus is Preferentially Associated with Memory for Spatial Context. *Journal of Cognitive Neuroscience*, 20(3):432–446.

Rubinov, M. and Sporns, O. (2010). Complex network measures of brain connectivity: Uses and interpretations. *NeuroImage*, 52(3):1059–1069.

Rudebeck, P. H. and Murray, E. A. (2014). The Orbitofrontal Oracle: Cortical Mechanisms for the Prediction and Evaluation of Specific Behavioral Outcomes. *Neuron*, 84(6):1143–1156.

Ruoss, K., Lövblad, K., Schroth, G., Moessinger, A. C., and Fusch, C. (2001). Brain Development (Sulci and Gyri) as Assessed by Early Postnatal MR Imaging in Preterm and Term Newborn Infants. *Neuropediatrics*, 32(2):69–74.

Saigal, S., Day, K. L., Van Lieshout, R. J., Schmidt, L. A., Morrison, K. M., and Boyle, M. H. (2016). Health, Wealth, Social Integration, and Sexuality of Extremely Low-Birth-Weight Prematurely Born Adults in the Fourth Decade of Life. *JAMA Pediatrics*, 170(7):678.

Sakoğlu, Ü., Pearlson, G. D., Kiehl, K. A., Wang, Y. M., Michael, A. M., and Calhoun, V. D. (2010). A method for evaluating dynamic functional network connectivity and task-modulation: application to schizophrenia. *Magnetic Resonance Materials in Physics, Biology and Medicine*, 23(5-6):351–366.

Samson, A. C., Kreibig, S. D., Soderstrom, B., Wade, A. A., and Gross, J. J. (2016). Eliciting positive, negative and mixed emotional states: A film library for affective scientists. *Cognition and Emotion*, 30(5):827–856.

Satterthwaite, T. D., Elliott, M. A., Gerraty, R. T., Ruparel, K., Loughead, J., Calkins, M. E., Eickhoff, S. B., Hakonarson, H., Gur, R. C., Gur, R. E., and Wolf, D. H. (2013). An improved framework for confound regression and filtering for control of motion artifact in the preprocessing of resting-state functional connectivity data. *NeuroImage*, 64:240–256.

Schnider, A. (2002). Early Cortical Distinction between Memories that Pertain to Ongoing Reality and Memories that Don't. *Cerebral Cortex*, 12(1):54–61.

Schnider, A. (2003). Spontaneous confabulation and the adaptation of thought to ongoing reality. *Nature Reviews Neuroscience*, 4(8):662–671.

Schnider, A. (2013). Orbitofrontal Reality Filtering. *Frontiers in Behavioral Neuroscience*, 7.

Schnider, A. (2018). *The Confabulating Mind*, volume 1. Oxford University Press.

Schnider, A., Bonvallat, J., Emond, H., and Leemann, B. (2005). Reality confusion in spontaneous confabulation. *Neurology*, 65(7):1117–1119.

Schnider, A. and Ptak, R. (1999). Spontaneous confabulators fail to suppress currently irrelevant memory traces. *Nature Neuroscience*, 2(7):677–681.

Schnider, A., Treyer, V., and Buck, A. (2000). Selection of Currently Relevant Memories by the Human Posterior Medial Orbitofrontal Cortex. *The Journal of Neuroscience*, 20(15):5880–5884.

Schnider, A., von Däniken, C., and Gutbrod, K. (1996). Disorientation in amnesia. *Brain*, 119(5):1627–1632.

Schonert-Reichl, K. A., Oberle, E., Lawlor, M. S., Abbott, D., Thomson, K., Oberlander, T. F., and Diamond, A. (2015). Enhancing cognitive and social–emotional development through a simple-to-administer mindfulness-based school program for elementary school children: A randomized controlled trial. *Developmental Psychology*, 51(1):52–66.

Senbabaoglu, Y., Michailidis, G., and Li, J. Z. (2014). Critical limitations of consensus clustering in class discovery. *Scientific Reports*, 4(6207).

Sgandurra, G., Biagi, L., Fogassi, L., Sicola, E., Ferrari, A., Guzzetta, A., Tosetti, M., and Cioni, G. (2018). Reorganization of the Action Observation Network and Sensory-Motor System in Children with Unilateral Cerebral Palsy: An fMRI Study. *Neural Plasticity*, 2018:1–15.

Shen, H., Li, Z., Qin, J., Liu, Q., Wang, L., Zeng, L. L., Li, H., and Hu, D. (2016). Changes in functional connectivity dynamics associated with vigilance network in taxi drivers. *NeuroImage*, 124:367–378.

Sherman, L. E., Rudie, J. D., Pfeifer, J. H., Masten, C. L., McNealy, K., and Dapretto, M. (2014). Development of the Default Mode and Central Executive Networks across early adolescence: A longitudinal study. *Developmental Cognitive Neuroscience*, 10:148–159.

Shi, F., Wang, L., Wu, G., Li, G., Gilmore, J. H., Lin, W., and Shen, D. (2014). Neonatal atlas construction using sparse representation. *Human Brain Mapping*, 35(9):4663–4677.

Siegel, J. S., Mitra, A., Laumann, T. O., Seitzman, B. A., Raichle, M., Corbetta, M., and Snyder, A. Z. (2017). Data Quality Influences Observed Links Between Functional Connectivity and Behavior. *Cerebral Cortex*, 27(9):4492–4502.

Siffredi, V., Spencer-Smith, M., Barrouillet, P., Vaessen, M., Leventer, R., Anderson, V., and Vuilleumier, P. (2017). Neural correlates of working memory in children and adolescents with agenesis of the corpus callosum: An fMRI study. *Neuropsychologia*, 106:71–82.

Simkin, D. R. and Black, N. B. (2014). Meditation and Mindfulness in Clinical Practice. *Child and Adolescent Psychiatric Clinics of North America*, 23(3):487–534.

Simony, E., Honey, C. J., Chen, J., Lositsky, O., Yeshurun, Y., Wiesel, A., and Hasson, U. (2016). Dynamic reconfiguration of the default mode network during narrative comprehension. *Nature Communications*, 7(May 2015):12141.

Smid, M., Stringer, E., and Stringer, J. (2016). A Worldwide Epidemic: The Problem and Challenges of Preterm Birth in Low- and Middle-Income Countries. *American Journal of Perinatology*, 33(03):276–289.

Smith, S. M. and Nichols, T. E. (2018). Statistical Challenges in "Big Data" Human Neuroimaging. *Neuron*, 97(2):263–268.

Smitha, K. A., Akhil Raja, K., Arun, K. M., Rajesh, P. G., Thomas, B., Kapilamoorthy, T. R., and Kesavadas, C. (2017). Resting state fMRI: A review on methods in resting state connectivity analysis and resting state networks. *Neuroradiology Journal*, 30(4):305–317.

Soares, J. M., Magalhães, R., Moreira, P. S., and Sousa, A. (2016). A Hitchhiker ' s Guide to Functional Magnetic Resonance Imaging. *Frontiers in Neuroscience*, 10(November):1–35.

Somandepalli, K., Kelly, C., Reiss, P. T., Zuo, X.-N., Craddock, R., Yan, C.-G., Petkova, E., Castellanos, F., Milham, M. P., and Di Martino, A. (2015). Short-term test–retest reliability of resting state fMRI metrics in children with and without attention-deficit/hyperactivity disorder. *Developmental Cognitive Neuroscience*, 15:83–93.

Sourty, M., Thoraval, L., Roquet, D., Armspach, J.-P., Foucher, J., and Blanc, F. (2016). Identifying Dynamic Functional Connectivity Changes in Dementia with Lewy Bodies Based on Product Hidden Markov Models. *Frontiers in Computational Neuroscience*, 10(June):1–11.

SOWELL, E. R., DELIS, D., STILES, J., and JERNIGAN, T. L. (2001). Improved memory functioning and frontal lobe maturation between childhood and adolescence: A structural MRI study. *Journal of the International Neuropsychological Society*, 7(3):312–322.

Spiers, H. J. and Maguire, E. A. (2007). A Navigational Guidance System in the Human Brain. *Hippocampus*, 626:618–626.

Spittle, A. J., Treyvaud, K., Lee, K. J., Anderson, P. J., and Doyle, L. W. (2018). The role of social risk in an early preventative care programme for infants born very preterm: a randomized controlled trial. *Developmental Medicine & Child Neurology*, 60(1):54–62.

Spreng, R. N., Mar, R. A., and Kim, A. S. N. (2009). The Common Neural Basis of Autobiographical Memory, Prospection, Navigation, Theory of Mind, and the Default Mode: A Quantitative Meta-analysis. *Journal of Cognitive Neuroscience*, 21(3):489–510.

Sprung, M., Münch, H. M., Harris, P. L., Ebesutani, C., and Hofmann, S. G. (2015). Children's emotion understanding: A meta-analysis of training studies. *Developmental Review*, 37:41–65.

Sripada, K., Bjuland, K. J., Sølsnes, A. E., Håberg, A. K., Grunewaldt, K. H., Løhaugen, G. C., Rimol, L. M., and Skranes, J. (2018). Trajectories of brain development in school-age children born preterm with very low birth weight. *Scientific Reports*, 8(1):15553.

St Clair-Thompson, H. L. and Gathercole, S. E. (2006). Executive functions and achievements in school: Shifting, updating, inhibition, and working memory. *Quarterly Journal of Experimental Psychology*, 59(4):745–759.

Staphorsius, A. S., Kreukels, B. P., Cohen-Kettenis, P. T., Veltman, D. J., Burke, S. M., Schagen, S. E., Wouters, F. M., Delemarre-van de Waal, H. A., and Bakker, J. (2015). Puberty suppression and executive functioning: An fMRI-study in adolescents with gender dysphoria. *Psychoneuroendocrinology*, 56:190–199.

Steuwe, C., Daniels, J. K., Frewen, P. A., Densmore, M., Theberge, J., and Lanius, R. A. (2015). Effect of direct eye contact in women with PTSD related to interpersonal trauma: psychophysiological interaction analysis of connectivity of an innate alarm system. *Psychiatry Research: Neuroimaging*, 232(2):162–167.

Tagliazucchi, E., Balenzuela, P., Fraiman, D., and Chialvo, D. R. (2012). Criticality in Large-Scale Brain fMRI Dynamics Unveiled by a Novel Point Process Analysis. *Frontiers in Physiology*, 3(15).

Tagliazucchi, E., Balenzuela, P., Fraiman, D., Montoya, P., and Chialvo, D. R. (2011). Spontaneous BOLD event triggered averages for estimating functional connectivity at resting state. *Neuroscience Letters*, 488(2):158–163.

Tarun, A., Behjat, H., Bolton, T., Abramian, D., and Van De Ville, D. (2020). Structural mediation of human brain activity revealed by white-matter interpolation of fMRI. *NeuroImage*, 213:116718.

Thézé, R., Manuel, A. L., Pedrazzini, E., Chantraine, F., Patru, M. C., Nahum, L., Guggisberg, A. G., and Schnider, A. (2019). Neural correlates of reality filtering in schizophrenia spectrum disorder. *Schizophrenia Research*, 204:214–221.

Thibault, R. T., MacPherson, A., Lifshitz, M., Roth, R. R., and Raz, A. (2018). Neurofeedback with fMRI: A critical systematic review. *NeuroImage*, 172:786–807.

Thomas Yeo, B. T., Krienen, F. M., Sepulcre, J., Sabuncu, M. R., Lashkari, D., Hollinshead, M., Roffman, J. L., Smoller, J. W., Zöllei, L., Polimeni, J. R., Fischl, B., Liu, H., and Buckner, R. L. (2011). The organization of the human cerebral cortex estimated by intrinsic functional connectivity. *Journal of Neurophysiology*, 106(3):1125–1165.

Thomason, M. E. (2009). Children in Non-Clinical Functional Magnetic Resonance Imaging (fMRI) Studies Give the Scan Experience a "Thumbs Up". *The American Journal of Bioethics*, 9(1):25–27.

Thomason, M. E., Scheinost, D., Manning, J. H., Grove, L. E., Hect, J., Marshall, N., Hernandez-andrade, E., Berman, S., Pappas, A., Yeo, L., Hassan, S. S., Constable, R. T., and Ment, L. R. (2017). Weak functional connectivity in the human fetal brain prior to preterm birth. *Nature Publishing Group*, (June 2016):1–10.

Thompson, D. K., Omizzolo, C., Adamson, C., Lee, K. J., Stargatt, R., Egan, G. F., Doyle, L. W., Inder, T. E., and Anderson, P. J. (2014). Longitudinal growth and morphology of the hippocampus through childhood: Impact of prematurity and implications for memory and learning. *Human Brain Mapping*, 35(8):4129–4139.

Thompson, D. K., Warfield, S. K., Carlin, J. B., Pavlovic, M., Wang, H. X., Bear, M., Kean, M. J., Doyle, L. W., Egan, G. F., and Inder, T. E. (2007). Perinatal risk factors altering regional brain structure in the preterm infant. *Brain*, 130(3):667–677.

Tobia, M. J., Hayashi, K., Ballard, G., Gotlib, I. H., and Waugh, C. E. (2017). Dynamic functional connectivity and individual differences in emotions during social stress. *Human Brain Mapping*, 38(12):6185–6205.

Togo, H., Rokicki, J., Yoshinaga, K., Hisatsune, T., Matsuda, H., Haga, N., and Hanakawa, T. (2017). Effects of Field-Map Distortion Correction on Resting State Functional Connectivity MRI. *Frontiers in Neuroscience*, 11.

Tommiska, V., Trominen, R., and V, F. (2003). Economic costs of care in extremely low birth weight infants during the first 2 years of life. *Pediatr Criti Care Med*, 4(157).

Treyer, V., Buck, A., and Schnider, A. (2003). Subcortical Loop Activation during Selection of Currently Relevant Memories. *Journal of Cognitive Neuroscience*, 15(4):610–618.

Treyer, V., Buck, A., and Schnider, A. (2006). Selection of currently relevant words: an auditory verbal memory study using positron emission tomography. *NeuroReport*, 17(3):323–327.

Twilhaar, E. S., de Kieviet, J. F., Bergwerff, C. E., Finken, M. J., van Elburg, R. M., and Oosterlaan, J. (2019). Social Adjustment in Adolescents Born Very Preterm: Evidence for a Cognitive Basis of Social Problems. *The Journal of Pediatrics*, 213:66–73.e1.

Twilhaar, E. S., Wade, R. M., De Kieviet, J. F., Van Goudoever, J. B., Van Elburg, R. M., and Oosterlaan, J. (2018). Cognitive outcomes of children born extremely or very preterm since the 1990s and associated risk factors: A meta-analysis and meta-regression. *JAMA Pediatrics*, 172(4):361–367.

Uddin, L. Q., Nomi, J. S., Hébert-Seropian, B., Ghaziri, J., and Boucher, O. (2018). Structure and Function of the Human Insula. *Journal of Clinical Neurophysiology*, 34(4):300–306.

van den Heuvel, M. P. and Hulshoff Pol, H. E. (2010). Exploring the brain network: A review on resting-state fMRI functional connectivity. *European Neuropsychopharmacology*, 20(8):519–534.

van den Heuvel, M. P. and Sporns, O. (2013). Network hubs in the human brain. *Trends in Cognitive Sciences*, 17(12):683–696.

Van Dijk, K. R. A., Hedden, T., Venkataraman, A., Evans, K. C., Lazar, S. W., and Buckner, R. L. (2010). Intrinsic Functional Connectivity As a Tool For Human Connectomics: Theory, Properties, and Optimization. *Journal of Neurophysiology*, 103(1):297–321.

Van Essen, D. C., Smith, S. M., Barch, D. M., Behrens, T. E., Yacoub, E., and Ugurbil, K. (2013). The WU-Minn Human Connectome Project: An overview. *NeuroImage*, 80:62–79.

Van Horn, J. D. and Toga, A. W. (2014). Human neuroimaging as a "Big Data" science. *Brain Imaging and Behavior*, 8(2):323–331.

Van Hus, J., Jeukens-Visser, M., Koldewijn, K., Holman, R., Kok, J., Nollet, F., and Van Wassenaer-Leemhuis, A. (2016). Early intervention leads to long-term developmental improvements in very preterm infants, especially infants with bronchopulmonary dysplasia. *Acta Paediatrica*, 105(7):773–781.

Vanderwal, T., Eilbott, J., and Castellanos, F. X. (2019). Movies in the magnet: Naturalistic paradigms in developmental functional neuroimaging. *Developmental Cognitive Neuroscience*, 36:100600.

Vidaurre, D., Smith, S. M., and Woolrich, M. W. (2017). Brain network dynamics are hierarchically organized in time. *Proceedings of the National Academy of Sciences*, 114(48):201705120.

Wager, T. D. (2011). NeuroSynth: a new platform for large-scale automated synthesis of human functional neuroimaging data. *Frontiers in Neuroinformatics*, 5.

Wager, T. D., Davidson, M. L., Hughes, B. L., Lindquist, M. A., and Ochsner, K. N. (2008). Prefrontal-Subcortical Pathways Mediating Successful Emotion Regulation. *Neuron*, 59(6):1037–1050.

Wahlen, A., Nahum, L., Gabriel, D., and Schnider, A. (2011). Fake or Fantasy: Rapid Dissociation between Strategic Content Monitoring and Reality Filtering in Human Memory. *Cerebral Cortex*, 21(11):2589–2598.

Wang, S., Yang, Y., Xing, W., Chen, J., Liu, C., and Luo, X. (2013). Altered neural circuits related to sustained attention and executive control in children with ADHD: An event-related fMRI study. *Clinical Neurophysiology*, 124(11):2181–2190.

Wechsler, D. (2014). *WISC-V: Technical and Interpretative Manual*. Bloomington: Pearson, 5th edition.

Wehrle, F. M., Michels, L., Guggenberger, R., Huber, R., Latal, B., O'Gorman, R. L., and Hagmann, C. F. (2018). Altered resting-state functional connectivity in children and adolescents born very preterm short title. *NeuroImage: Clinical*, 20:1148–1156.

Wen, X., Rangarajan, G., and Ding, M. (2013). Is Granger Causality a Viable Technique for Analyzing fMRI Data? *PLoS ONE*, 8(7).

Western, P. and Patrick, J. (1988). Effects of focusing attention on breathing with and without apparatus on the face. *Respiration Physiology*, 72(1):123–130.

White, T., Muetzel, R., Schmidt, M., Langeslag, S. J., Jaddoe, V., Hofman, A., Calhoun, V. D., Verhulst, F. C., and Tiemeier, H. (2014a). Time of Acquisition and Network Stability in Pediatric Resting-State Functional Magnetic Resonance Imaging. *Brain Connectivity*, 4(6):417–427.

White, T. P., Symington, I., Castellanos, N. P., Brittain, P. J., Froudist Walsh, S., Nam, K. W., Sato, J. R., Allin, M. P., Shergill, S. S., Murray, R. M., Williams, S. C., and Nosarti, C. (2014b). Dysconnectivity of neurocognitive networks at rest in very-preterm born adults. *NeuroImage: Clinical*, 4:352–365.

Whitlow, C. T., Casanova, R., and Maldjian, J. A. (2011). Effect of Resting-State Functional MR Imaging Duration on Stability of Graph Theory Metrics of Brain Network Connectivity. *Radiology*, 259(2):516–524.

Wilke, M., Hauser, T.-K., Krägeloh-Mann, I., and Lidzba, K. (2014). Specific impairment of functional connectivity between language regions in former early preterms. *Human Brain Mapping*, 35(7):3372–3384.

Witt, S., Weitkämper, A., Neumann, H., Lücke, T., and Zmyj, N. (2018). Delayed theory of mind development in children born preterm: A longitudinal study. *Early Human Development*, 127:85–89.

Wolke, D., Johnson, S., and Mendonça, M. (2019). The Life Course Consequences of Very Preterm Birth. *Annual Review of Developmental Psychology*, 1(3):1–24.

Worsley, K. and Friston, K. (1995). Analysis of fMRI Time-Series Revisited–Again. *NeuroImage*, 2:172–181.

Wozniak, J. R., Mueller, B. A., Muetzel, R. L., Bell, C. J., Hoecker, H. L., Nelson, M. L., Chang, P.-N., and Lim, K. O. (2011). Inter-Hemispheric Functional Connectivity Disruption in Children With Prenatal Alcohol Exposure. *Alcoholism: Clinical and Experimental Research*, 35(5):849–861.

Wu, C. W., Chen, C.-L., Liu, P.-Y., Chao, Y.-P., Biswal, B. B., and Lin, C.-P. (2011). Empirical Evaluations of Slice-Timing, Smoothing, and Normalization Effects in Seed-Based, Resting-State Functional Magnetic Resonance Imaging Analyses. *Brain Connectivity*, 1(5):401–410.

Wu, Y., Wang, J., Zhang, Y., Zheng, D., Zhang, J., Rong, M., Wu, H., Wang, Y., Zhou, K., and Jiang, T. (2016). The Neuroanatomical Basis for Posterior Superior Parietal Lobule Control Lateralization of Visuospatial Attention. *Frontiers in Neuroanatomy*, 10.

Yaari, M., Rotzak, N. L., Mankuta, D., Harel-Gadassi, A., Friedlander, E., Eventov-Friedman, S., Bar-Oz, B., Zucker, D., Shinar, O., and Yirmiya, N. (2018). Preterm-infant emotion regulation during the still-face interaction. *Infant Behavior and Development*, 52:56–65.

Yaesoubi, M., Allen, E. A., Miller, R. L., and Calhoun, V. D. (2015). Dynamic coherence analysis of resting fMRI data to jointly capture state-based phase , frequency , and time-domain information. *NeuroImage*, 120:133–142.

Yaple, Z. and Arsalidou, M. (2018). N -back Working Memory Task: Meta-analysis of Normative fMRI Studies With Children. *Child Development*, 89(6):2010–2022.

Yoshida, K., Shimizu, Y., Yoshimoto, J., Takamura, M., Okada, G., Okamoto, Y., Yamawaki, S., and Doya, K. (2017). Prediction of clinical depression scores and detection of changes in whole-brain using resting-state functional MRI data with partial least squares regression. *PLoS ONE*, 12(7):1–21.

Yuan, W., Altaye, M., Ret, J., Schmithorst, V., Byars, A. W., Plante, E., and Holland, S. K. (2009). Quantification of head motion in children during various fMRI language tasks. *Human Brain Mapping*, 30(5):1481–1489.

Zabelina, D. L. and Andrews-Hanna, J. R. (2016). Dynamic network interactions supporting internally-oriented cognition. *Current Opinion in Neurobiology*, 40:86–93.

Zalesky, A. and Breakspear, M. (2015). Towards a statistical test for functional connectivity dynamics. *NeuroImage*, 114:466–470.

Zanesco, A. P., King, B. G., MacLean, K. A., and Saron, C. D. (2018). Cognitive Aging and Long-Term Maintenance of Attentional Improvements Following Meditation Training. *Journal of Cognitive Enhancement*, 2(3):259–275.

Zang, Y. F., Yong, H., Chao-Zhe, Z., Qing-Jiu, C., Man-Qiu, S., Meng, L., Li-Xia, T., Tian-Zi, J., and Yu-Feng, W. (2007). Altered baseline brain activity in children with ADHD revealed by resting-state functional MRI. *Brain and Development*, 29(2):83–91.

Zhang, J., Díaz-Román, A., and Cortese, S. (2018). Meditation-based therapies for attention-deficit/hyperactivity disorder in children, adolescents and adults: a systematic review and meta-analysis. *Evidence Based Mental Health*, 21(3):87–94.

Zhang, L., Zuo, X.-N., Ng, K. K., Chong, J. S. X., Shim, H. Y., Ong, M. Q. W., Loke, Y. M., Choo, B. L., Chong, E. J. Y., Wong, Z. X., Hilal, S., Venketasubramanian, N., Tan, B. Y., Chen, C. L.-H., and Zhou, J. H. (2020). Distinct BOLD variability changes in the default mode and salience networks in Alzheimer's disease spectrum and associations with cognitive decline. *Scientific Reports*, 10(1):6457.

Zhang, Z. G., Hu, L., Hung, Y. S., Mouraux, A., and Iannetti, G. D. (2012). Gamma-Band Oscillations in the Primary Somatosensory Cortex–A Direct and Obligatory Correlate of Subjective Pain Intensity. *Journal of Neuroscience*, 32(22):7429–7438.

Zhong, Y., Wang, H., Lu, G., Zhang, Z., Jiao, Q., and Liu, Y. (2009). Detecting Functional Connectivity in fMRI Using PCA and Regression Analysis. *Brain Topography*, 22(2):134–144.

Zhuang, J., Peltier, S., He, S., LaConte, S., and Hu, X. (2008). Mapping the connectivity with structural equation modeling in an fMRI study of shape-from-motion task. *NeuroImage*, 42(2):799–806.

Zhuang, X., Walsh, R. R., Sreenivasan, K., Yang, Z., Mishra, V., and Cordes, D. (2018). Incorporating spatial constraint in co-activation pattern analysis to explore the dynamics of resting-state networks: An application to Parkinson's disease. *NeuroImage*, 172(September 2017):64–84.

Zmyj, N., Witt, S., Weitkämper, A., Neumann, H., and Lücke, T. (2017). Social Cognition in Children Born Preterm: A Perspective on Future Research Directions. *Frontiers in Psychology*, 8.

Zöller, D., Sandini, C., Karahanoğlu, F. I., Padula, M. C., Schaer, M., Eliez, S., and Van De Ville, D. (2019). Large-Scale Brain Network Dynamics Provide a Measure of Psychosis and Anxiety in 22q11.2 Deletion Syndrome. *Biological Psychiatry: Cognitive Neuroscience and Neuroimaging*, 4(10):881–892.

Zöller, D., Schaer, M., Scariati, E., Padula, M. C., Eliez, S., and Van De Ville, D. (2017). Disentangling resting-state BOLD variability and PCC functional connectivity in 22q11.2 deletion syndrome. *NeuroImage*, 149:85–97.

Zubiaurre-Elorza, L., Soria-Pastor, S., Junque, C., Sala-Llonch, R., Segarra, D., Bargallo, N., and Macaya, A. (2012). Cortical Thickness and Behavior Abnormalities in Children Born Preterm. *PLoS ONE*, 7(7):e42148.

Zwicker, J. G., Missiuna, C., Harris, S. R., and Boyd, L. A. (2011). Brain activation associated with motor skill practice in children with developmental coordination disorder: an fMRI study. *International Journal of Developmental Neuroscience*, 29(2):145–152.

LORENA GONÇALVES DE ALCÂNTARA E FREITAS KRIKLER

linkedin.com/in/lorenafreitas/ researchgate.net/profile/Lorena_Freitas2

EDUCATION

2020 (Present) **PhD Electrical Engineering – École Polytechnique Fédérale de Lausanne (EPFL), Switzerland**
Courses: Signal Processing for Brain Imaging; Adaptation and Learning; Open Science in Practice.
Thesis title: "Dynamics of Brain Function in Preterm-Born Young Adolescents".

2015 **MRes, MSc Neurosciences** - Neurasmus, Erasmus Mundus Joint Masters Degree

Year 1: MRes Neuroscience, **Vrije Universiteit Amsterdam, Netherlands** (Cum Laude).
Year 2: MSc Medical Neuroscience, **Humboldt University of Berlin, Germany.**

2011 **BSc Computer Science** - **Federal University of Uberlândia, Brazil**
Relevant courses: Machine Learning; Image Processing; Information Retrieval; Project Management.
Exchange following Year 1 of the Information Systems MSc at **ENSIMAG, Grenoble, France**.

HONOURS AND AWARDS

2017 **Swiss Society for Neuroscience Travel Fellowship**
Awarded for the presentation of my project at the OHBM 2017 conference in Vancouver, Canada.

2015 **Cum Laude, Vrije Universiteit Amsterdam, The Netherlands**
The highest honours awarded by Vrije Universiteit Amsterdam for a Masters Degree.

2013 – 2015 **Full Erasmus Mundus Scholarship**
Awarded to the 2% top applicants of the Neurasmus Joint Masters Program in my year.

RESEARCH EXPERIENCE

2016 – Present Jun **Doctoral Candidate – École Polytechnique Fédérale de Lausane and University of Geneva**
Developing advanced signal processing and machine learning techniques to study brain function dynamics in children, within an interdisciplinary collaboration; Teaching Image Processing I and II, and Signal Processing for Functional Brain Imaging at Masters level; Supervising MSc student projects.

Keywords: *Time series analysis, unsupervised machine learning, MATLAB.*

2015 – 2016 Aug – Jan **Research Assistant – Centre for Bio-Inspired Technology - Imperial College London**
Collected and analysed multimodal data from surgical patients at Hammersmith Hospital to automatically monitor awareness and anaesthetics delivery during surgery.

Keywords: *Multimodal time-series analysis, mutual information, ECG+EEG analysis, MATLAB.*

2014 – 2015 Dec – Jul **Intern, MSc Thesis – Neurotechnology Group, Computer Science Dpt., Technische Universität Berlin**
Developed an algorithm based on dimensionality reduction that rejects noise artefacts from EEG signals in real time, to improve Brain-Computer Interfaces for patients with locked-in syndrome.

Keywords: *LDA classification, supervised and unsupervised machine learning, EEG, MATLAB.*

2014 Jan – Jul **Intern, MSc project – Center for Neurogenomics and Cognition Research (CNCR) Amsterdam**
Developed and lead a research study and analysis to enable a neurofeedback-based Brain-Computer Interface for attentional control. Trained 100+ BSc students to carry out their own projects.

Keywords: *Spectral EEG analysis, artefact removal, neurofeedback, experiment design, MATLAB.*

PROFESSIONAL EXPERIENCE

2012 – 2013 **Software Deployment Analyst - DEVEX S/A (now Hexagon Mining), Belo Horizonte, Brazil**

Provided software consultancy for the automation and optimisation of production in high end mining firms. Managed projects and small teams (2–4 people). My final project increased our client's productivity by 20% in two months.

2010 – 2012 **Software Engineer (iOS) - Shockmonkey Studios, Uberlândia, Brazil**

Developed iOS applications in Objective-C using an agile methodology (SCRUM). The final app I helped develop reached the top 5 most downloaded for its category in the whole country. Supervised interns and helped manage project sprints.

PROGRAMMING SKILLS

MATLAB (*advanced*), Python (Pandas; Numpy; Scikit-learn; Keras; OpenCV: *intermediate*), C, C# .NET, Java, PL/SQL (*previous experience*).

LANGUAGE SKILLS

Portuguese (*Native*); English (*Fluent*); French (*Advanced*); Italian (*Intermediate*); Spanish (*Intermediate*) Dutch (*Elementary*); German (*Elementary*).

LIST OF PUBLICATIONS

Freitas, L. G. A., Bolton, T. A. W., Krikler, B. E., Jochaut, D., Giraud, A. L., Hüppi, P. S., & Van De Ville, D. (2020). Time-resolved effective connectivity in task fMRI: Psychophysiological interactions of Co-activation patterns. *NeuroImage*, 212.

Liverani, M. C.*, **Freitas, L. G. A.***, Siffredi, V., Mikneviciute, G., Martuzzi, R., Meskaldij, D., Borradori Tolsa,C., Ha-Vinh Leuchter, R., Schnider, A., Van De Ville, D., and Hüppi, P. S. (2020). Get real: Orbitofrontal cortex mediates the ability to sense reality in early adolescents. *Brain and Behavior*, 10 (4): e01552.

Bolton TAW**, Freitas, L.G.A**., Jochaut D., Giraud A.L., Van De Ville D. Neural responses in autism during movie watching : Inter-individual response variability co-varies with symptomatology. *Neuroimage*. 2020 : 116571.

Adam-Darque, A., **Freitas, L.G.A.**, Grouiller, F., Sauser, J., Lazeyras, F., Van De Ville, D., Pollien, P., Garcia, C., Bergonzelli, G., Hüppi., P.S., Ha-Vihn Leuchter, R. (2020) Shedding Light on Excessive Crying in Babies. *Pediatric Research*, DOI: https://doi.org/10.1038/s41390-020-1048-6.

Viaña J.N.M, **Freitas L.**, Severo M.C., Gilbert F. (2016). Decoded Neurofeedback: Eligibility, Applicability, and Reliability Issues for Use in Schizophrenia and Major Depressive Disorder. *AJOB Neuroscience* 7 (2), 127-129.

POSTER PRESENTATIONS

Freitas, L. G. A., Liverani, M. C., Siffredi, V., Borradori Tolsa,C., Ha-Vinh Leuchter, R., Schnider, A., Van De Ville, D., and Hüppi, P. S. (2019) "Get Real: the orbitofrontal cortex mediates pre-teenagers' sense of reality", Organization for Human Brain Mapping, Rome, Italy.

Freitas, L. G. A., Liverani, M. C., Siffredi, V., Borradori Tolsa,C., Ha-Vinh Leuchter, R., Schnider, A., Van De Ville, D., and Hüppi, P. S. (2019) "*Orbitofrontal cortex mediates pre-teens' sense of reality*", Alpine Brain Imaging Meeting, Champéry, Switzerland.

Freitas, L. G. A., Bolton, T. A. W., Krikler, B. E., Jochaut, D., Giraud, A. L., Hüppi, P. S., & Van De Ville, D (2018) *"PPI-CAPs: fMRI dynamics during task performance***"**, Second International Workshop on Modelling the Progression Of Neurological Disease (EuroPOND2018), Geneva, Switzerland.

Freitas, L. G. A., Bolton, T. A. W., Krikler, B. E., Jochaut, D., Giraud, A. L., Hüppi, P. S., & Van De Ville, D (2018) **"***Psychophysiological interaction of co-activation patterns: tracking fMRI dynamics during task***"**, Alpine Brain Imaging Meeting, Champéry, Switzerland.

Freitas, L. G. A., Bolton, T. A. W., Krikler, B. E., Jochaut, D., Giraud, A. L., Hüppi, P. S., & Van De Ville, D (2017) **"***Psychophysiological interaction of co-activation patterns (PPI-CAPs): tracking task-dependent brain activity***"**, Organization for Human Brain Mapping, Vancouver, Canada.

Freitas, L. G. A., Adam-Darque, A., Van De Ville D., Huppi P. S., (2017) **"***PPI analysis reveals altered connectivity in preterm infants listening to their mother's voice***",** Alpine Brain Imaging Meeting, Champéry, Switzerland.

Freitas, L. G. A., Adam-Darque, A., Van De Ville D., Huppi P. S., (2016) *"Altered connectivity in preterm infants listening to their mother's voice revealed by PPI analysis"*, EPFL Bioengineering Institute Scientific Day, Geneva, Switzerland.

ORAL PRESENTATIONS

Freitas L.G.A., (2018) "*Time-resolved effective connectivity in task-based fMRI: Psychophysiological Interactions of Co-activation Patterns (PPI- CAPs).*" BBL/CIBM/CB Research day, Geneva, Switzerland.

Freitas L.G.A., (2018) "*Time-resolved effective connectivity in task-based fMRI: Psychophysiological Interactions of Co-activation Patterns (PPI- CAPs).*" Second International Workshop on Modelling the Progression Of Neurological Disease (EuroPOND2018), Geneva, Switzerland.

Freitas L.G.A., *(2017) "Can differences in early functional connectivity in healthy newborns exposed to olfactory stimulation help us understand crying behaviour at 6 weeks of life?"*, jENS: 2nd Congress of joint European Neonatal Societies, Venice, Italy.

EXTRACURRICULAR PROJECTS AND COURSES

- 2020 project: A multi-class image recognition project in Python, employing all steps of the data science lifecycle including data acquisition through web scraping; data scrubbing; multi-class classification using a deep convolutional network; and application of the results as part of a hackathon challenge (libraries: BeautifulSoup, Keras).
- 2020 course: Innosuisse Business Training Course – 48h of lectures from industrial experts on market analysis, financial planning, product development, presentation skills.
- 2019 project: A machine learning-based age classification project using the NHANES open access medical dataset, in Python (main python libraries: Pandas; Numpy; Scikit-learn).
- 2019 project: A video manipulation tool to generate a static image of background scenes after removing transient objects such as passers by, in Python (main library: OpenCV).